



LUND UNIVERSITY

Minimum Power Losses Based Optimal Power Flow for Iraqi National Super Grid (INSG) and its Effect on Transient Stability

Algburi, Sameer

2007

[Link to publication](#)

Citation for published version (APA):

Algburi, S. (2007). *Minimum Power Losses Based Optimal Power Flow for Iraqi National Super Grid (INSG) and its Effect on Transient Stability*. [Doctoral Thesis (monograph), University of Technology Iraq].

Total number of authors:

1

General rights

Unless other specific re-use rights are stated the following general rights apply:

Copyright and moral rights for the publications made accessible in the public portal are retained by the authors and/or other copyright owners and it is a condition of accessing publications that users recognise and abide by the legal requirements associated with these rights.

- Users may download and print one copy of any publication from the public portal for the purpose of private study or research.
- You may not further distribute the material or use it for any profit-making activity or commercial gain
- You may freely distribute the URL identifying the publication in the public portal

Read more about Creative commons licenses: <https://creativecommons.org/licenses/>

Take down policy

If you believe that this document breaches copyright please contact us providing details, and we will remove access to the work immediately and investigate your claim.

LUND UNIVERSITY

PO Box 117
221 00 Lund
+46 46-222 00 00

Republic of Iraq
Ministry of Higher Education and
Scientific Research
University of Technology



Minimum Power Losses Based Optimal Power Flow for Iraqi National Super Grid (INSG) and its Effect on Transient Stability

A thesis

Submitted to the Department of Technical Education of
University of Technology in a partial fulfillment of the requirements
for the Degree of Doctor of Philosophy in
Educational Technology/Electrical Engineering

by

Samir Sadon Mustafa Al-Jubory

supervised by

Dr. Nihad M. Al-Rawi

Dr. Samira A. Al-Mosawi

Certification

We certify that this thesis entitled "Minimum Power Losses Based Optimal Power Flow for Iraqi National Super Grid INSG and its Effect on Transient stability" was prepared under our supervision at the Department of Technical Education, University of Technology, Baghdad, in the partial fulfillment of the requirements for the degree of Doctor of Philosophy in Educational Technology/ Electrical Engineering.

Signature:

Name: Dr.Nihad M. Al-Rawi

Prof. /inElect. Eng.

Date: /1/2007

Signature:

Name: Samira M. Al-Mosawi

Prof. /in Educational Technology

Date: /1/2007

Examining committee certificate

We certify that we have read this thesis entitled "Minimum Power Losses Based Optimal Power Flow for Iraqi National Super Grid INSG and its Effect on Transient stability" and, as an examining committee examined the student (**Samir S. Mustafa**) in its content and that, in our opinion, it meet the standards of a thesis for degree of doctor of philosophy in Educational Technology/Electrical Engineering.

Signature:

Name: Krikor S. Krikor
Prof. /in Elect.Eng.
(Chairman)

Signature:

Name: Dr.Dhary Yousif
Asst.Prof./in Elect.Eng.
(Member)

Signature:

Name: Dr.Adil Hameed Ahmad
Asst.Prof./in Elect.Eng.
(Member)

Signature:

Name: Esmaeel M. Jabir
Asst.Prof./in Elect.Eng.
(Member)

Signature:

Name: Dr.Anaam M. Al-Sadik
Prof. /in Educational Technology
(Member)

Signature:

Name: Nihad M. Al-Rawi
Prof. /in Elect.Eng.
(Supervisor)

Signature:

Name: Dr.Samira A. Al-Mosawi
Prof. /in Educational Technology
(Supervisor)

Approved for Technical Education Department, University of Technology, Baghdad

Signature:

Name: Dr. Dhary Yousif
Head of Technical Education Department

To my family

with my love

ACKNOWLEDGMENT

I would like to express my deep sense of gratitude to my supervisors Dr.Nihad Al-Rawi and Dr. Samira Al-Mosawi for their valuable guidance suggestions and continuous encouragement during the development of this work.

Many thanks to the staff of Technical Education Department for their assistance during this work.

I would like to thank all my colleagues at the Ph.D specially to Siham Ahmad.

Special thanks are extended to Dr. Abdul Rahman and Mr. Faris Rofa in the Technical College/Kirkuk and Mr.Ashor at the Technical Institute/Kirkuk, Dr. Afaneen in Elec. Eng . Dep . and Ahmed Mohamad in Alqaa center for their continuous help.

Samir

Abstract

In the present work Optimal Power Flow (OPF) with minimum net work losses for Iraqi National Super Grid (400kv) INSG which consist of 19 load buses and 6 generating buses was studied. The losses were calculated and compared with that in case of ordinary load flow which is equal to 37592 MW according to data of generation and load on 2/1/2003. Mathematical model using Lagrange method programmed in Matlab5.3 language was used to reduce network active power losses by injecting active and reactive power in the network load buses according to the sensitivity of each bus to reduce network losses with respect to injection power in the buses. It was found that minimum losses in the network is equal to 21.824MW in case of injecting 180,200,210 and 300MW in the load buses 7, 8, 9 and 11 respectively. Also the minimum losses in the network are equal to 32.64MW in case of injecting 150,120,120,120,100 and 310MVAR in the load buses 5, 7, 8,9,10 and 11 respectively. Optimal generation for the present six generating units which gives minimum network losses was calculated. The effect of removing transmission lines and generating units on OPF was studied for six different operating cases.

Also the effect of three phase faults in the middle of transmission lines on OPF and transient stability was studied. In this work step by step integration method has been used. It was found that the worst case takes place in the case of three phase fault in the middle of transmission line (3-4) HAD-QAM which causes system instability.

List of Contents

Abstract	I
List of Contents	II-V
List of Abbreviations	VI
List of Symbols	VII
The Names of the Stations	VII

Chapter One *Introduction and Literature Survey*

1.1	<i>Introduction</i>	1
1.2	<i>Methodology of the Research</i>	2
1.2.1	<i>Research Problem</i>	2
1.2.2	<i>Aim of the Research</i>	2
1.2.3	<i>Research Importance</i>	2
1.2.4	<i>Research Limitations</i>	3
1.3	<i>Literature Survey</i>	3
1.4	<i>Scope and Organization of the Thesis</i>	9

Chapter Two *Power Flow and Transient Stability Problem*

2.1	<i>Introduction</i>	10
2.2	<i>Simulation</i>	10
2.2.1	<i>Simulation Techniques</i>	11
2.2.2	<i>Simulation Model Used in this Work</i>	12
2.3	<i>Network Modeling</i>	15
2.3.1	<i>Line Modeling</i>	15
2.3.2	<i>Generator Modeling</i>	16
2.3.3	<i>Load Modeling</i>	16
2.4	<i>Power Flow Problem</i>	17
2.5	<i>Bus Types</i>	17
2.6	<i>Solution to the P.F Problem</i>	18

2.6.1	<i>Newton-Raphson Method</i>	18
2.6.2	<i>Equality and Inequality Constraints</i>	21
2.7	<i>Optimal Power Flow</i>	21
2.7.1	<i>Introduction</i>	21
2.7.2	<i>Goals of the OPF</i>	21
2.7.3	<i>Nonlinear Programming Methods Applied to OPF Problems</i>	24
2.7.4	<i>Analysis of System Optimization and Security Formulation of the Optimization Problems</i>	25
2.7.5	<i>Linear Programming Technique (LP)</i>	29
2.8	<i>Transient Stability</i>	29
2.8.1	<i>Introduction</i>	29
2.8.2	<i>Power Transfer between Two Equivalent Sources</i>	31
2.8.3	<i>The Power Angle Curve</i>	31
2.8.4	<i>Transiently Stable and Unstable Systems</i>	33
2.8.5	<i>The Swing Equation</i>	34
2.8.6	<i>Step-by-Step Solution of the Swing Curve</i>	35

Chapter Three *Optimal Power Flow with Transient Stability*

3.1	<i>Introduction</i>	39
3.2	<i>Optimal Design Using Mathematical Model</i>	39
3.3	<i>Optimization Solution Approaches</i>	40
3.3.1	<i>Graphical Method</i>	40
3.3.2	<i>Analytical Technique</i>	40
3.3.2.1	<i>The Kuhn-Tucker Conditions</i>	41
3.3.2.2	<i>Sufficient and Necessary Conditions</i>	42
3.3.3	<i>Numerical Technique</i>	43
3.3.4	<i>Experimental Technique</i>	43
3.4	<i>Optimal Control of Reactive Power Flow for Real Power Loss Minimization</i>	43
3.5	<i>Reactive Power Allocation</i>	44
3.6	<i>Optimal Placement of Generation Units</i>	44
3.7	<i>Mathematical Analysis for Reactive Power Allocation and Optimal Placement of Generation Units</i>	45

3.8	<i>Optimum Power Flow Operation with Transient Stability</i>	52
3.9	<i>Stability-Constrained OPF Formulation</i>	53
3.10	<i>Stability-Constrained OPF Procedure</i>	55

Chapter Four *The Application of the Developed Program on INSG*

4.1	<i>Introduction</i>	57
4.2	<i>General Description of the Iraqi National Super Grid (INSG) System</i>	57
4.3	<i>The Program Used</i>	60
4.4	<i>The Educational Program</i>	61

Chapter Five *Results and Discussion*

5.1	<i>Power Losses Reduction</i>	67
5.1.1	<i>Injecting Active Power</i>	67
5.1.2	<i>Injecting Reactive Power</i>	80
5.1.3	<i>Injecting Equal Amount of Active Power at the same Time</i>	93
5.1.4	<i>Injecting Equal Amount of Reactive Power at the same Time</i>	96
5.1.5	<i>Optimal Quantity and Placement of Active Power Injection at Load Buses</i>	99
5.1.6	<i>Optimal Quantity and Placement of Reactive Power Injection at Load Buses</i>	100
5.1.7	<i>Control of Active Power at Generation Buses</i>	101
5.1.8	<i>Load Flow Losses with Multi Contingencies</i>	111
5.1.8.1	<i>Removing the Line 1-6 (BAJ-KRK)</i>	112
5.1.8.2	<i>Removing the Line 3-4 (HAD-QAM)</i>	114
5.1.8.3	<i>Removing Lines 1-6 (BAJ-KRK) and 3-4 (HAD-QAM)</i>	115
5.1.8.4	<i>Removing Lines 1-6 (BAJ-KRK), 3-4 (HAD-QAM) and 18-19 (HRT-QRN)</i>	116

5.1.8.5	<i>Removing Line 1-6 (BAJ-KRK) and Generation at Bus 22 (HAD)</i>	117
5.1.8.6	<i>Removing Line 1-6 (BAJ-KRK) and Generation at Bus 25 (HRT)</i>	118
5.2	<i>Transient Stability</i>	119
5.3	<i>Transient Stability with Optimal Power Flow Case Studies</i>	119
5.3.1	<i>Three Phase Fault in the Middle of Line 1-6 (BAJ-KRK)</i>	119
5.3.2	<i>Three Phase Fault in the Middle of Line 3-4 (HAD-QAM)</i>	123
5.3.3	<i>Three Phase Fault in the Middle of Line 18-19 (HRT-QRN)</i>	126
5.3.4	<i>Improvement of System Stability in case of Faults in the Middle of Line (3-4)</i>	129

Chapter Six *Conclusions & Suggestions for Future Works*

6.1	<i>Conclusions</i>	133
6.2	<i>Suggestions for Futures Works</i>	134

	<i>References</i>	135
	<i>Appendix</i>	
<i>Appendix A:</i>	<i>Sensitivity</i>	a-c
<i>Appendix B:</i>	<i>Derivation of the Swing Equation</i>	d-e
<i>Appendix C:</i>	<i>The Load & Generation of the Iraqi National Super Grid System (400 kV)</i>	f
<i>Appendix D:</i>	<i>INSG System Line Data</i>	g
<i>Appendix E:</i>	<i>Machine's Parameters</i>	h
<i>Appendix F:</i>	<i>Limits of Generation and Load Buses</i>	i

List of Abbreviations

ACSR	Aluminum Conductor Steel Reinforced
COI	Center of Inertia
FACTS	Flexible AC Transmission System
INRG	Iraqi Northern Region Grid
INSG	Iraqi National Super Grid
LP	Linear Programming
MVA	Mega Volt Amper
MVAR	Mega Volt Amper Reactive
MW	Megawatt
NP	Nonlinear Programming
N-R	Newton-Raphson
OPF	Optimal Power Flow
OPFWTS	Optimal power flow with Transient Stability
ORPF	Optimal Reactive Power Flow

SBSI	Step By Step Integration
SVC	Static VAR Compensator
TAA	Twin Aluminum Alloy
TCR	Thyristor Controlled Reactor
TCSC	Thyristor Controlled series Compensation
TS	Transient Stability
TSC	Thyristor switched Capacitor
VAR	Volt Amper Reactive
SBSI	Step By Step Integration

List of Symbols

B	Sucseptance
C	Capacitor
F	Frequency
G	Conductance
H	Inertia Constant
I_R	Receiving end current of TL
I_s	Sending end current of TL
k	Number of iterations
m	Number of machines
n	Number of buses
P	Active Power
Q	Reactive Power
R	Resistance
T	Torque
V_R	Receiving end voltage of Transmission Line
V_s	Sending end voltage of Transmission Line
V_t	Terminal Voltage
X	Reactance
X_c	Capacitive reactance
X_L	Inductive reactance
Y	Admittance
ω	Angular Velocity
δ	Rotor Angle

The Names of the Stations

BAB	Babel
BAJ	Baji
BGE	Baghdad East
BGN	Baghdad North
BGS	Baghdad South
BGW	Baghdad West
BQB	Baquba
HAD	Haditha
HRT	Hartha
KAZ	Khour-Al-Zubair
KDS	Kadissia
KRK	Kirkuk
KUT	KUT
MOS	Mousil
MSB	Mussayab
NAS	Nasiriya
QAM	Qaim
QRN	Qurna
SDM	Sed Al-Mousil

Chapter One

Introduction and Literature Survey

Chapter One

Introduction and Literature Survey

1.1 Introduction:

A practical electric power system is a nonlinear network, which is generally governed by a large number of differential equations (defined by the dynamics of the generators and the loads as well as their controllers) and algebraic equations (described by the current balance equations of the transmission network). An operating point of a power system is not only a stable equilibrium of the differential and algebraic equations, but also satisfy all of the static equality and inequality constraints at the equilibrium such as upper and lower bounds of generators and voltages of all buses. A feasible operation point should withstand the fault and ensure that the power system moves to a new stable equilibrium after the clearance of the fault without violating equality and inequality constraints even during transient period of dynamics.

As it is of great importance that power systems must be designed to operate at highest degree of efficiency, security and reliability, i.e. to be stable under any probable disturbance, a study providing information concerned with the capability of the system to remain stable during major disturbance is therefore needed.

In large-scale power systems with many synchronous machines interconnected by complicated transmission networks, transient stability studies are best performed with a digital computer program. For a specified disturbance, the computer program Matlab5.3 solves, step by step, a set of algebraic power-flow equations describing synchronous generators. Newton Raphson method has been applied to network solution, while

modified Euler's and Runge-Kutta methods have been applied to the solution of the differential equations in transient stability analysis.

The network configuration and parameters as well as protection philosophy are principal factors affecting the transient performance of power systems. Different methods have been used for improving and enhancing transient stability of power system.

1.2 Methodology of the Research:

1.2.1 Research Problem:

Although study optimal power flow and the proper location of active and reactive power units for INSG and its effect on transient stability is an important problem, there is no study which deals with it.

1.2.2 Research Objectives:

The main goals of this research are:

- 1- Studying optimal power flow for Iraqi National Super Grid with optimal loss reduction using linear and non linear programming methods.
- 2- Studying the effect of optimal power flow on transient stability in case of sudden major faults.
- 3- Reducing the active power losses in INSG Network.
- 4- Allocation of the optimal active and reactive power at all buses.
- 5- Designing instructional program to be used by electrical engineers.

1.2.3 Research Importance:

The importance of this study can be described briefly:

- 1- It is the first attempt to study INSG optimal power flow and its effect on transient stability.

- 2- The research gives suggestions to develop the 400 kV system and the best places to install generation and compensation, also its optimal magnitudes to reach optimal system loss reduction.

1.2.4 Research Boundaries:

The limitations of the research are:

- 1- The study uses MATLAB 5.3 programming language.
- 2- The case study of the research is applied to the Iraqi National Super Grid INSG.
- 3- The input data for the new program represents the loading and generation of the 2nd of Jan. 2003 according to the latest data which can be obtained from the Iraqi National Control Center.

1.3 Literature Survey:

According to the great importance of the proper allocation of the active and reactive power and its effect on transient stability with optimal power flow, there have a large number of studies that deal with this subject: Azhar Said Al-Fahady, “**A New Approaches in Compensation Techniques Applied for INRG Systems**”, 1997, Mosul.

In this study six different schemes using series and shunt compensation are investigated. Two analytical approaches are described, the first is based on minimizing the energy transmission cost, and the second is based on maximizing an objective function defined by the difference between the equivalent cost of the increase in the power level transmitted over the line and other costs associated with the line including the costs of series and extra power losses due to the higher current carried over the compensated line. Comparison between the six schemes from the economical point of view is investigated. The procedure is applied to INRG

system for enhancement of power transmitted over the existing (400 kV) lines [1].

Deqiang Gan, “**A transient Stability Constrained OPF**”, 1999.

In this work, swing equations are converted to numerically equivalent algebraic equations and then integrated into a standard OPF formulation. In this way standard nonlinear programming techniques can be applied to the problem [2].

Ahmad Nasser Bahjat Al-Sammak, “**A New Method for Transient Stability Study with Application to INRG (Iraqi Northern Region Grid)**”, 1999, Mosul.

A new modeling technique for the simulation of transient stability studies of power system has been introduced using numerical analysis as a principal tool of calculation aided with computer programs. The trapezoidal method has been selected as a numerical analysis method.

The existing Iraqi Northern Region Grid has been selected in this study. The study shows that the circuit breakers must always be maintained to fasten the response of the system to the faults. The study also shows the effect of using auto-reclosing circuit breakers during the transient state with abnormal conditions, which increase the stability of the systems to the faults. The used programming language is Fortran 90 [3].

W. Rosehart, “**Optimal Power Flow Incorporating Voltage Collapse Constraints**”, 2000.

This paper presents applications of optimization techniques to voltage collapse studies. First a maximum distance to voltage collapse algorithm that incorporates constraints on the current operating conditions is presented. Second, an optimal power flow formulation that incorporates voltage-stability criteria is proposed. The algorithms are tested on a 30-bus system using a standard power flow model, where the effect of limits on the maximum loading point is demonstrated [4].

Sangahm Kim, “**Generation Redispatch Model to Enhance Voltage Security in Competitive Power Market Using Voltage Stability Constrained Optimal Power Flow VSCOPF**”, 2001.

This paper shows the impact of incorporation of voltage security constraint into optimal power flow formulation in which the active power dispatch problem is associated with guaranteeing adequate voltage security levels in power systems. The objective function is chosen to minimize fuel optimization problem of the following forms:

$$\begin{aligned} \min f(x) \\ \text{s.t } g(x) = 0 \\ \underline{h} \leq h(x) \leq \bar{h} \end{aligned}$$

where $g(x)$ is equality constraints generally represented by the load flow equations and $h(x)$ is the inequality constraints with lower limits \underline{h} and upper limits \bar{h} . In this paper primal dual interior point algorithm (PDIPM) is utilized to solve the VSCOPF problems. The proposed VSCOPF formulation was implemented in a computer program and tested on simple 3-bus system and IEEE 30-bus test system [5].

Luonan Chen, “**Optimal Operation Solutions of Power Systems with Transient Stability Constrains**”, 2001.

The author showed that is not easy to deal with the computation of an optimal operation point in power systems since it is a nonlinear optimization problem. In this work OPF with transient stability constraints (OTS) was equivalently converted into an optimization problem in the Euclidean space via a constraint transcription which can be viewed as an initial value problem for all disturbances and solved by any standard nonlinear programming techniques adopted by OPF. The transformed OTS problem has the same variables as those of OPF.

This work proposes a new method for OTS based on the functioned transformation techniques, which convert infinite-dimensional OTS into a finite-dimensional optimization problem, thereby making OTS tractable even for large scale system with a large number of contingencies [6].

Mohammed Ali Abdullah Al-Rawi, “**Transient Stability Improvement Using Series Capacitors with Application to Iraqi National Super Grid (INSG)**”, 2002, Mosul.

Maintaining and improving transient stability using series capacitor compensation technique has been presented in this work.

Simulation with mathematical modeling for transient stability of power system has been introduced using modified Euler’s iterative numerical integration method. The existing INSG system has been chosen for this study. It has been shown that the series capacitor compensation is an effective tool to improve the stability of power systems. The research includes 13 cases with different faults on the investigated system [7].

William Rosehart “**Optimal Placement of Distributed Generation**”, 2002

In this paper, a lagrangian based approach is used to determine optimal locations for placing distributed generators and enhancing system stability. The approach was analyzed using IEEE 30-bus system [8].

Yue Yuan *et al.*, “**A Study of Transient Stability Constrained Optimal Power Flow with Multi-contingency**”, 2002.

This paper illustrates the necessity for multi-contingency transient stability constrained optimal power flow MC-SCOPF through the result of single-contingency SCOPF of Japan IEEJ WESTIO model system. The problem was formulated and demonstrated on this system.

A solution to MC-SCOPF problem was proposed by the primal-dual Newton Interior Point Method (IPM) for nonlinear programming (NLP). Because MC-SCOPF contains a large number of variables and constraints,

the success of the solution needs fast algorithm together with efficiently exploiting sparsity programming technique.

All of the contingencies are three-phase grounding fault and removed 70ms later by opening one of the double lines. For all machines -100 degree and $+100$ degree was assigned as the lower and upper limits of angles with respect to center of inertia COI. The step-width Δt is fixed to be 0.005 second and the maximum integration period T_{\max} is set to be 2.0 second for the purpose of studying first swing transients [9].

Al-Suhamei W.S., “**Minimizing Losses in the Northern Network**”, 2002.

In this work, the capability of minimizing active power losses to the minimum possible limit within operation constraints in Iraqi northern region grid with voltage level (400 kV and 132 kV) has been presented by using optimal reactive power control techniques. The problem is solved by using Lagrangian method. Two test situations were used, minimum load situation and maximum load situation [10].

Afaneen Anwar Abood Al-Khazragy, “**Implementation of Geographic Information System (GIS) in Real-Time Transient Stability**”, 2004.

This research is concerned in developing a transient stability program using the Direct Method of Lyapunov. The network under consideration is the Iraqi Super Grid Network 400kV.

The database system in the National Control Center of Iraq was improved by using the facilities of the GIS (Geographic Information System) which was applied to develop a real-time transient stability program which has the ability to sense any changes in the network under consideration, and operates automatically with a suitable time (3 seconds).

This work developed and investigated a direct method for transient stability analysis using the energy approach method [11].

M. Rodriquez Montancs “**Voltage Sensitivity Based Technique for Optimal Placement of Switched Capacitors**”, 2005.

This paper produced sensitivity analysis technique to solve the optimal allocation and sizing of capacitors on power systems and its effect on voltage stability. The proposed methodology is mainly characterized by assuming linear behaviors for the reactive problem to minimize the sum of voltage magnitude deviation from the specified voltage. Voltage sensitivity index was used as indicator of voltage stability. The proposed approach has been tested on IEEE 14-bus and 30-bus systems [12].

Comparison with this work

Case studies: Various case studies have been used in literature survey. INSG was used in ref.[9] and[3],INRG in ref.[5,7&1],IEEE 30 bus in ref.[2,4&10]and 10 machines 39 bus in ref.[12]and [11].In this work the case study is INSG.

Language: FORTRAN language has been used in ref. [9, 5&7], the other studies used MATLAB tools. This work used MATLAB version 5.3.

Studying time: Clearing time (t_c) used to clear fault is 0.07 sec-0.1 sec. Total integration time (T) is 1sec-2sec.In this work t_c and T are 0.15 sec and 1.5 sec respectively.

Methods to solve transient stability: Numerical analysis by trapezoidal rule, Range Kutta, Modified Euler and other methods were used to solve transient stability. In this work step by step integration method has been used because it is robust and provides all relevant system swing information.

Methods to solve OPF: LP or Quasi Newton methods were used in ref. [8] and [12]. Interior Point Method was used in ref. [6] and [4]; other methods were used in other ref. In this work Lagrange method with sensitivity analysis were used to search for optimal placement of active and reactive power.

Objectives: Minimizing operation cost, improving stability, enhancement of power transmission or minimizing active power losses were the objectives of the studies in literature survey.

Optimal placement of active and reactive power to reduce losses and their effect on transient stability are the objectives of this work.

1.4 Scope and Organization of the Thesis:

This thesis consists of six chapters including the current one.

Chapter 2: gives introduction to networks modeling, power flow problem, optimal power flow, and transient stability.

Chapter 3: discusses the optimal power flow with transient stability (OPFWTS). Also the chapter gives a formulation of stability constrained OPF and its objective function. The flow charts are included.

Chapter 4: illustrates the application of the new program written in MATLAB 5.3 to INSG.

Chapter 5: provides the results and discussion of the research.

Chapter 6: provides the conclusions of this research. Suggestions are presented for future works.

Appendices: are provided at the end of the thesis.

Chapter Two

Power Flow and Transient Stability Problem

Chapter Two

Power Flow and Transient Stability Problem

2.1 Introduction:

All analyses in the engineering sciences start with the formulation of appropriate models. A mathematical model is a set of equations or relations, which appropriately describe the interactions between different quantities in the time frame studies and with the desired accuracy of a physical or engineering component or system. Hence, depending on the purpose of the analysis different models might be valid. In many engineering studies the selection of correct model is often the most difficult part of the study.

2.2 Simulation:

Simulation is an educational tool that is commonly used to teach processes that are infeasible to practice in the real world. Software process education is a domain that has not yet taken full advantage of benefits of simulation.

Simulation is a powerful tool for the analysis of new system designs, retrofits to existing systems and proposed changes to operating rules. Conducting a valid simulation is both an art and a science.

A simulation model is a descriptive model of a process or system, and usually includes parameters that allow the model to be configurable, that is, to represent a number of somewhat different systems or process configurations.

As a descriptive model, we can use a simulation model to experiment with, evaluate and compare any number of system alternatives. Evaluation,

comparison and analysis are the key reasons for doing simulation. Prediction of system performance and identification of system problems and their causes are the key results [13-16]. Simulation is most useful in the following situations:

- 1- There is no simple analytic model.
- 2- The real system has some level of complexity, interaction or interdependence between various components, which makes it difficult to grasp in its entirety. In particular, it is difficult or impossible to predict the effect of proposed changes.
- 3- Designing a new system, and facing a new different demand.
- 4- System modification of a type that we have little or no experience and hence face considerable risk.
- 5- Simulation with animation is an excellent training and educational device, for managers, supervisors, and engineers. In systems of large physical scale, the simulation animation may be the only way in which most participants can visualize how their work contributes to overall system success or problems [17, 18].

2.2.1 Simulation Techniques:

Simulation techniques are fundamental to aid the process of large-scale design and network operation.

Simulation models provide relatively fast and inexpensive estimates of the performance of alternative system configuration and / or alternative operating procedures. The value and usage of simulation have increased due to improvement in both computing power and simulation software.

In order for the simulation to be a successful educational tool, it must be based on an appropriate economic model with correct “fundamental laws” of software engineering and must encode them quantitatively into accurate mathematical relationship [19-23].

2.2.2 Simulation Model Used in this Work:

The simulation model used in this work is (**Law and McComas Approach**)[24] which is called Seven Steps Approach for conducting a successful simulation study as shown in Figure (2.1), which presents techniques for building valid and credible simulation models, and determines whether a simulation model is an accurate representation of the system for the particular objectives of the study. In this approach, a simulation model should always be developed for a particular set of objectives, where a model that is valid for one objective may not be for another. The important activities that take place in the seven steps model are used in this work:

Step 1. Formulation the Problem

The following things are studied in this step:

- 1- The overall objectives of the study.
- 2- The scope of the model.
- 3- The system configuration to be modeled.
- 4- The time frame for the study and the required resources.

Step 2. Collection of information/Data and Construction a Conceptual Model

- 1- Collecting information on the system layout and operating procedures.
- 2- Collecting data to specify model parameters.
- 3- Documentation of the model assumptions, algorithms and data summaries.

Step 3. Validation of Conceptual Model

If errors or omissions are discovered in the conceptual model, it must be updated before proceeding to programming in step 4.

Step 4. Programming the Model

- 1- Programming the conceptual model in a programming language.
- 2- Verification (debugging) of the computer program.

Step 5. The Programmed Model Validity

- 1- If there is an existing system (as in this work), then compare model performance measures with the comparable performance measures collected from the system.
- 2- Sensitivity analyses should be performed on the programmed model to see which model factors have the greatest effect on the performance measured and, thus, have to be modeled carefully.

Step 6. Designing and Analyzing Simulation Experiments

Analyzing the results and deciding if additional experiments are required.

Step 7. Documenting and Presenting the Simulation Results

The documentation for the model should include a detailed description of the computer program, and the results of the study [24].

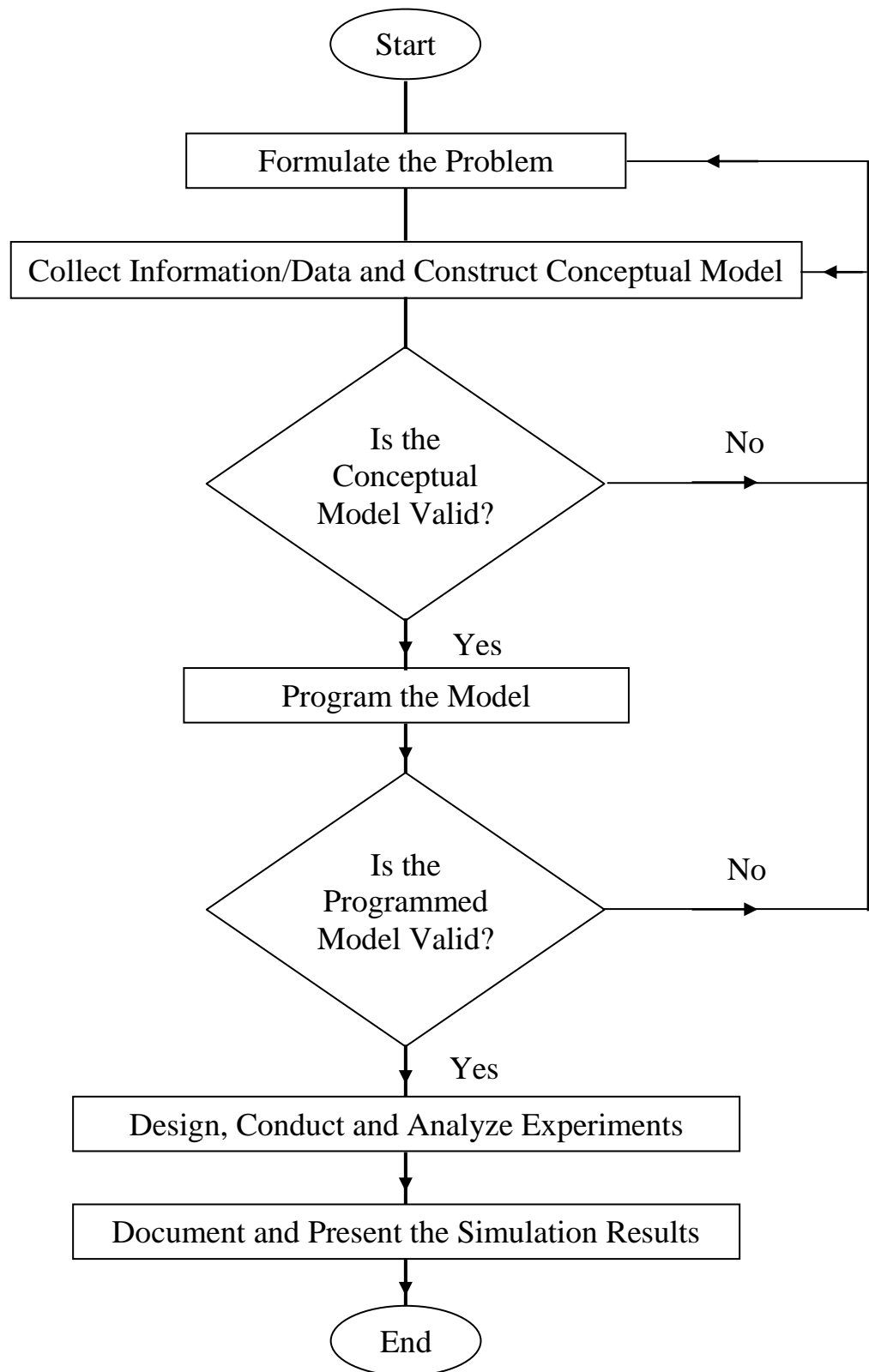


Figure (2.1): Law and McComas Simulation Model [24]

2.3 Network Modeling:

Transmission plant components are modeled by their equivalent circuits in terms of inductance, capacitance and resistance. Among many methods of describing transmission systems to comply with Kirchhoff's laws, two methods, mesh and nodal analysis are normally used. Nodal analysis has been found to be particularly suitable for digital computer work, and almost exclusively used for routine network calculations.

2.3.1 Line Modeling:

The equivalent π -model of a transmission line section is shown in Figure (2.2) and it is characterized by parameters:

$$Z_{km} = R_{km} + jX_{km} = \text{series impedance } (\Omega)$$

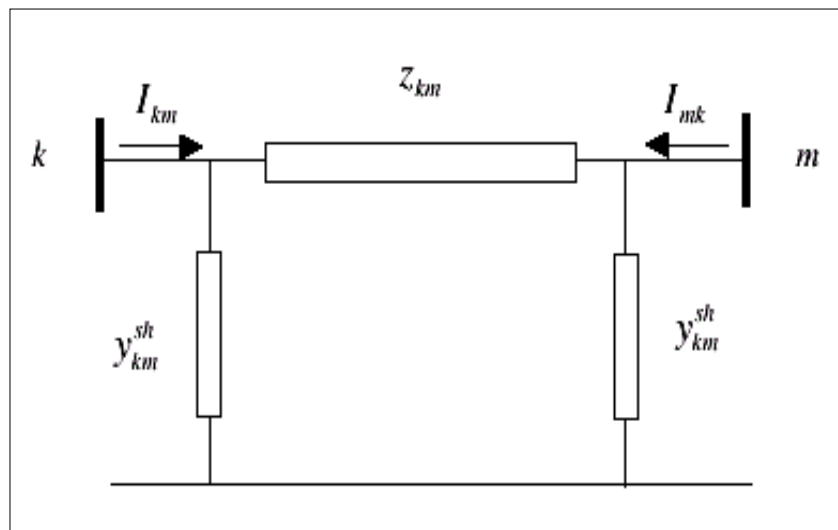


Figure (2.2): Equivalent (π - Model) of a Transmission Line [25]

$$Y_{km} = Z_{km}^{-1} = G_{km} + jB_{km} = \text{series admittance (siemens).}$$

$$Y_{km}^{sh} = G_{km}^{sh} + jB_{km}^{sh} = \text{shunt admittance (siemens).}$$

where:

G_{km} and G_{km}^{sh} are series and shunt conductance respectively.

B_{km} and B_{km}^{sh} are series and shunt Susceptance respectively.

The value of G_{km}^{sh} is so small that it could be neglected [25, 26].

2.3.2 Generator Modeling:

In load flow analysis, generators are modeled as current injections as shown in Figure (2.3).

In steady state a generator is commonly controlled so that the active power injected into the bus and the voltage at the generator terminal are kept constant. Active power from the generator is determined by the turbine control and must of course be within the capability of the turbine generator system. Voltage is primarily determined by reactive power injection into the node, and since the generator must operate within its reactive capability curve, it is not possible to control the voltage outside certain limits [25].

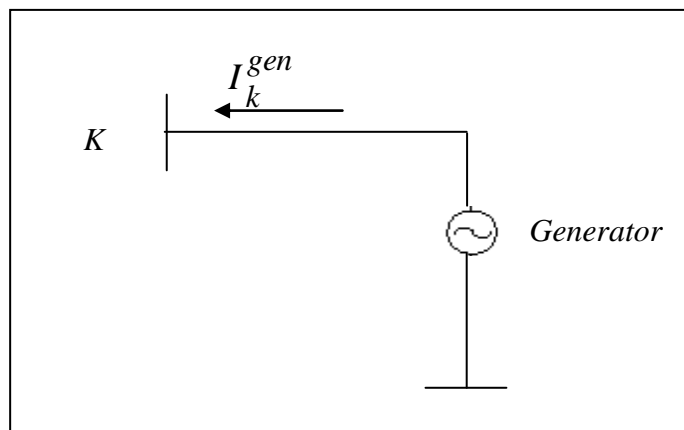


Figure (2.3): Generator Modeling [25]

2.3.3 Load Modeling:

Accurate representation of electric loads in power system is very important in stability calculations. Electric loads can be treated in many ways during the transient period. The common representation of loads are static impedance or admittance to ground, constant current at fixed power factor, constant real and reactive power, or a combination of these representations [27]. For a constant current and a static admittance representation of a load, the following equations are used respectively:

$$I_{Lo} = \frac{P_L - jQ_L}{V_L^*} \quad (2.1)$$

$$Y_{Lo} = \frac{P_L - jQ_L}{V_L^* V_L} \quad (2.2)$$

where:

P_L and Q_L are the scheduled bus loads.

V_L is calculated bus voltage.

I_{Lo} current flows from bus L to ground.

2.4 Power Flow Problem:

The power flow problem can be formulated as a set of non-linear algebraic equality/inequality constraints. These constraints represent both Kirchhoff's laws and network operation limits. In the basic formulation of the power flow problem, four variables are associated with each bus (network node) k:

- V_k – voltage magnitude.
- δ_k – voltage angle.
- P_k – net active power (algebraic sum of generation and load).
- Q_k – net reactive power (algebraic sum of generation and load) [25, 28].

2.5 Bus Types:

Depending on which of the above four variables are known (scheduled) and which ones are unknown (to be calculated), the basic types of buses can be defined as in Table (2-1).

Table (2.1): Power Flow Bus Specification [29]

Bus Type	Active Power, P	Reactive Power, Q	Voltage Magn., E 	Voltage Angle, θ
Constant Power Load, Constant Power Bus	Scheduled	Scheduled	Calculated	Calculated
Generator/Synchronous Condenser, Voltage Controlled Bus	Scheduled	Calculated	Scheduled	Calculated
Reference / Swing Generator, Slack Bus	Calculated	Calculated	Scheduled	Scheduled

2.6 Solution to the PF Problem:

In all realistic cases the power flow problem cannot be solved analytically and hence iterative solutions implemented in computers must be used. Gauss iteration with a variant called Gauss-Seidel iterative method and Newton Raphson method are some of the solutions methods of PF problem. A problem with the Gauss and Gauss-Seidel iteration schemes is that convergence can be very slow and sometimes even the iteration does not converge although a solution exists. Therefore more efficient solution methods are needed, Newton-Raphson method is one such method that is widely used in power flow computations [25, 30].

2.6.1 Newton-Raphson Method [25]:

A system of nonlinear algebraic equations can be written as:

$$f(x) = 0 \quad (2.3)$$

where x is an (n) vector of unknowns and (f) is an (n) vector function of (x). Given an appropriate starting value x^0 , the Newton-

Raphson method solves this vector equation by generating the following sequence:

$$\left. \begin{aligned} J(x^v) \Delta x^v &= -f(x^v) \\ x^{v+1} &= x^v + \Delta x^v \end{aligned} \right\} \quad (2.4)$$

where $J(x^v) = \frac{\partial f(x)}{\partial x}$ is the Jacobian matrix.

The Newton-Raphson algorithm for the n-dimensional case is thus as follows:

1. Set $v=0$ and choose an appropriate starting value x^0 .
2. Compute $f(x^v)$.
3. Test convergence:
If $|f_i(x^v)| \leq \epsilon$ for $i=1, 2, \dots, n$, then x^v is the solution otherwise go to 4.

4. Compute the Jacobian matrix $J(x^v)$.

5. Update the solution

$$\left. \begin{aligned} \Delta x^v &= -J^{-1}(x^v) f(x^v) \\ x^{v+1} &= x^v + \Delta x^v \end{aligned} \right\} \quad (2.5)$$

6. Update iteration counter $v+1 \rightarrow v$ and go to step 2. Note that the linearization of $f(x)$ at x^v is given by the Taylor expansion.

$$f(x^v + \Delta x^v) \approx f(x^v) + J(x^v) \Delta x^v \quad (2.6)$$

where the Jacobian matrix has the general form:

$$J = \frac{\partial f}{\partial x} = \begin{bmatrix} \frac{\partial f_1}{\partial x_1} & \frac{\partial f_1}{\partial x_2} & \dots & \frac{\partial f_1}{\partial x_n} \\ \frac{\partial f_2}{\partial x_1} & \frac{\partial f_2}{\partial x_2} & \dots & \frac{\partial f_2}{\partial x_n} \\ \vdots & \vdots & \ddots & \vdots \\ \frac{\partial f_n}{\partial x_1} & \frac{\partial f_n}{\partial x_2} & \dots & \frac{\partial f_n}{\partial x_n} \end{bmatrix} \quad (2.7)$$

To formulate the Newton-Raphson iteration of the power flow equation, firstly, the state vector of unknown voltage angles and magnitudes is ordered such that:

$$x = \begin{bmatrix} \delta \\ V \end{bmatrix} \quad (2.8)$$

And the nonlinear function f is ordered so that the first component corresponds to active power and the last ones to reactive power:

$$f(x) = \begin{bmatrix} P(x) \\ Q(x) \end{bmatrix} \quad (2.9)$$

$$f(x) = \begin{bmatrix} P_2(x) - P_2 \\ \vdots \\ P_m(x) - P_m \\ \hline Q_2(x) - Q_2 \\ Q_n(x) - Q_n \end{bmatrix} \quad (2.10)$$

In eq. (2.10) the function $P_m(x)$ are the active power which flows out from bus k and the P_m are the injections into bus k from generators and loads, and the functions $Q_n(x)$ are the reactive power which flows out from bus k and Q_n are the injections into bus k from generators and loads. The first $m-1$ equations are formulated for PV and PQ buses, and the last $n-1$ equations can only be formulated for PQ buses. If there are N_{PV} PV buses and N_{PQ} PQ buses, $m-1 = N_{PV} + N_{PQ}$ and $n-1 = N_{PQ}$.

The load flow equations can be written as:

$$f(x) = \begin{bmatrix} P(x) \\ Q(x) \end{bmatrix} = 0 \quad (2.11)$$

And the functions $P(x)$ and $Q(x)$ are called active and reactive power mismatches. The updates to the solutions are determined from the equation:

$$J(x^v) \begin{bmatrix} \Delta\delta^v \\ \Delta V^v \end{bmatrix} + \begin{bmatrix} P(x^v) \\ Q(x^v) \end{bmatrix} = 0 \quad (2.12)$$

The Jacobian matrix J can be written as:

$$J = \begin{bmatrix} \frac{\partial P}{\partial \delta} & \frac{\partial P}{\partial V} \\ \frac{\partial Q}{\partial \delta} & \frac{\partial Q}{\partial V} \end{bmatrix} \quad (2.13)$$

2.6.2 Equality and Inequality Constraints [25]:

The complex power injection at bus k is:

$$S_k = P_k + jQ_k = E_k I_k^* = V_k e^{j\delta_k} I_k^* \quad (2.14)$$

$$\text{where } I_k = \sum Y_{km} E_m \quad (2.15)$$

E_m : complex voltage at bus $m = V_m e^{j\delta}$

$$\text{So } I_k = \sum_{m=1}^N (G_{km} + jB_{km}) V_m e^{j\delta_m} \quad (2.16)$$

$$\text{And } I_k^* = \sum_{m=1}^N (G_{km} - jB_{km}) V_m e^{-j\delta_m} \quad (2.17)$$

$$S_k = V_k e^{j\delta_k} \sum_{m=1}^N (G_{km} - jB_{km}) (V_m e^{-j\delta_m}) \quad (2.18)$$

Where N is the number of buses

The expression for active and reactive power injections is obtained by identifying the real and imaginary parts of eq. (2.18), yielding:

$$P_k = V_k \sum V_m (G_{km} \cos \delta_{km} + B_{km} \sin \delta_{km}) \quad (2.19)$$

$$Q_k = V_k \sum V_m (G_{km} \sin \delta_{km} - B_{km} \cos \delta_{km}) \quad (2.20)$$

Complex power S_{km} flows from bus k to bus m is given by:

$$P_{km} = V_k^2 G_{km} - V_k V_m G_{km} \cos \delta_{km} - V_k V_m B_{km} \sin \delta_{km} \quad (2.21)$$

$$Q_{km} = -V_k^2 (B_{km} + B_{km}^{sh}) + V_k V_m B_{km} \cos \delta_{km} - V_k V_m G_{km} \sin \delta_{km} \quad (2.22)$$

The active and reactive power flows in opposite directions, P_{mk} and Q_{mk} can be obtained in the same way:

$$P_{mk} = V_m^2 G_{km} - V_k V_m G_{km} \cos \delta_{km} + V_k V_m B_{km} \sin \delta_{km} \quad (2.23)$$

$$Q_{mk} = -V_m^2 (B_{km} + B_{km}^{sh}) + V_k V_m B_{km} \cos \delta_{km} + V_k V_m G_{km} \sin \delta_{km} \quad (2.24)$$

The active and reactive power losses of the lines are easily obtained as:

$$P_{km} + P_{mk} = \text{active power losses.}$$

$$Q_{km} + Q_{mk} = \text{reactive power losses.}$$

where:

$k = 1, \dots, n$ (n is the number of buses in the network).

Or: active power loss is calculated using the following equation:

$$P_{loss} = \sum_{i=1}^N \sum_{\substack{j=1 \\ j \neq i}}^N \frac{r_{ij}}{|V_i||V_j|} [(P_i P_j + Q_i Q_j) \cos(\delta_i - \delta_j) + (Q_i P_j - P_i Q_j) \sin(\delta_i - \delta_j)] \quad (2.25)$$

also

$$P_{loss} = \sum_{i=1}^N \sum_{\substack{j=1 \\ j \neq i}}^N G_{ij} [|V_i|^2 + |V_j|^2 - 2|V_i||V_j| \cos(\delta_i - \delta_j)] \quad (2.26)$$

V_k, V_m : voltage magnitudes at the terminal buses of branch k-m.

δ_k, δ_m : voltage angles at the terminal buses of branch k-m.

P_{km} : active power flow from bus k to bus m.

Q_{km} : reactive power flow from bus k to bus m.

Q_k^{sh} = component of reactive power injection due to the shunt element (capacitor or reactor) at bus k ($Q_k^{sh} = b_k^{sh} V_m^2$)

A set of inequality constraints imposes operating limits on variables such as the reactive power injections at PV buses (generator buses) and voltage magnitudes at PQ buses (load buses):

$$V_k^{\min} \leq V_k \leq V_k^{\max}$$

$$Q_k^{\min} \leq Q_k \leq Q_k^{\max}$$

When no inequality constraints are violated, nothing is affected in the power flow equations, but if the limit is violated, the bus status is changed and it is enforced as an equality constraint at the limiting value [25].

2.7 Optimal Power Flow:

2.7.1 Introduction:

The OPF problem has been discussed since 1962 by Carpentier [31]. Because the OPF is a very large, non-linear mathematical programming problem, it has taken decades to develop efficient algorithms for its solution.

Many different mathematical techniques have been employed for its solution. The majority of the techniques in the references [32-37] use one of the following methods:

- 1- Lambda iteration method.
- 2- Gradient method.
- 3- Newton's method.
- 4- Linear programming method.
- 5- Interior point method.

The first generation of computer programs that aimed at a practical solution of the OPF problem did appear until the end of the sixties. Most of these used a gradient method i.e. calculation of the first total derivatives of the objective function related to the independent variables of the problem. These derivatives are known as the gradient vector [38].

2.7.2 Goals of the OPF:

Optimal power flow (OPF) has been widely used in planning and real-time operation of power systems for active and reactive power dispatch to minimize generation costs and system losses and improve voltage profiles.

The primary goal of OPF is to minimize the costs of meeting the load demand for a power system while maintaining the security of the system [39]. The cost associated with the power system can be attributed to the cost of generating power (megawatts) at each generator, keeping each device in the power system within its desired operation range. This will

include maximum and minimum outputs for generators, maximum MVA flows on transmission lines and transformers, as well as keeping system bus voltages within specified ranges.

OPF program is to determine the optimal Operation State of a power system by optimizing a particular objective while satisfying certain specified physical and operating constraints.

Because of its capability of integrating the economic and secure aspects of the concerned system into one mathematical formulation, OPF has been attracting many researchers. Nowadays, power system planners and operators often use OPF as a powerful assistant tool both in planning and operating stage [2]. To achieve these goals, OPF will perform all the steady-state control functions of power system.

These functions may include generator control and transmission system control. For generators, the OPF will control generator MW outputs as well as generator voltage. For the transmission system, the OPF may control the tap ratio or phase shift angle for variable transformers, switched shunt control, and all other flexible ac transmission system (FACTS) devices [31,40].

2.7.3 Nonlinear Programming Methods Applied to OPF Problems:

In a linear program, the constraints are linear in the decision variables, and so is the objective function. In a nonlinear program, the constraints and/or the objective function can also be nonlinear function of the decision variables [41].

In the last three decades, many nonlinear programming methods have been used in the solution of OPF problems, resulting in three classes of approaches:

- a) Extensions of conventional power flow method. In this type of approach, a sequence of optimization problem is alternated with solutions of conventional power flow.
- b) Direct solution of the optimality conditions for Newton's method. In this type of methodology, the approximation of the Lagrangian function by a quadratic form is used, the inequality constraints being handled through penalty functions.
- c) Interior point algorithm, has been extensively used in both linear and nonlinear programming. With respect to optimization algorithm, some alternative versions of the primal-dual interior point algorithm have been developed. One of the versions more frequently used in the OPF is the Predictor-corrector interior point method, proposed for linear programming. This algorithm aims at reducing the number of iterations to the convergence [42-49].

2.7.4 Analysis of System Optimization and Security Formulation of the Optimization Problems:

Optimization and security are often conflicting requirements and should be considered together. The optimization problem consists of minimizing a scalar objective function (normally a cost criterion) through the optimal control of vector $[u]$ of control parameters, i.e.

$$\text{Min } f ([x], [u]) \quad (2.27)$$

subject to:

- ◆ equality constraints of the power flow equations:

$$[g ([x], [u])] = 0 \quad (2.28)$$

- ◆ inequality constraints on the control parameters (parameter constraints):

$$V_{i, \min} \leq V_i \leq V_{i, \max}$$

- ◆ dependent variables and dependent functions (functional constraints):

$$X_{i, \min} \leq X_i \leq X_{i, \max}$$

$$h_i ([x], [u]) \leq 0 \quad (2.29)$$

Examples of functional constraints are the limits on voltage magnitudes at PQ nodes and the limits on reactive power at PV nodes.

The optimal dispatch of real and reactive powers can be assessed simultaneously using the following control parameters:

- ◆ Voltage magnitude at slack node.
- ◆ Voltage magnitude at controllable PV nodes.
- ◆ Taps at controllable transformers.
- ◆ Controllable power P_{Gi} .
- ◆ Phase shift at controllable phase-shifting transformers.
- ◆ Other control parameters.

We assume that only part (P_{Gi}) of the total net power (P_{Ni}) is controllable for the purpose of optimization.

The objective function can then be defined as the sum of instantaneous operating costs over all controllable power generation:

$$f ([x], [u]) = \sum_i c_i (P_{Gi}) \quad (2.30)$$

where c_i is the cost of producing P_{Gi} .

The minimization of system losses is achieved by minimizing the power injected at the slack node.

The minimization of the objective function $f ([x], [u])$ can be achieved with reference to the Lagrange function (L).

$$L = f ([x], [u]) - [\lambda]^T \cdot [g] \quad (2.31)$$

For minimization, the partial derivatives of L with respect to all the variables must be equal to zero, i.e. setting them equal to zero will then give the necessary conditions for a minimum:

$$\left[\frac{\partial L}{\partial \lambda} \right] \equiv [g] = 0 \quad (2.32)$$

$$\left[\frac{\partial L}{\partial x} \right] \equiv \left[\frac{\partial f}{\partial x} \right] - \left[\frac{\partial g}{\partial x} \right]^T \cdot [\lambda] = 0 \quad (2.33)$$

$$\left[\frac{\partial L}{\partial u} \right] \equiv \left[\frac{\partial f}{\partial u} \right] - \left[\frac{\partial g}{\partial u} \right]^T \cdot [\lambda] = 0 \quad (2.34)$$

When we have found $[\lambda]$ from equation (2.33), $[\nabla f]$ the gradient of the objective function (f) with respect to $[u]$ can now be calculated when the minimum has been found, the gradient components will be:

$$\frac{\partial f}{\partial u_i} \begin{cases} = 0 & \text{if } V_{\min} \leq V_i \leq V_{\max} \\ > 0 & \text{if } V_i = V_{\max} \\ < 0 & \text{if } V_i = V_{\min} \end{cases} \quad (2.35)$$

A simplified flow diagram of an optimal power flow program is shown in Figure (2.4) [49].

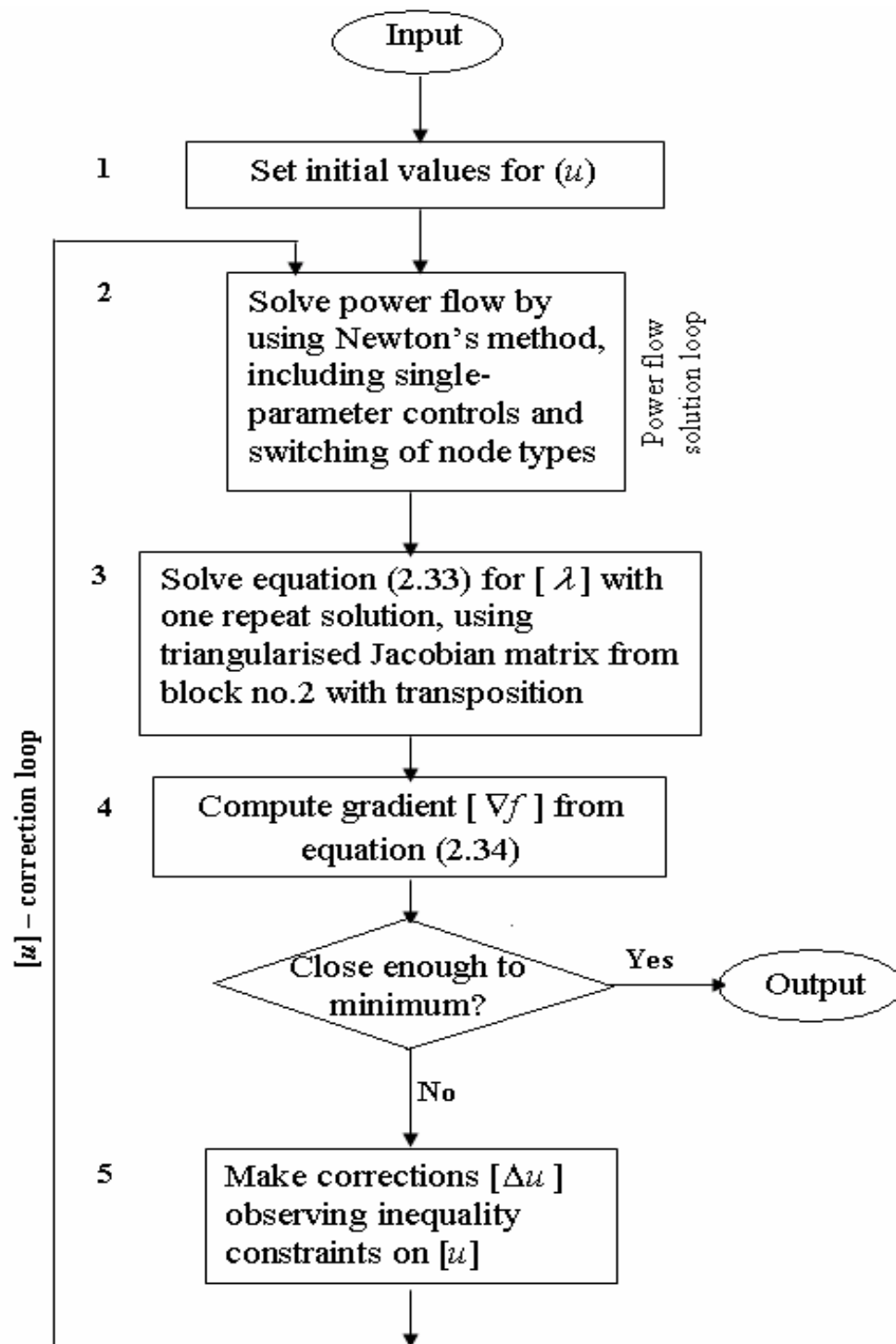


Figure (2.4): Flow Chart of the Optimal Power Flow [49]

2.7.5 Linear Programming Technique (LP):

The nonlinear power loss equation is:

$$P_{\text{loss}} = \sum_{i=1}^N \sum_{j=1}^N G_{ij} [|V_i|^2 + |V_j|^2 - 2|V_i||V_j|\cos(\delta_i - \delta_j)] \quad (2.36)$$

The linearized sensitivity model relating the dependent and control variables can be obtained by linearizing the power equations around the operating state. Despite the fact that any load flow techniques can be used, N-R load flow is most convenient to use to find the incremental losses as shown in Appendix (A). The change in power system losses, ΔP_L , is related to the control variables by the following equation [32]:

$$\Delta P_L = \begin{bmatrix} \frac{\partial P_L}{\partial V_1} & \dots & \frac{\partial P_L}{\partial V_m} & \dots & \frac{\partial P_L}{\partial Q_{m+1}} & \dots & \frac{\partial P_L}{\partial Q_{m+w}} \end{bmatrix} \begin{bmatrix} \Delta V_1 \\ \vdots \\ \Delta V_m \\ \Delta Q_{m+1} \\ \Delta Q_{m+w} \end{bmatrix} \quad (2.37)$$

2.8 Transient Stability:

2.8.1 Introduction:

Power system stability may be defined as the property of the system, which enables the synchronous machines of the system to respond to a disturbance from a normal operating condition so as to return to a condition where their operation is again normal.

Stability studies are usually classified into three types depending upon the nature and order of disturbance magnitude. These are:

- 1- Steady-state stability.
- 2- Transient stability.
- 3- Dynamic stability.

Our major concern here is transient stability (TS) study. TS studies aim at determining if the system will remain in synchronism following major disturbances such as:

- 1- Transmission system faults.
- 2- Sudden or sustained load changes.
- 3- Loss of generating units.
- 4- Line switching.

Transient stability problems can be subdivided into first swing and multi-swing stability problems. In first swing stability, usually the time period under study is the first second following a system fault.

If the machines of the system are found to remain in synchronism within the first second, the system is said to be stable. Multi-swing stability problems extend over a longer study period.

In all stability studies, the objective is to determine whether or not the rotors of the machines being perturbed return to constant speed operation. We can find transient stability definitions in many references such as [50-57].

A transient stability analysis is performed by combining a solution of the algebraic equations describing the network with a numerical solution of the differential equations describing the operation of synchronous machines. The solution of the network equations retains the identity of the system and thereby provides access to system voltages and currents during the transient period. The modified Euler and Runge-Kutta methods have been applied to the solution of the differential equations in transient stability studies [37, 58].

2.8.2 Power Transfer between Two Equivalent Sources:

For a simple lossless transmission line connecting two equivalent generators as shown in Figure (2.5), it is well known that the active power, P , transferred between two generators can be expressed as:

$$p = \frac{E_s * E_R}{X} * \sin \delta \quad (2.38)$$

where E_s is the sending-end source voltage magnitude, E_R is the receiving-end source voltage magnitude, δ is the angle difference between two sources and X is the total reactance of the transmission line and the two sources (X_s, X_R) [50, 59].

$$X = X_s + X_L + X_R \quad (2.39)$$

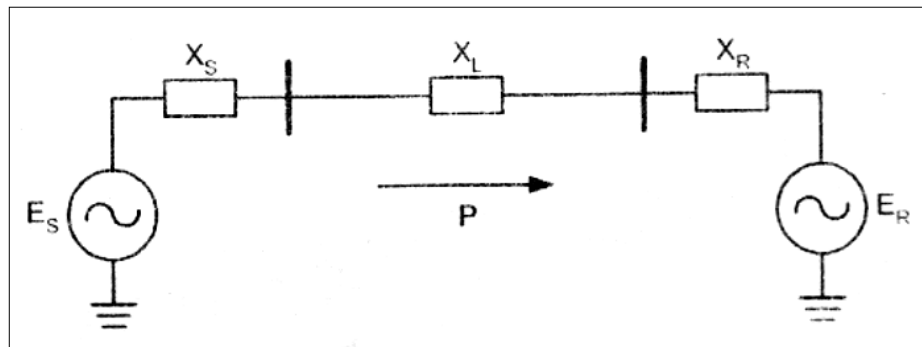


Figure (2.5): A Two-Source System [50]

2.8.3 The Power Angle Curve:

With fixed E_s , E_R and X values, the relationship between P and δ can be described in a power angle curve as shown in Figure (2.6). Starting from $\delta = 0$, the power transferred increases as δ increases. The power transferred between two sources reaches the maximum value P_{MAX} when δ is 90 degrees. After that point, further increase in δ will result in a decrease of power transfer. During normal operations of a generation system without losses, the mechanical power P_0 from a prime mover is converted into the same amount of electrical power and transferred over the transmission line. The angle difference under this balanced normal operation is δ_0 [50, 58].

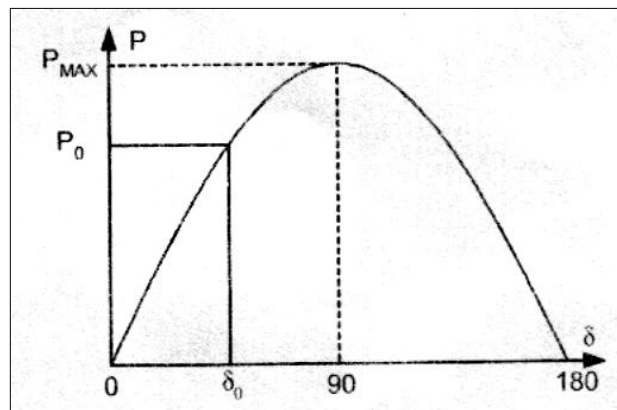


Figure (2.6): The Power Angle Curve [50]

2.8.4 Transiently Stable and Unstable Systems:

During normal operations of a generator, the output of electric power from the generator produces an electric torque that balances the mechanical torque applied to the generator rotor shaft. The generator rotor therefore runs at a constant speed with this balance of electric and mechanical torques. When a fault reduces the amount of power transmission, the electric torque that counters the mechanical torque is also decreased. If the mechanical power is not reduced during the period of the fault, the generator rotor will accelerate with a net surplus of torque input.

Assume that the two-source power system in Figure (2.5) initially operates at a balance point of δ_0 , transferring electric power P_0 . After a fault, the power output is reduced to P_F , the generator rotor therefore starts to accelerate, and δ starts to increase. At the time that the fault is cleared when the angle difference reaches δ_C , there is decelerating torque acting on the rotor because the electric power output P_C at the angle δ_C is larger than the mechanical power input P_0 . However, because of the inertia of the rotor system, the angle does not start to go back to δ_0 immediately. Rather, the angle continues to increase to δ_F when the energy lost during

deceleration in area 2 is equal to the energy gained during acceleration in area 1. This is the so-called equal-area criterion [50, 60].

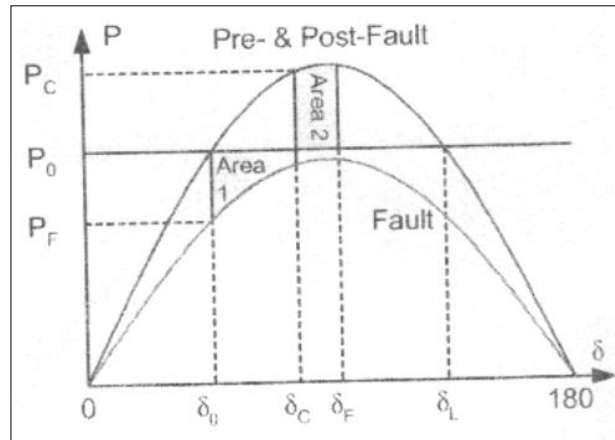


Figure (2.7): A Transiently Stable System [50]

If δ_F is smaller than δ_L , then the system is transiently stable as shown in Figure (2.7). With sufficient damping, the angle difference of the two sources eventually goes back to the original balance point δ_0 . However, if area 2 is smaller than area 1 at the time the angle reaches δ_L , then further increase in angle δ will result in an electric power output that is smaller than the mechanical power input. Therefore, the rotor will accelerate again and δ will increase beyond recovery. This is a transiently unstable scenario, as shown in Figure (2.8). When an unstable condition exists in the power system, one equivalent generator rotates at a speed that is different from the other equivalent generator of the system. We refer to such an event as a loss of synchronism or an out-of-step condition of the power system.

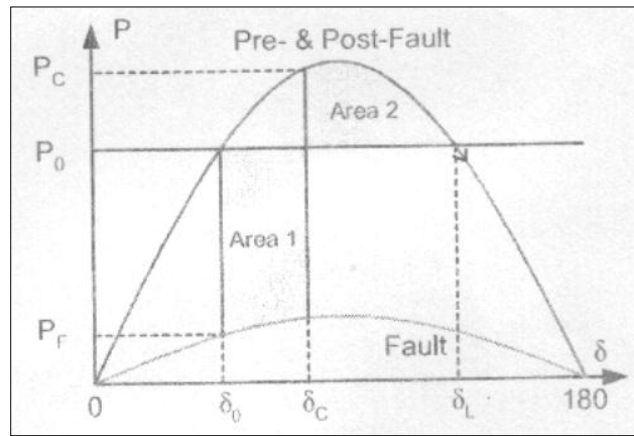


Figure (2.8): A Transiently Unstable System [50]

2.8.5 The Swing Equation:

Electromechanical oscillations are an important phenomenon that must be considered in the analysis of most power systems, particularly those containing long transmission lines. In normal steady state operation all synchronous machines in the system rotate with the same electrical angular velocity, but as a consequence of disturbances one or more generators could be accelerated or decelerated and there is risk that they can fall out of step i.e. lose synchronism. This could have a large impact on system stability and generators losing synchronism must be disconnected otherwise they could be severely damaged. The differential equation describing the rotor dynamics is[25]:

$$J \frac{d^2 \theta_m}{dt^2} = T_m - T_e \quad (2.40)$$

where:

J = the total moment of inertia of the synchronous machine (kg m^2).

θ_m = the mechanical angle of the rotor (rad.).

T_m = mechanical torque from turbine or load (N.m). Positive T_m corresponds to mechanical power fed into the machine, i.e. normal generator operating in steady state.

T_e = electrical torque on the rotor (N.m). Positive T_e is the normal generator operation. Sometimes equation (2.40) is expressed in terms of frequency (f) and inertia constant (H) then the swing equation becomes:

$$\frac{H}{180f} \frac{d^2\theta}{dt^2} = P_m - P_e \quad (2.41)$$

The swing equation is of fundamental importance in the study of power oscillations in power systems. The derivation of this equation is given in Appendix (B) [25].

2.8.6 Step-by-Step Solution of the Swing Curve:

For large systems we depend on the digital computer which determines δ versus t for all the machines in the system. The angle δ is calculated as a function of time over a period long enough to determine whether δ will increase without limit or reach a maximum and start to decrease although the latter result usually indicates stability. On an actual system where a number of variables are taken into account it may be necessary to plot δ versus t over a long enough interval to be sure that δ will not increase again without returning in a low value.

By determining swing curves for various clearing times the length of time permitted before clearing a fault can be determined. Standard interrupting times for circuit breakers and their associated relays are commonly (8, 5, 3 or 2) cycles after a fault occurs, and thus breaker speeds may be specified. Calculations should be made for a fault in the position, which will allow the least transfer of power from the machine, and for the most severe type of fault for which protection against loss of stability is justified.

A number of different methods are available for the numerical evaluation of second-order differential equations in step-by-step computations for small increments of the independent variable. The more

elaborate methods are practical only when the computations are performed on a digital computer by making the following assumptions:

- 1- The accelerating power P_a computed at the beginning of an interval is constant from the middle of the preceding interval considered.
- 2- The angular velocity is constant throughout any interval at the value computed for the middle of the interval. Of course, neither of the assumptions is true, since δ is changing continuously and both P_a and ω are functions of δ . As the time interval is decreased, the computed swing curve approaches the true curve. Figure (2.9) will help in visualizing the assumptions. The accelerating power is computed for the points enclosed in circles at the ends of the $n-2$, $n-1$, and n intervals, which are the beginning of the $n-1$, n and $n+1$ interval. The step curve of P_a in Figure (2.9) results from the assumption that P_a is constant between mid points of the intervals.

Similarly, ω_r , the excess of angular velocity ω over the synchronous angular velocity ω_s , is shown as a step curve that is constant throughout the interval at the value computed for the midpoint. Between the ordinates $n-\frac{3}{2}$ and $n-\frac{1}{2}$ there is a change of speed caused by the constant accelerating power. The change in speed is the product of the acceleration and the time interval, and so

$$\omega_{r,n-1/2} - \omega_{r,n-3/2} = \frac{d^2\delta}{dt^2} \Delta t = \frac{180f}{H} P_{a,n-1} \Delta t \quad (2.42)$$

The change in δ over any interval is the product of ω_r for the interval and the time of the interval. Thus, the change in δ during the $n-1$ interval is:

$$\Delta \delta_{n-1} = \delta_{n-1} - \delta_{n-2} = \Delta t \omega_{r,n-3/2} \quad (2.43)$$

and during the n^{th} interval.

$$\Delta \delta_n = \delta_n - \delta_{n-1} = \Delta t \omega_{r,n-1/2} \quad (2.44)$$

Subtracting Eq. (2.43) from Eq. (2.44) and substituting Eq. (2.42) in the resulting equation to eliminate all values of ω , yields:

$$\Delta \delta_n = \Delta \delta_{n-1} + k P_{a,n-1} \quad (2.45)$$

$$\text{where } k = \frac{180f}{H} (\Delta t)^2 \quad (2.46)$$

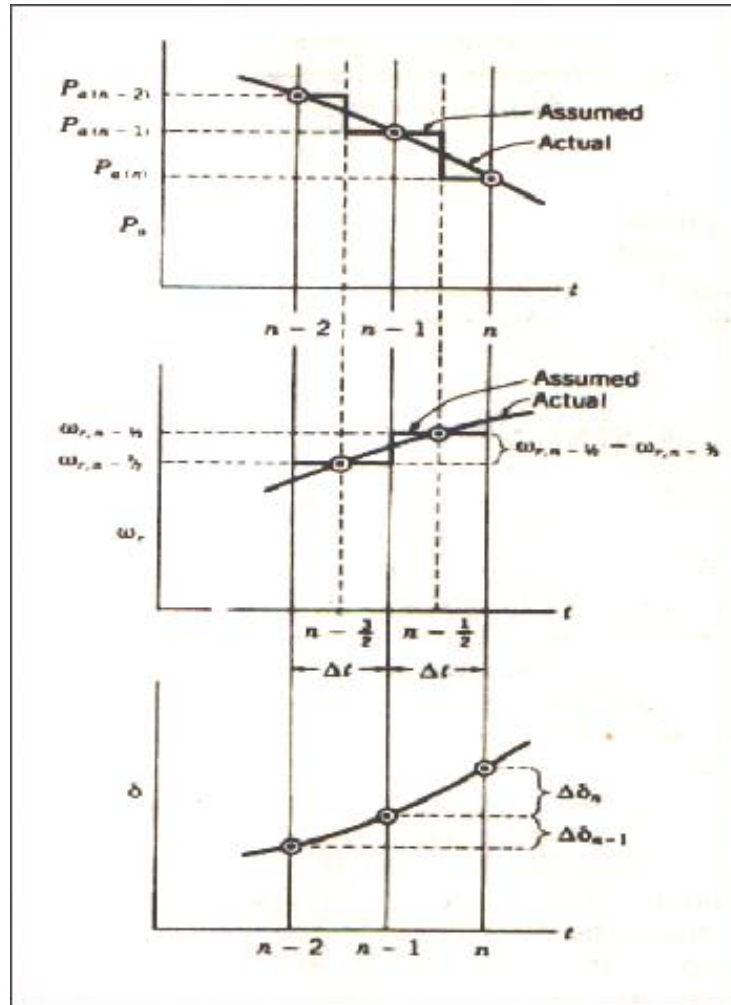


Figure (2.9): Actual and Assumed Values of P_e , ω_r and δ as a Function of Time [37]

Equation (2.45) is the important one for the step-by-step solution of the swing equation with the necessary assumptions enumerated, for it shows how to calculate the change in δ during an interval if the change in δ for the previous interval and the accelerating power for interval are known.

Equation (2.45) shows that, subject to stated assumptions, the change in torque angle during a given interval is equal to change in torque angle during the preceding interval plus the accelerating power at the beginning of the interval times k .

The accelerating power is calculated at the beginning of each new interval. The solution progresses through enough intervals to obtain points for plotting the swing curve. Greater accuracy is obtained when the duration of the intervals is small. An interval of 0.05s is usually satisfactory.

The occurrence of a fault causes a discontinuity in the accelerating power P_a which is zero before the fault and a definite amount immediately following the fault. The discontinuity occurs at the beginning of the interval, when $t=0$. Reference to Figure (2.9) shows that our method of calculation assumes that the accelerating power computed at the beginning of an interval is constant from the middle of the preceding interval to the middle of the interval considered. When the fault occurs, we have two values of P_a at the beginning of an interval, and we must take the average of these two values at our constant accelerating power [37].

Chapter Three

*Optimal Power Flow
with Transient Stability (OPFWTS)*

Chapter Three

Optimal Power Flow

With Transient Stability (OPFWTS)

3.1 Introduction:

A number of researches have tried to incorporate the transient stability constraints directly into OPF, mainly by approximating the differential equations to difference (or algebraic) equations. The major advantage is that these approaches handle the operational problems systematically in contrast to the conventional heuristics. The methodologies adopted for OPF such as successive linear programming or the quasi-Newton method can be used to solve the OTS by adding extra constraints.

3.2 Optimal Design Using Mathematical Model:

To describe optimization concepts and methods we need a general mathematical statement for the optimum design problem. All design problems can easily be transcribed into the following standard form [61, 62]:

$$\min f(\underline{x})$$

subject to:

$$g_i(\underline{x}) \leq 0 \quad i = 1, \dots, n_g$$

$$h_k(\underline{x}) = 0 \quad k = 1, \dots, m_h$$

Where $\underline{x} = \{x_1 \dots x_n\} \in \mathfrak{R}$ (design variables).

$f(\underline{x})$ the objective function.

$g_i(\underline{x})$ inequality constraints.

$h_k(\underline{x})$ equality constraints.

3.3 Optimization Solution Approaches [62]:

The goal of a good optimization model is to obtain useful numerical values. Once the problem has been formulated, four ways exist to obtain a solution and these are summarized as follows:

3.3.1 Graphical Method:

The objective function is plotted in terms of the decision variables. This method is limited to two-dimensional problems (problems with no more than two design variables). Plotting the constraints is the first step, the next step includes plotting the objective function $f(x)$. We give different values to the constant C and proceed to plot the objective function several times. Once the objective function is plotted we then find the minimum C such that all the constraints are satisfied.

3.3.2 Analytical Technique:

The analytical technique, to be discussed here, is the classical method of Lagrange multipliers. Consider that each constraint has a scalar multiplier associated with it, called the Lagrange multiplier.

Consider the following optimization problem:

$$\min f(\underline{x})$$

subject to:

$$h(\underline{x}) = 0$$

$$g(\underline{x}) \leq 0$$

where $\underline{x} = \{x_1, x_2\}$, the design variables. Let the optimum point be \underline{x}^* .

The necessary conditions for optimality can be written in vector form as: $\nabla f|_{x^*} + \mu \nabla h|_{x^*} + \lambda \nabla g|_{x^*} = 0$ (3.1)

where (μ, λ) are LaGrange multipliers which measure the change in the objective function with respect to the constraint.

In general, we use what is known as the Lagrangian, or the Lagrange function, in writing the necessary conditions. The Lagrangian is denoted as (L) and defined using the objective and constraint functions as follows:

$$L(\underline{x}, \mu, \lambda) = f(\underline{x}) + \mu h(\underline{x}) + \lambda g(\underline{x}) \quad (3.2)$$

The Lagrangian function is treated as a function dependent on the design variables and the Lagrange multipliers. To find candidate optimum points of design variables and Lagrange multipliers, we find where the Lagrangian is stationary, i.e.

$$\nabla L(\underline{x}^*, \mu, \lambda) = \nabla f \Big|_{\underline{x}=\underline{x}^*} + \mu \nabla h \Big|_{\underline{x}=\underline{x}^*} + \lambda \nabla g_i \Big|_{\underline{x}=\underline{x}^*} = 0 \quad (3.3)$$

By rearranging the above equation we can get a geometrical interpretation. Thus:

$$\nabla f \Big|_{\underline{x}=\underline{x}^*} = -\mu \nabla h \Big|_{\underline{x}=\underline{x}^*} - \lambda \nabla g_i \Big|_{\underline{x}=\underline{x}^*} \quad (3.4)$$

3.3.2.1 The Kuhn-Tucker Conditions:

The Kuhn-Tucker (K-T) conditions are a set of necessary conditions for constraint optimality. The K-T conditions define a stationary point of the Lagrangian: $\nabla L = \underline{0}$

If the vector \underline{x}^* is a good candidate for the optimum design, the following conditions must be satisfied:

1. The point \underline{x}^* must be feasible; gradient of the Lagrangian with respect to the design variables must be zero. By feasible we understand that all constraints are satisfied and the function is defined at the design point.

$$h_k \Big|_{\underline{x}=\underline{x}^*} = 0 \quad k = 1, \dots, m_h$$

$$g_i \Big|_{\underline{x}=\underline{x}^*} + s_i^2 = 0 \quad i = 1, \dots, n_g$$

$$f \Big|_{\underline{x}=\underline{x}^*} = \text{exists}$$

where s is a slack variable which makes an inequality constraint an equality one by adding this variable.

2. The Lagrange multipliers for equality constraints (μ_k) are free in sign, i.e. they can be positive, negative or zero. The Lagrange multipliers for inequality constraints (λ_i) must be nonnegative.

$$\mu_k \rightarrow \text{of any sign} \quad \lambda_i \geq 0$$

If the constraint is inactive at the optimum, its associated Lagrange multiplier is zero. If it is active ($g_i = 0$), then the associated multiplier must be non negative.

3. The Lagrangian must be stationary with respect to the design variables:

$$\left. \frac{\partial f}{\partial \underline{x}} \right|_{\underline{x}=\underline{x}^*} + \sum_{k=1}^{m_h} \mu_k \left. \frac{\partial h_k}{\partial \underline{x}} \right|_{\underline{x}=\underline{x}^*} + \sum_{i=1}^{n_g} \lambda_i \left. \frac{\partial g_i}{\partial \underline{x}} \right|_{\underline{x}=\underline{x}^*} = \underline{0} \quad (3.5)$$

3.3.2.2 Sufficient and Necessary Conditions:

The second-order necessary and sufficient conditions can distinguish between the minimum, maximum and inflection points. The second-order test consists in evaluating the Hessian of the Lagrangian with respect to the design variables, at the design point $L^* = (\underline{x}^*, \underline{\mu}^*, \underline{\lambda}^*)$, ensuring it is positive definite. In other words:

$$\underline{H}(L^*) = \begin{bmatrix} \frac{\partial^2 L}{\partial x_1^2} & \frac{\partial^2 L}{\partial x_1 \partial x_2} & \dots & \frac{\partial^2 L}{\partial x_1 \partial x_n} \\ \frac{\partial^2 L}{\partial x_2 \partial x_1} & \frac{\partial^2 L}{\partial x_2^2} & \dots & \frac{\partial^2 L}{\partial x_2 \partial x_n} \\ \vdots & \vdots & \ddots & \vdots \\ \frac{\partial^2 L}{\partial x_n \partial x_1} & \frac{\partial^2 L}{\partial x_n \partial x_2} & \dots & \frac{\partial^2 L}{\partial x_n^2} \end{bmatrix}_{(\underline{x}=\underline{x}^*, \underline{\mu}=\underline{\mu}^*, \underline{\lambda}=\underline{\lambda}^*)} \quad (3.6)$$

Only if all the Kuhn-Tucker conditions are satisfied and the Hessian of the Lagrangian is positively definite, then the design point is an isolated minimum point.

3.3.3 Numerical Technique:

Numerical techniques are usually used in nonlinear optimization problems. Numerical methods for nonlinear optimization problems are needed because the analytical methods for solving some problems are either too cumbersome or not applicable at all.

3.3.4 Experimental Technique:

This technique does not require a mathematical model of the physical system because the actual process is used. An experiment is performed on the process and the result is compared to that of the preceding experiment, in order to decide where to locate the next one. This procedure is continued until the optimum is achieved.

3.4 Optimal Control of Reactive Power Flow for Real Power Loss Minimization:

It is possible to minimize the system losses by reactive power redistributions in the system to improve the voltage profiles and to minimize the system losses. Reactive power distributions in the system can be controlled by the following controllable variables:

- Transformer taps.
- Generator voltages.
- Switchable shunt capacitors and inductors (switchable VAR sources).

These control variables (state variables) have their upper and lower permissible limits. Any changes to these state variables have the effect of changing the system voltage profiles and the reactive power output of generators and the system losses. Thus the problem is to find the set of adjustments to the state variables required to minimize the system losses [63-65].

3.5 Reactive Power Allocation:

The purpose of a reactive power allocation study is to determine the amount of reactive power addition required at selected buses to get a certain voltage profile and to minimize the number of locations. Voltage control and real power loss coupled with engineering judgment are indices which can give better location for reactive power devices. For small changes in reactive power, there is a linear relationship between reactive power and total active power losses [8, 66].

3.6 Optimal Placement of Generation Units:

In most large electrical power systems, most of the electrical power is generated from large generating stations. However with increased electricity costs, the corporation of smaller scale, dispersed or distributed generation in electrical power systems is becoming more popular. Two optimization formulations are examined, one to determine generator locations based on minimizing losses and the other based on enhancing system stability.

Proper placement of generation units will reduce losses, while improper placement may actually increase system losses. Proper placement will also free available capacity for transmission of power and reduce equipment stress.

Electric power systems designed with generating units that are widely scattered and interconnected by long transmission lines may suffer significant losses. The losses depend on the line resistance and currents and are usually referred to as thermal losses. While the line resistances are fixed, the currents are a complex function of the system topology and the location of generation and load. Using the load data collected on 2/1/2003 which can be obtained from the Iraqi Control Center (Appendix C), algorithm was applied to determine the best placement of new units in

order to maximize power available and minimize losses on the system for a given load [8].

3.7 Mathematical Analysis for Reactive Power Allocation and Optimal Placement of Generation Units:

The analysis objective is to find the partial derivatives (sensitivity) of active power loss with respect to active and reactive power injected at all buses except slack bus.

$$[SEN] = [\partial P_L / \partial P \quad \partial P_L / \partial Q] \quad (3.7)$$

The results of sensitivity vector $[SEN]$ are used as an indicator to the efficiency of the system to reduce losses in case of installing generation units or shunt capacitors at these buses.

The following matrix $[D]$ is the partial derivative of real losses with respect to voltage magnitude at load buses and voltage angles at all buses except slack bus. Figure (3.1) is a flow chart illustrating the best buses to install optimal generation units and shunt capacitors.

$$[D] = \frac{\partial f}{\partial x} = \begin{bmatrix} \partial P_{loss} / \partial \delta_2 \\ \partial P_{loss} / \partial \delta_3 \\ \partial P_{loss} / \partial \delta_N \\ \partial P_{loss} / \partial V_2 \\ \partial P_{loss} / \partial V_3 \\ \partial P_{loss} / \partial V_{NL+1} \end{bmatrix} \quad (3.8)$$

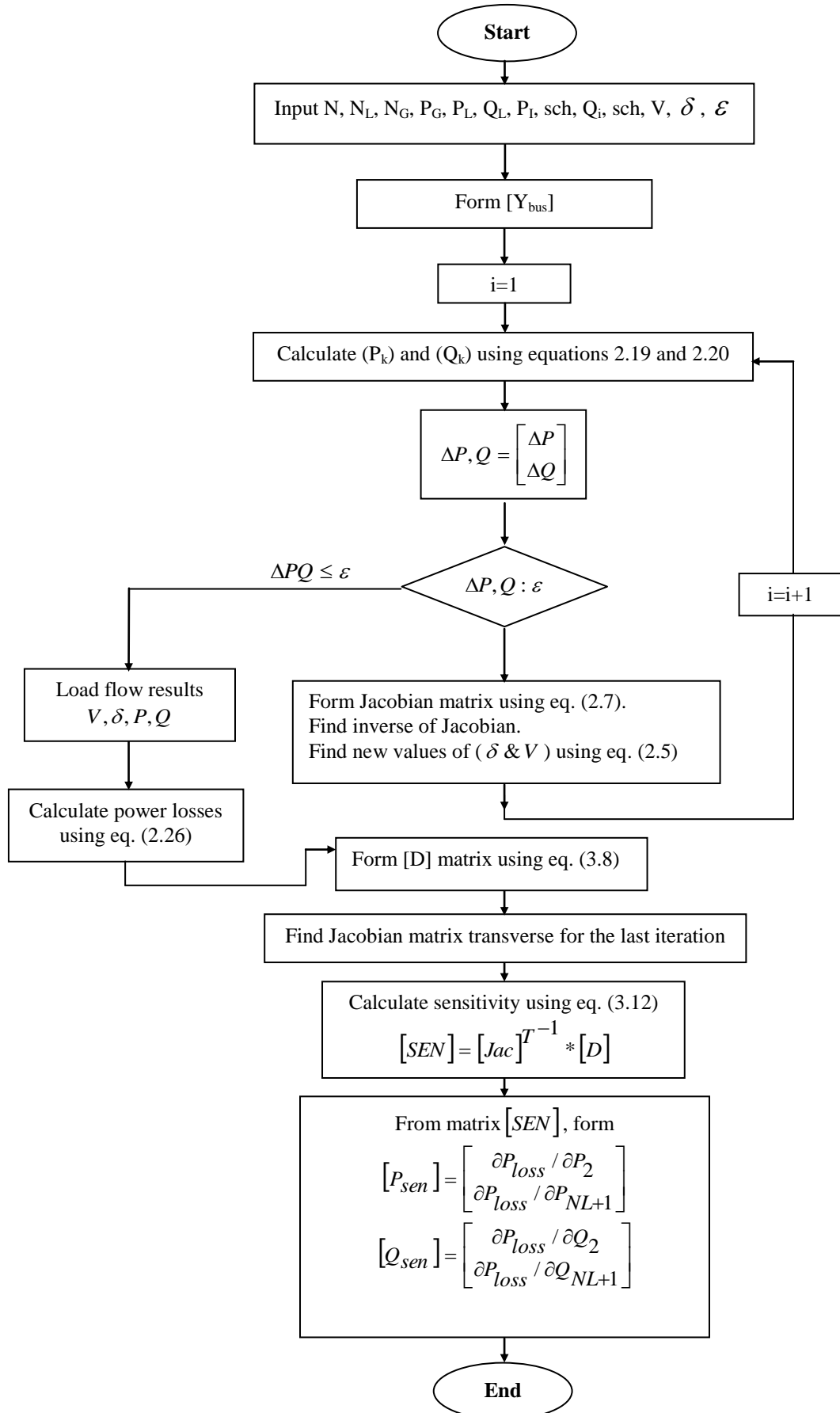


Figure (3.1): Flow Chart Illustrating the Best Buses to Install Optimal Generating Units and Reactive Power

The components of $[D]$ are calculated as follows:

$$\frac{\partial P_{loss}}{\partial \delta_i} = 2 \sum_{\substack{j=1 \\ j \neq i}}^N G_{ij} [V_i |V_j| \sin(\delta_i - \delta_j)] \quad (3.9)$$

$$\frac{\partial P_{loss}}{\partial V_i} = 2 \sum_{\substack{j=1 \\ j \neq i}}^N G_{ij} [V_i | - |V_j| \cos(\delta_i - \delta_j)] \quad (3.10)$$

The mathematical analysis needs also Jacobian matrix $[Jac]$ which is used before in power flow problem, then:

$$[Jac]^T [SEN] = [D] \quad (3.11)$$

$$\text{then } [SEN] = [Jac]^T^{-1} [D] \quad (3.12)$$

$$\begin{bmatrix} P_{sen} \\ Q_{sen} \end{bmatrix} = \begin{bmatrix} \frac{\partial P_L}{\partial P} \\ \frac{\partial P_L}{\partial Q} \end{bmatrix} = [Jac]^T^{-1} \begin{bmatrix} \frac{\partial P_L}{\partial \delta} \\ \frac{\partial P_L}{\partial V} \end{bmatrix} \quad (3.13)$$

where $[J]$ is the Jacobian matrix of Newton-Raphson load flow.

$$\text{Then } P_{sen} = \begin{bmatrix} \frac{\partial P_{loss}}{\partial P_2} \\ \frac{\partial P_{loss}}{\partial P_{NL+1}} \end{bmatrix} \quad (3.14)$$

$$\text{And } Q_{sen} = \begin{bmatrix} \frac{\partial P_{loss}}{\partial Q_2} \\ \frac{\partial P_{loss}}{\partial Q_{NL+1}} \end{bmatrix} \quad (3.15)$$

The following matrix represents derivative of active power losses w.r.t generation voltages:

$$\frac{\partial f}{\partial u} = \begin{bmatrix} \frac{\partial P_{loss}}{\partial V_1} \\ \frac{\partial P_{loss}}{\partial V_2} \\ \vdots \\ \frac{\partial P_{loss}}{\partial V_{NG}} \end{bmatrix} \quad (3.16)$$

$$\text{where } \frac{\partial P_{loss}}{\partial V_i} = 2 \sum_{\substack{j=1 \\ j \neq i}}^{NG} G_{ij} [V_i | - |V_j| \cos(\delta_i - \delta_j)]$$

$$\frac{\partial g}{\partial u} = \begin{bmatrix} \frac{\partial P_2}{\partial V_1} & \frac{\partial P_2}{\partial V_2} & \dots & \frac{\partial P_2}{\partial V_N} \\ \vdots & & & \\ \frac{\partial P_N}{\partial V_1} & \frac{\partial P_N}{\partial V_2} & \dots & \frac{\partial P_N}{\partial V_N} \\ \frac{\partial Q_2}{\partial V_1} & \frac{\partial Q_2}{\partial V_2} & \dots & \frac{\partial Q_2}{\partial V_N} \\ \vdots & & & \\ \frac{\partial Q_{N_{L+1}}}{\partial V_1} & \frac{\partial Q_{N_{L+1}}}{\partial V_2} & & \frac{\partial Q_{N_{L+1}}}{\partial V_N} \end{bmatrix} \quad (3.17)$$

where $\left[\frac{\partial g}{\partial u} \right]$ represents partial derivative of injected power to bus voltages.

$$\text{Gradient } [\nabla f] = \left[\frac{\partial f}{\partial u} \right] + \left[\frac{\partial g}{\partial u} \right]^T * [SEN] \quad (3.18)$$

where $[\nabla f]$ represent the sensitivity of losses w.r.t control variables.

$$\text{Hessian } [H] = \frac{\partial^2 P_{loss}}{\partial V_i \partial V_j} = \begin{bmatrix} \frac{\partial^2 P_{loss}}{\partial V_1^2} & \dots & \frac{\partial P_{loss}}{\partial V_1 \partial V_{NG}} \\ \frac{\partial^2 P_{loss}}{\partial V_2 \partial V_1} & \dots & \frac{\partial P_{loss}}{\partial V_2 \partial V_{NG}} \\ \vdots & & \\ \frac{\partial^2 P_{loss}}{\partial V_{NG} \partial V_1} & \dots & \frac{\partial P_{loss}}{\partial V_N^2 G} \end{bmatrix} \quad (3.19)$$

where $[H]$ represents the second partial derivative for P_{loss} w.r.t control variables.

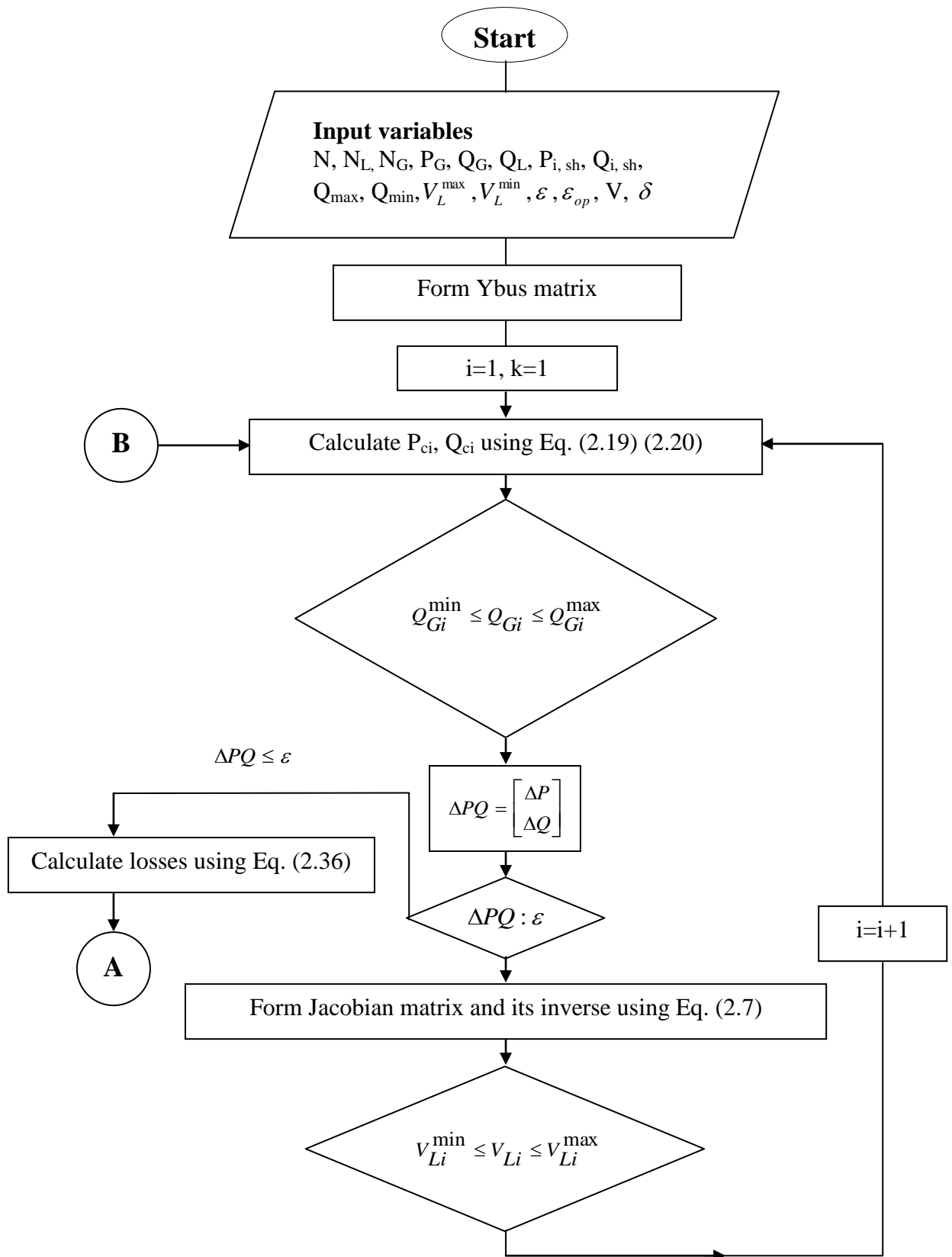
$$[\Delta u] = \begin{bmatrix} \Delta V_1 \\ \Delta V_2 \\ \vdots \\ \Delta V_{NG} \end{bmatrix} = -[H]^{-1} * [\nabla f] \quad (3.20)$$

As shown in Figure (3.2), if $[\Delta u] \leq \epsilon$ optimum, where $\epsilon_{opt.} = 0.001$, then P_{loss} represents minimum losses in the system. Otherwise control variables have to be developed as follows:

$$\begin{bmatrix} V_1 \\ V_2 \\ \vdots \\ V_{NG} \end{bmatrix}^{K+1} = \begin{bmatrix} V_1 \\ V_2 \\ \vdots \\ V_{NG} \end{bmatrix}^K + \begin{bmatrix} \Delta V_1 \\ \Delta V_2 \\ \vdots \\ \Delta V_{NG} \end{bmatrix}^K \quad (3.21)$$

where P_{sen} = partial derivative of real losses with respect to real power injected at load buses.

Q_{sen} = partial derivative of real losses with respect to reactive power injected at load buses. Appendix (A) shows loss sensitivities in details.



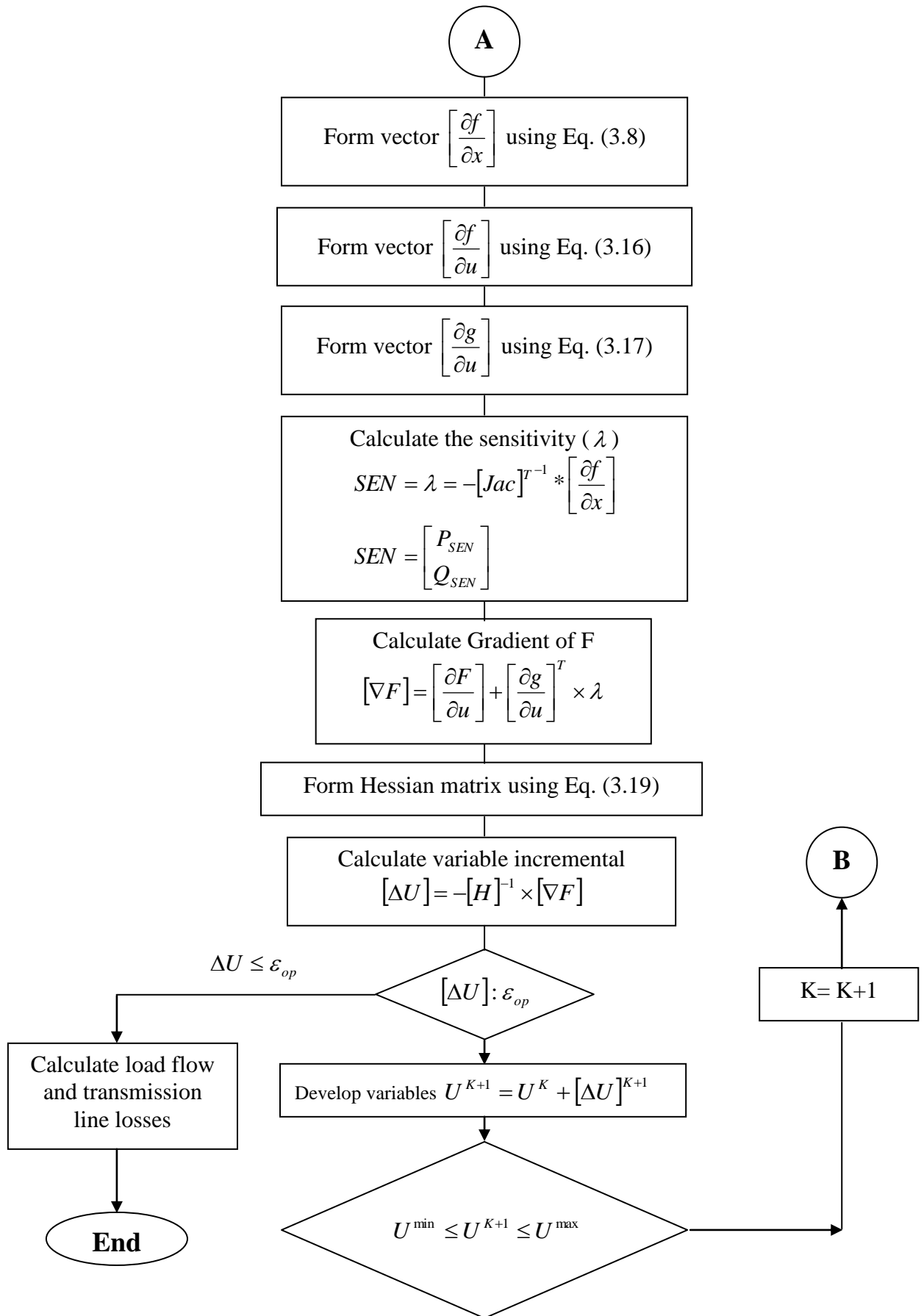


Figure (3.2): Using Non-Linear Optimization Programming (Lagrange Method) to Reduce Losses

3.8 Optimum Power Flow Operation with Transient Stability:

A practical electric power system is a nonlinear network, which is generally governed by a large number of differential and algebraic equations (*DAE*). For instance, the ordinary differential equations are defined by the dynamics of the generators and the loads as well as their controllers, conversely algebraic equalities are described by the current balance equations of the transmission network corresponding to the Kirchoff's law at each bus or node and internal static behaviors of passive devices (e.g. shunt capacitors and static loads). An operation point of a power system not only is a stable equilibrium of *DAEs*, but also must satisfy all of static equality and inequality constraints at the equilibrium, such as upper and lower bounds of generators and voltages of all buses. Besides, as a dynamic security requirement, when any of a specified set of disturbances (e.g. outages of generators or transmission lines) occurs, a feasible operation point should withstand the fault and ensure that the power system moves to a new stable equilibrium after the clearance of the fault without violating equality and inequality constraints even during transient period of the dynamics. These conditions for all of the specified credible contingencies are called transient stability constraints.

Conventionally, a trial solution to the operation point in power systems is first solved by (*OPF*) problem that is defined as a static nonlinear optimization problem without the transient stability constraints. In other words, (*OPF*) is to minimize operating costs of a power system, transmission losses or other appropriate objective functions at the specified time instance subject to the static equalities and inequalities, by determining an equilibrium corresponding to all of operational variables, such as power outputs of generators, transformer tap positions, phase shifter angle positions, shunt capacitors, reactors, voltage values, etc. Then the obtained trial solution is an optimal operation point.

The trial solution often has to be modified so as eventually to meet the transient stability. However, converting differential equations into algebraic equations by discretizing scheme may not only suffer from the inaccuracy of computation because of the approximation but also cause convergence difficulties due to introduction of a large number of variables and equations at each time step to the original (OPF) [6].

3.9 Stability-Constrained OPF Formulation:

A standard OPF problem can be formulated as follows [2]:

$$\text{Min } f(P_g) \quad (3.22)$$

S.T

$$P_g - P_L - P(V, \theta) = 0 \text{ active power flow equations} \quad (3.23)$$

$$Q_g - Q_L - Q(V, \theta) = 0 \text{ reactive power flow equations} \quad (3.24)$$

$$S(V, \theta) - S^M \leq 0 \quad (3.25)$$

$$V^m \leq V \leq V^M \quad (3.26)$$

$$P_g^m \leq P_g \leq P_g^M \quad (3.27)$$

$$Q_g^m \leq Q_g \leq Q_g^M \quad (3.28)$$

where:

f : objective function, can be defined as operation cost, transmission loss, as well as special objectives.

P_g : generator active power.

Q_g : generator reactive power.

P_L : real power demand.

Q_L : reactive power demand.

$P(V, \theta)$: real network injections.

$Q(V, \theta)$: reactive network injections.

$S(V, \theta)$: apparent power across the transmission lines.

S^M : thermal limits for the transmission lines.

V : bus voltage magnitude.

θ : bus voltage angle.

Also we have the following ‘swing’ equation [68]:

$$\frac{d\delta_i}{dt} = \omega_i \quad (3.29)$$

$$\frac{d\delta_i}{dt} = \frac{\pi f_0}{2H_i} \left[P_{gi} - \frac{1}{\bar{x}d_i} (E_i V_{xi} \sin \delta_i - E_i V_{yi} \cos \delta_i) \right] \quad (3.30)$$

$$= D_i (P_{gi}, E_i, V_{xi}, V_{yi}, \delta_i, \omega_i)$$

$$\begin{bmatrix} G & -B \\ B & G \end{bmatrix} \begin{bmatrix} V_x \\ V_y \end{bmatrix} = \begin{bmatrix} I_x \\ I_y \end{bmatrix} \quad (3.31)$$

where:

G = real part of the bus admittance matrix.

B = reactive part of the bus admittance matrix.

V_x = real part of bus voltage.

V_y = imaginary part of bus voltage.

f_0 = nominal system frequency

H_i = inertia of i^{th} generator.

ω_i = rotor speed of i^{th} generator.

δ_i = rotor angle of i^{th} generator.

$$I_{xi} = \frac{E_i \sin \delta_i}{\bar{x}d}, \quad I_{yi} = \frac{E_i \cos \delta_i}{\bar{x}d} \quad (\text{generator buses})$$

$$I_{xi} = 0, \quad I_{yi} = 0 \quad (\text{non-generator buses})$$

We require that a solution to the stability-constrained OPF with respect to the following constraint for each i :

$$\bar{\delta}_i = \delta_i - \frac{\sum_{k=1}^{n_g} H_k \delta_k}{\sum_{k=1}^{n_g} H_k} \leq 100^\circ \quad (3.32)$$

where:

n_g = number of generators.

$\bar{\delta}_i$ = the rotor angle with respect to a center of inertia reference frame.

Rotor angle is used to indicate whether the system is stable.

A solution to a stability-constrained OPF would be a set of generator set-points that satisfy equations (3.22) – (3.32) for a set of credible contingencies.

3.10 Stability-Constrained OPF Procedure:

A standard OPF is solved to see if the solution considers stability constraints. If the solution does, then this solution is also the final solution of stability constrained OPF. If the solution does not respect stability constraints, then a complete stability constrained OPF must be solved, as shown in Figure (3.3) where Kuhn-Tucker condition shown in the figure is the optimality condition for the algebraic Nonlinear Programming.

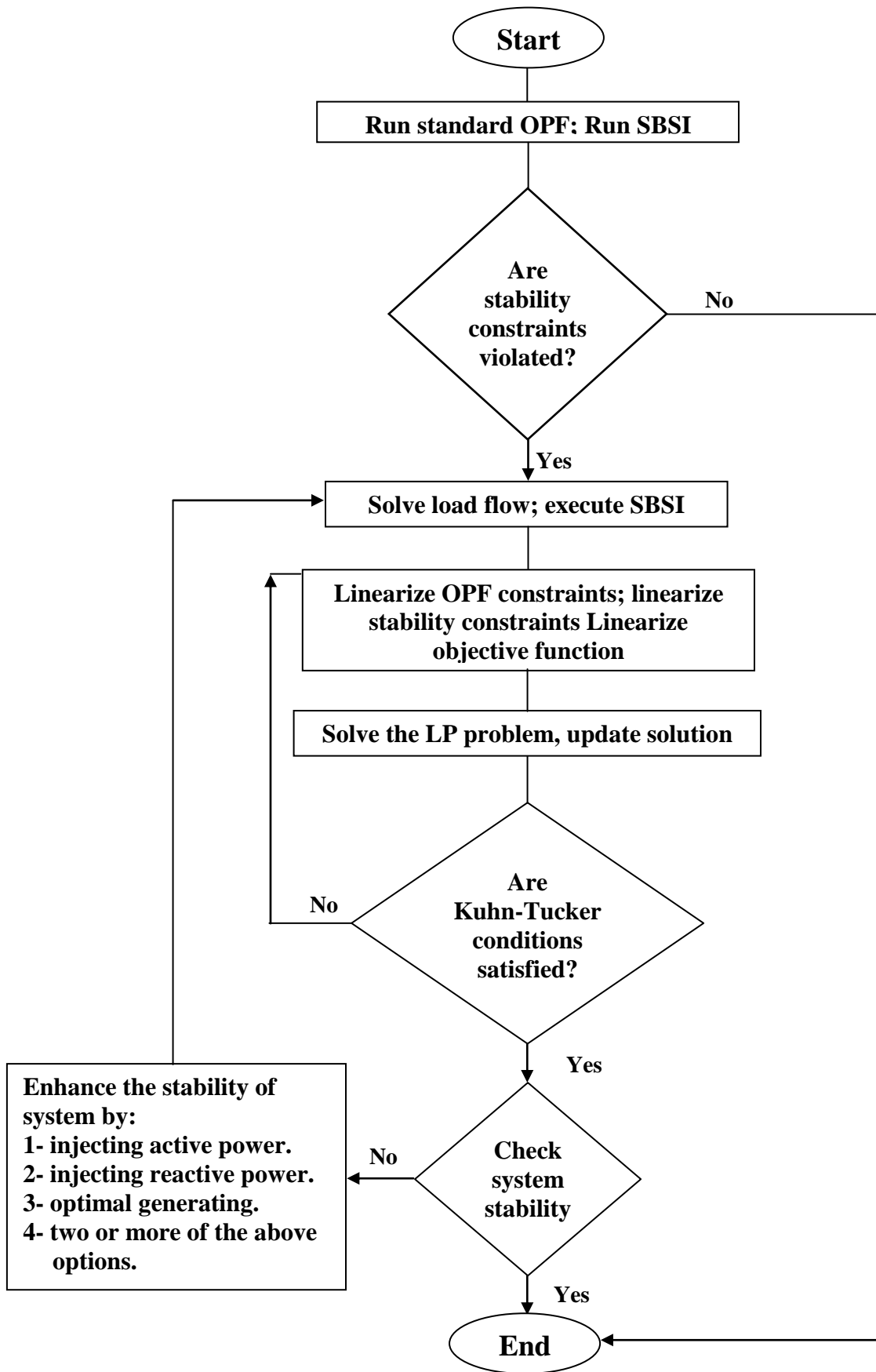


Figure (3.3): A Procedure for the Stability Constrained OPF

Chapter Four

*The Application of the
Developed Program to the Iraqi National
Super Grid*

Chapter Four

The Application of the Developed Program to the INSG

4.1 Introduction:

The Electrical Energy Generation companies try always to improve the system performance through reducing the active power losses. This problem is investigated by using a mathematical model to find the best location to inject active and reactive power at selected local buses.

In this work the INSG 400 kV has been taken as an example and interesting results have been found.

The objective function of the study is to minimize the system total power loss. The control variables include generator voltage, active power generation, the reactive power generation of VAR sources (capacitive or inductive). The constraints of the load flow are voltage limits at load buses, VAR voltage limits of the generators, and VAR source limits.

OPF and swing equations were solved sequentially. Integration format is used in step-by-step integration (SBSI) and that in the algebraic nonlinear problem should be consistent.

Lagrangian method was applied to find the best solution to optimal load flow. The process was repeated according to control variables. Also different constraints were used according to objective function.

4.2 General Description of the Iraqi National Super Grid (INSG) System:

INSG network consists of 19 busbars and 27 transmission lines; the total length of the lines is 3711 km., six generating stations are connected to the grid. They are of various types of generating units, thermal and hydro

turbine kinds, with different capabilities of MW and MVAR generation and absorption.

Figure (4.1) shows the single line diagram of the INSG (400) kV system [69]. The diagram shows all the busbars, the transmission lines connecting the busbars with their lengths in km marked on each one of them. The per unit data of the system is with the following base values:

Base voltage is 400 kV, base MVA is 100 MVA, and base impedance is 1600Ω . In the single-line diagram the given loads represent the actual values of the busbar's loads. The busbars are numbered and named in order to simplify the input data to the computer programs (the load flow and transient stability programs), which are employed in this thesis. The load and generation of INSG system on the 2nd of January 2003 are tabulated in Appendix (C). Lines and machines parameters are tabulated in Appendixes D, and E and used for a program formulated in MATLAB version (5.3).

The transmission system parameters for both types of conductors (TAA and ACSR) are given in p.u /km in Table (4.1) at the base of 100 MVA [7, 69].

Table (4.1): Transmission Lines Parameters

Conductor Type	R (p.u/km)	X (p.u/km)	B (p.u/km)
TAA *	0.2167×10^{-4}	0.1970×10^{-4}	0.5837×10^{-2}
ACSR **	0.2280×10^{-4}	0.1908×10^{-4}	0.5784×10^{-2}

*TAA is Twin Aluminum Alloy.

** ACSR is Aluminum Conductor Steel-Reinforced.

The cross-section area of the conductors in Table (4.1) is $551 \times 2 \text{ mm}^2$ bundle. These overhead lines can be over loaded 25% more than thermal

limits with these types of conductors. Each 1 mm² can handle 1.25 ampere [7].

The INSG system configuration has been taken as given in Figure (4.1) without any rearrangement and reduction of system buses.

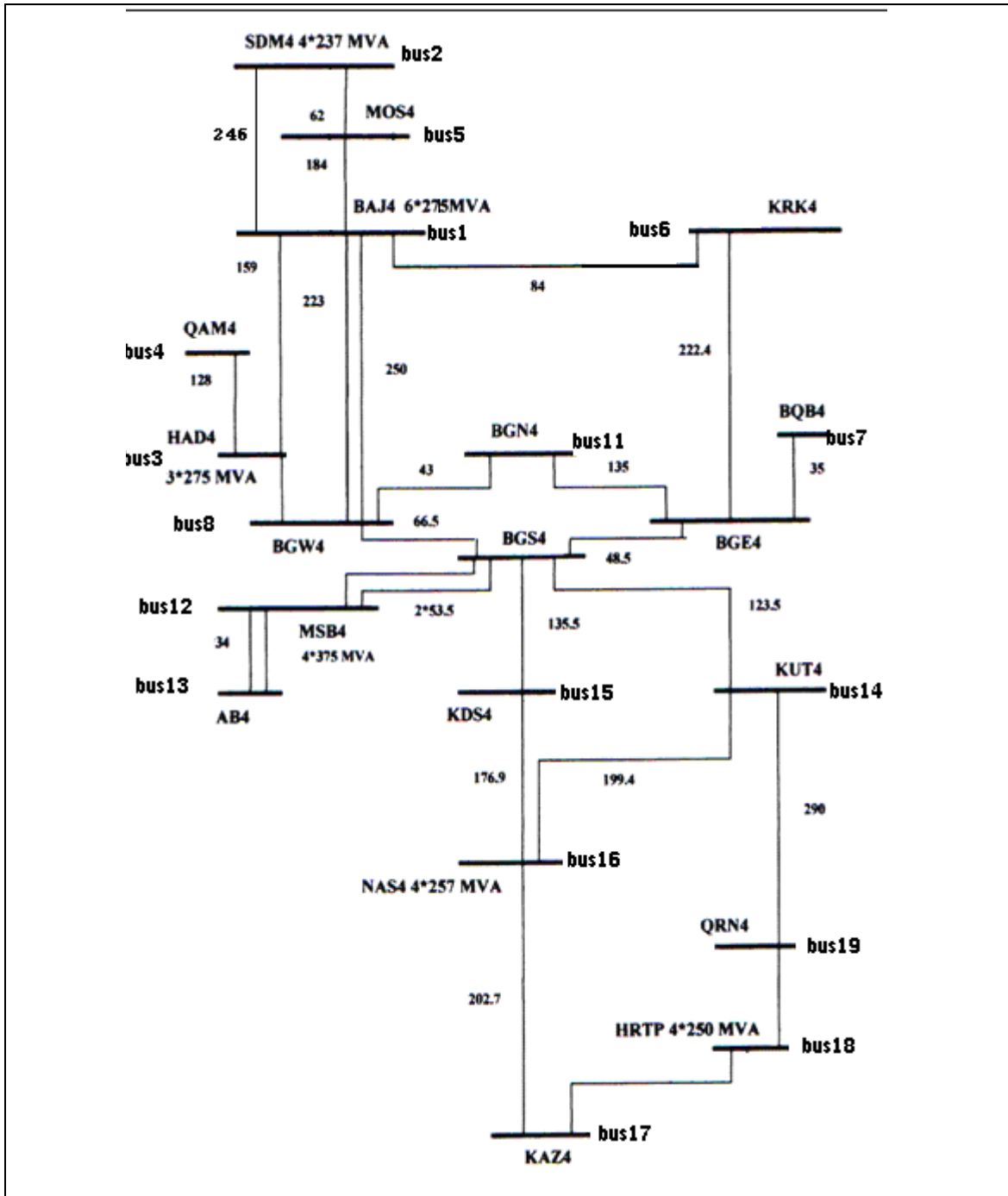


Figure (4.1): Configuration of the 400 kV Network [69]

4.3 The Program Used:

A problem for electric power system students is the solution to problems in text books. In the case of load flow problem, most of the efforts is focused on iterative calculations, not on how the problem is solved. The same is true for stability studies.

A software package [58] is developed to perform electrical power system analysis on a personal computer. The software is capable of performing admittance calculations, load flow studies, optimal load flow studies and transient stability analysis of electric power systems.

It is intended for electric power system students, and is realized in such a manner that a problem can be solved using alternative methods.

Each step during calculations can be visualized. The program has been developed under MATLAB 5.3 for Microsoft Windows. The students are also able to see the inner structure of the program. Load flow analysis is performed by means of Newton-Raphson or Fast-Decoupled methods. Gradient method is used for optimal power flow analysis. This feature enables the power system students to examine differences in the performance of alternative algorithms. A simplified model is used for transient stability, which takes the data from the load flow module. After defining the fault duration, fault clearance time and total analysis time, modified-Euler method is used. The results are displayed and written to corresponding output files. The graphs for angle vs. time for each generator in the system are plotted.

4.4 The Instructional Program:

Power Analysis User Manual

In MATLAB command window, the program is called by typing:

```
>> Main_program
```

which results in the main program menu as shown in Figure (4.2).

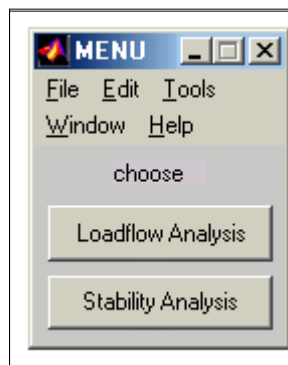


Figure (4.2): Main Program Menu

Load Flow Analysis:

1. Choosing the load flow option, a sub menu is displayed. This menu provides the choice of power flow with and without contingency as shown in Figure (4.3).

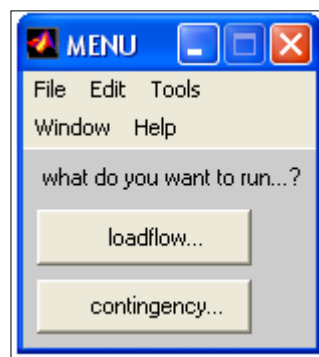


Figure (4.3): Sub Menu of Load Flow Analysis

2. Choosing the Load Flow without contingency, the program will ask the user to enter the data file name. The results consist of two text files (bus result.txt and flow result.txt). The bus result contains: bus number, name, voltage magnitude and phase in degrees, generated and demand power, total series and shunt losses as shown in Figure (4.4). Flow result.txt contains the over loaded lines, the power flow through the lines from send to receive and vice verse as shown in Figure (4.5).

```

LOAD FLOW BUS RESULTS
Name      |V|          angle(deg)      PG(MW)      QG(MVAR)
BAJG      399.9996    -0.00032593     0            0
SDMG      400.0001     6.3145         0            0
HADG      400         0.73618        0            0
QAM4      398.9524    -0.082643     0            0
MOS4      394.1607     3.2424        0            0
KRK4      394.4911    -2.7952        0            0
BQB4      373.5296    -9.2764        0            0
BGW4      382.455     -6.8138        0            0
BGE4      376.1397    -8.6367        0            0
BGS4      391.5996    -6.5426        0            0
BGN4      375.7272    -8.5621        0            0
MSBG      399.9983    -5.5487        0            0
BAB4      398.0503    -5.6635        0            0
KUT4      400.656     -5.0389        0            0
KDS4      392.4906    -5.8886        0            0
NSRG      400.0003    -1.0043        0            0
KAZ4      394.1097    -3.9273        0            0
HRTG      399.9999    -2.6124        0            0
QRN4      402.6102    -3.4641        0            0
BAJ4      400         0              570.5925     100.4455
SDM4      400         6.3149         700          -23.22485
HAD4      400         0.73647       500          -0.8474983
MSB4      400         -5.5484       600          420.6564
NSR4      400         -1.004        650          -69.14344
HRT4      400         -2.6121       380          35.9855
TOTAL
THE TOTAL AMOUNT OF SERIES LOSSES ARE 37.59249-330.18861
THE TOTAL AMOUNT OF SHUNT LOSSES ARE 0+1922.31691
463.8716

```

Figure (4.4): Load Flow Bus Results

NS	Name	NR	Name	P(Mw)
2	SDMG	21	SDM4	-700
5	MOS4	2	SDMG	-455.4206
5	MOS4	1	BAJG	155.4206
1	BAJG	2	SDMG	-233.3049
1	BAJG	20	BAJ4	-570.5925
4	QAM4	3	HADG	-60
3	HADG	22	HAD4	-500
1	BAJG	3	HADG	-45.1666
3	HADG	8	BGW4	294.6566
1	BAJG	8	BGW4	238.7362
1	BAJG	8	BGW4	267.6415
1	BAJG	6	KRK4	296.9418
9	BGE4	7	BQB4	150.2395
8	BGW4	11	BGN4	340.7821
11	BGN4	9	BGE4	39.3459
8	BGW4	10	BGS4	-51.5339
9	BGE4	10	BGS4	-388.5388
13	BAB4	12	MSBG	-50
13	BAB4	12	MSBG	-50
12	MSBG	23	MSB4	-600
10	BGS4	12	MSBG	-188.9261
10	BGS4	12	MSBG	-188.9261
10	BGS4	15	KDS4	-41.4485
10	BGS4	14	KUT4	-124.3212

Figure (4.5): Line Flow Results

3. Choosing the Load Flow with contingency, a sub menu is displayed; this menu provides the choice of different contingencies as shown in Figure (4.6).

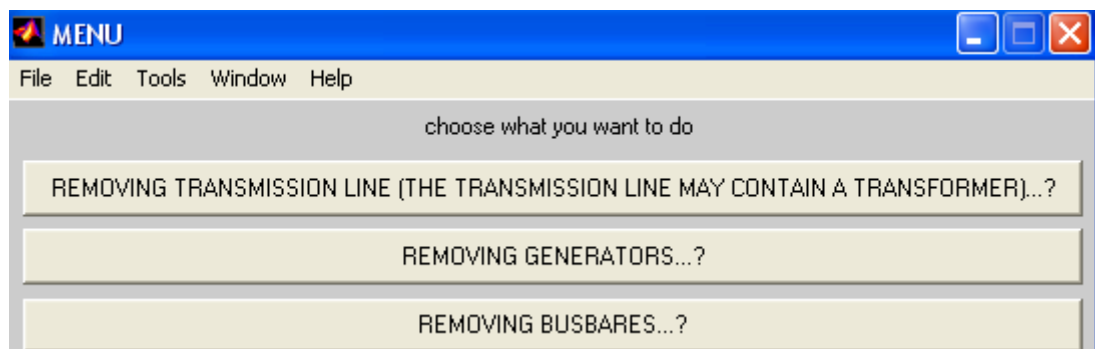


Figure (4.6): Sub Menu of Load Flow with Contingency

4. Choosing one or many of these options gives a system with new configuration. The result consists of two text files similar to that without contingency, but according to the new configuration. The

user has a lot of alternatives to study the system with many contingencies.

Transient Stability Analysis:

1. Choosing the T.S option in the main program, the program will ask for the data file name. The results are displayed at each time step and graphs for angle vs. time for each generator in the system are plotted as shown in Figure (4.7) for one of the generators.

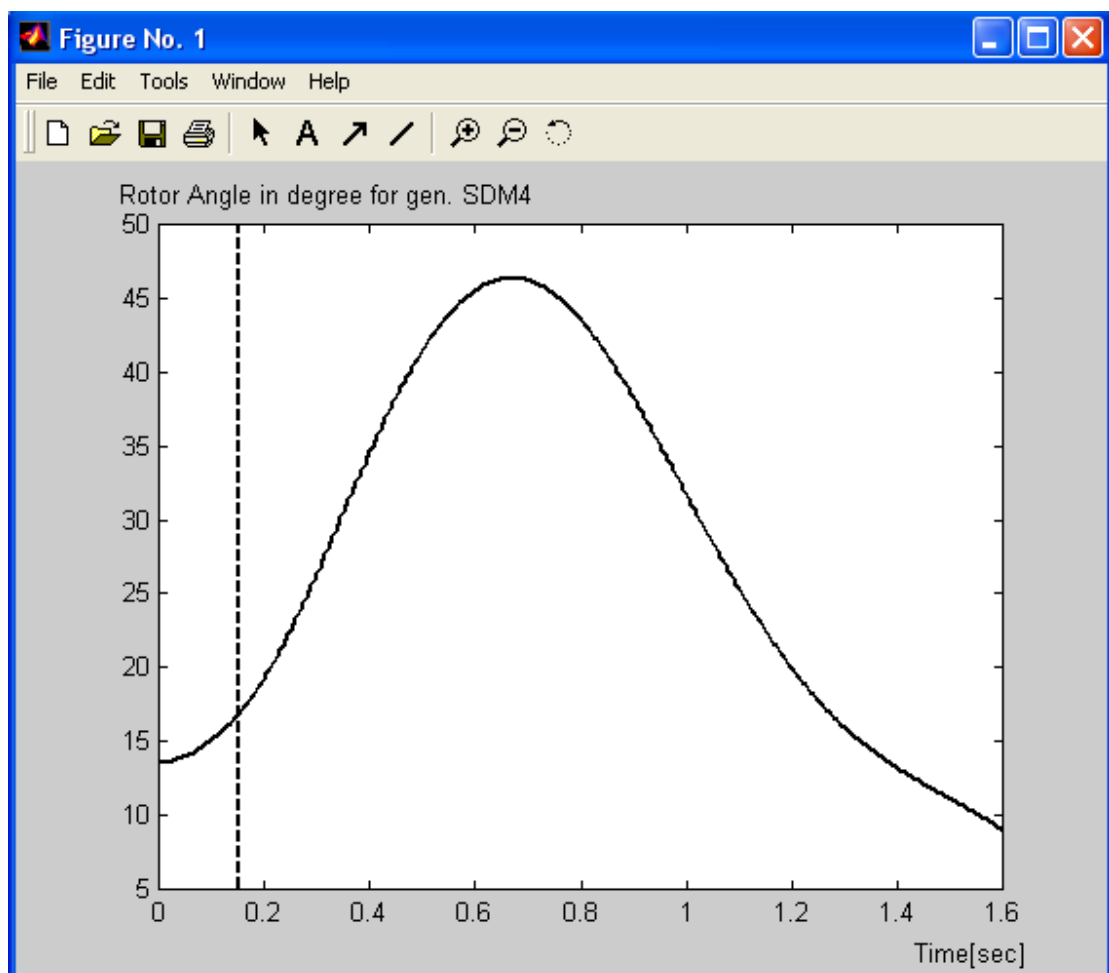


Figure (4.7): Swing Curve for SDM Generation Bus

2. Choosing any type of three phase fault (Line fault, generator fault and load fault) will give a new situation of system stability and a new plot for swing curve is plotted.

Optimal Load Flow:

1. Choosing the OPF option, a sub menu is displayed. This menu provides a choice of minimum losses calculation, bus sensitivity to decrease losses w.r.t real power injecting and bus sensitivity to decrease losses w.r.t reactive power injection as shown in Figure (4.8).

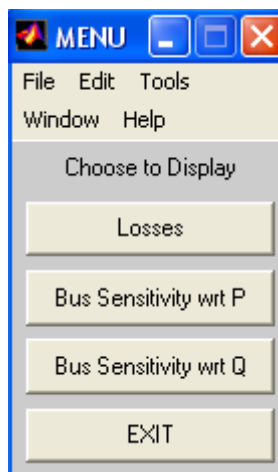
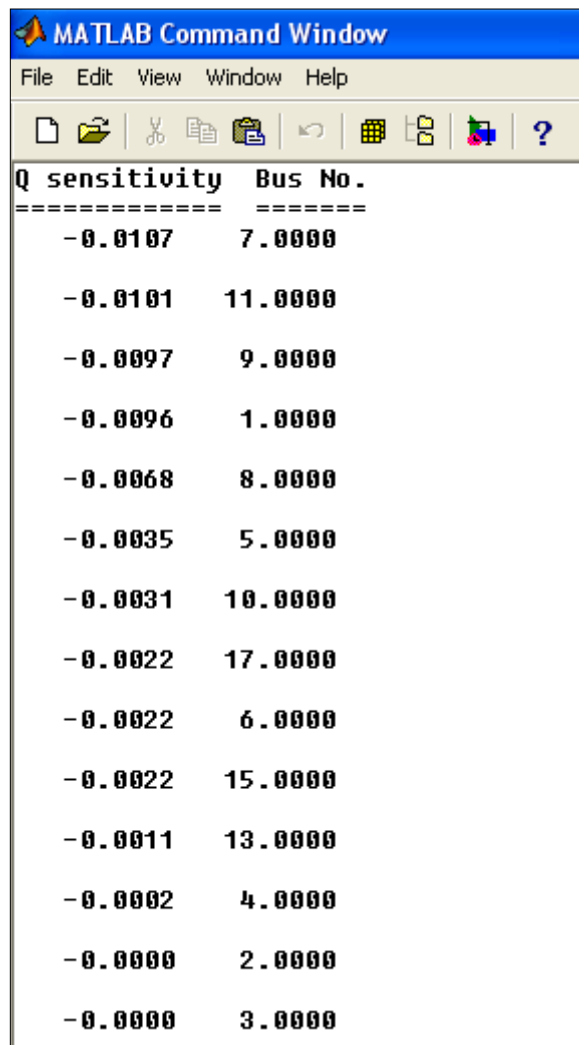


Figure (4.8): Optimal Load Flow

2. Choosing (losses) option will give the magnitude of total system losses.
3. Choosing (P sensitivity) or (Q sensitivity) will give the sequence of the buses according to these sensitivities to reduce system losses with respect to real or reactive power injection in load buses or power generated in generation buses, this will give the best allocation for generator or shunt capacitor in the system which gives minimum losses as shown in Figure (4.9).



The image shows a screenshot of the MATLAB Command Window. The window title is "MATLAB Command Window" and it has a menu bar with "File", "Edit", "View", "Window", and "Help". Below the menu bar is a toolbar with various icons. The main area of the window displays a table with two columns: "Q sensitivity" and "Bus No.". The table is separated from the rest of the window by a dashed line. The data in the table is as follows:

Q sensitivity	Bus No.
-0.0107	7.0000
-0.0101	11.0000
-0.0097	9.0000
-0.0096	1.0000
-0.0068	8.0000
-0.0035	5.0000
-0.0031	10.0000
-0.0022	17.0000
-0.0022	6.0000
-0.0022	15.0000
-0.0011	13.0000
-0.0002	4.0000
-0.0000	2.0000
-0.0000	3.0000

Figure (4.9): Sequence of Bus Sensitivities w.r.t Reactive Power Injection

Chapter Five

Results and Discussion

Chapter Five

Results and Discussion

5.1 Power Losses Reduction:

Power losses reduction depends on the sensitivities of the system losses with respect to state variables. The method of finding the sensitivities is presented in Appendix (A).

5.1.1 Injecting Active Power:

Power loss sensitivity (P_{sen}) was calculated using equation (3.14).

The values of partial derivatives $\partial P_{loss}/\partial P_i$ which represents the efficiency to reduce system power losses with respect to real power injecting at the buses except the slack bus, are tabulated in Table (5.1). High negative partial derivative at any bus means that the system has high efficiency to reduce active power losses when injecting active power in that bus. On the other hand positive partial derivative $\partial P_{loss}/\partial P_i$ at buses (3, 5, and 2) means that system power losses increase in case of injecting real power in these buses. The procedure to find P_{sen} is shown in Figure (3.1) which is a flow chart to find the best buses to install generation units and reactive power. The best buses to accept injecting active power are those with high negative partial derivative $\frac{\partial P_{loss}}{\partial P_i}$.

Table (5.2) and Figures (5.1)-(5.13) show that active power losses decrease when increasing injection power to the point where the active power losses start to increase again, at this point losses partial derivative (sensitivity) becomes equal or next to zero. Injecting real power at buses must not exceed the value, which gives maximum loss reduction.

Table (5.3) and Figure (5.14) show the values of active power injection at each load bus, which gives maximum real power loss reduction. Injecting real power at bus 9 (BGE) gives max system loss reduction equal to $\frac{37.592 - 22.67}{37.592} \times 100\% = 39.69\%$. On the other hand injecting real power at bus 16 (NSR) gives max system loss reduction equal to $\frac{37.592 - 37.49}{37.592} \times 100\% = 0.27\%$, for the other buses loss reduction lies between these two values.

Table (5.1): The Partial Derivative of Losses (Sensitivity) with Respect to Active Power Injection

No.	Bus No.	$\partial P_{\text{loss}} / \partial P_{\text{injection}}$
1.	7	- 0.0392
2.	9	- 0.0361
3.	11	- 0.0359
4.	8	- 0.0279
5.	10	- 0.0258
6.	15	- 0.0230
7.	13	- 0.0214
8.	12	- 0.0207
9.	23	- 0.0207
10.	14	- 0.0188
11.	17	- 0.0152
12.	19	- 0.0126
13.	6	- 0.0110
14.	18	- 0.0096
15.	25	- 0.0096
16.	16	- 0.0034
17.	24	- 0.0034
18.	4	- 0.0004
19.	1	0.0000
20.	20	0.0000
21.	3	0.0031
22.	22	0.0031
23.	5	0.0136
24.	2	0.0268
25.	21	0.0268

Table (5.2): Effect of Injecting Real Power on Sensitivity and Losses

P_i [Mw]	Bus No. 4		Bus No. 5		Bus No. 6	
	$\partial P_{\text{loss}}/\partial P_i$	Losses [Mw]	$\partial P_{\text{loss}}/\partial P_i$	Losses [Mw]	$\partial P_{\text{loss}}/\partial P_i$	Losses [Mw]
0	- 0.0004	37.592	0.0136	37.592	- 0.0110	37.592
10	0.0007	37.593	0.0141	37.72	- 0.0107	37.48
50	0.0049	37.70	0.0162	38.32	- 0.0095	37.062
100	0.0101	38.08	0.0189	39.19	- 0.0079	36.612
150			0.0216	40.18	- 0.0049	35.946
300					- 0.0019	35.59
350					- 0.0004	35.528
400					0.0011	35.544

Table (5.2) (continued): Effect of Injecting Real Power on Sensitivity and Losses

P_i [Mw]	Bus No. 7		Bus No. 8		Bus No. 9	
	$\partial P_{\text{loss}}/\partial P_i$	Losses [Mw]	$\partial P_{\text{loss}}/\partial P_i$	Losses [Mw]	$\partial P_{\text{loss}}/\partial P_i$	Losses [Mw]
0	- 0.0392	37.592	- 0.0279	37.592	- 0.0361	37.592
10	- 0.0347	37.190	- 0.0253	37.3	- 0.0319	37.21
50	- 0.0324	35.653	- 0.024	36.18	- 0.0303	35.77
100	- 0.0296	33.889	- 0.0224	34.868	- 0.0283	34.090
150	- 0.0268	32.298			- 0.0263	32.52
200	- 0.0239	30.877	- 0.0209	32.515	- 0.0243	31.07
250	- 0.0211	29.6238				
300	- 0.0183	28.535	- 0.0175	30.524	- 0.0203	28.53
350	- 0.0155	27.61				
400	- 0.0127	26.847	- 0.0141	28.89	- 0.0163	26.46
450	- 0.0098	26.244				
500	- 0.0070	25.800	- 0.0107	27.611	- 0.0123	24.85
550	- 0.0042	25.514				
600	- 0.0014	25.383	- 0.0073	26.678	- 0.0084	23.68
625	0.0000	25.37				
650	0.0014	25.40				
700	0.0042	25.58	- 0.0039	26.08	- 0.0044	22.96
750	0.0072	26.41	- 0.0023	25.92	- 0.0027	22.76
800			- 0.0006	25.84	- 0.0005	22.67
825			0.0003	25.83		
850	0.0142	27.05	0.0011	25.84	0.0000	22.69
900			0.0026	25.92	0.0034	22.82
950					0.0054	23.05
1000			0.0061	26.35		

Table (5.2) (continued): Effect of Injecting Real Power on Sensitivity and Losses

P_i [Mw]	Bus No. 10		Bus No. 11		Bus No. 13	
	$\partial P_{\text{loss}}/\partial P_i$	Losses [M36.11w]	$\partial P_{\text{loss}}/\partial P_i$	Losses [Mw]	$\partial P_{\text{loss}}/\partial P_i$	Losses [Mw]
0	- 0.0258	37.592	- 0.0359	37.592	- 0.0214	37.592
10	- 0.0244	37.32	- 0.0354	37.22	- 0.0207	37.29
50	- 0.0226	36.28	- 0.0336	35.79	- 0.0179	36.25
100	- 0.0202	35.11	- 0.0313	34.118	0.0144	35.28
150	- 0.0185	34.07	- 0.0290	32.563	- 0.0110	34.66
200	- 0.0156	33.16	- 0.0268	31.12	- 0.0076	34.406
225					- 0.0058	34.407
250	- 0.0137	32.38	- 0.0245	29.81	- 0.0042	34.494
300	- 0.0110	31.73	- 0.0223	28.61	- 0.0001	34.92
350			- 0.0201	27.53	0.0024	35.69
400	- 0.0064	30.80	- 0.0179	26.56	0.0054	36.8
450			- 0.0157	25.70	0.0090	38.24
500	- 0.0019	30.37	- 0.0122	24.96	0.0122	40.00
550	0.0004	30.35	- 0.0113	24.33		
600	0.0027	30.44	- 0.0091	23.81		
700	0.0060	31.008	- 0.0048	23.10		
800	0.0124	32.057	- 0.0005	22.832		
825			0.0005	22.831		
850			0.0015	22.85		
900			0.0035	22.98		
950			0.0054	23.22		

Table (5.2) (continued): Effect of Injecting Real Power on Sensitivity and Losses

P_i [Mw]	Bus No. 14		Bus No. 15		Bus No. 17	
	$\partial P_{\text{loss}}/\partial P_i$	Losses [Mw]	$\partial P_{\text{loss}}/\partial P_i$	Losses [Mw]	$\partial P_{\text{loss}}/\partial P_i$	Losses [Mw]
0	- 0.0188	37.592	- 0.0230	37.592	- 0.0152	37.592
10	- 0.0180	37.39	- 0.0215	37.35	- 0.0136	37.43
50	- 0.0144	36.67	- 0.0178	36.48	- 0.0074	36.95
100	- 0.0101	35.99	- 0.0132	35.63	0.0003	36.71
125					0.0041	36.74
200	- 0.0013	35.32	- 0.0039	34.67	0.0154	37.74
225	0.0008	35.30	- 0.0015	34.59		
250	0.0030	35.33	0.0008	34.56		
300	0.0073	35.57	0.0053	34.70	0.0305	39.64
350	0.0115	36.03				
400	0.0158	36.72	0.0148	35.71		
450						
500			0.0241	37.68		

Table (5.2) (continued): Effect of Injecting Real Power on Sensitivity and Losses

P_i [Mw]	Bus No. 19	
	$\partial P_{\text{loss}}/\partial P_i$	Losses [Mw]
0	- 0.0126	37.592
10	- 0.0111	37.456
50	- 0.0050	37.071
75	- 0.0012	36.959
100	0.0026	36.946
125	0.0063	37.031
150	0.0103	37.21
200	0.0175	37.86

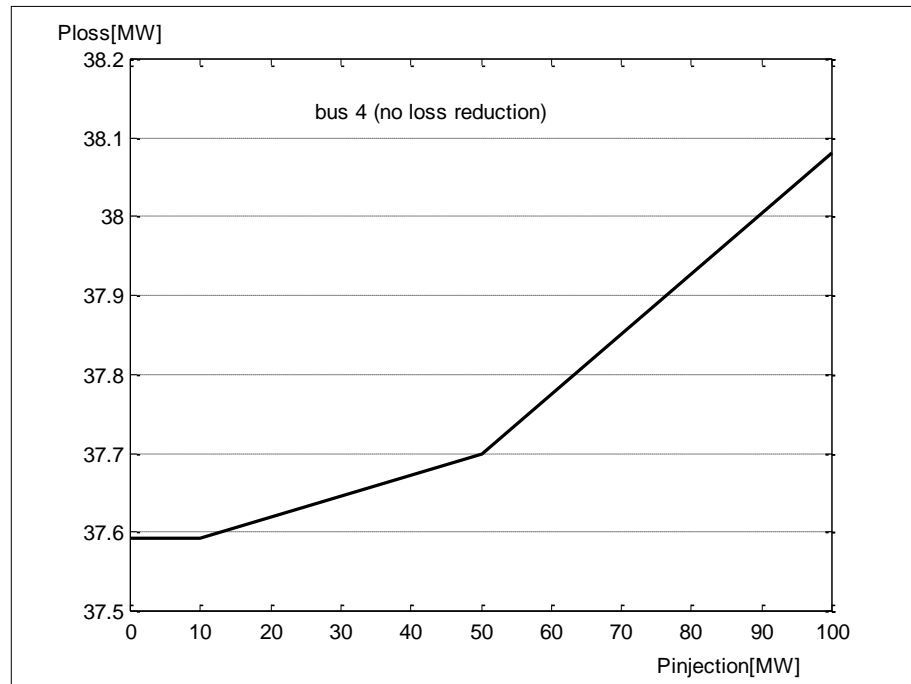


Figure (5.1): P_{loss} vs. $P_{\text{injection}}$ at Bus 4 (QAM)

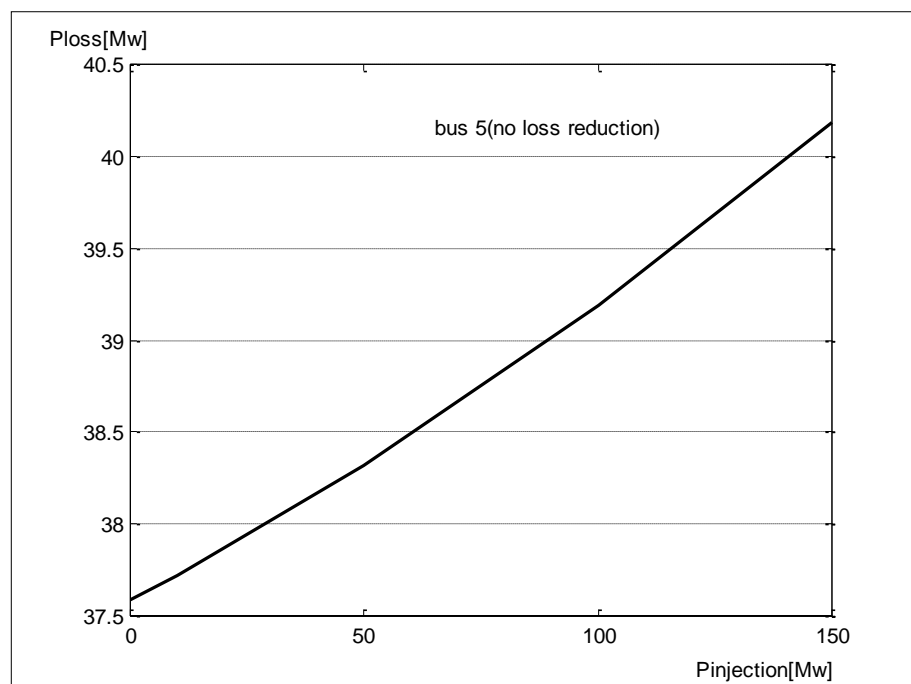


Figure (5.2): P_{loss} vs. $P_{\text{injection}}$ at Bus 5 (MOS)

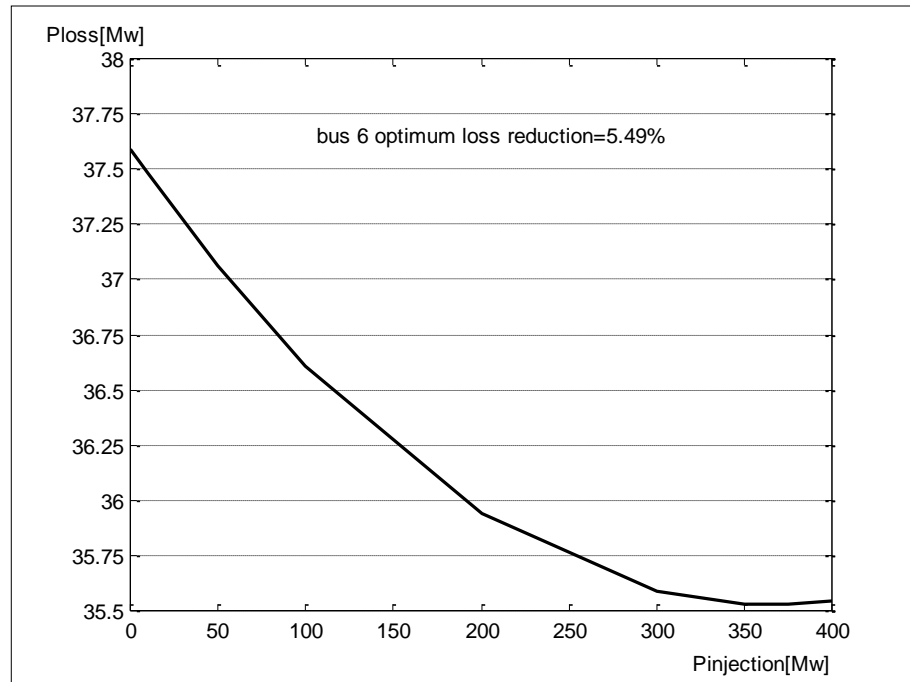


Figure (5.3): P_{loss} vs. $P_{\text{injection}}$ at Bus 6 (KRK)

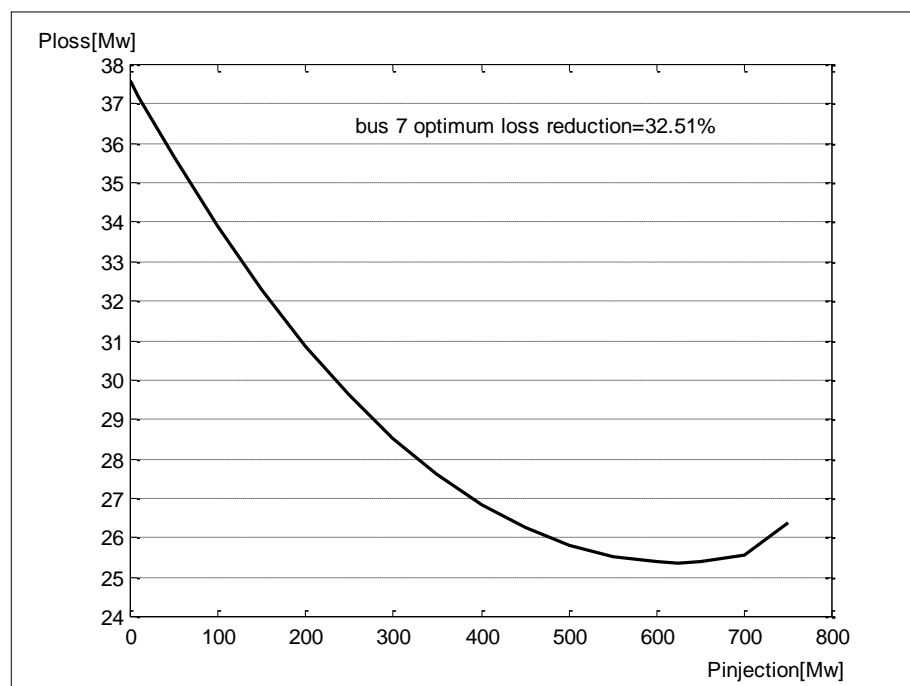


Figure (5.4): P_{loss} vs. $P_{\text{injection}}$ at Bus 7 (BQB)

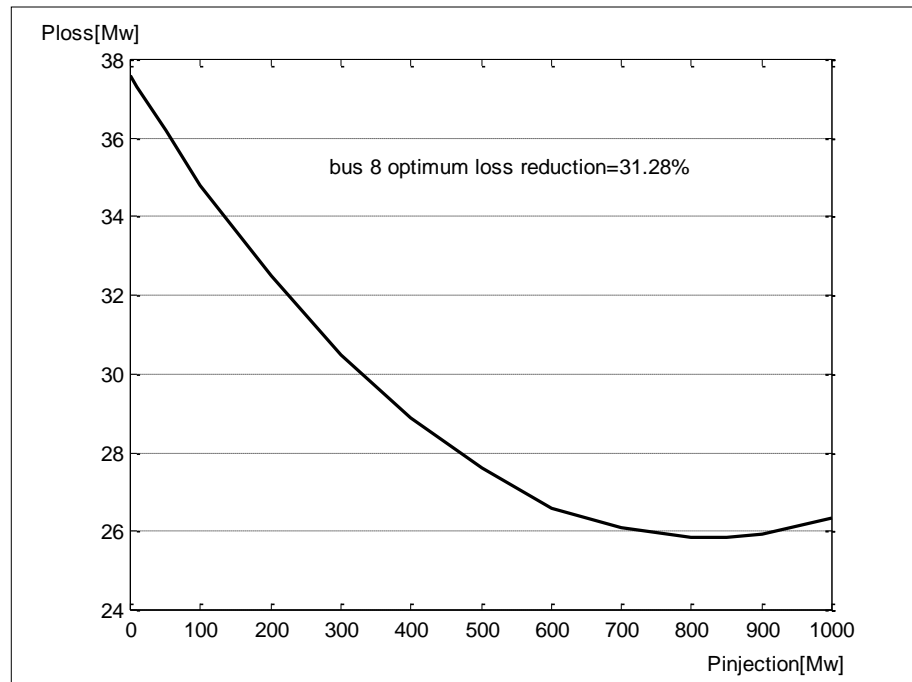


Figure (5.5): P_{loss} vs. P_{injection} at Bus 8 (BGW)

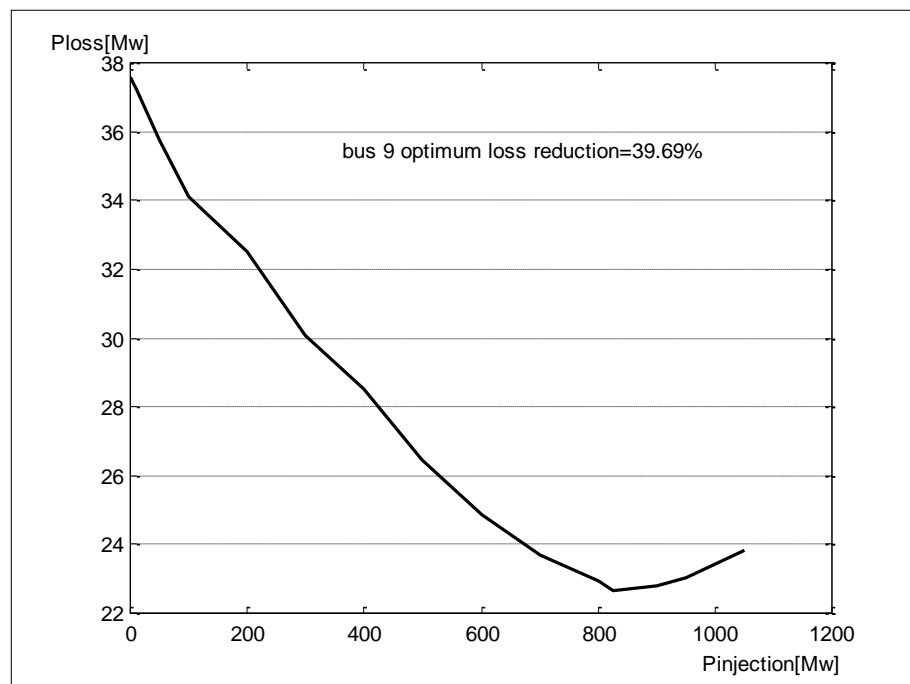


Figure (5.6): P_{loss} vs. P_{injection} at Bus 9 (BGE)

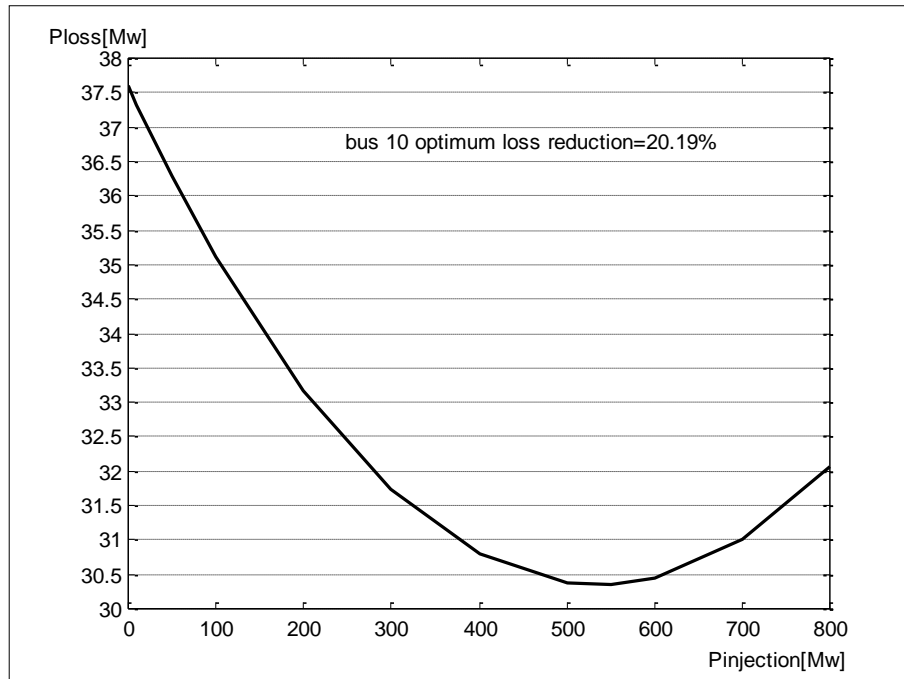


Figure (5.7): P_{loss} vs. $P_{\text{injection}}$ at Bus 10 (BGS)

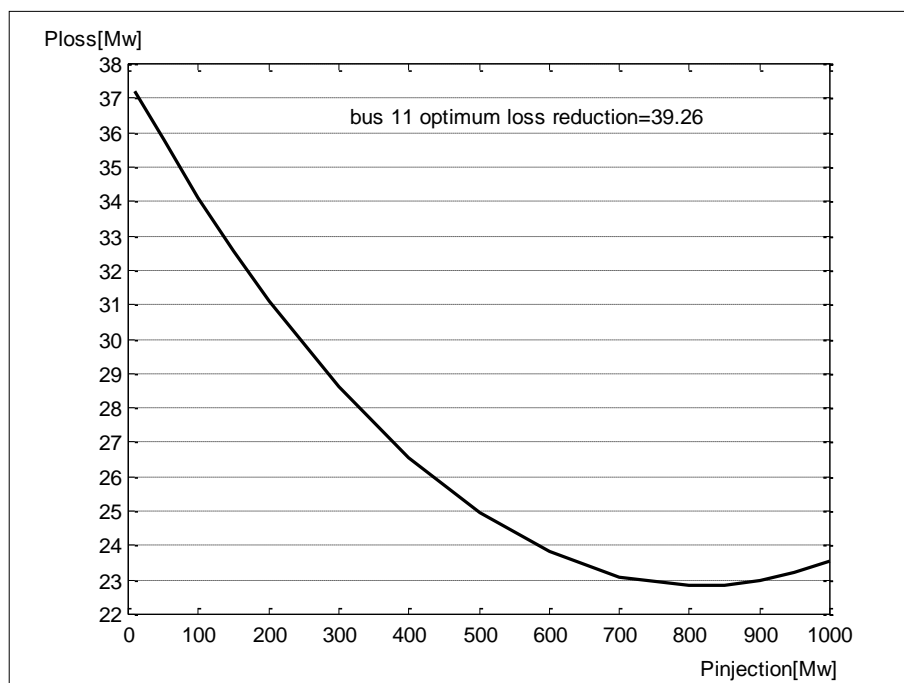


Figure (5.8): P_{loss} vs. $P_{\text{injection}}$ at Bus 11 (BGN)

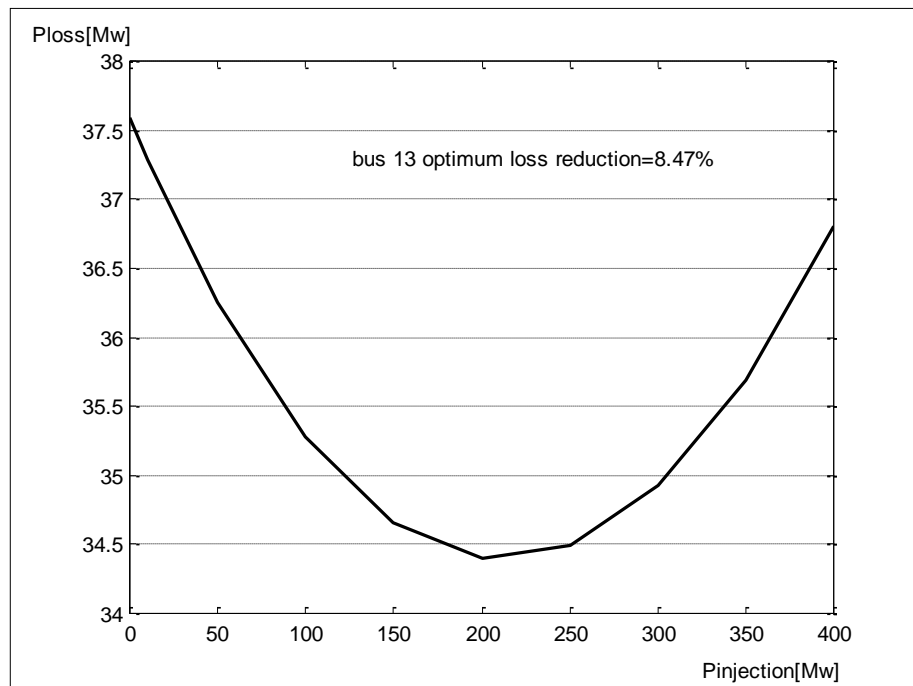


Figure (5.9): P_{loss} vs. $P_{\text{injection}}$ at Bus 13 (BAB)

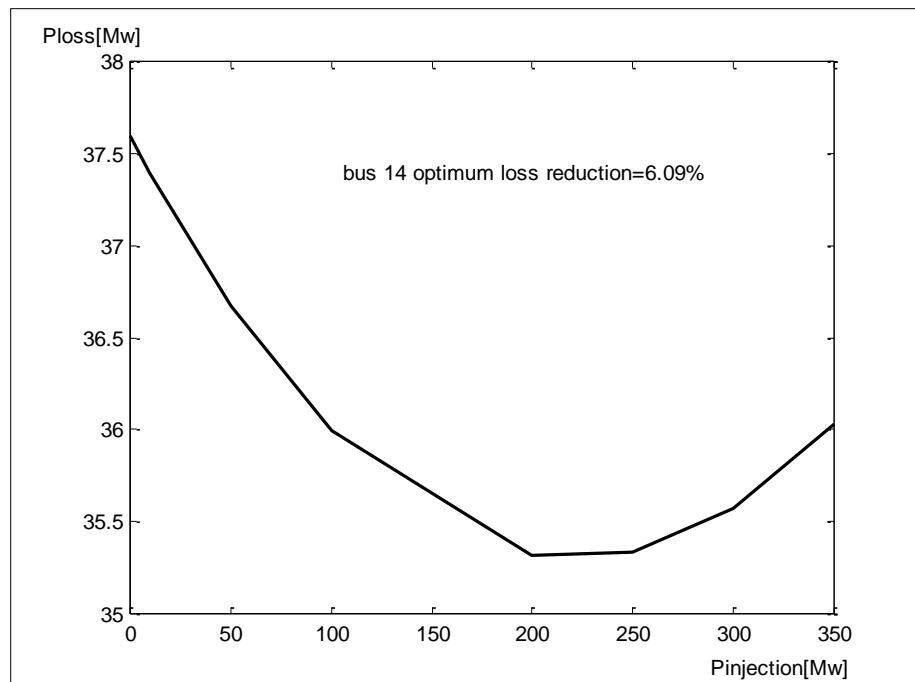


Figure (5.10): P_{loss} vs. $P_{\text{injection}}$ at Bus 14 (KUT)

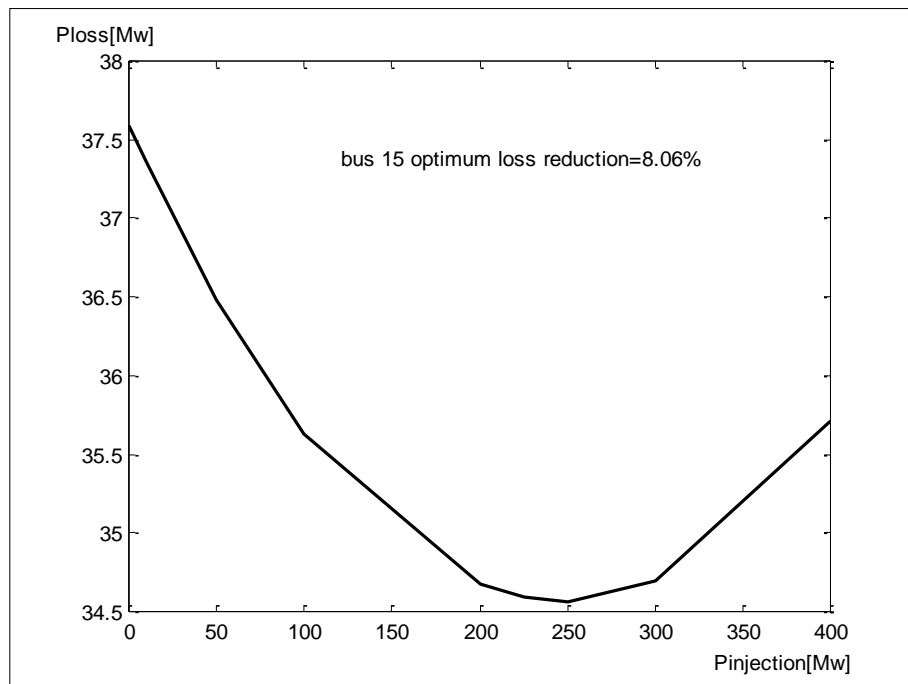


Figure (5.11): P_{loss} vs. $P_{\text{injection}}$ at Bus 15 (KDS)

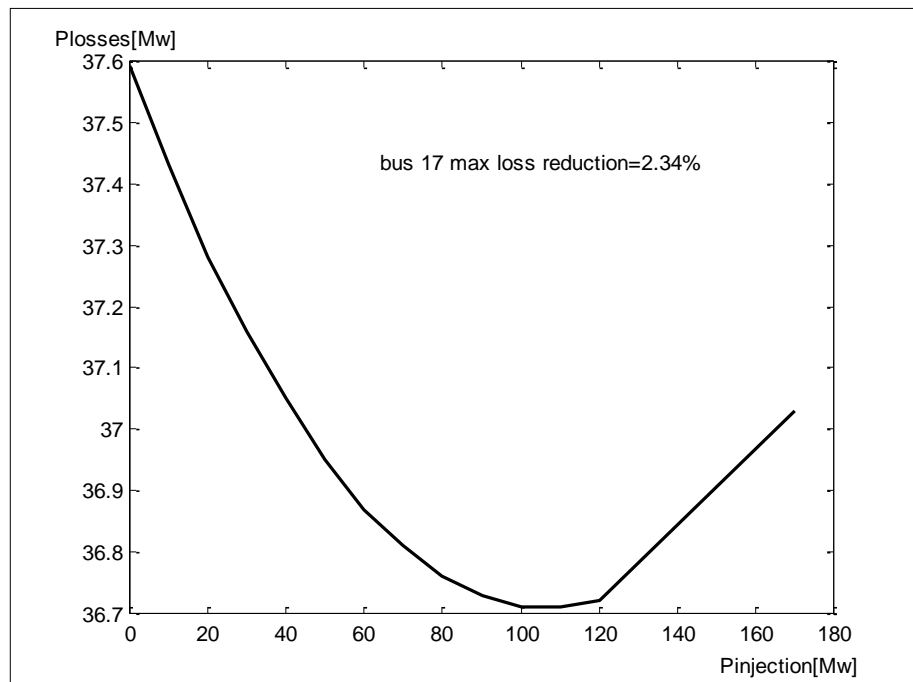


Figure (5.12): P_{loss} vs. $P_{\text{injection}}$ at Bus 17 (KAZ)

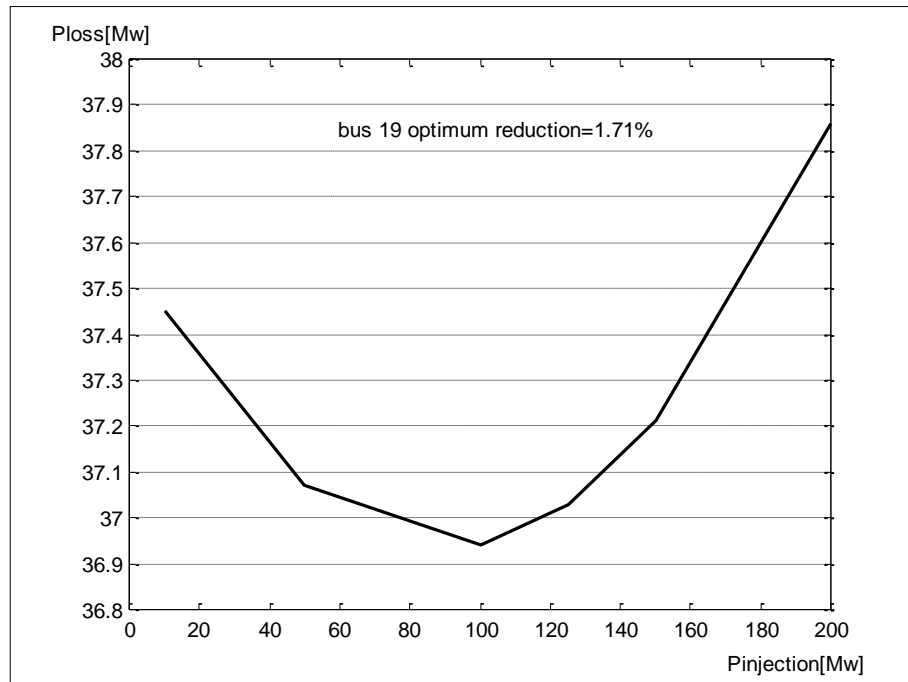


Figure (5.13): P_{loss} vs. P_{injection} at Bus 19 (QRN)

Table (5.3): The Injection of Real Power which Gives Max Loss Reduction

Bus No.	P _{injection} [Mw]	Minimum losses [Mw]	Max. loss Reduction %
9	800	22.67	39.69
11	825	22.83	39.26
7	625	25.37	32.51
8	825	25.83	31.28
10	550	30.35	20.19
12	350	33.71	10.32
13	200	34.406	8.47
15	250	34.56	8.06
14	225	35.30	6.09
6	350	35.528	5.49
17	100	36.71	2.34
19	100	36.946	1.71
18	75	37.197	1.05
16	50	37.49	0.27

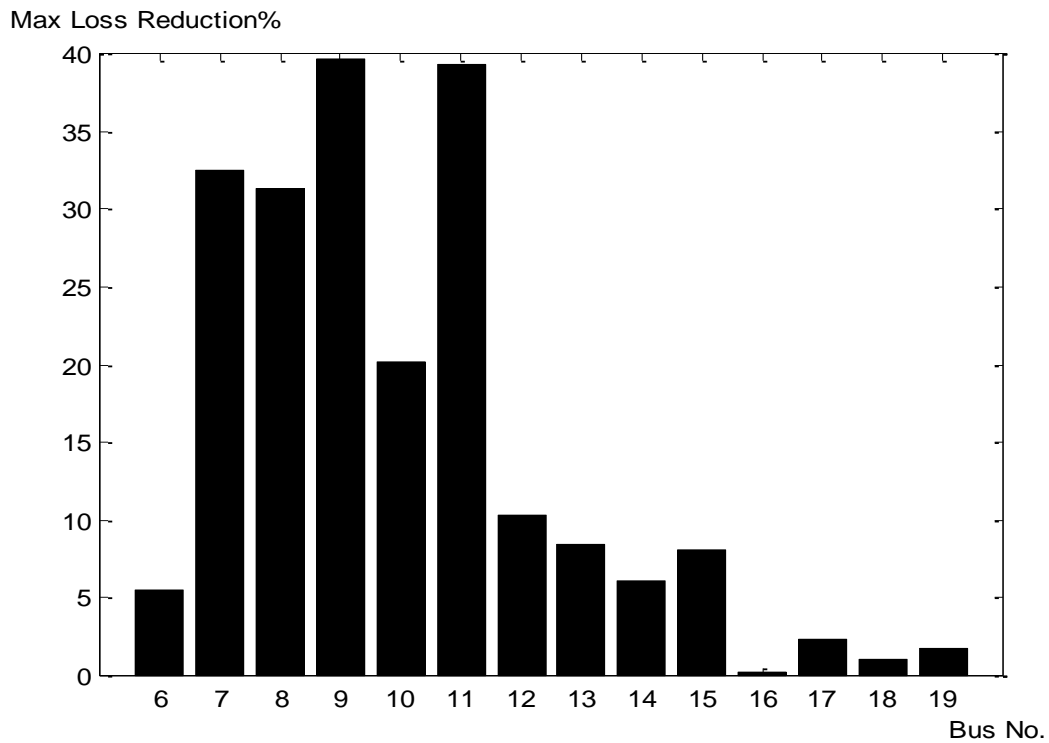


Figure (5.14): Loss Reduction for Injecting Real Power at some Buses

5.1.2 Injecting Reactive Power:

Power loss sensitivity (Q_{sen}) was calculated using equation (3.15). The values of partial derivative $\partial P_{loss}/\partial Q_i$ which represent the efficiency to reduce system power losses with respect to reactive power injection at buses except the slack bus, are tabulated in Table (5.4). High negative partial derivative at the bus means that the system has high efficiency to reduce active power losses when injecting reactive power in that bus. On the other hand positive partial derivative $\partial P_{loss}/\partial Q_i$ at buses (14, 19) means that system power losses increase in case of injecting reactive power.

Sensitivity to reactive power Q_{sen} was calculated using the procedure mentioned in section 5.1.1 according to flowchart in Figure (3.1). The best buses are those with high negative partial derivative $\frac{\partial P_{loss}}{\partial Q_i}$.

Table (5.5) and Figures (5.15)-(5.24) show that active power losses decrease when increasing injection reactive power to the point where the active power losses start to increase, at this point losses partial derivatives $\partial P_{\text{loss}}/\partial Q_i$ become equal or next to zero. Because partial derivatives (sensitivity) at buses 14, 19 are positive so injecting inductive reactive power decreases system active power losses as shown in Table (5.6) and Figures (5.25) and (5.26).

Table (5.7) and Figure (5.27) show the value of reactive power injection that gives maximum real power loss reduction. Injecting reactive power at bus 9 (BGE) gives max loss reduction:

$$\text{Loss reduction} = \frac{37.592 - 33.24}{37.592} \times 100\% = 11.57\%$$

Also max loss reduction when injecting reactive power at bus 13 (BAB) is equal to $\frac{37.592 - 37.56}{37.592} \times 100\% = (0.085\%)$. For the other buses loss reduction lies between these two values.

Table (5.4): The Partial Derivative of Losses (Sensitivity) with Respect to Reactive Power Injection

No.	Bus No.	$\partial P_{\text{loss}} / \partial Q_{\text{injection}}$
1	7	- 0.0107
2	11	- 0.0101
3	9	- 0.0097
4	8	- 0.0068
5	5	- 0.0035
6	10	- 0.0031
7	15	- 0.0022
8	17	- 0.0022
9	6	- 0.0022
10	13	- 0.0011
11	4	- 0.0002
12	14	+ 0.0015
13	19	+ 0.0019

Table (5.5): Effect of Injecting Reactive Power on Sensitivity and Losses

Q_i [MAR]	Bus No. 4		Bus No. 5		Bus No. 6	
	$\partial P_{\text{loss}}/\partial Q_i$	Losses [Mw]	$\partial P_{\text{loss}}/\partial Q_i$	Losses [Mw]	$\partial P_{\text{loss}}/\partial Q_i$	Losses [Mw]
0	- 0.0002	37.592	- 0.0035	37.592	- 0.0022	37.592
10	0.0004	37.593	- 0.0033	37.56	- 0.0019	37.557
20	0.0010	37.599	- 0.0031	37.53	- 0.0016	37.526
30	0.0015	37.612	- 0.0028	37.50	- 0.0013	37.49
40	0.0021	37.63	- 0.0026	37.48	- 0.0011	37.47
50	0.0027	37.65	- 0.0024	37.46	- 0.0008	37.44
100			- 0.0013	37.38	0.0007	37.38
150			- 0.0002	37.36	0.0020	37.386
200			0.0009	37.40	0.0034	37.46

Table (5.5) (continued): Effect of Injecting Reactive Power on Sensitivity and Losses

Q_i [MVAR]	Bus No. 7		Bus No. 8		Bus No. 9	
	$\partial P_{\text{loss}}/\partial Q_i$	Losses [Mw]	$\partial P_{\text{loss}}/\partial Q_i$	Losses [Mw]	$\partial P_{\text{loss}}/\partial Q_i$	Losses [Mw]
0	- 0.0107	37.592	- 0.0068	37.592	- 0.0097	37.592
10	- 0.0103	37.43	- 0.0067	37.48	- 0.0095	37.53
20	- 0.0098	37.28				
50	- 0.0086	36.85	- 0.0060	37.07	- 0.0087	36.78
100	- 0.0066	36.23	- 0.0051	36.61	- 0.0076	35.99
150	- 0.0047	35.72				
200	- 0.0028	35.31	- 0.0026	35.833	- 0.0055	35.21
250	- 0.0010	35.00				
300	0.0007	34.79	- 0.0019	35.244	- 0.0035	34.39
350	0.0024	34.678				
400	0.0040	34.649	- 0.0002	34.836	- 0.0015	33.80
450			0.0006	34.63		
500	0.0072	34.825	0.0013	34.602	0.0003	33.42
600			0.0028	34.53	0.0021	33.24
650			0.0036	34.56	0.0030	33.257
700			0.0043	34.62	0.0033	33.2586

Table (5.5) (continued): Effect of Injecting Reactive Power on Sensitivity and Losses

Q_i [MVAR]	Bus No. 10		Bus No. 11		Bus No. 13	
	$\partial P_{\text{loss}}/\partial Q_i$	Losses [Mw]	$\partial P_{\text{loss}}/\partial Q_i$	Losses [Mw]	$\partial P_{\text{loss}}/\partial Q_i$	Losses [Mw]
0	- 0.0031	37.592	- 0.0101	37.592	- 0.0011	37.592
10	- 0.0030	37.54	- 0.0098	37.446	- 0.0008	37.6
50	- 0.0027	37.34	- 0.0089	36.89	- 0.0006	37.56
100	- 0.0022	37.12	- 0.0078	36.25	- 0.0001	37.74
150	- 0.0018	36.93	- 0.0066	35.69	0.0004	38.11
200	- 0.0013	36.76	- 0.0055	35.195	0.0009	38.68
250	- 0.0009	36.61	- 0.0045	34.75		
300	- 0.0002	36.48	- 0.0034	34.38		
400	0.0004	36.30	- 0.0013	33.81		
500	0.0012	36.21	0.0007	33.46		
600	0.0021	36.217	0.0026	3.32		
650	0.0025	36.219	0.0035	33.33		
700			0.0044	33.39		

Table (5.5) (continued): Effect of Injecting Reactive Power on Sensitivity and Losses

Q_i [MVAR]	Bus No. 15		Bus No. 17	
	$\partial P_{\text{loss}}/\partial Q_i$	Losses [Mw]	$\partial P_{\text{loss}}/\partial Q_i$	Losses [Mw]
0	- 0.0022	37.592	- 0.0022	37.592
10	- 0.0018	37.55	- 0.0020	37.565
50	- 0.0003	37.43	- 0.0012	37.479
100	0.0016	37.37	- 0.0003	37.418
150	0.0034	37.41	0.0007	37.406
200			0.0016	37.44

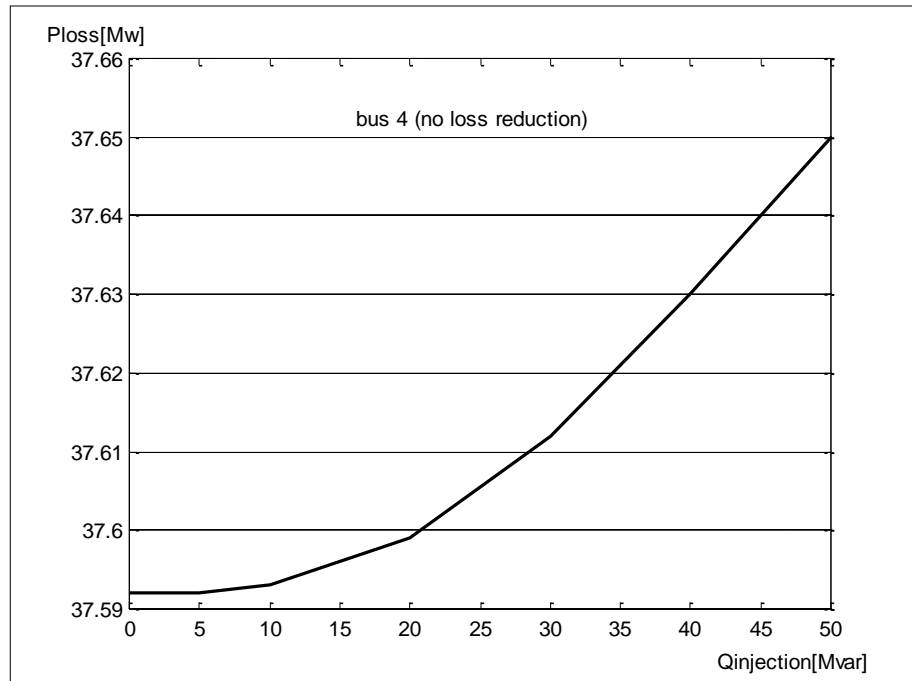


Figure (5.15): P_{loss} vs. $Q_{\text{injection}}$ for Bus 4 (QAM)

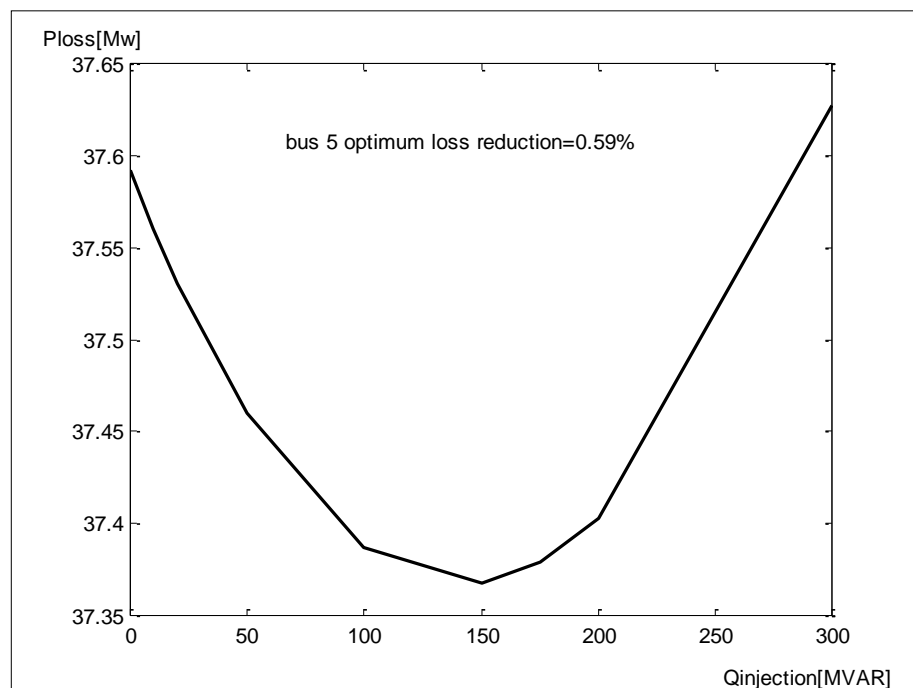


Figure (5.16): P_{loss} vs. $Q_{\text{injection}}$ for Bus 5 (MOS)

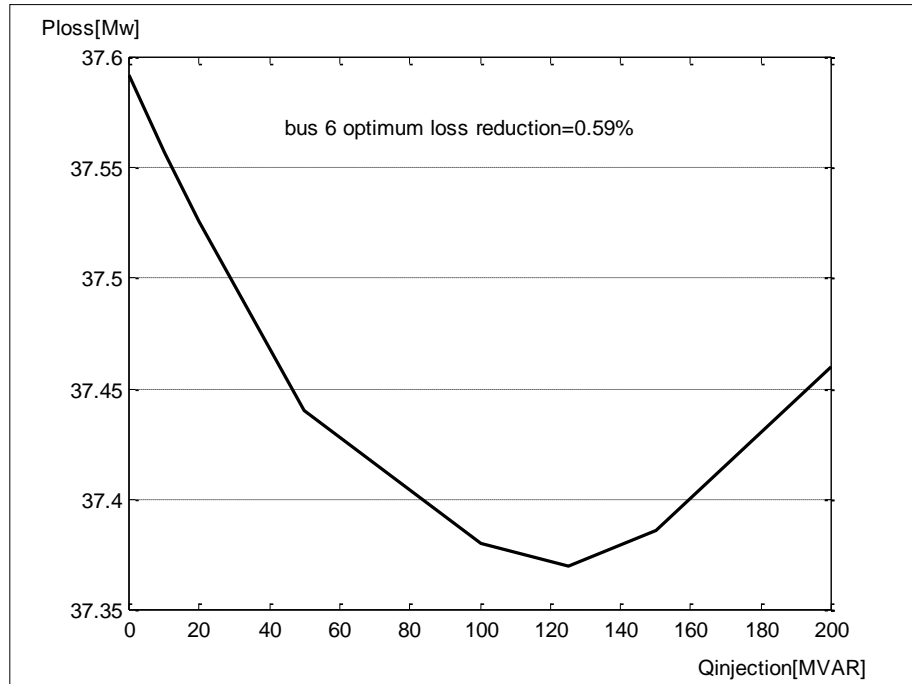


Figure (5.17): P_{loss} vs. $Q_{\text{injection}}$ for Bus 6 (KRK)

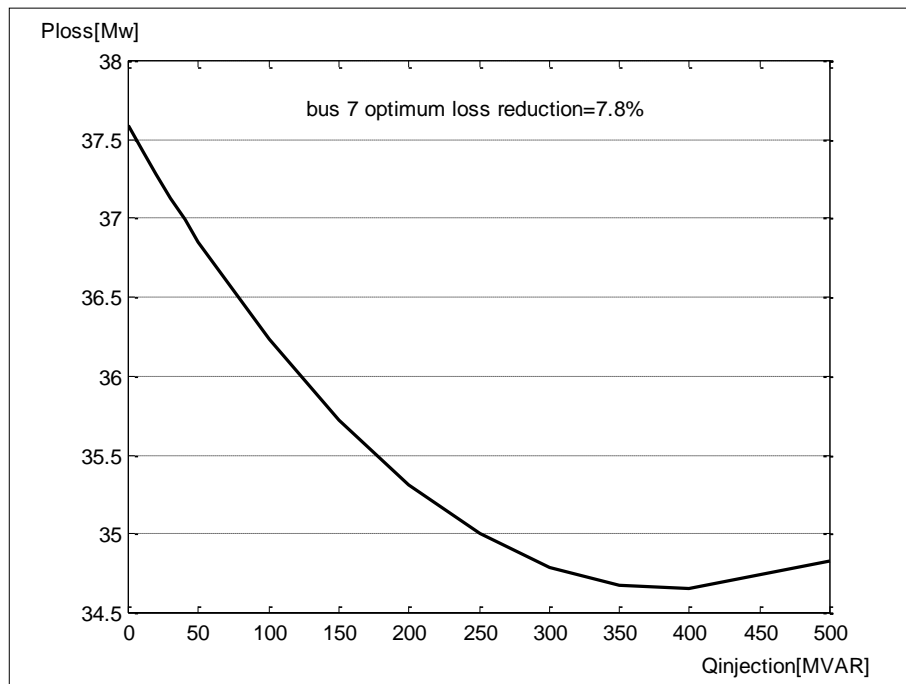


Figure (5.18): P_{loss} vs. $Q_{\text{injection}}$ for Bus 7 (BQB)

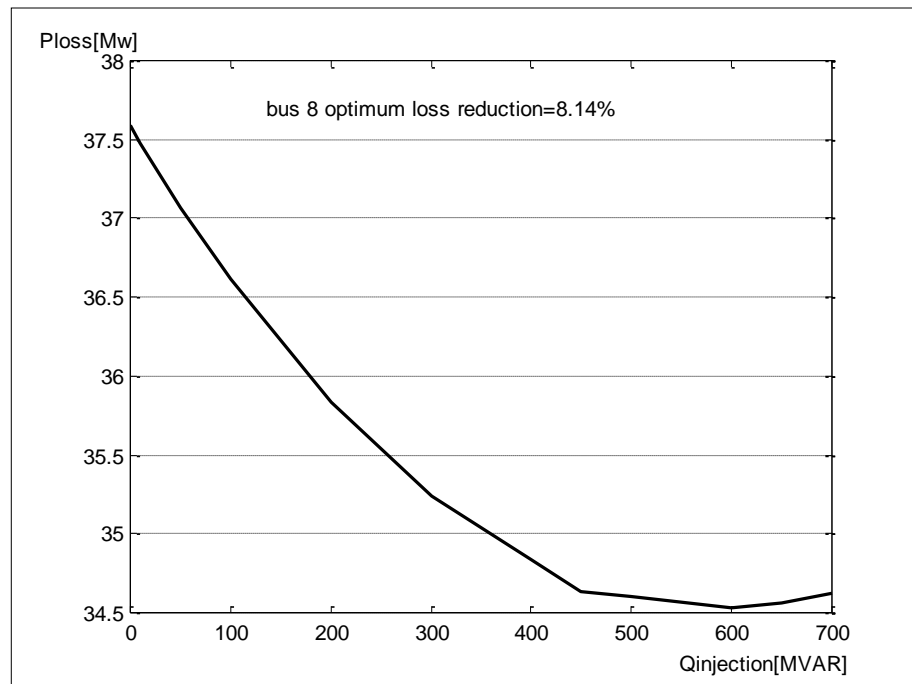


Figure (5.19): P_{loss} vs. $Q_{\text{injection}}$ for Bus 8 (BGW)

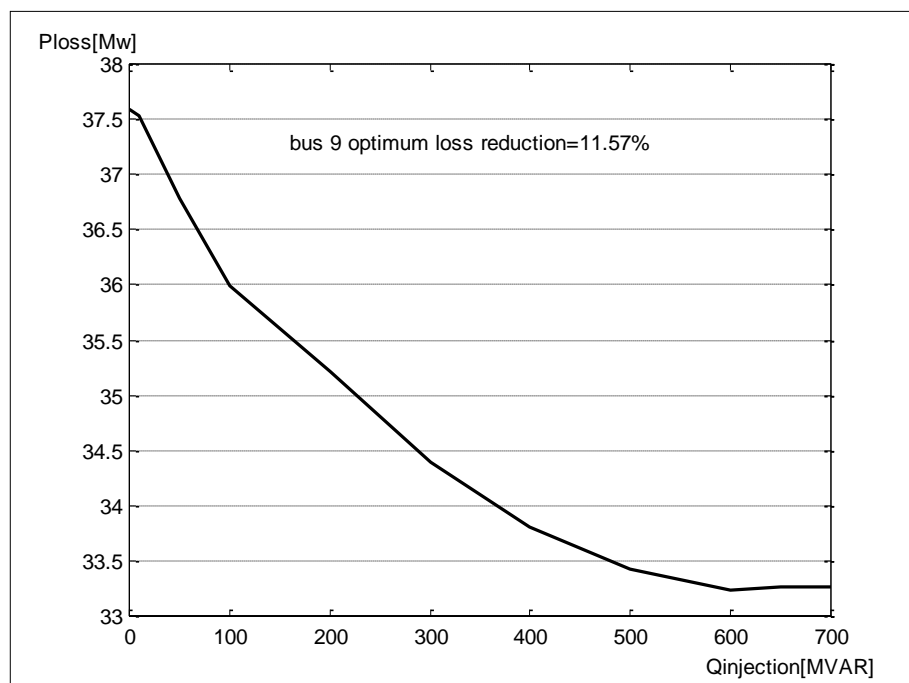


Figure (5.20): P_{loss} vs. $Q_{\text{injection}}$ for Bus 9 (BGE)

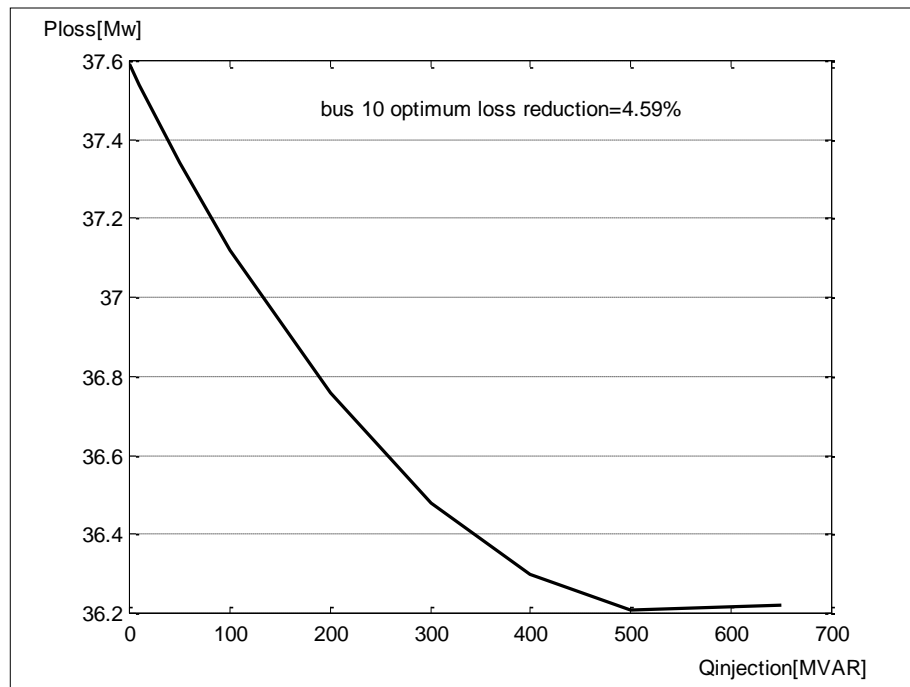


Figure (5.21): P_{loss} vs. $Q_{\text{injection}}$ for Bus 10 (BGS)

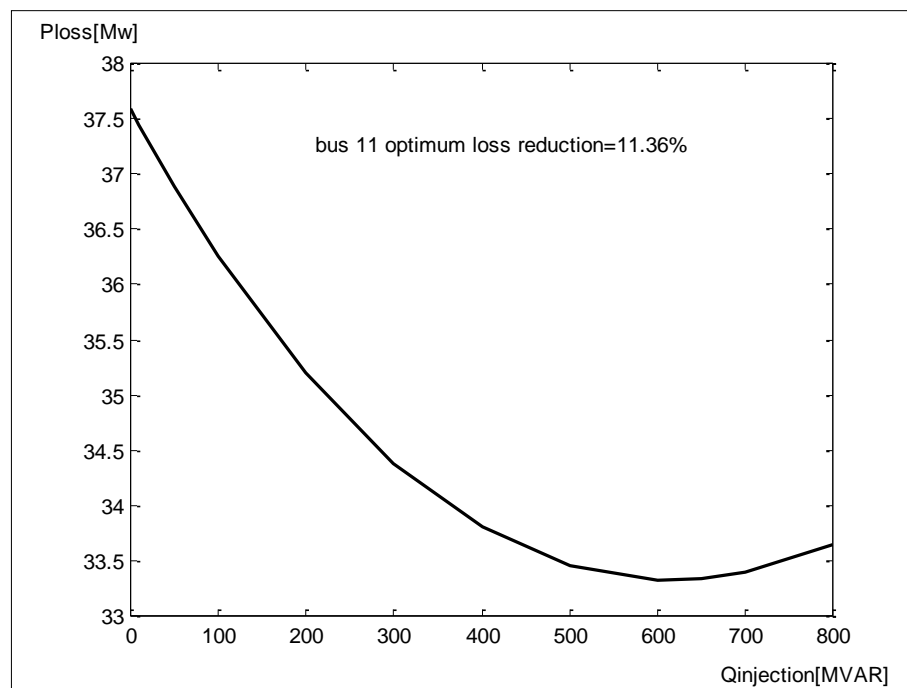


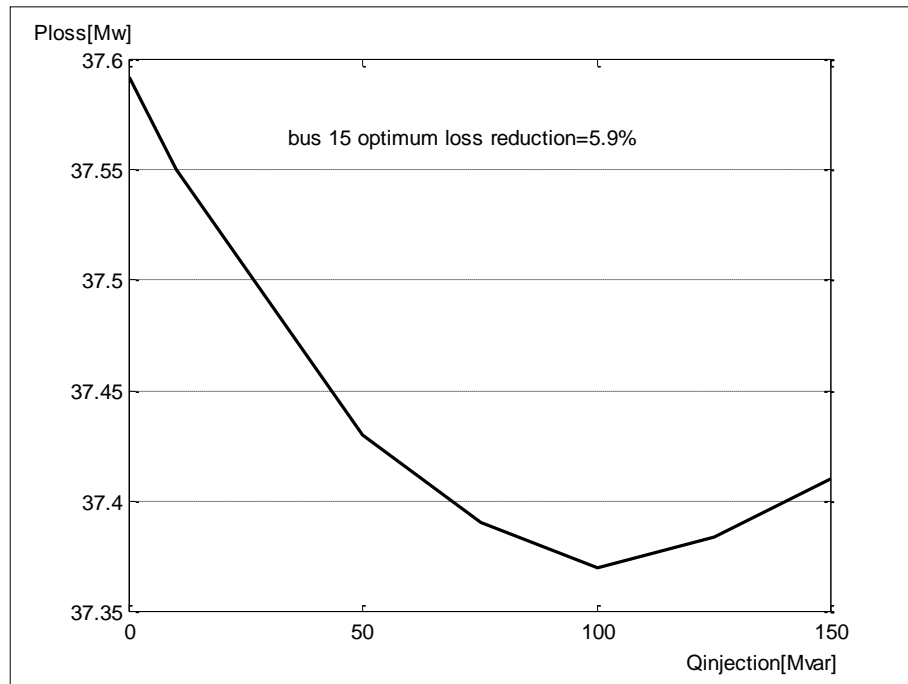
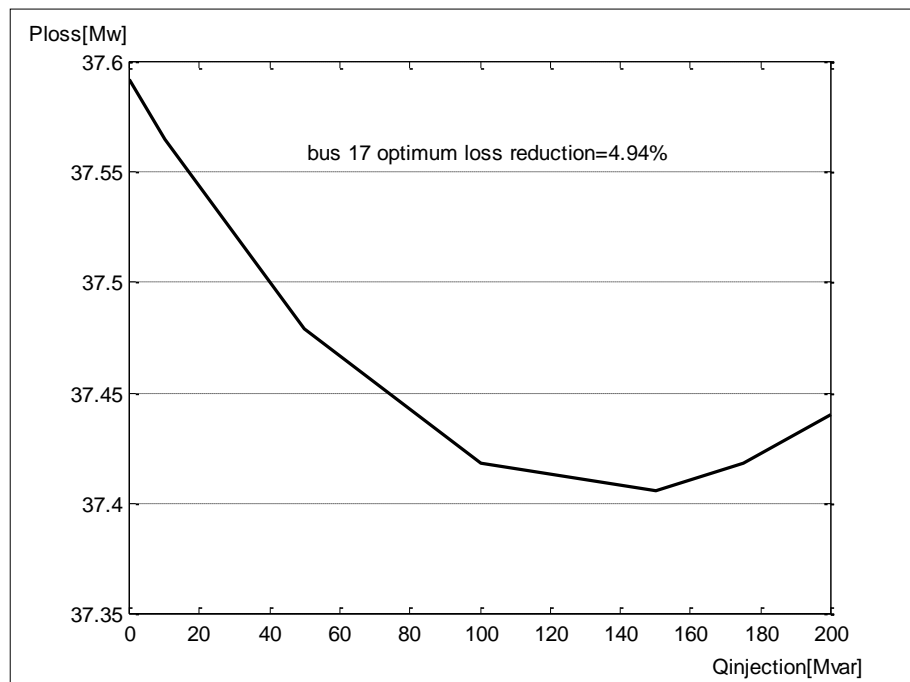
Figure (5.22): P_{loss} vs. $Q_{\text{injection}}$ for Bus 11 (BGN)**Figure (5.23): P_{loss} vs. $Q_{\text{injection}}$ for Bus 15 (KAD)****Figure (5.24): P_{loss} vs. $Q_{\text{injection}}$ for Bus 17 (KAZ)**

Table (5.6): Effect of Injecting Reactive Power on Sensitivity and Losses at Buses 14 (KUT) and 19 (QRN)

Q_i [MVAR]	Bus No. 14		Bus No. 19	
	$\partial P_{\text{loss}}/\partial Q_i$	Losses [Mw]	$\partial P_{\text{loss}}/\partial Q_i$	Losses [Mw]
- 100	- 0.0015	37.72	- 0.0004	37.549
- 90	- 0.0012	37.69	- 0.0002	37.543
- 80	- 0.0009	37.66	0.0000	37.539
- 70	- 0.0005	37.648	0.0003	37.537
- 60	- 0.0002	37.631	0.0005	37.538
- 50	0.0001	37.616	0.0007	37.5418
- 40	0.0004	37.605	0.0010	37.547
- 30	0.0007	37.597	0.0012	37.555
- 20	0.0010	37.5927	0.0014	37.565
- 10	0.0012	37.5910	0.0016	37.577
0	0.0015	37.592	0.0019	37.592
5	0.0016	37.594		
10	0.0018	37.596	0.0021	37.609
20			0.0023	37.628
30			0.0025	37.650
50	0.0030	37.64		

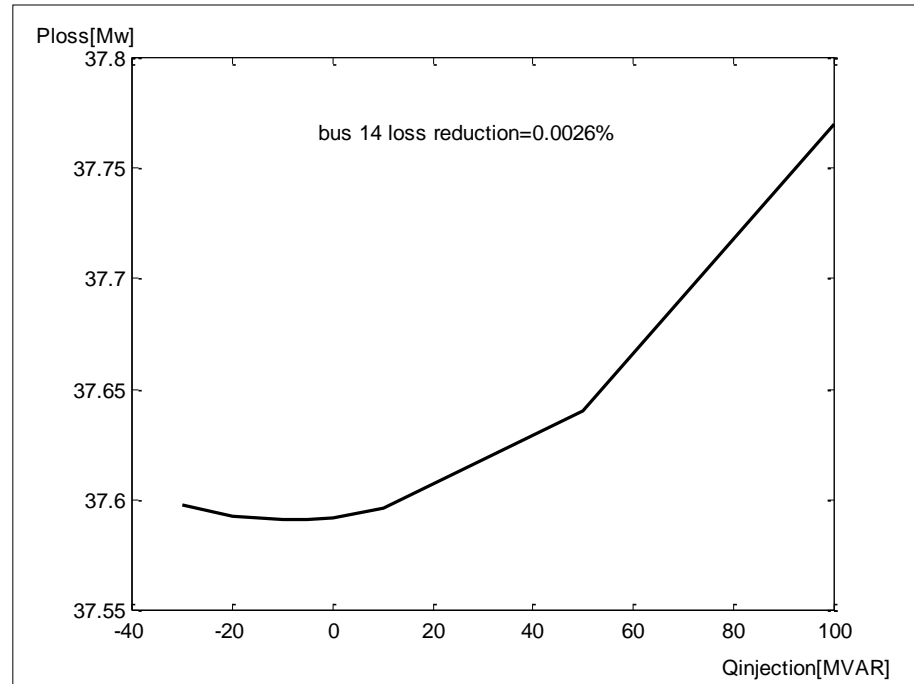


Figure (5.25): P_{loss} vs. $Q_{\text{injection}}$ for Bus 14 (KUT)

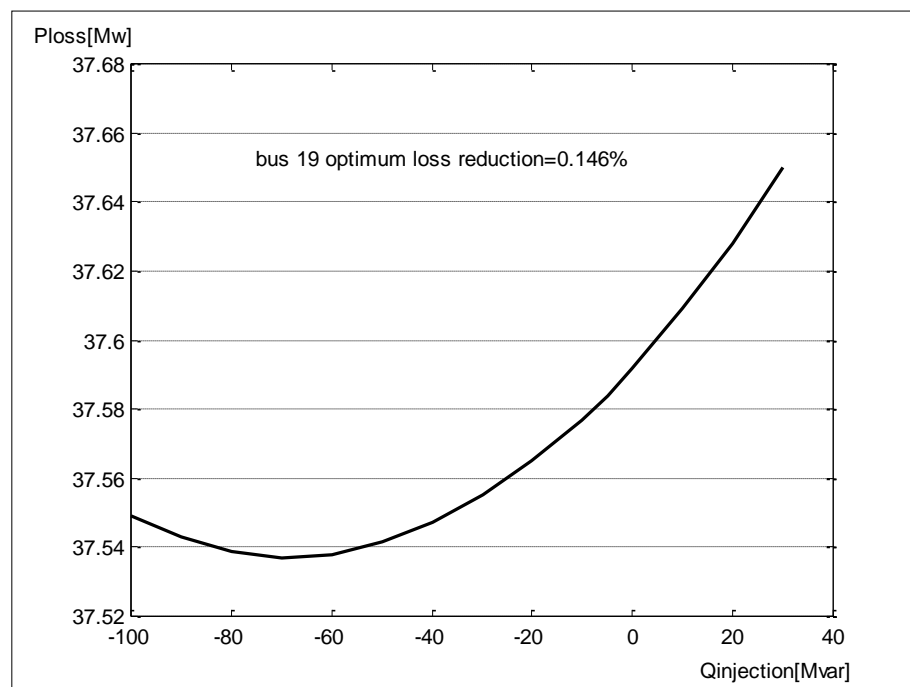


Figure (5.26): P_{loss} vs. $Q_{\text{injection}}$ for Bus 19 (QRN)

Table (5.7): Injection Reactive Power which Gives Max Loss Reduction

Bus No.	$Q_{inj.}$ [MVAR]	Minimum Losses [Mw]	Max. losses Reduction %
9	600	33.24	11.57
11	600	33.32	11.36
8	600	34.53	8.14
7	300	34.78	7.48
15	100	37.37	5.9
17	150	37.406	4.94
10	500	36.21	3.67
5	150	37.368	0.595
6	125	37.37	0.59
13	50	37.56	0.085

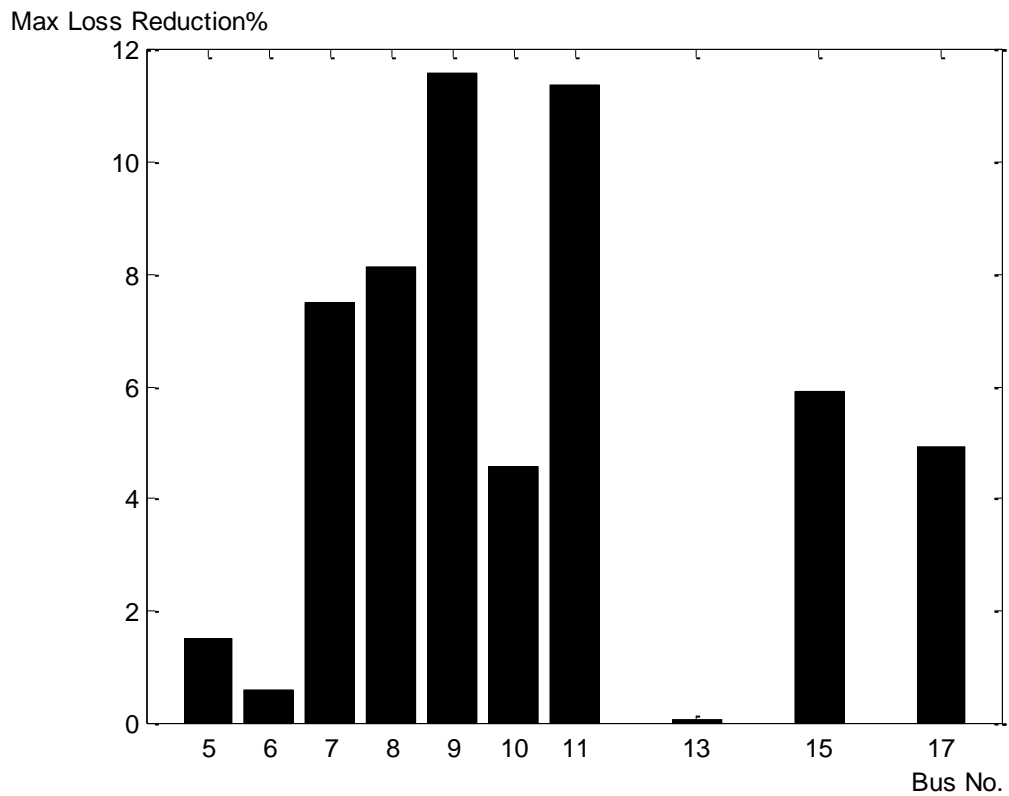


Figure (5.27): Loss Reduction for Injecting Reactive Power at some buses

5.1.3 Injecting Equal Amount of Active Power at the Same Time:

The first six buses in Table (5.1) i.e. (7, 8, 9, 10, 11, 15) have been chosen as the best buses in loss sensitivity (P_{sen}) to the injection of active power. Table (5.8) and Figure (5.28) show the system total losses when injecting equal amount of active power at mean time. Injecting total active power equal to (840 Mw) i.e. 140 Mw to each one of the six buses at the same time gives total system losses equal to 25.069 Mw. So:

$$\text{Loss reduction} = \frac{37.592 - 25.069}{37.592} \times 100\% = 33.31\% .$$

Notice that injecting active power affects slightly the sequence of buses with the best sensitivity as shown in Table (5.9) and Figure (5.29).

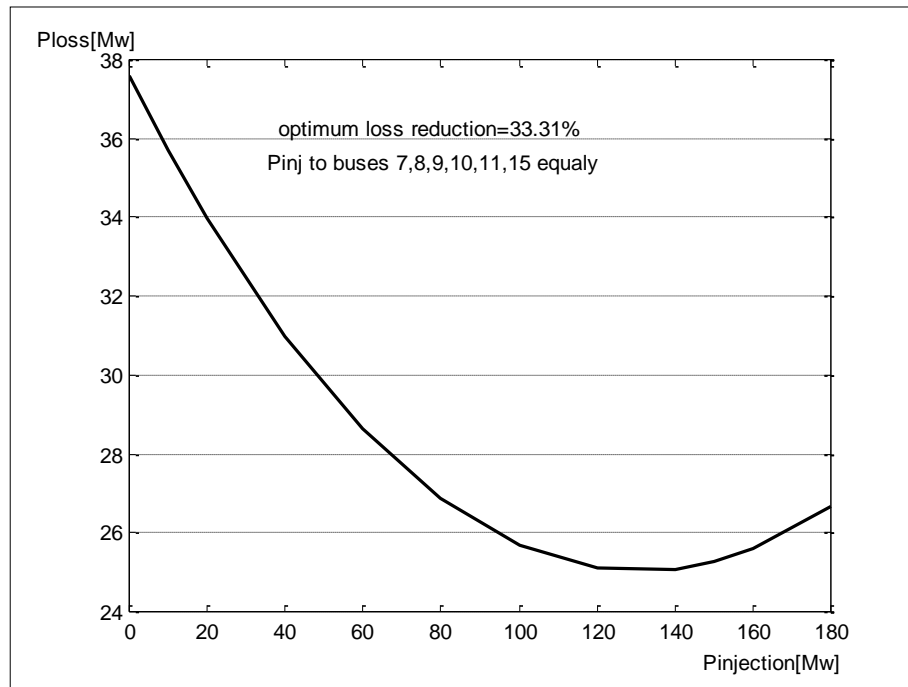


Figure (5.28): P_{loss} vs P_{inj} at Buses 7, 8, 9,10,11,15 Equally at the Same Time

Table (5.9): Effect of Injecting (100 Mw) on the Sequence of Buses Sensitivity

	Before insertion Pin		After insertion Pin	
	Bus No.	$\partial P_{\text{loss}}/\partial P_i$	Bus No.	$\partial P_{\text{loss}}/\partial P_i$
1.	7	- 0.0392	7	- 0.0182
2.	9	- 0.0361	11	- 0.0170
3.	11	- 0.0359	9	- 0.0168
4.	8	- 0.0279	8	- 0.0125
5.	10	- 0.0258	10	- 0.0066
6.	15	- 0.0230	15	0.0001

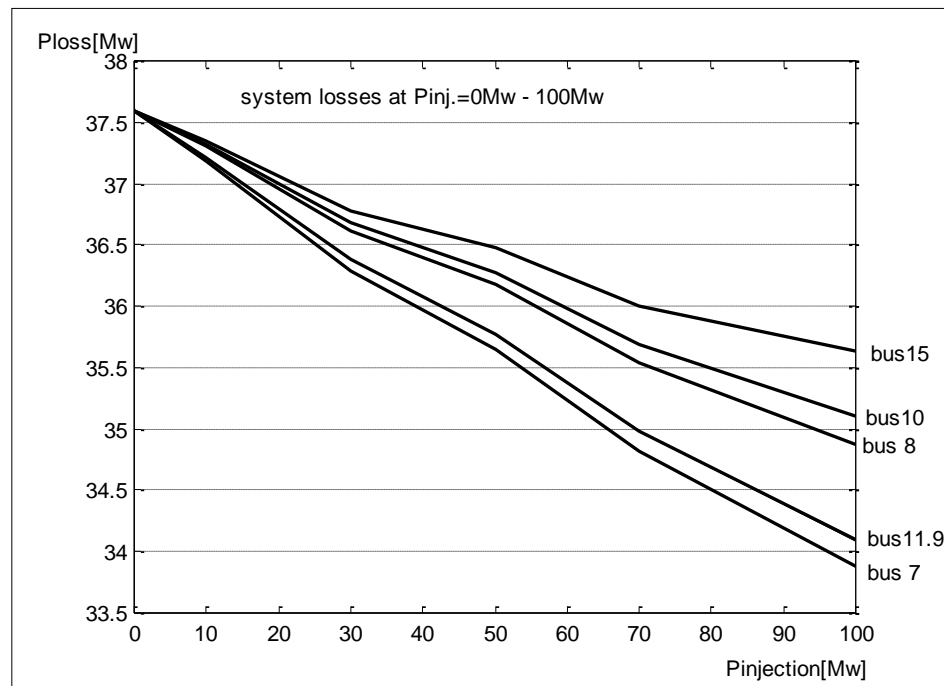


Figure (5.29): P_{loss} vs P_{inj} at Buses 7, 8, 9, 10, 11, 15 Individually

5.1.4 Injecting Equal Amount of Reactive Power at the Same Time:

The first eight buses in Table (5.4) i.e. (5, 6, 7, 8, 9, 10, 11, 15) have been chosen as the best buses in loss sensitivity (Q_{sen}) to the injection of reactive power. Table (5.10) and Figure (5.30) show the relationship between loss reduction and amount of reactive power injected in the eight buses at the same time. Injecting 1040 MVAR i.e. (130 MVAR) at each load bus gives total system losses equal to 33.2827 Mw:

$$\text{Loss reduction} = \frac{37.592 - 33.282}{37.592} \times 100\% = 11.46\%$$

Injecting reactive power affects slightly the sequence of buses with the best sensitivity to reduce losses as shown in Table (5.11) and Figure (5.31).

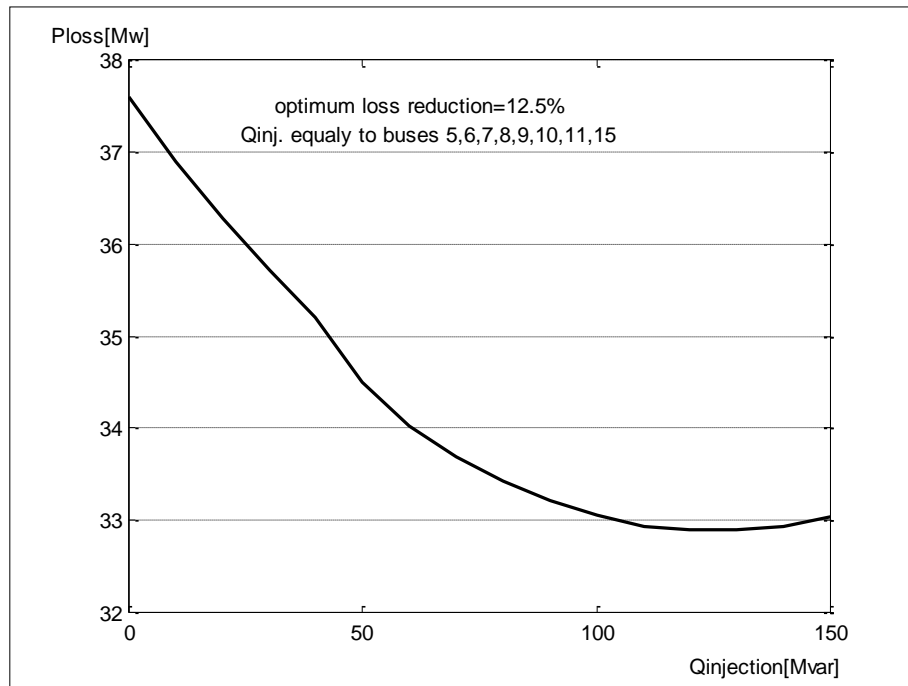


Figure (5.30): P_{loss} vs Q_{inj} . at Buses 5,6,7,8,9,10,11,15 Equally at the Same Time

Table (5.11): Buses Sensitivity Sequence when Injecting (80 MVAR)

	Before Injection		After Injection	
	Bus No.	$\partial P_{\text{loss}} / \partial Q_i$	Bus No.	$\partial P_{\text{loss}} / \partial Q_i$
1.	7	- 0.0107	11	- 0.0031
2.	11	- 0.0101	9	- 0.0028
3.	9	- 0.0097	7	- 0.0023
4.	8	- 0.0068	8	- 0.0019
5.	5	- 0.0035	5	- 0.0017
6.	10	- 0.0031	10	+ 0.0003
7.	15	- 0.0022	6	+ 0.0016
8.	6	- 0.0022	15	+ 0.0024

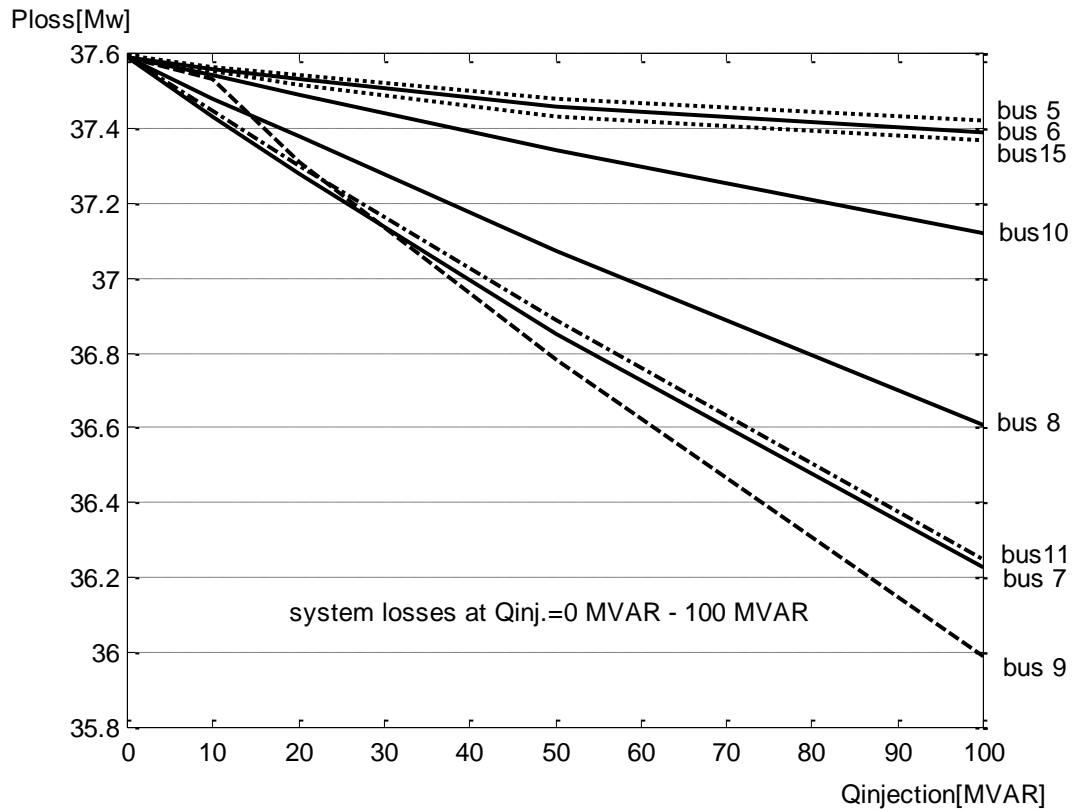


Figure (5.31): P_{loss} vs Q_{inj} . at Buses 5, 6,7,8,9,10,11,15 Individually

5.1.5 Optimal Quantity and Placement of Active Power Injection at Load Buses:

The optimal power injection at all buses is obtained by adding in steps small real power (U) equal to (5 Mw) in each step at the buses with the negative partial derivative of power losses with respect to real injection power (sensitivity) as shown before in Table (5.1).

The addition of active power to each bus is stopped when sensitivity at that bus becomes zero or positive, the overall addition is stopped when sensitivity in all buses becomes zero or positive, at the same time this process must satisfy the constraints including reactive power limits of the generators as shown in (Appendix F) where the load bus voltage limit is pulse minus 0.05.

The injecting of 180,200,210 and 300 Mw i.e. total power injected is equal to (890 Mw) at the buses 7,8,9,11 respectively (which were chosen in

section 5.1.3 as the best buses) gives total system losses equal to 21.824 Mw. So:

$$\text{Loss Reduction} = \frac{37.592 - 21.824}{37.592} \times 100\% = 41.94\% .$$

To compare the optimum result with the losses when injecting equal amount of power as mentioned in section (5.1.3), divide total injecting power which gives optimum results by the number of buses then injecting equal amount of active power = $\frac{890}{6} = 148.33Mw$.

Injecting 148.33 Mw at each bus at the same time gives power loss equal to 25.25 Mw and losses reduction equal to (32.8 %) according to Table (5.8).

41.94 – 32.8 = 9.14 % is the difference between losses reduction in case of optimal addition of real power to load buses and addition with equal amount of real power.

5.1.6 Optimal Quantity and Placement of Reactive Power Injection at Load Buses:

The procedure is similar to that for injecting optimal active power at the buses. In this case and according to flow chart in Figure (3.2), injecting U= (5 MVAR) at each load bus is stopped when sensitivity of power losses with respect to reactive power injected becomes zero or positive and satisfies the constraints including reactive power limits of the generators and load buses voltages as shown in (Appendix F).

The total reactive power to be added is equal to (920 MVAR) which gives total system losses equal to 32.64 Mw and losses reduction equal (13.17 %). To compare the optimal result with that taken when injecting equal amount of reactive power, divide total injecting power which gives optimal results by eight which is the number of the best buses that were

chosen in section 5.1.4 as the more sensitive buses, then injecting equal amount of reactive power = $\frac{920}{8} = 115\text{MVAR}$.

Injecting 115 MVAR at each one of the eight buses at the same time gives power loss equal to 33.309 Mw and reduction equal to (11.39 %) as shown before according to Table (5.10).

Saving Loss Reduction = $13.17 - 11.39 = 1.78\%$ between the two cases.

5.1.7 Control of Active Power at Generation Buses:

The sensitivities $\partial P_{\text{loss}}/\partial P_g$ at the generation buses (2, 3, 12, 16 and 18) were calculated according to equation (3.14). The results give indication of the system efficiency to reduce losses when generating active power at these buses, as shown in Tables (5.12)-(5.16) and Figures (5.32)-(5.41).

If sensitivity value at any bus is negative, then increasing power generation at that bus reduces system losses. On the other hand if the sensitivity value at any bus is positive, the system losses decrease in case of reducing power generation at that bus.

Optimal power generation was calculated using procedure similar to that implemented in section (5.1.5). Generation at each bus is increased by (10 Mw) at each step until the sensitivity at the bus becomes zero or positive, i.e. the system losses start to increase. Table (5.17) and Figures (5.42) and (5.43) show active power generation at each generation bus which gives minimum losses equal to (25.95 Mw) with optimal losses reduction equal to (30.96 %).

Table (5.12): System Losses and Sensitivities at Generation Bus 2 (SDM)

$P_{\text{generation}}$ [Mw]	Losses [Mw]	Sensitivity $\frac{\partial P_{\text{Loss}}}{\partial P_g}$	$P_{\text{generation}}$ [Mw]	Losses [Mw]	Sensitivity $\frac{\partial P_{\text{Loss}}}{\partial P_g}$
0	32.789	- 0.0131	625	35.747	0.0225
100	31.75	- 0.0074	650	36.327	0.0239
150	31.45	- 0.0045	660	36.569	0.0245
200	31.29	- 0.0016	670	36.816	0.0251
250	31.28	+ 0.0012	680	37.069	0.0256
300	31.41	0.0041	690	37.328	0.0262
400	32.113	0.0098	700	37.592	0.0268
500	33.375	0.0155	710	37.862	0.0273
525	33.779	0.0169	720	38.137	0.0279
550	34.212	0.0183	730	38.419	0.0285
575	34.692	0.0197	740	38.705	0.0290
600	35.202	0.0211	750	38.998	0.0296

Table (5.13): System Losses and Sensitivities at Generation Bus 3 (HAD)

$P_{\text{generation}}$ [Mw]	Losses [Mw]	Sensitivity $\frac{\partial P_{\text{Loss}}}{\partial P_g}$
300	37.925	- 0.0062
325	37.77	- 0.0050
350	37.662	- 0.0039
375	37.576	- 0.0027
400	37.52	- 0.0015
425	37.493	- 0.0004
450	37.496	0.0008
460	37.506	0.0013
470	37.520	0.0017
480	37.539	0.0022
490	37.563	0.0027
500	37.592	0.0031
510	37.625	0.0036
520	37.664	0.0041
530	37.706	0.0045
540	37.754	0.0050

**Table (5.14): System Losses and Sensitivities at Generation Bus 12
(MSB)**

$P_{\text{generation}}$ [Mw]	Losses [Mw]	Sensitivity $\frac{\partial P_{\text{Loss}}}{\partial P_g}$
550	38.796	- 0.0249
575	38.173	- 0.0222
600	37.592	- 0.0207
625	37.153	- 0.0190
650	36.553	- 0.0177
675	36.095	- 0.016
700	35.678	- 0.0147
750	34.965	- 0.0117
800	34.413	- 0.0087
850	34.021	- 0.0058
900	33.787	- 0.0028
950	33.711	0.0002
975	33.732	0.0016
1000	33.792	0.0031

**Table (5.15): System Losses and Sensitivities at Generation Bus 16
(NSR)**

$P_{\text{generation}}$ [Mw]	Losses [Mw]	Sensitivity $\frac{\partial P_{\text{Loss}}}{\partial P_g}$
600	37.984	- 0.0090
625	37.752	- 0.0062
650	37.592	- 0.0034
675	37.505	- 0.0007
700	37.49	0.0021
725	37.54	0.0049
750	37.677	0.0076
775	37.87	0.0104
800	38.15	0.0131
825	38.49	0.0158
850	38.90	0.0185
875	39.39	0.0213
900	39.99	0.0240

**Table (5.16): System Losses and Sensitivities at Generation Bus 18
(HRT)**

$P_{\text{generation}}$ [Mw]	Losses [Mw]	Sensitivity $\frac{\partial P_{\text{Loss}}}{\partial P_g}$
380	37.592	- 0.0096
400	37.39	- 0.0065
425	37.24	- 0.0027
450	37.19	0.0012
475	37.24	0.0050
500	37.389	0.0089
525	37.634	0.0127
550	37.97	0.0165
575	38.41	0.0203
600	38.953	0.0240

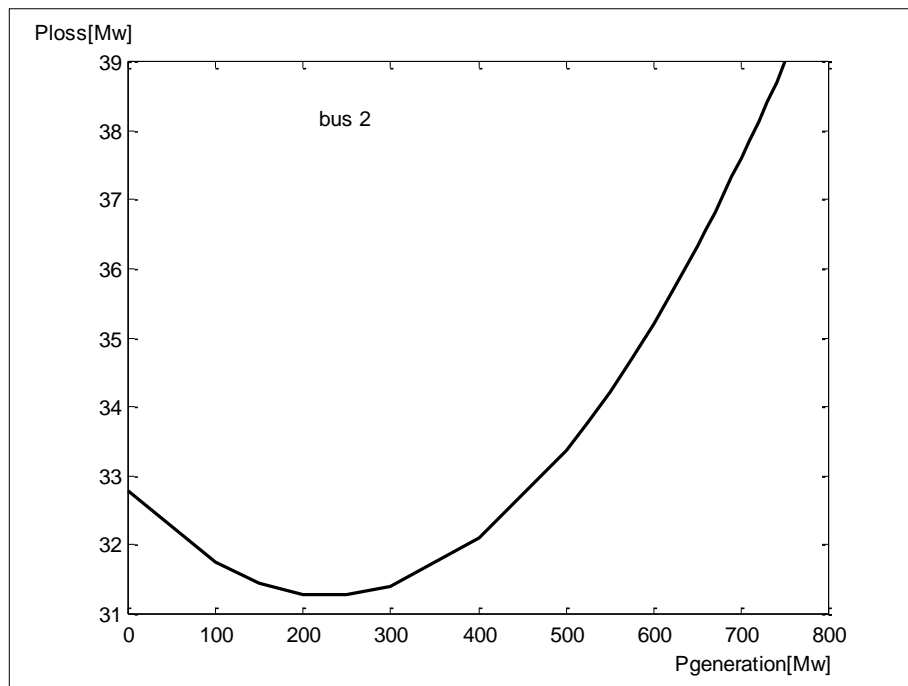


**Figure (5.32): Relationship between Generation and System Losses at
Bus 2 (MOS)**

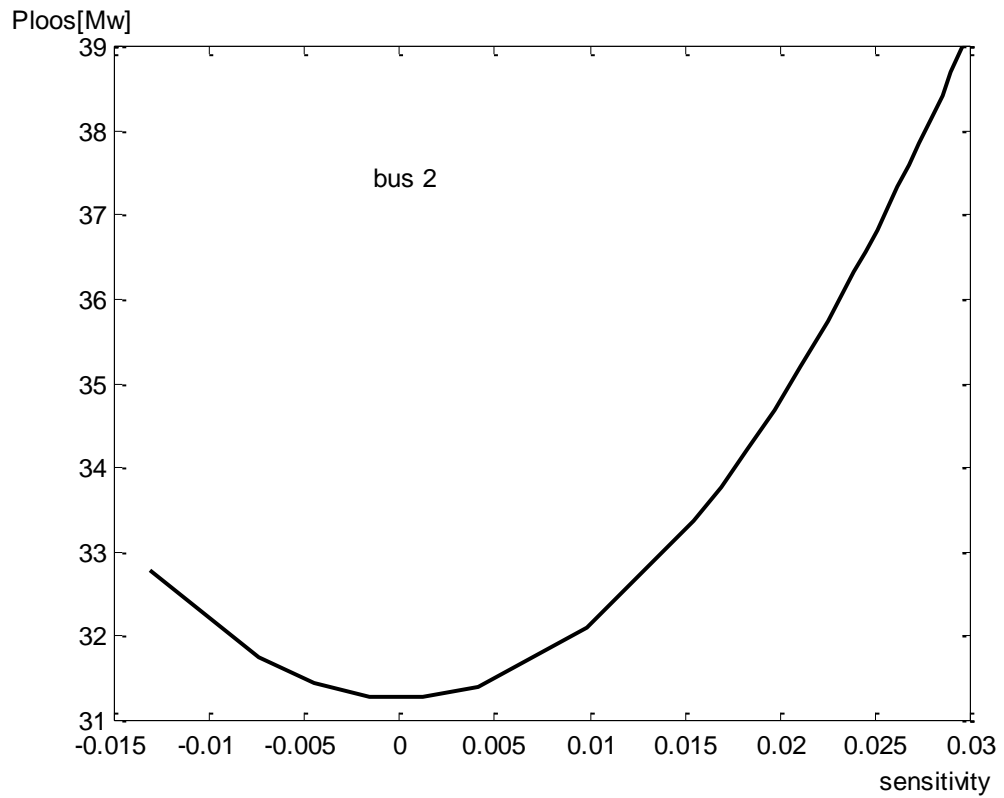


Figure (5.33): Relationship between Sensitivity and System Losses at Bus 2 (MOS)

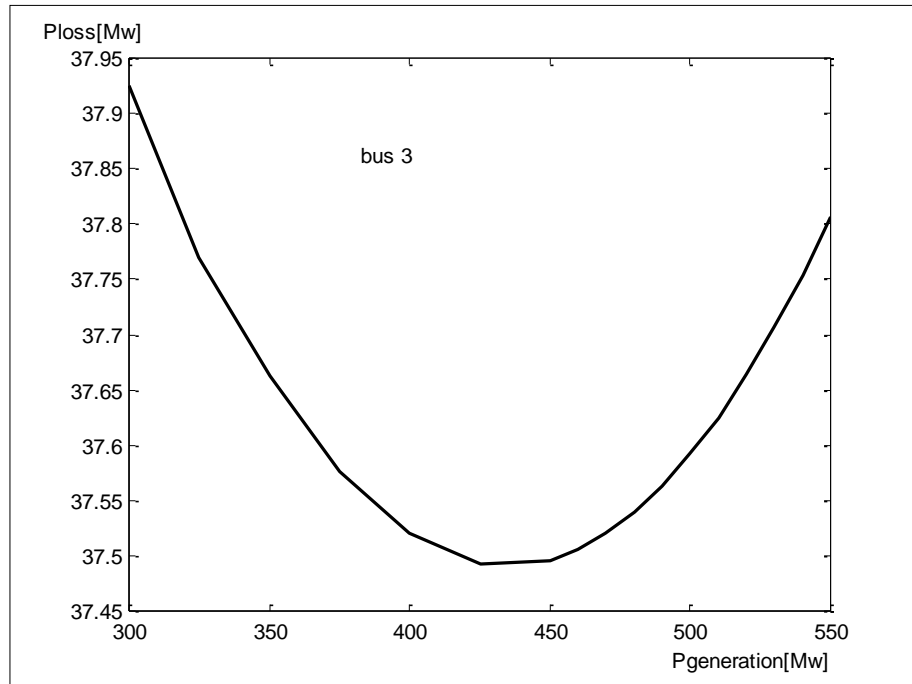


Figure (5.34): Relationship between Generation and System Losses at Bus 3 (HAD)

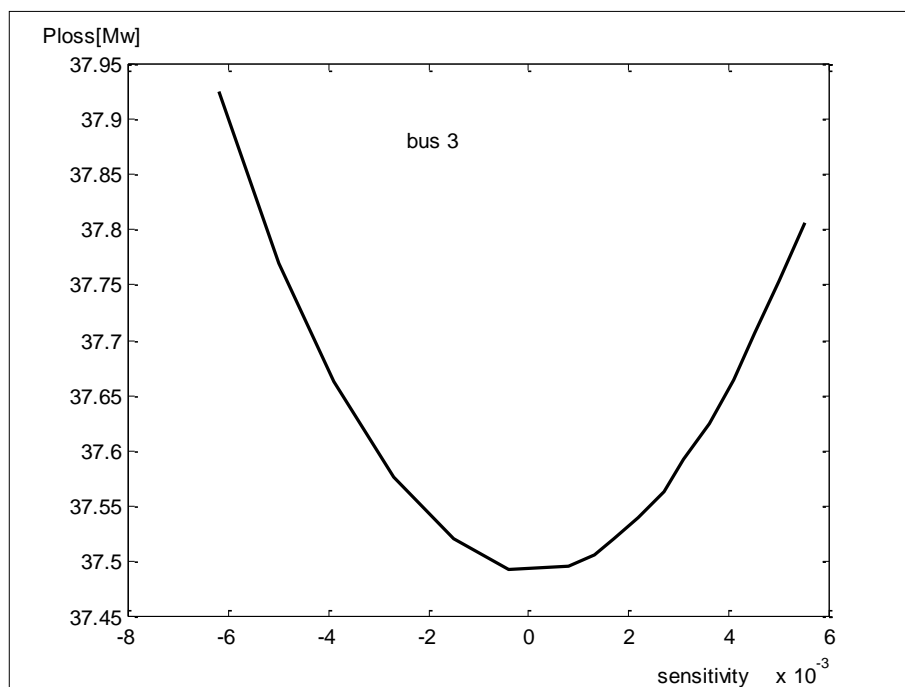


Figure (5.35): Relationship between Sensitivity and System Losses at Bus 3 (HAD)

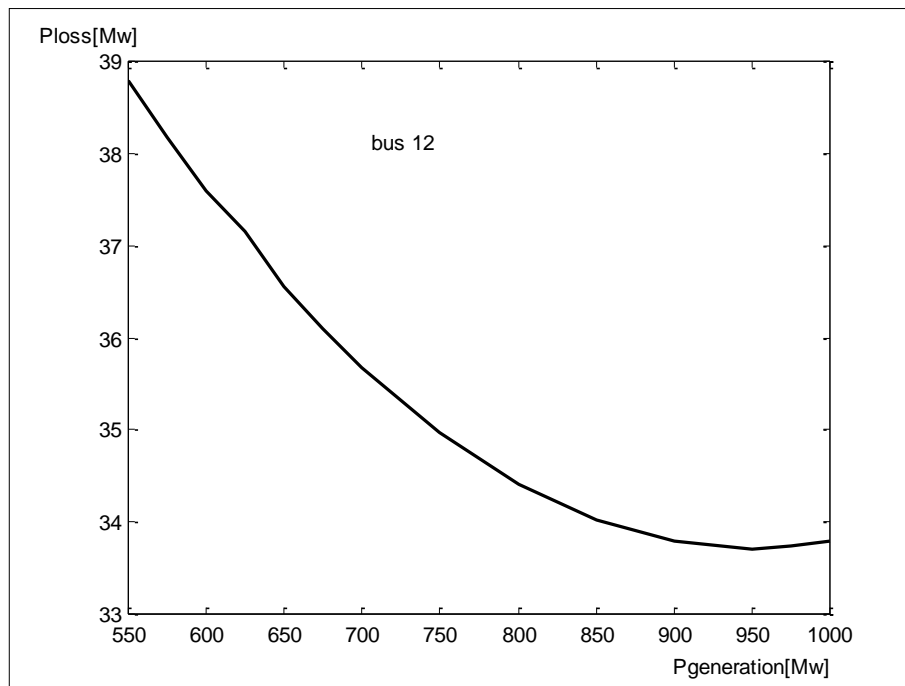


Figure (5.36): Relationship between Generation and System Losses at Bus 12 (MSB)

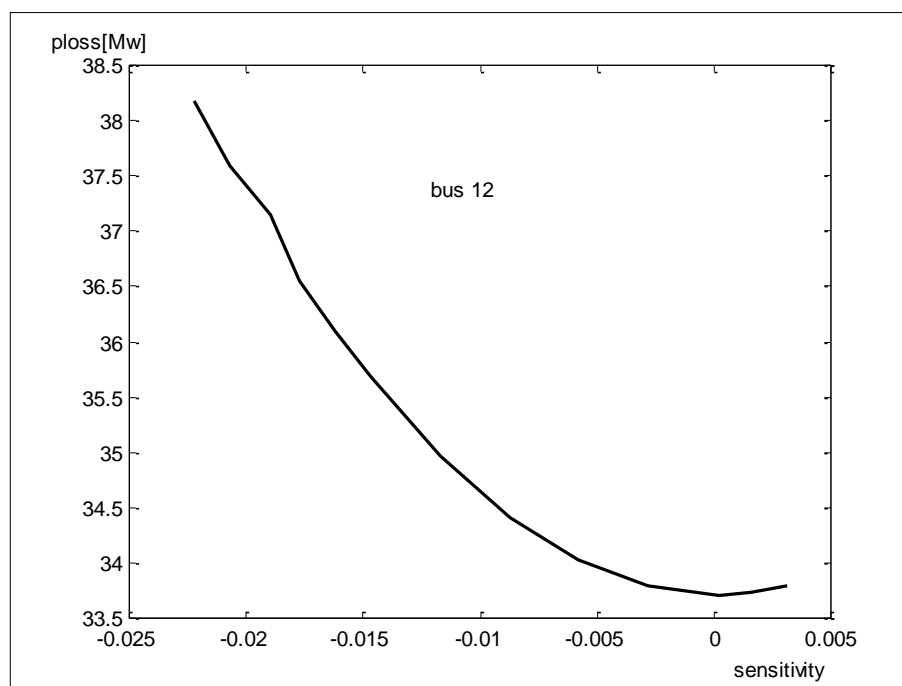


Figure (5.37): Relationship between Sensitivity and System Losses at Bus 12 (MSB)

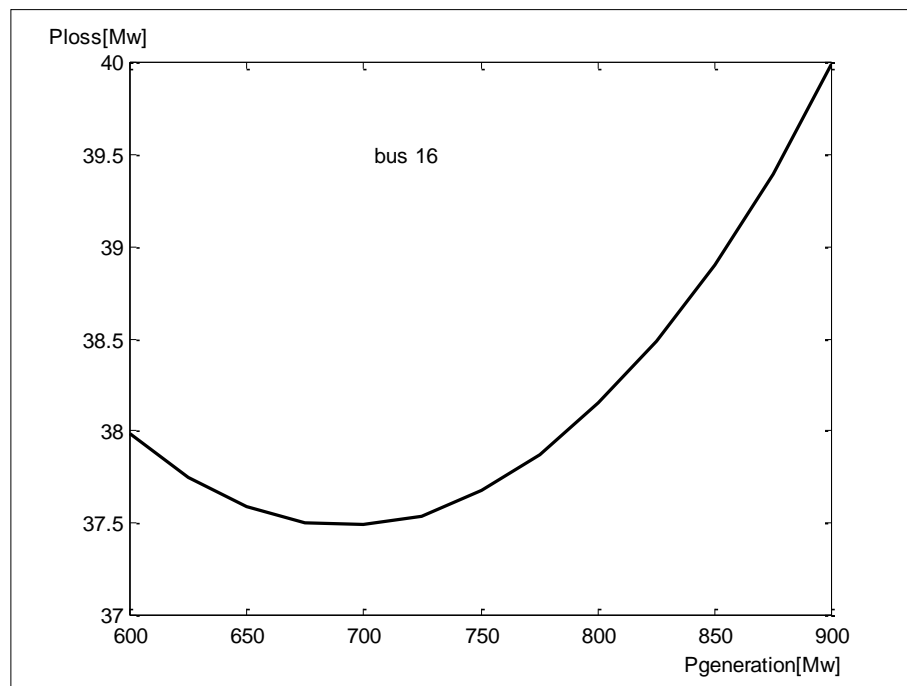


Figure (5.38): Relationship between Generation and System Losses at Bus 16 (NSR)

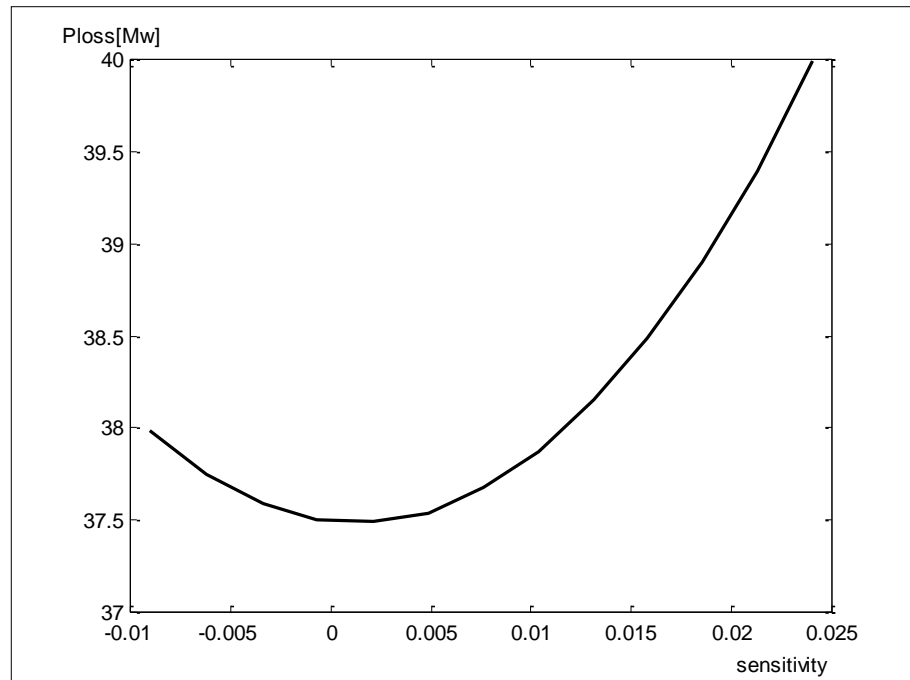


Figure (5.39): Relationship between Sensitivity and System Losses at Bus 16 (NSR)

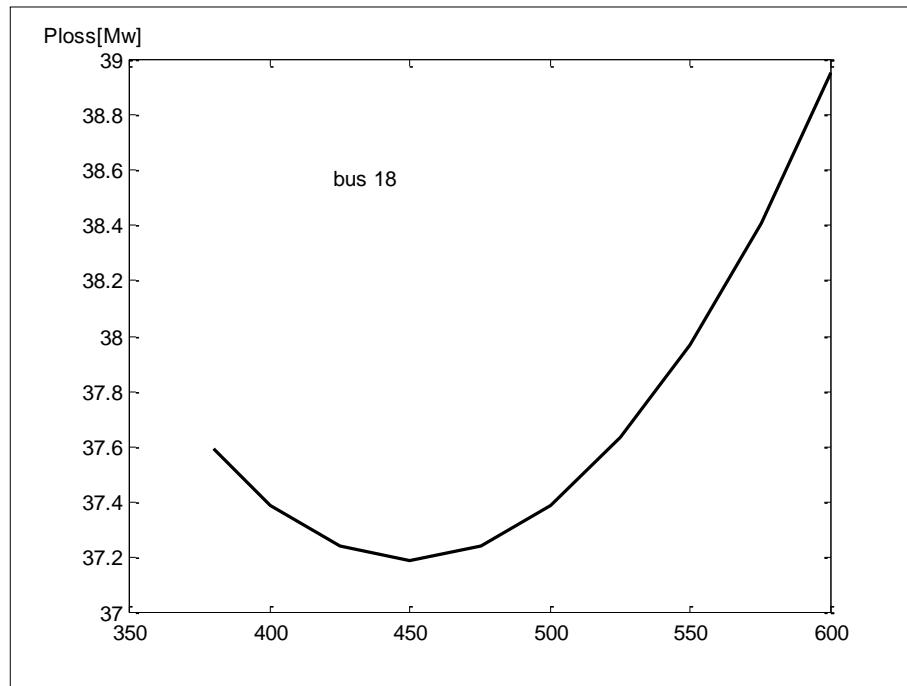


Figure (5.40): Relationship between Generation and System Losses at Bus 18 (HRT)

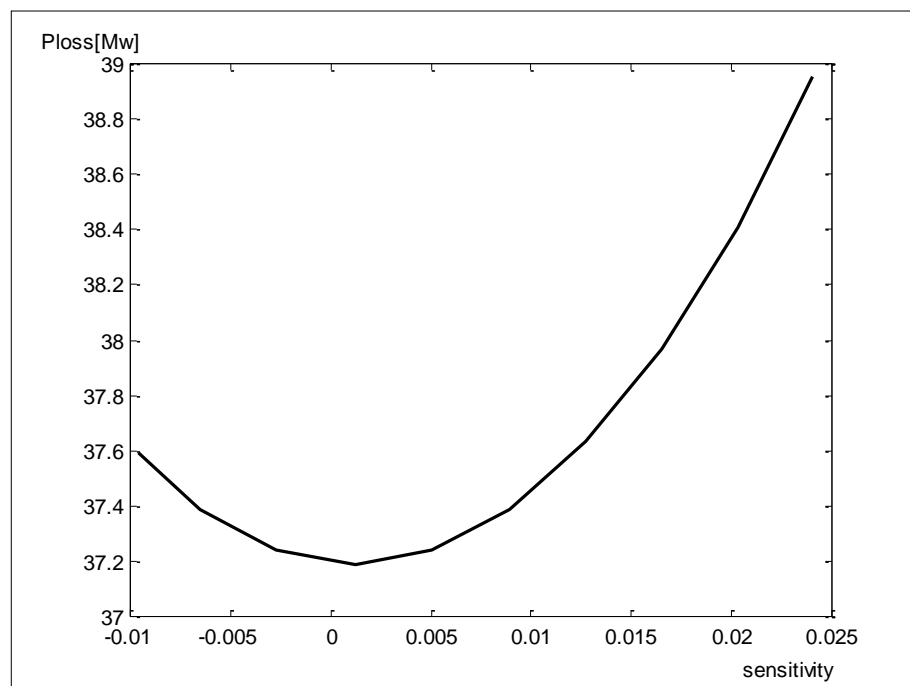


Figure (5.41): Relationship between Sensitivity and System Losses at Bus 18 (HRT)

Table (5.17): Active Power Generations which Give Optimal Losses Reduction

Generation Bus Number	Generation [Mw]
2 SDM	250
3 HAD	350
12 MSB	1000
16 NSR	500
18 HRT	400

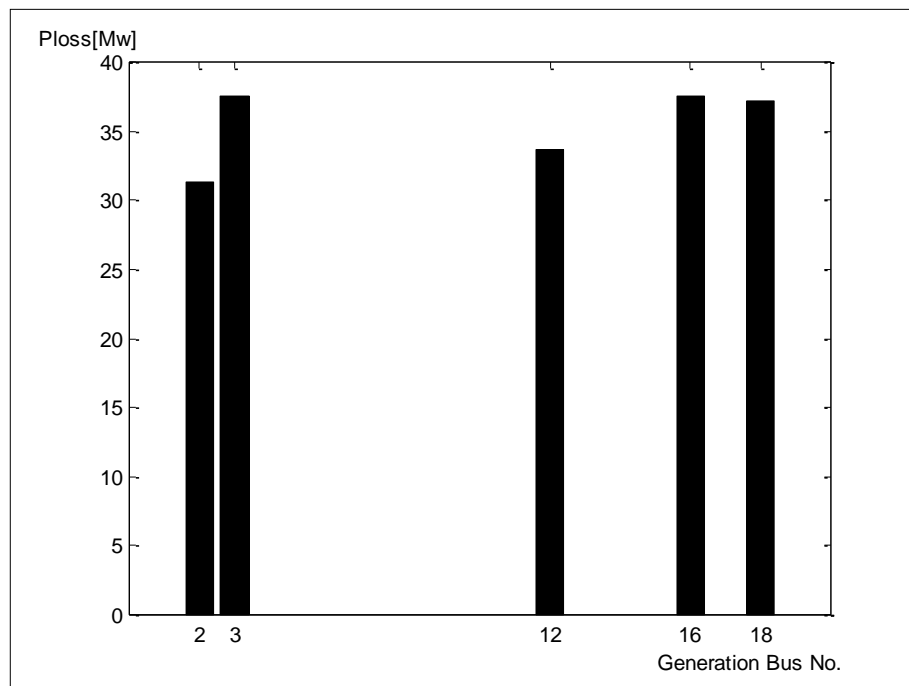


Figure (5.42): Generation Effect of Each Generating Bus Individually on System Losses

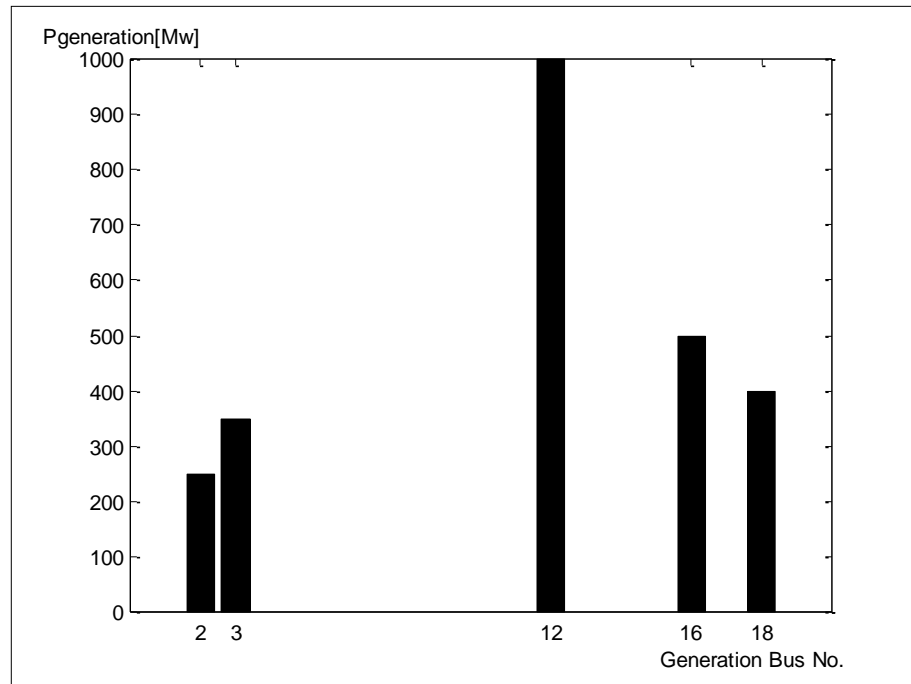


Figure (5.43): System Optimal Power Generation which Gives Minimum Losses

5.1.8 Load Flow Losses with Multi Contingencies:

Multi contingencies like removing transmission line, generating unit and bus bar, were studied and compared at different operating cases which are:

- 1- Ordinary load flow according to data in Appendix (B).
- 2- Optimal power injection at load buses as mentioned in section (5.1.5).
- 3- Optimal power generation at generation buses according to the results in Table (5.17).
- 4- Optimal active and reactive power injection at load buses as mentioned in sections (5.1.5) and (5.1.6) respectively.
- 5- Optimal power generation at generation buses and injection at load buses according to the results in Table (5.17) and section (5.1.5) respectively.

6- Optimal reactive power injection at load buses as mentioned in section (5.1.6).

Loss reduction in case of any contingency=

ordinary LF losses-modified LF losses/ordinary LF losses x 100%

5.1.8.1 Removing the Line 1-6 (BAJ-KRK):

Removing the line (1-6) does not isolate BAJ or KRK or any bus bar in the system. Minimum losses were calculated. According to each case mentioned in section (5.1.8), Table (5.18) and Figure (5.44) show losses in the system in case of different operating cases. Optimal generation with optimal injection of active power give minimum losses equal to 17.808 Mw and losses reduction equal to $\frac{48.315 - 17.808}{48.315} \times 100\% = 63.14\%$.

System losses for other operating cases lie between ordinary LF losses (48.315 Mw) and losses in case of optimal Pgeneration with Pinjection simultaneously (17.808 Mw).

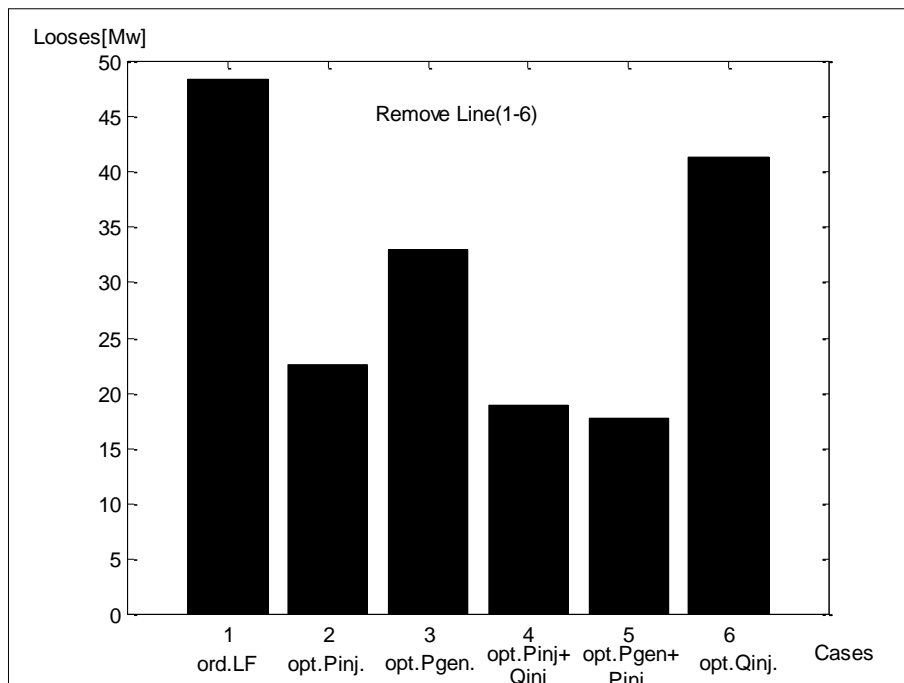


Figure (5.44): Minimum Losses for Different Cases when Removing Line 1-6 (BAJ-KRK)

5.1.8.2 Removing the Line 3-4 (HAD-QAM):

Removing the line (3-4) isolates (QAM) from the system. The system is unstable according to ordinary LF results in Appendix (C). Table (5.18) and Figure (5.45) show system losses in case of different operating cases. Injecting optimal active and reactive power at load buses (case 4) makes the system stable with minimum losses equal to (20.98 Mw) and losses reduction equal to $\frac{36.439 - 20.98}{36.439} \times 100\% = 42.42\%$.

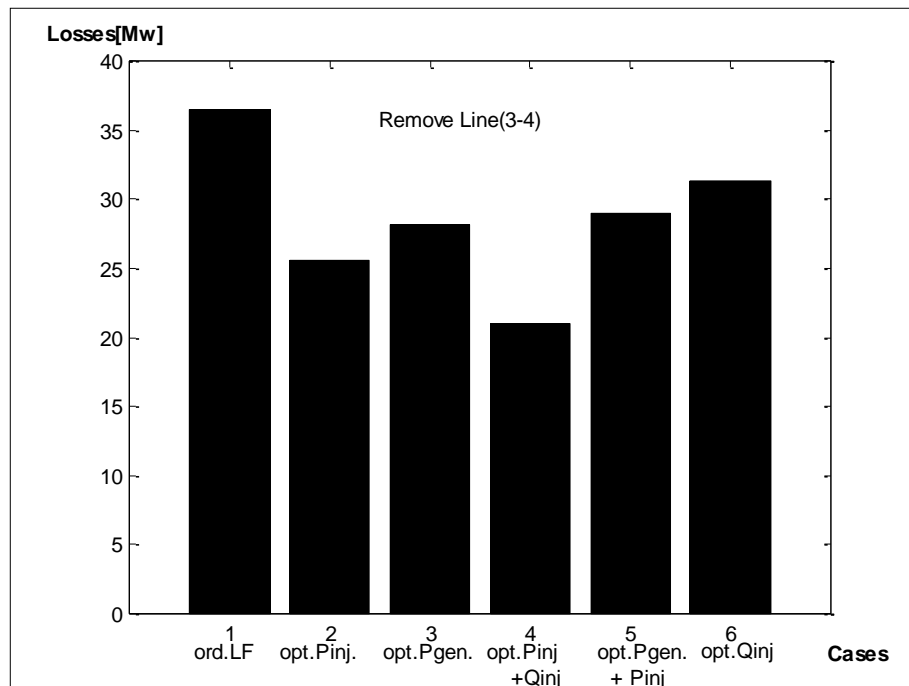


Figure (5.45): Minimum Losses for Different Cases when Removing Line 3-4 (HAD-QAM)

5.1.8.3 Removing Lines 1-6 (BAJ-KRK) and 3-4 (HAD-QAM):

Removing two lines is a multi-contingency case, these lines become not a part of the system. Figure (5.46) and Table (5.18) show system losses in case of different operating cases. Injecting optimal active and reactive power at load buses (case 4) gives minimum losses equal to (20.93 Mw) and losses reduction equal to $\frac{47.28 - 20.93}{47.28} \times 100\% = 55.73\%$.

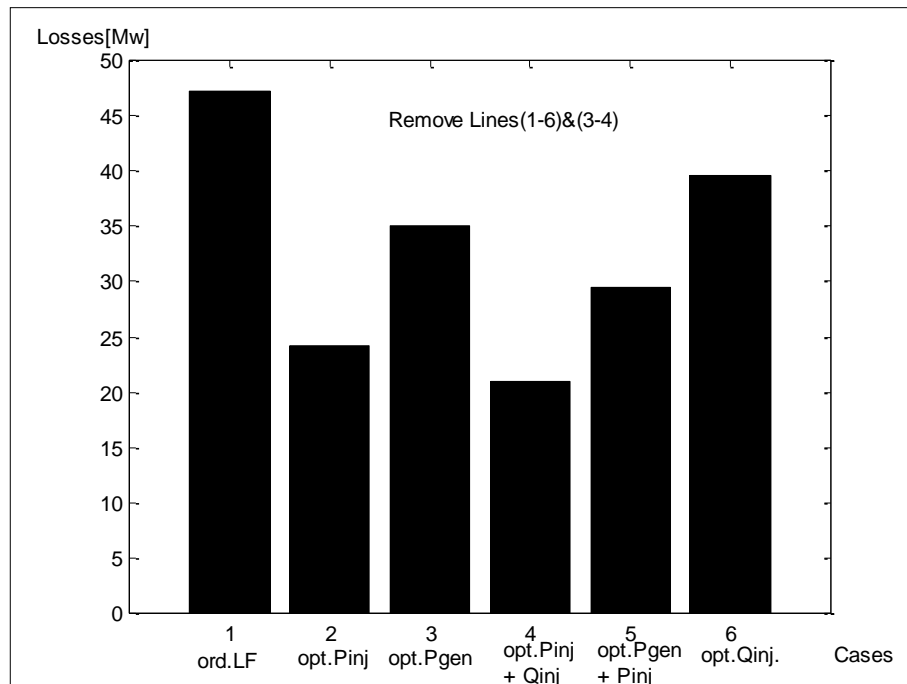


Figure (5.46): Minimum Losses for Different Cases when Removing Lines (1-6) (BAJ-KRK) and (3-4) (HAD-QAM)

5.1.8.4 Removing Lines 1-6 (BAJ-KRK), 3-4 (HAD-QAM) and 18-19 (HRT-QRN):

This case is also multi-contingency case. Figure (5.47) and Table (5.18) show that injecting optimal active and reactive power at load buses (case 4) gives minimum losses equal to (23.56 Mw) and losses reduction equal to $\frac{49.894 - 23.56}{49.894} \times 100\% = 52.7\%$.

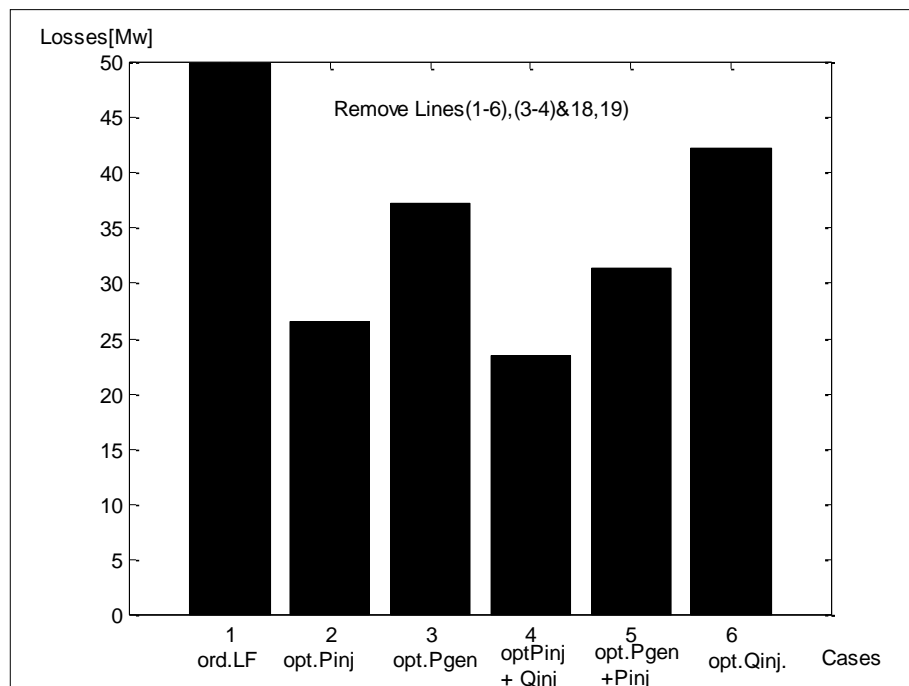


Figure (5.47): Minimum Losses for Different Cases when Removing Lines (1-6) (BAJ-KRK), (3-4) (HAD-QAM) and (18-19) (HRT-QRN)

5.1.8.5 Removing line 1-6 (BAJ-KRK) and Generation at Bus 22 (HAD):

In this multi-contingency case, line (1-6) and generator plant (HAD) are no more a part of the system. Figure (5.48) and Table (5.18) show that optimal active generating and injecting optimal active power at load buses (case 5) give minimum losses of (17.11 Mw) and loss reduction is equal to $\frac{56.08 - 17.11}{56.08} \times 100\% = 69.49\%$.

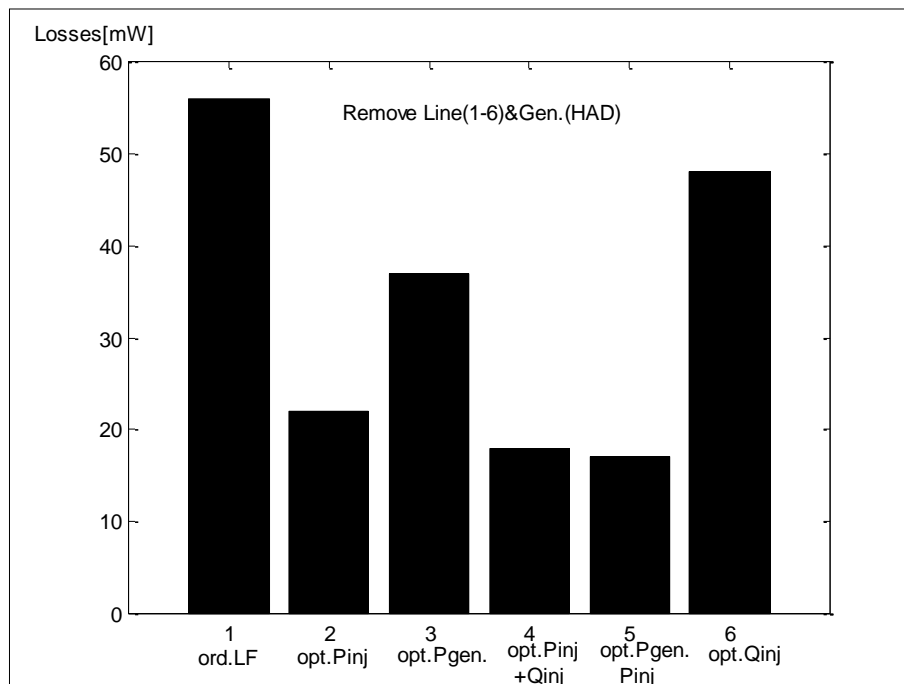


Figure (5.48): Minimum Losses for Different Cases when Removing Lines (1-6) (BAJ-KRK) and Generation (HAD)

5.1.8.6 Removing Line 1-6 (BAJ-KRK) and Generation at bus 25(HRT):

In this case line (1-6) and generator plant (HRT) are no more a part of the system. Figure (5.49) and Table (5.18) show that optimal active generating and injecting active power at load buses (case 5) give minimum losses of (20.71 Mw) and loss reduction is equal to $\frac{74.04 - 20.71}{74.04} \times 100\% = 72.02\%$.

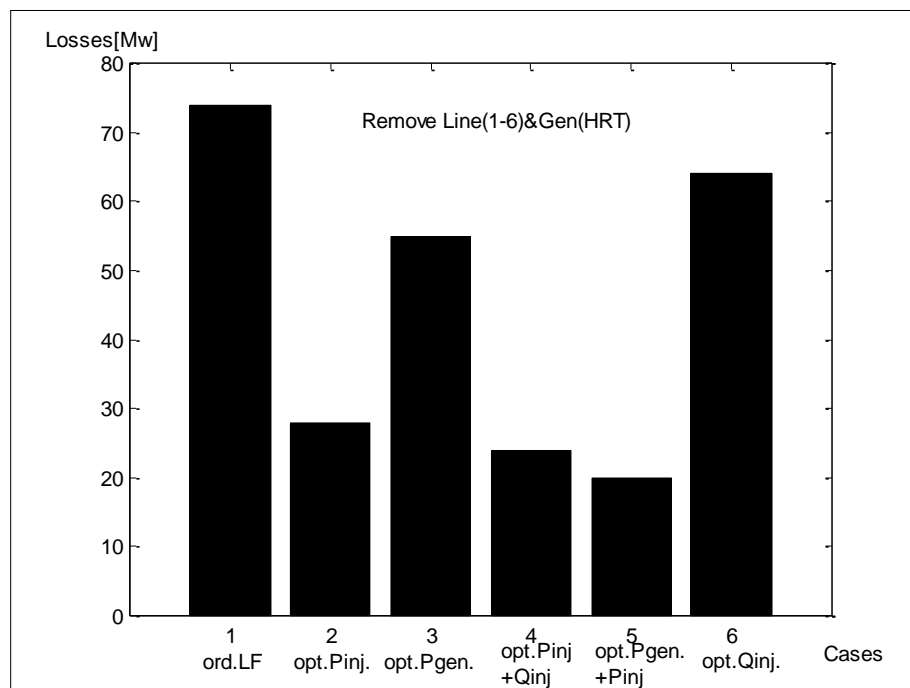


Figure (5.49): Minimum Losses for Different Cases when Removing Lines (1-6) and Generation (HRT)

5.2 Transient Stability Program:

The Transient Stability calculations were carried out using the step by step modified Euler iterative solution of the differential equations describing machines behavior of INSG system.

The solution took into account a time step of 0.05 second and total solution time period of 1.5 second. The program performs transient calculations with different types of faults at any point on the system with 0.15 second clearing time (t_c). Rotor angles were taken as an indicator of transient stability in this work. The improvement in transient stability is the difference between the amplitudes of swing curves for two cases, i.e. the difference between rotor angles before and after improvement, divided by the angle before improvement.

5.3 Transient Stability with Optimal Power Flow Case Studies:

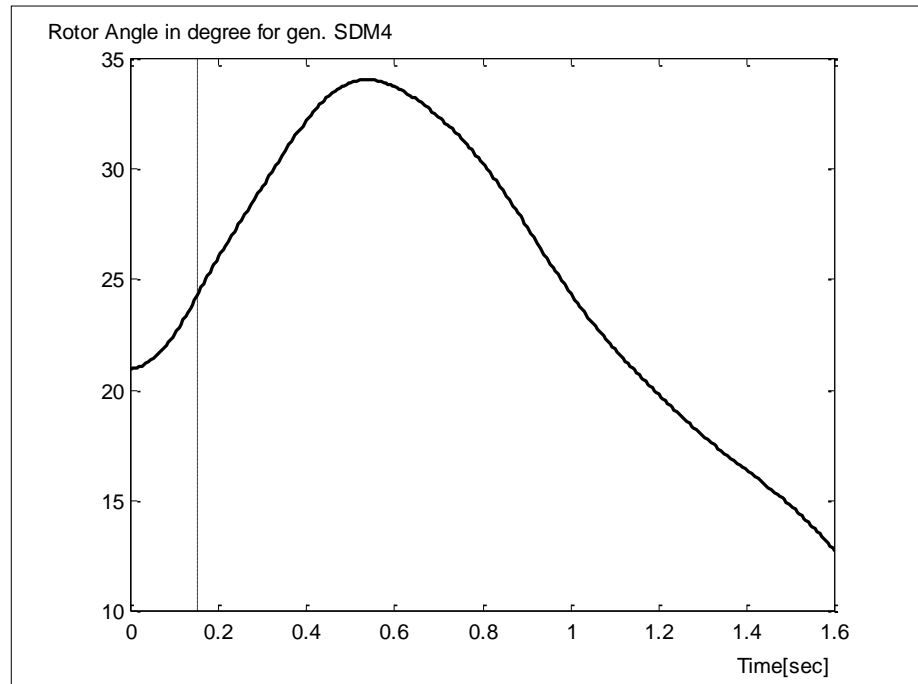
The effects of OPF constrained minimum losses on transient stability were studied, the results were compared with transient stability in case of implementing load flow results of INSG. Three generation buses from the north, west and south of Iraq were selected to study the situation of the network under consideration in detail, these buses are 2 (SDM), 3 (HAD) and 16 (NSR).

5.3.1 Three Phase Fault in the Middle of Line (1-6) (BAJ-KRK):

Although the system is stable in case of three phase fault in the middle of line 1-6 (i.e. BAJ-KRK) with ordinary load flow, the system becomes more stable with OPF.

Swing curves of SDM, HAD and NSR power plants which represent their stability as shown in Figures (5.50), (5.52) and (5.54) respectively were improved when OPF were implemented as shown in Figures (5.51),

(5.53) and (5.55). According to the amplitudes of swing curves, stability improvement were equal to 16.6%, 84% and 82.5% for SDM, HAD and



NSR power plants respectively.

Figure (5.50): Swing Curve for (SDM) Generating Machine for Fault in the Middle of Line (1-6) with Ordinary Load Flow

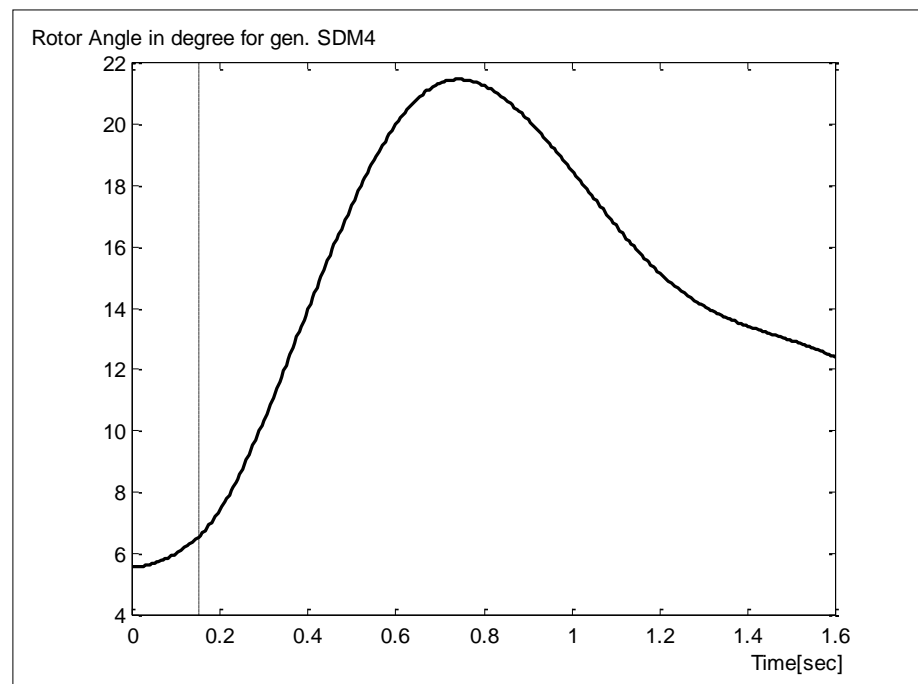


Figure (5.51): Swing Curve for (SDM) Generating Machine for Fault in the Middle of Line (1-6) with OPF

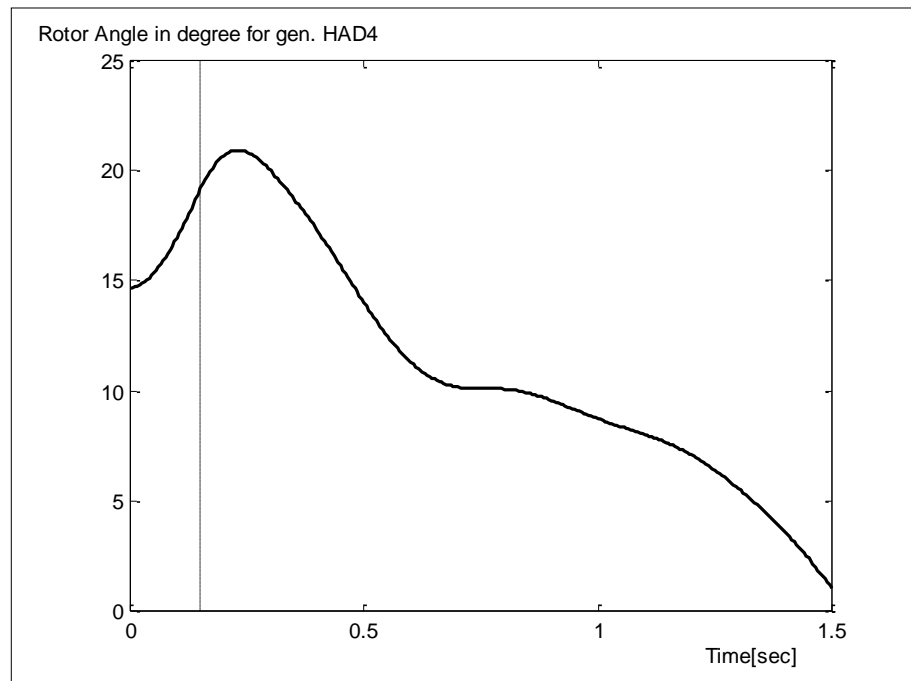


Figure (5.52): Swing Curve for (HAD) Generating Machine for Fault in the Middle of Line (1-6) with Ordinary Load Flow

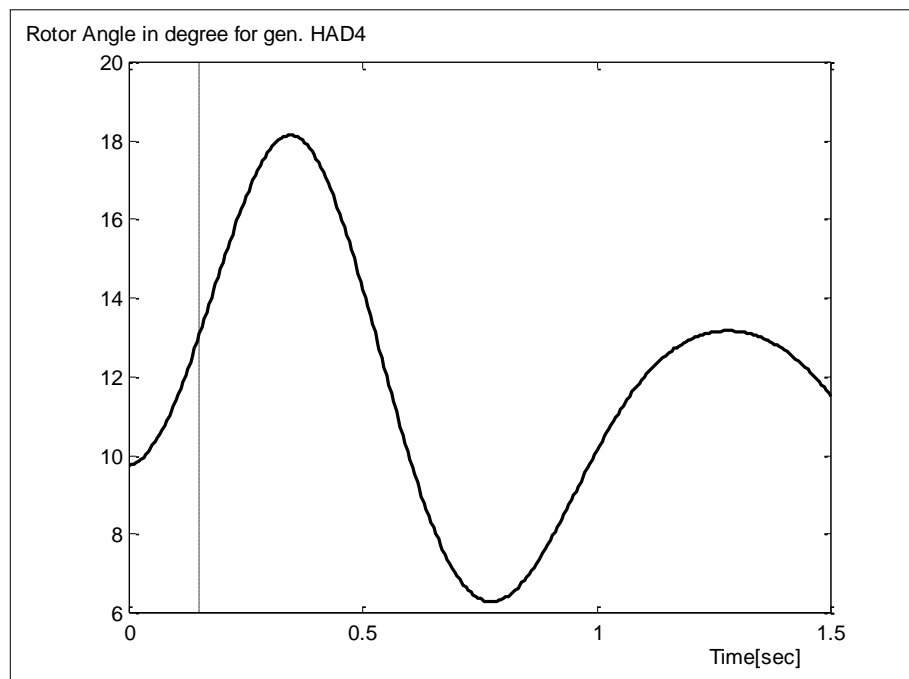


Figure (5.53): Swing Curve for (HAD) Generating Machine for Fault in the Middle of Line (1-6) with OPF

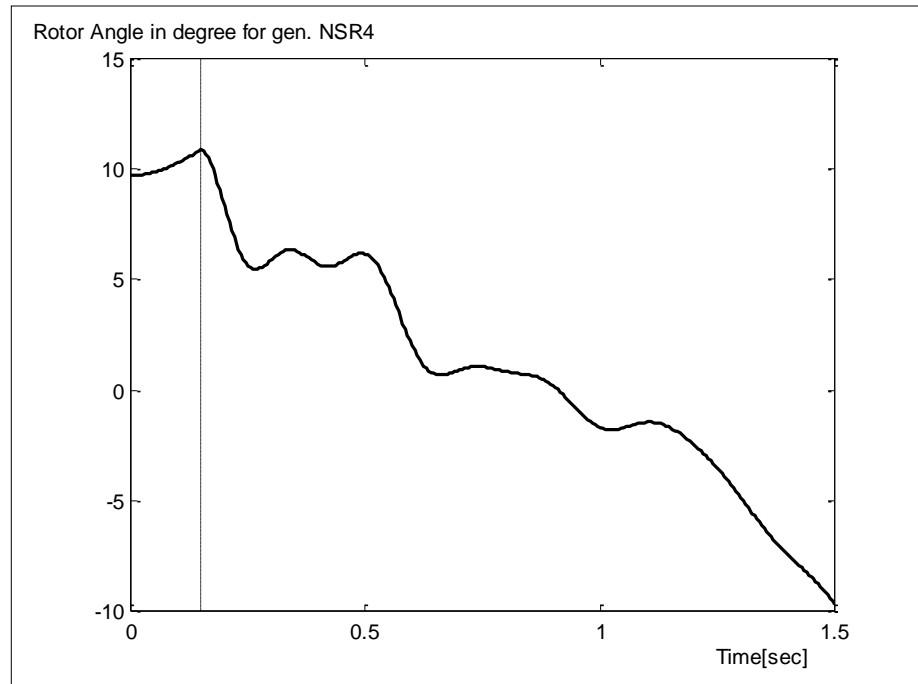


Figure (5.54): Swing Curve for (NSR) Generating Machine for Fault in the Middle of Line (1-6) with Ordinary Load Flow

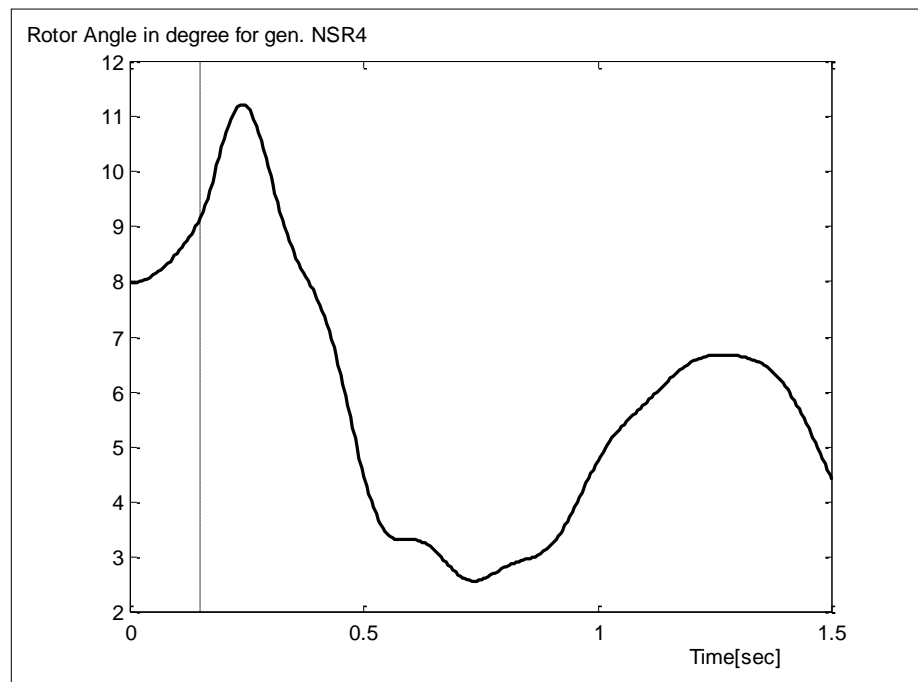


Figure (5.55): Swing Curve for (NSR) Generating Machine for Fault in the Middle of Line (1-6) with OPF

5.3.2 Three Phase Fault in the Middle of Line (3-4) (HAD-QAM):

The system is unstable in case of three phase fault in the middle of line (3-4) (i.e. HAD-QAM) with ordinary load flow because SDM plant is out of synchronism as shown in Figures (5.56), (5.58) and (5.60). The system becomes more stable when implementing OPF as shown in Figures (5.57), (5.59) and (5.61) for SDM, HAD and NSR power plants, stability improvement is equal to 70%, 71.1% and 61.3% respectively.

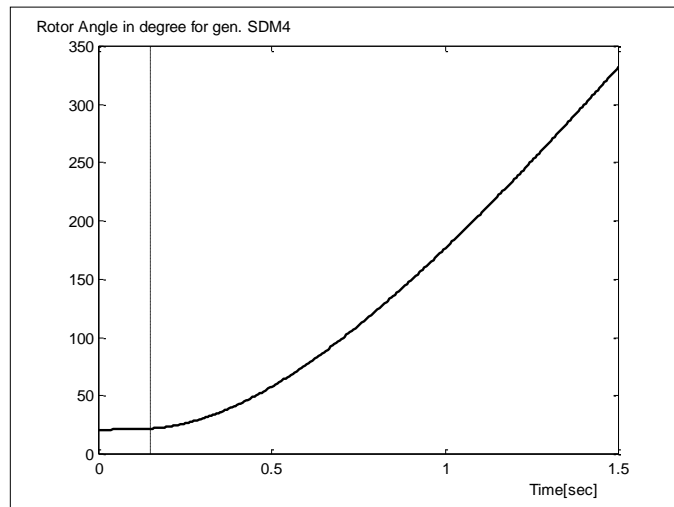


Figure (5.56): Swing Curve for (SDM) Generating Machine for Fault in the Middle of Line (3-4) with Ordinary Load Flow

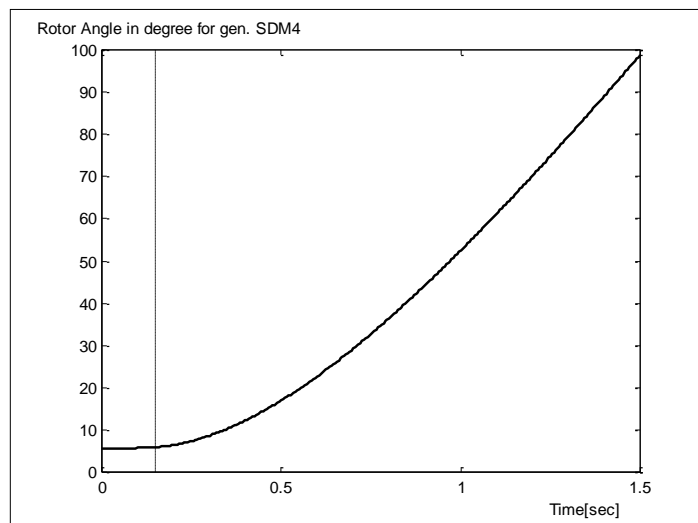


Figure (5.57): Swing Curve for (SDM) Generating Machine for Fault in the Middle of Line (3-4) with OPF

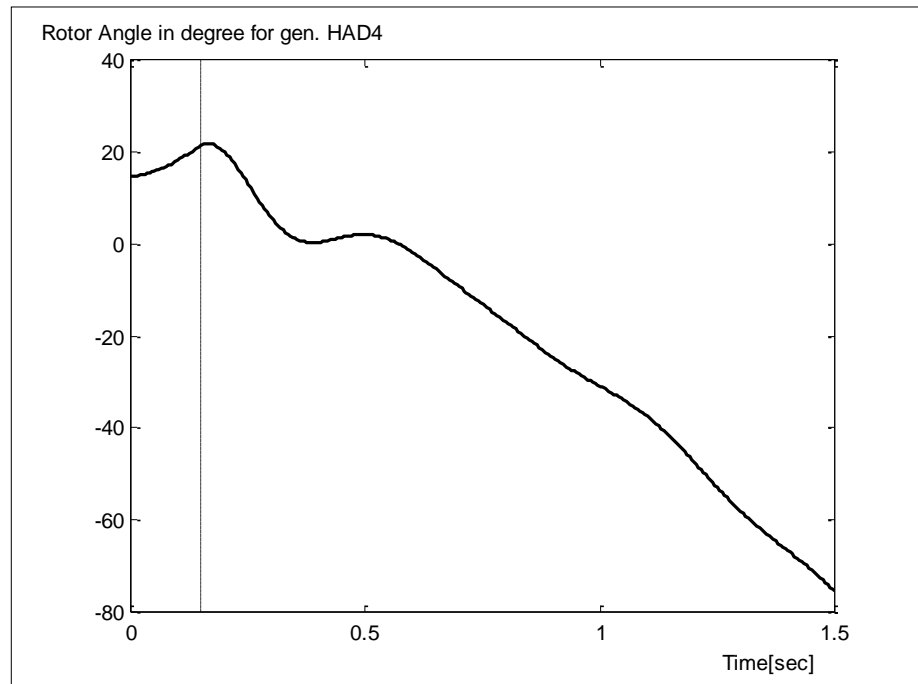


Figure (5.58): Swing Curve for (HAD) Generating Machine for Fault in the Middle of Line (3-4) with Ordinary Load Flow

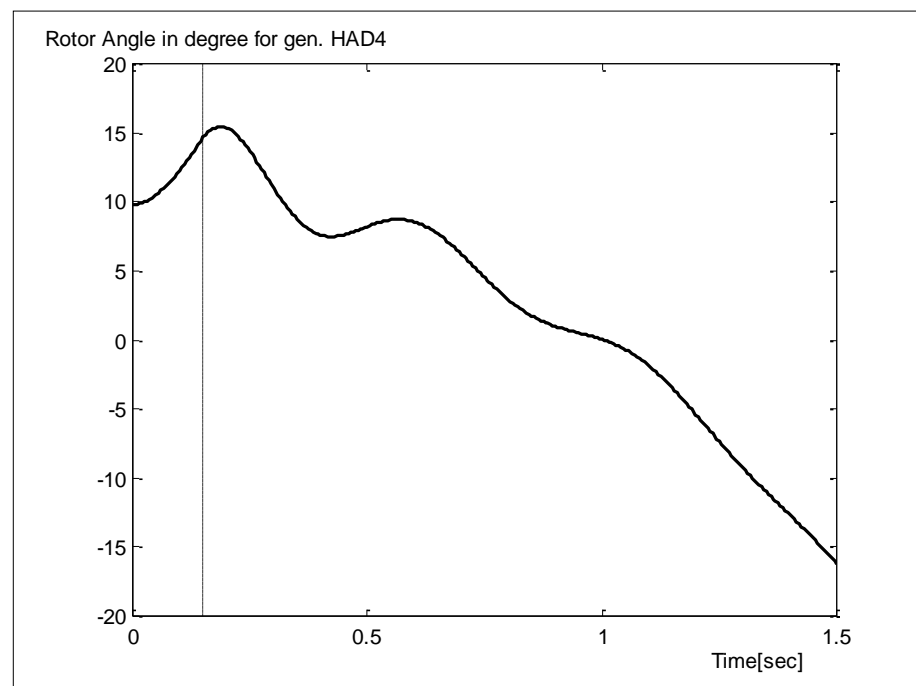


Figure (5.59): Swing Curve for (HAD) Generating Machine for Fault in the Middle of Line (3-4) with OPF

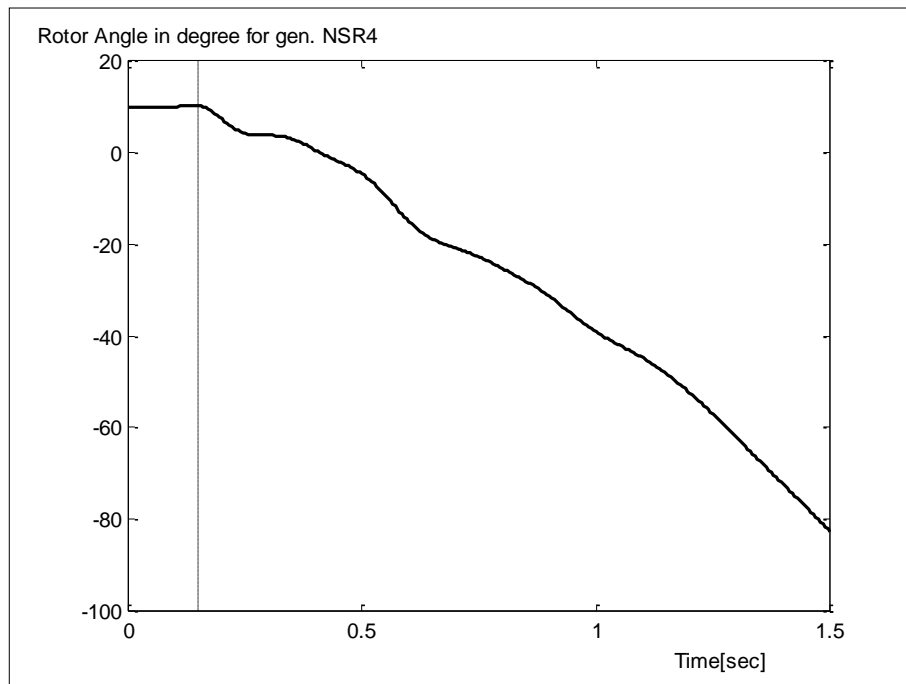


Figure (5.60): Swing Curve for (NSR) Generating Machine for Fault in the Middle of Line (3-4) with Ordinary Load Flow

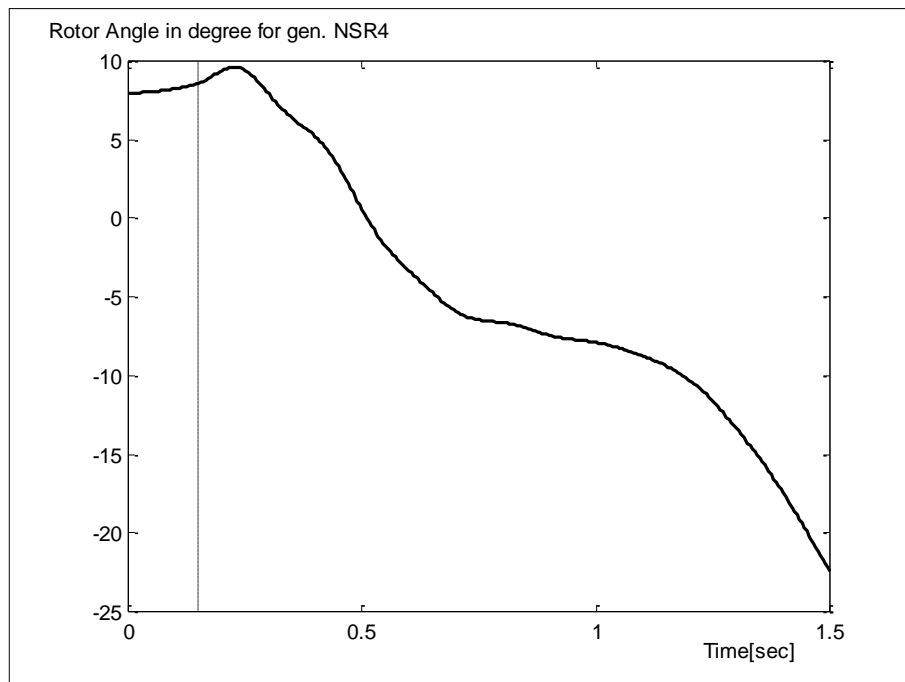


Figure (5.61): Swing Curve for (NSR) Generating Machine for Fault in the Middle of Line (3-4) with OPF

5.3.3 Three Phase Fault in the Middle of Line 18-19 (HRT-QRN):

Although the system is stable in case of three phase fault in the middle of line (18-19) (i.e. HRT-QRN) with ordinary load flow, the system becomes more stable with the results of OPF.

Swing curves of SDM, HAD and NSR power plants as shown Figures (5.62), (5.64) and (5.66) respectively were improved when OPF were implemented as shown in Figures (5.63), (5.65) and (5.67) by 65.2%, 80.4% and 64% respectively.

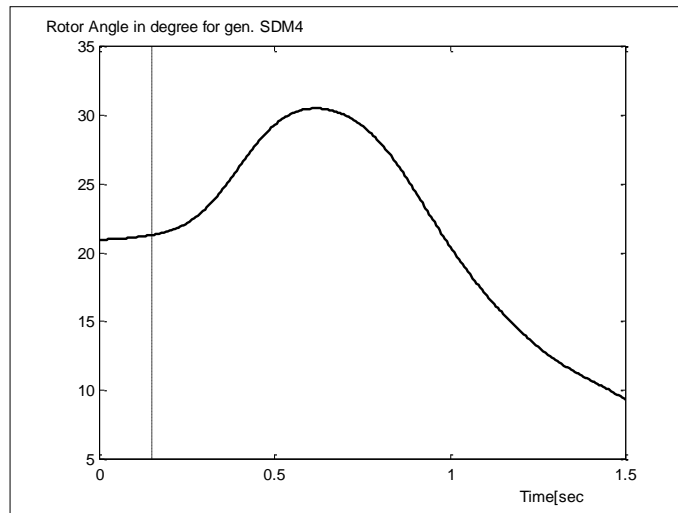


Figure (5.62): Swing Curve for (SDM) Generating Machine for Fault in the Middle of Line (18-19) with Ordinary Load Flow

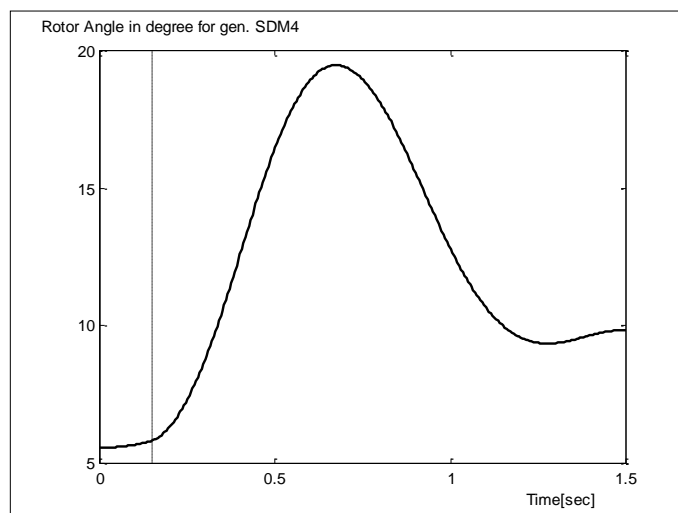


Figure (5.63): Swing Curve for (SDM) Generating Machine for Fault in the Middle of Line (18-19) with OPF

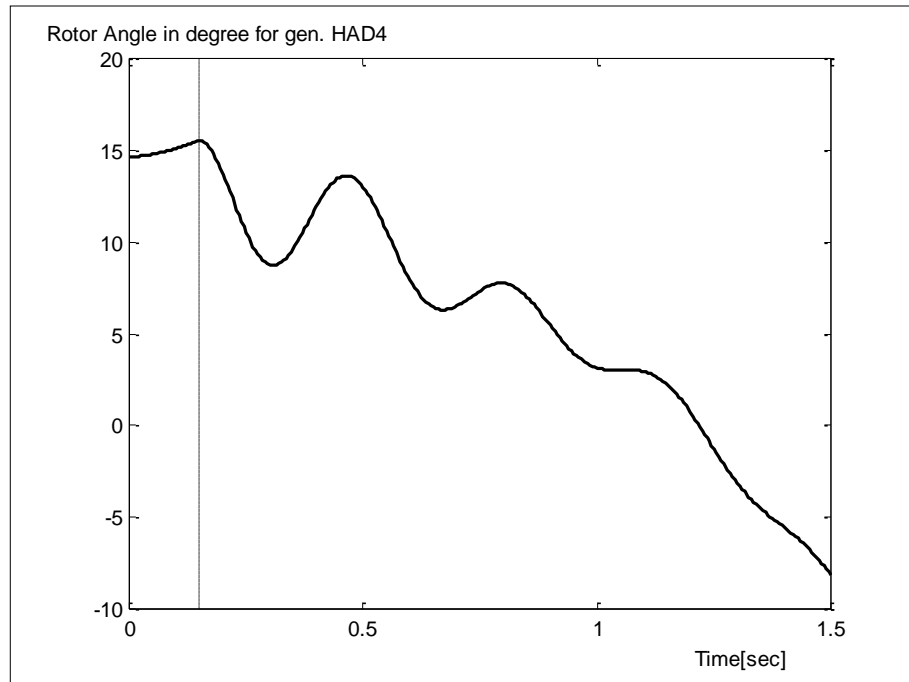


Figure (5.64): Swing Curve for (HAD) Generating Machine for Fault in the Middle of Line (18-19) with Ordinary Load Flow

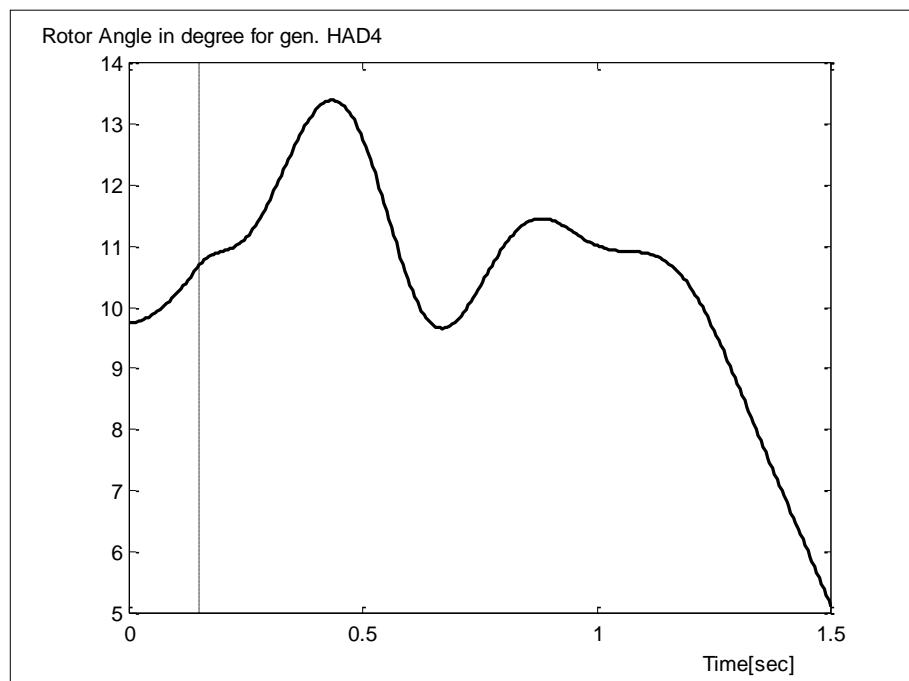


Figure (5.65): Swing Curve for (HAD) Generating Machine for Fault in the Middle of Line (18-19) with OPF

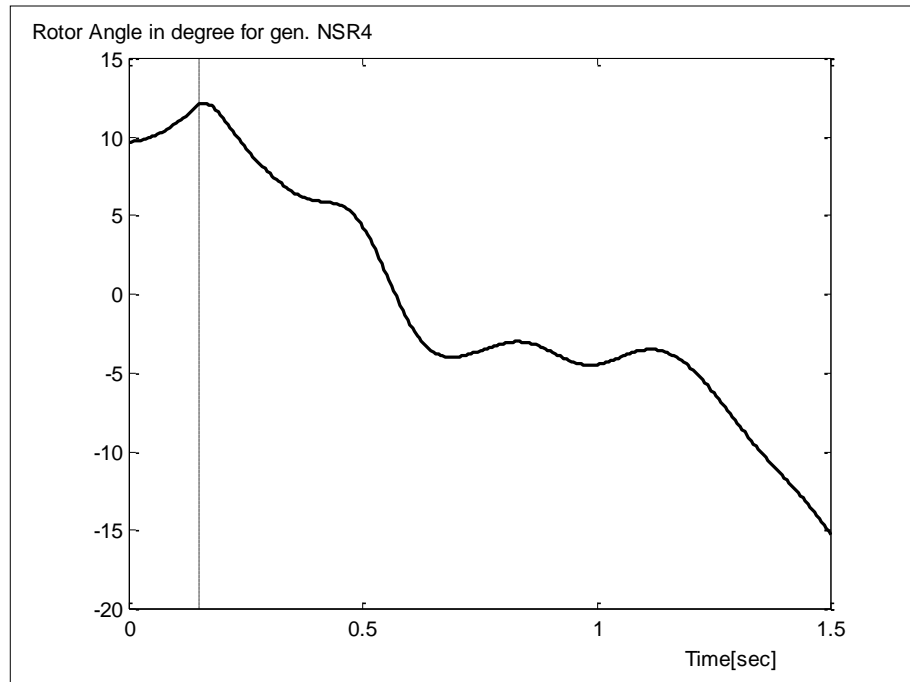


Figure (5.66): Swing Curve for (NSR) Generating Machine for Fault in the Middle of Line (18-19) with Ordinary Load Flow

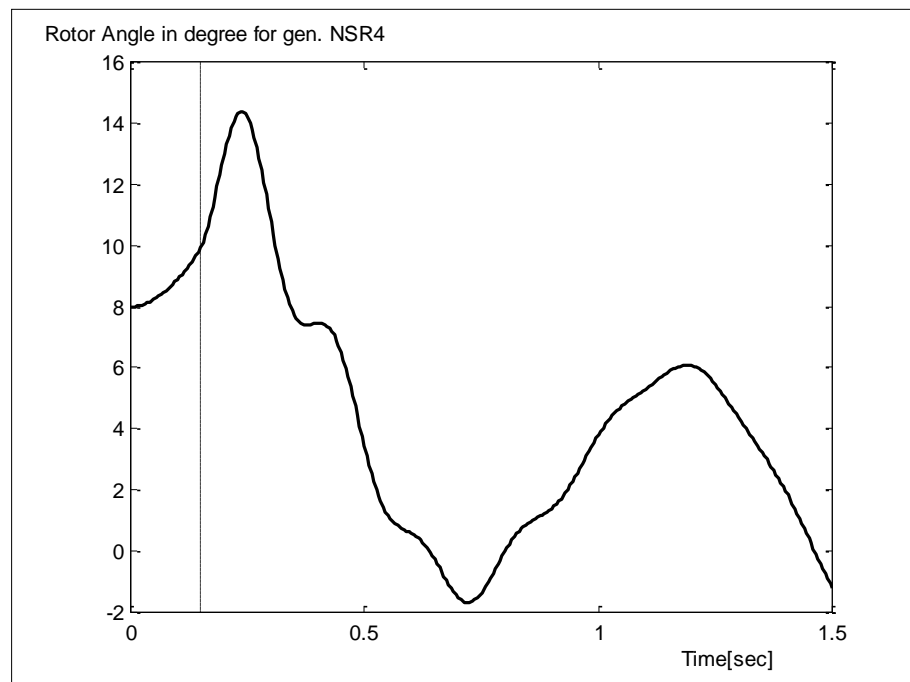


Figure (5.67): Swing Curve for (NSR) Generating Machine for Fault in the Middle of Line (18-19) with OPF

5.3.4 Improvement of System Stability in Case of Faults in the Middle of Line (3-4)

The problem of the network is the instability, during both ordinary and optimal load flows, in case of three phase fault in the middle of line 3-4 (HAD-QAM) because this fault will lead SDM bus to swing away from the stability and will cause the instability of the system. To overcome this problem a new configuration of the network will solve this problem. If the radial path 1-3-4 (BAJ-HAD-QAM) as shown in Figure (4.1) is changed to a loop path 1-4-3-8-1 (BAJ-QAM-HAD-BGE-BAJ), the system becomes stable for both ordinary and OPF as shown in swing curves Figures (5.68)-(5.73).

Ordinary load flow : without modification TS for SDM,HAD and NSR buses as shown before in Figures 5.56,5.58 and 5.60 was improved using new suggested (modified) configuration. The improvements in stability are equal to 96.4%, 63.8% and 59.6% for SDM, HAD and NSR buses as shown in Figures 5.68-5.70 respectively.

OPF: without modification TS for SDM, HAD and NSR buses as shown before in Figures 5.57, 5.59 and 5.61 was improved using new configuration. The improvements in stability are equal to 97.4%, 67.9% and 50.8% for SDM, HAD and NSR buses as shown in Figures 5.71-5.73 respectively.

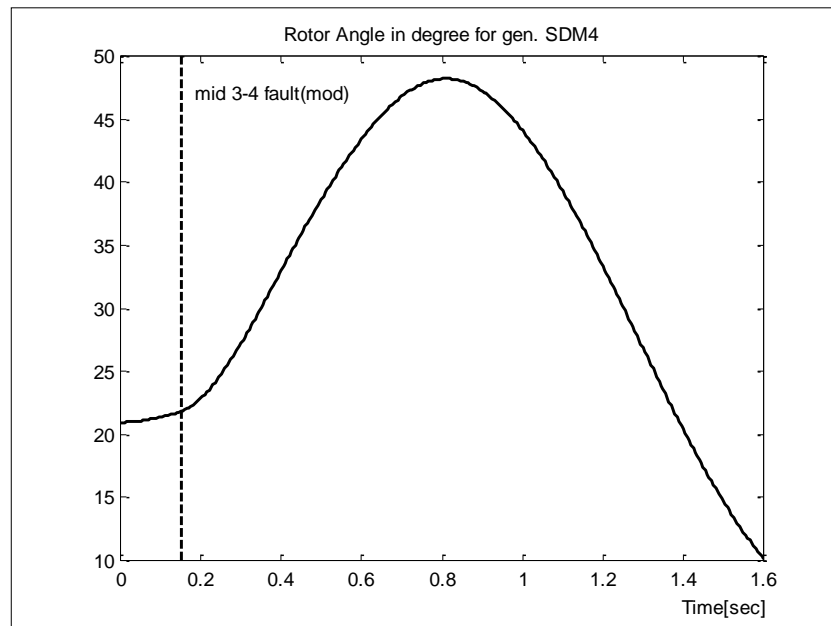


Figure (5.68): The Effect of Modification of the Network Configuration on the Swing Curve (SDM) Generators for Fault in the Mid. of Line (3-4)(HAD-QAM) with Ordinary LF

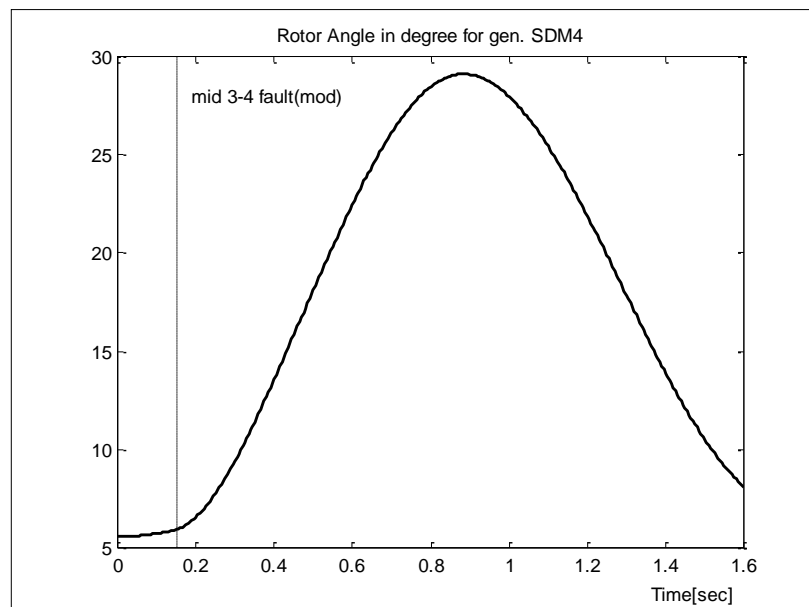


Figure (5.71): The Effect of Modification of the Network Configuration on the Swing Curve (SDM) Generators for Fault in the Mid. of Line (3-4)with OPF

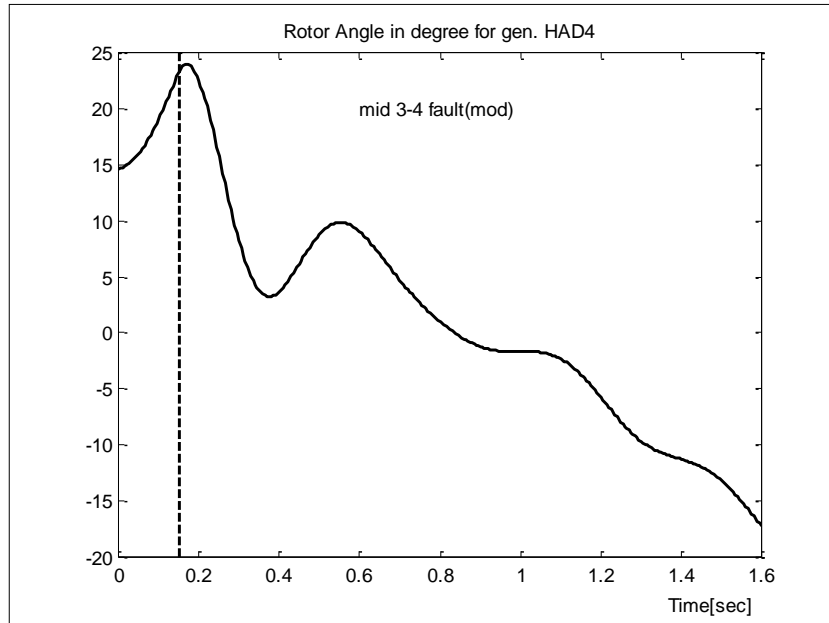


Figure (5.69): The Effect of Modification of the Network Configuration on the Swing Curve (HAD) Generators for Fault in the Mid. of Line (3-4)(HAD-QAM) with Ordinary LF

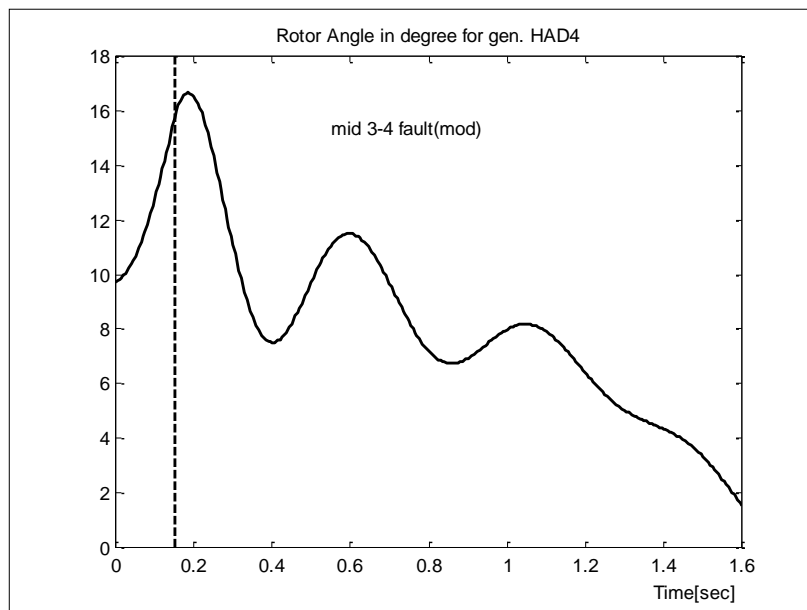


Figure (5.72): The Effect of Modification of the Network Configuration on the Swing Curve (HAD) Generators for Fault in the Mid. of Line (3-4) (HAD-QAM) with OPF

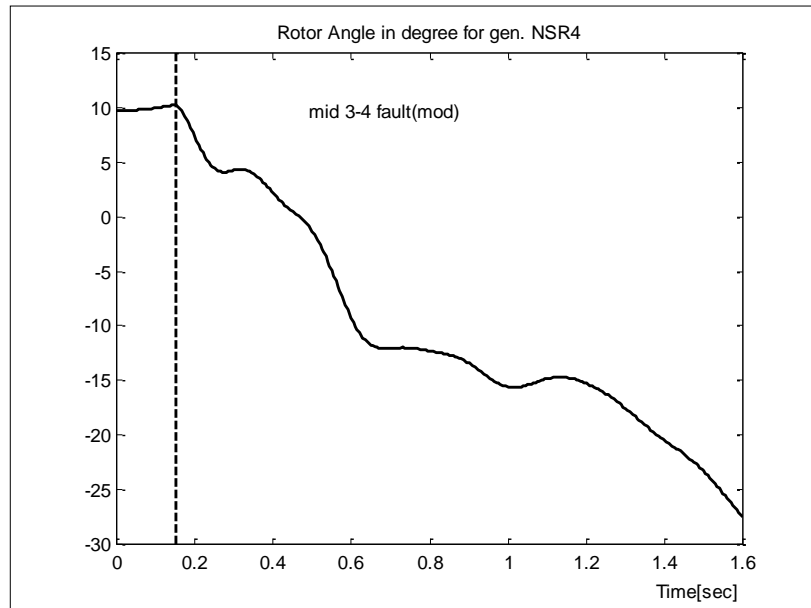


Figure (5.70): The Effect of Modification of the Network Configuration on the Swing Curve (NSR) Generators for Fault in the Mid. of Line (3-4) (HAD-QAM) with Ordinary LF

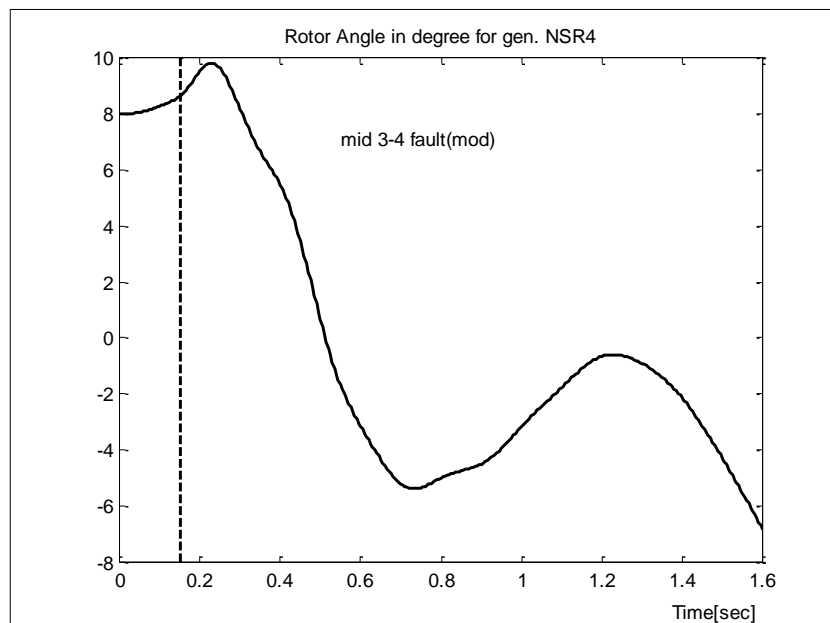


Figure (5.73): The Effect of Modification of the Network Configuration on the Swing Curve (NSR) Generators for Fault in the Mid. of Line (3-4)(HAD-QAM) with OPF

Chapter Six

Conclusions and Suggestions for Future Works

Chapter Six

Conclusions and Suggestions for Future Works

6.1 Conclusions:

- 1- Each load bus in the system has its sensitivity to decrease losses with respect to active and reactive power injection in the bus.
- 2- Bus sensitivities which are the partial derivatives of real power losses w.r.t active and reactive power injection, are tabulated in Table (5.1) and (5.4). The values give indication of the power needed at load buses in INSG.
- 3- Proper placement of generation units will reduce losses, while improper placement may actually increase system losses.
- 4- Also proper placement of generation units will free available capacity for transmission of power as shown in data results. This is better than that for available placement.
- 5- The efficiency of reactive power to reduce losses is less than the ability of generation units because the values of $\partial P_{\text{loss}}/\partial P_{\text{inj}}$ are higher than $\partial P_{\text{loss}}/\partial Q_{\text{inj}}$ as shown in Tables (5.1) and (5.4).
- 6- The first six buses in Table (5.1) are the best to reduce active power losses, so these buses (7, 9, 11, 8, 10 & 15) are chosen as the best places to get minimum losses, which give maximum loss reduction equal to 41.94% when injecting total amount of active power equal to 890 Mw.
- 7- The first eight buses in Table (5.4) are the best buses to reduce active power loss with respect to Q_{inj} which give max loss reduction equal to 13.17% when injecting total amount of reactive power equal to 920 MVAR.

- 8- Comparison between stability with OPF and stability with ordinary power flow according to the rotor time angle curves indicates that the stability is much better with OPF.
- 9- The problem of system instability when a fault takes place in the middle of line (3-4) can be enhanced using optimal OPF in case of optimal generation or real and reactive power injection in load buses.
- 10- The best case to operate generation plants in Iraqi power system is to operate them at optimal power generation as shown in Table (5.17) which gives optimal loss reduction equal to 30.96%.
- 11- For the present 400 kV network the system remains unstable in case of three phase fault in the middle of line 3-4 (HAD-QAM) even for OPF. The system becomes stable if a new configuration is used.
- 12- Designing instructional program under widows to be used by engineers may help to understand the effect of OPF on TS.

6.2 Suggestions for Futures Works:

- 1- Using series capacitors to enhance transient stability (TS) constrained optimal power flow (OPF).
- 2- Enhancement of TS constrained OPF using new configurations for Iraqi transmission line network, like changing the paths of transmission lines.
- 3- Using Neural Network to study OPF and its effects on transient stability TS.
- 4- Studying the effect of proper allocation of active and reactive units to reduce losses from Iraqi 132 kV.

References

- [1] Al-Fahady A. S., **New Approaches in Compensation Techniques Applied for INRG System**, Ph. D. Thesis, University of Mosul, 1997, Mosul.
- [2] Ray D. Zimmerman, “**A Transient Stability Constrained Optimal Power Flow**”, Bulk Power System Dynamics and Control IV- Restructing, August 24-28, Santorini, Greece, 2000.
- [3] Al-Sammak A. Nasser, **A New Method for Transient Study with Application to INRG**”, M. Sc. thesis, University of Mosul, Electrical Engineering Department, 1999, Mosul.
- [4] Rosehart W. and Claudio C., “**Optimal Power Flow Incorporating Voltage Collapse Constraints**”, proceeding of the 1999 IEEE-PES summer meeting Edmonton, 1999, USA.
- [5] Kim S., “**Generation Redispatch Model to Enhance Voltage Security in Competitive Power Market using Stability Constrained Optimal Power Flow**”, www.ee.server, Korea. Ac. Kr, 2001, Korea.
- [6] Chen L. *et al.*, “**Optimal Operation Solutions of Power Systems with Transient Stability Constraints**”, IEEE Trans. on Circuits and Systems, Vol. 48, No. 3, March 2001, USA.
- [7] Al Rawi M. Ali, **Transient Stability Improvement Using Series Capacitors with Application to Iraqi National Super Grid** , Ph.D. Thesis, University of Mosul, 2002, Mosul.
- [8] William R., “**Optimal Placement of Distributed Generation**”, www.psc2.org, 2002, USA.
- [9] Yue Yuan, “**A study of Transient Stability Constrained Optimal Power Flow with Multi-Contingency**”, T.IEE Japan, Vol. 122-B, No. 7, 2002, Japan.

-
- [10] Al-Suhamei W. S. , **Minimizing losses in the Northern Network**, M Sc. Thesis, University of Mosul, 2002, Mosul.
- [11] Al-Khazragy A. Abood , **Implementation of Geographic Information System (GIS) in Real-Time Transient Stability**, Ph.D. thesis, University of Technology, Baghdad, 2004.
- [12] Rodriguez M. Montanes, “**Voltage Sensitivity Based Technique for Optimal Placement of Switched Capacitors**”, 15th PSCC, Lieg, Session 16, paper 4, 22-26 August 2005.
- [13] Carson J.S., “**Introduction to Modeling and Simulation**”, Proceedings of the 2003 winter simulation conference, USA, 2003.
- [14] Carson J.S, “**Introduction to Modeling and Simulation**”, Proceedings of the 2004 winter simulation conference, USA, 2004.
- [15] Navarro I. R, “**Object-Oriented Modeling and Simulation of Power Systems Using Modelica**”, www.dynasim.se, 2000.
- [16] Larsson M., “**Object Stab-A Modelica Library for Power System Stability studies**”, www.modelica.org/workshop 2000.
- [17] Bauer D. and Yukel M., “**A Case Study in Meta-Simulation Design and Performance Analysis for Large-Scale Networks**”, www.informs-sim.org, 2004.
- [18] Jaijeet S. Roychowdhury, "**Efficient Transient Simulation of Lossy Interconnect**", www.sigh.org/archives/paper/1991.
- [19] Emily O., “**Challenges in Using an Economic Cost Model for Software Engineering Simulation**”, Proceedings of the 2004 winter simulation conference, USA, 2004.
- [20] Barton R.R., “**Designing Simulation Experiments**”, Proceedings of the 2004 winter simulation conference, USA, 2004.

-
- [21] Navarro E.O. and Hoek A.V., “**Design and Evaluation of an Educational Software Process Simulation Environment and Associated Model**”, www.informs-sim.org, 2004.
- [22] Nance E., “**Thoughts and Musings on Simulation Education**”, Proceeding of the 2001 winter simulation conference, pp. 1567-1570, 2001.
- [23] He D., “**Enhancing Simulation Education with a Virtual Presentation Tool**”, www.informs-sim.org, 2004.
- [24] Averill M. Law and Michael G. McComas, “**How to Build Valid and Credible Simulation Models**”, Proceedings of the 2001 winter simulation conference, 2001.
- [25] Anderson G., “**Modeling and Analysis of Electric Power Systems**” EEH-Power Systems Laboratory, ETH Zurich, March 2003.
- [26] Lee Y. M., “**Power Grid Transient Simulation in Linear Time Based on Transmission Line Modeling Alternating Direction Implicit Method**”, IEEE Trans. on Computer-Aided Design, Vol. 21, No. 11, November 2002.
- [27] Eric H. Allen, “**Interaction of Transmission Network and Load Phasor Dynamics in Electric Power Systems**”, IEEE Transactions on Circuits and Systems, Vol. 47, No. 11, November, 2000.
- [28] Al Rashidi M., “**Power Flow Program**”, ECED 3101: Power Systems 1, July 13th, 2004.
- [29] Baldwin T., “**Power System Operation and Control**”, Florida State University, www.research.caps.fsu.edu/eel6266, 2004.
- [30] Tapan K. Saha, “**Applications of Load Flow Analysis**”, www.itee.uq.edu.au.pdf, 2004.
- [31] James D. Weber, “**Implementation of a Newton-Based Optimal Power Flow into A Power System Simulation Environment**”, [www.power.world.com/Document library](http://www.power.world.com/Document%20library), 1997.

-
- [32] Selman N. H., **Minimum Energy Loss Based Reactive Power Flow**, M. Sc. Thesis, University of Technology, 2005.
- [33] Antonio J. and Maria J., “**Optimal Power Flow Algorithm Based on TABU Search for Meshed Distribution Networks**”, www.pscoco2.org, 2002.
- [34] Quek R., “**Power Transfer Capability Assessment**”, www.innovexpo.itee.uq.edu.au/ 2002.
- [35] Pajic S., “**Sequential Quadratic Programming-Based Contingency Constrained Optimal Power Flow**”, M. Sc. Thesis, Worcester polytechnic institute, www.wpi.edu. April 2003.
- [36] Kristiansen T., “**Utilizing Mat Power in Optimal Power Flow**”, www.ksg.haward.edu, 2002.
- [37] Stevenson W. D., “**Elements of Power System Analysis**”, McGraw-Hill Book co. 4th edition, 1985.
- [38] Etienne J., “**A Reduced Gradient Method with Variable Base Using Second Order Information, Applied to the Constrained and Optimal Power Flow**”, www.system.seurope.be/pdf, 2000.
- [39] Claudio C., “**Comparison of Voltage Security Constrained Optimal Power Flow Techniques**”, Proc. IEEE-PES Summer meeting Vancouver, BC, July 2001.
- [40] Michael M., “**Investigation of Voltage Stability of the IEEE 14 bus Power System**”, www.itee.uq.edu.
- [41] Graves S., “**Nonlinear Programming**”, www.ocw.mit.edu, summer 2003.
- [42] Edgardo D. Castronuovo, “**A largest-step Central-Path Algorithm Applied to the Optimal Power Flow Problem**”, www.fee.unicamp.lor, 2000.
- [43] Momoh J. A. *et al.*, “**Challenges to Optimal Power Flow**”, IEEE Power Engineering. Winter meeting, January 21-25, 1996.

-
- [44] Al Augaidee M. Obaid, **Optimal Load Flow**, M. Sc. Thesis, University of Mosul, 2002.
- [45] Nakada F., “**Loop Power Flow Control by Series Controllable Reactance’s for Optimal Power Flow Management**”, 14th PSCC, Sevilla, 24-28 June, 2002.
- [46] Rosehart W., “**Multi-Objective Optimal Power Flow to Evaluate Voltage Security Costs in Power Networks**”, IEEE Trans. Power Systems, October 2002.
- [47] Milano F., “**Multiobjective Optimization for Pricing System Security in Electricity Markets**”, IEEE Trans. On Power Systems, Vol. 18, No. 2, May 2003.
- [48] Zhao Y., “**Non linear Programming**”, www.ucd.ie/economic/staff,
- [49] Castronuovo E. D., “**New Versions of Nonlinear Interior Point Methods Applied to the Optimal Power Flow Problem**”, www.optimization-online.org, 2002.
- [50] Demetrios A. Tziouvaras, “**Out-Of-Step Protection Fundamentals and Advancements**”, www.selinc.com/6163 pdf.
- [51] Anupindi K. *et al.*, “**Parallel Differential-Algebraic Equation Solvers for Power System Transient Stability Analysis**”, Nigara Mohawk, Power Corporation, the New York Science and Technology Foundation.
- [52] Shin-Min Hsu, “**Power Systems-Basic Concepts and Applications**”, www.PDHcenter.com.
- [53] Saha T., “**Power Systems and Reliability-Lecture Notes on Stability**”, www.itee.uq.edu, 2002.
- [54] Ernst D. *et al.*, “**Power Systems Stability Control: Reinforcement Learning Framework**”, www.montefiore.ulg.ac.be/ 2003. Pdf.
- [55] Kundur K., “**System Stability**”, www.ee.und.ac.za/ coursemain, 2004.

-
- [56] Bankar H., “**Transient Stability Lecture 10**”, www.ece.mcgill.ca/~inf464, 2003.
- [57] Khedkar M. K. *et al.*, “**Transient Stability Analysis by Transient Energy Function Method: Closest and Controlling Unstable Equilibrium Point Approach**”, www.ieindia.org/publish, 2004.
- [58] Al Azawi Faiq *et al.*, “**Power System Analysis Programs**”, Al Nahreen University, August 2001.
- [59] Yiqiao L., “**Calculation of the probability Density Function of Critical Clearing Time in Transient Stability Analysis**”, proceeding of the 35th Hawaii International Conference on System Sciences, 2002.
- [60] Keith M. *et al.*, “**Application of Out-Of-Step Relaying for Small Generators in Distributed Generation**”, www.neiengineering.com/papers, 2004.
- [61] Yong T. and Lasseter R., “**OPF Formulation in Market of Retail Wheeling**”, www.pserc.cornell.edu, 1999.
- [62] John R., “**Engineering Design Optimization**”, www.me.uprm.edu/vgoyal/inme4058, 2003.
- [63] Mamandur K.R.C., “**Optimal control of Reactive Power Flow for Improvements in Voltage Profiles and for Real Power Loss Minimization**”, IEEE Trans. on power apparatus and systems, vol. PAS-100, No. 7, July 1981.
- [64] Cai L., “**Robust Coordinated of FACTS Devices in Large Power System**”, www.ub.uni.duisburg.de/EDT-db, 2004.
- [65] J. D. Glover, “**Power System Analysis and Design**”, PNS publishing company, 1998.
- [66] Venkataraman A., “**Optimal Reactive Power Allocation**”, IEEE Trans. on power systems, vol. PWRS-2, No. 1, Feb. 1987.

- [67] Staniulis R., **“Reactive Power Valuation”**,
www.lea.th.se/publications, 2001.
- [68] Peter W. Sauer, **"Power System Dynamics and Stability"**, Prentice Hall, USA, 1998.
- [69] Al-Khazragy A. Afaneen **Automated Mapping Facilities Management Geographic Information System of a Power System**, M. Sc. Thesis, University of Technology, Baghdad, 1998.

Appendix A

Sensitivity

A method of finding the sensitivities of the system losses with respect to the state variables is presented in this appendix. The procedure starts by calculating the sensitivities of the losses with respect to the real and reactive power injections at all the buses except the slack bus. Quoting the final equation in matrix notation as:

$$\begin{bmatrix} \frac{\partial P_L}{\partial P_i} \\ \frac{\partial P_L}{\partial Q_i} \end{bmatrix} = [J^t]^{-1} \begin{bmatrix} \frac{\partial P_L}{\partial \delta_i} \\ \frac{\partial P_L}{\partial V_i} \end{bmatrix} \quad (\text{A.1})$$

where $[J]$ is the Jacobian matrix of the N-R load flow. The elements of the vectors $\frac{\partial P_L}{\partial \delta_i}$ and $\frac{\partial P_L}{\partial V_i}$ can be determined very easily by differentiating the equation (2.36) in the chapter two with respect to δ_i and V_i respectively.

$$\frac{\partial P_L}{\partial \delta_i} = 2 \sum_{i=1}^N \sum_{\substack{j=1 \\ j \neq i}}^N G(i, j) [V_i V_j \sin(\delta_i - \delta_j)] \quad (\text{A.2})$$

$$\frac{\partial P_L}{\partial V_i} = 2 \sum_{i=1}^N \sum_{\substack{j=1 \\ j \neq i}}^N G(i, j) [V_i - V_j \cos(\delta_i - \delta_j)] \quad (\text{A.3})$$

Thus, using the relationship of equation (A.1), the loss sensitivity of the system real power losses to real and reactive power injection variations at each bus can be calculated.

Using the values of $\frac{\partial P_L}{\partial P_i}$ and $\frac{\partial P_L}{\partial Q_i}$ of equation (A.1), the loss sensitivities with respect to the control variables of the VAR control

problem can be determined. They are developed below for transformer taps, generator voltages and for switchable VAR sources.

1- Loss sensitivity with respect to generator terminal voltages ($\frac{\partial P_L}{\partial V}$):

Changing the terminal voltage at a generator bus results in the modified VAR injection at that bus. Hence, the loss sensitivity with respect to generator terminal voltage can be given by:

$$\frac{\partial P_L}{\partial V_q} = \frac{\partial P_L}{\partial Q_q} \frac{\partial Q_q}{\partial V_q}; q = 2, 3, \dots, M \quad (\text{A.4})$$

The term $\frac{\partial Q_q}{\partial V_q}$ can be calculated as the Jacobian matrix calculation

and $\frac{\partial P_L}{\partial Q_q}$ is already calculated by equation (A.1). Thus $\frac{\partial P_L}{\partial V_q}$ for all the

controllable generator terminal voltages can be calculated and utilized.

2- Loss sensitivity with respect to the terminal voltage of the slack

generator ($\frac{\partial P_L}{\partial V_1}$):

Any changes to the terminal voltages of the slack generator results in modified reactive power injections at all the other generators and in reactive power injection errors at all the load buses connected to bus 1.

$$\frac{\partial P_L}{\partial V} = \sum_{\alpha} \frac{\partial P_L}{\partial Q_{\alpha}} \left(-\frac{\partial Q_{\alpha}}{\partial V_1} \right) + \frac{\partial P_L}{\partial Q_2} \frac{\partial Q_2}{\partial V_1} + \frac{\partial P_L}{\partial Q_3} \frac{\partial Q_3}{\partial V_1} + \dots + \frac{\partial P_L}{\partial Q_M} \frac{\partial Q_M}{\partial V_1} \quad (\text{A.5})$$

Where α is the set of all the load buses connected to bus-1. Values of

$\frac{\partial P_L}{\partial Q_{\alpha}}$, $\frac{\partial P_L}{\partial Q_2}$, ..., $\frac{\partial P_L}{\partial Q_M}$ are readily available from equation (A.1). Values of

$\frac{\partial Q_{\alpha}}{\partial V_1}$ can be calculated as in the Jacobian formulation.

3- Loss sensitivity with respect to the reactive powers of the switchable

VAR sources ($\frac{\partial P_L}{\partial Q_{m+w}}$):

These values are already calculated and can readily be taken from equation (A.1).

Appendix B

Derivation of the Swing Equation

The differential equation describing the rotor dynamics is

$$J \frac{d^2 \theta_m}{dt^2} = T_m - T_e \quad (1)$$

where:

J = The total moment of inertia of the synchronous machine (kg m^2).

θ_m = The mechanical angle of the rotor (rad).

T_m = Mechanical torque from turbine or load (N. m). Positive T_m corresponds to mechanical power fed into the machine, i.e. normal generator operating in steady state.

T_e = Electrical torque on the rotor (N.m). Positive T_e in normal generator operation.

If eq. (1) is multiplied with the mechanical angular velocity ω_m .

$$\omega_m J \frac{d^2 \theta}{dt^2} = P_m - P_e \quad (2)$$

where:

$P_m = T_m \omega_m$ = mechanical power acting on the rotor (W).

$P_e = T_e \omega_m$ = electrical power acting on the rotor (W).

$\omega_m = \frac{\omega_e}{p/2}$ The relationship between mechanical angular velocity of

rotor and electrical frequency of the system.

Where p is the number of the poles.

$$\frac{2}{p} \omega_m J \frac{d^2 \theta_e}{dt^2} = P_m - P_e \quad (3)$$

Where the left hand side can be re-arranged.

$$2 \frac{2}{p\omega_m} \left(\frac{1}{2} \omega_m^2 J \right) \frac{d^2\theta_e}{dt^2} = P_m - P_e \quad (4)$$

If eq. (4) is divided by the rating of the machines, and the result is:

$$\frac{2}{\omega_e} \frac{\frac{1}{2} \omega_m^2 J d^2\theta_e}{S dt^2} = \frac{P_m - P_e}{S} \quad (5)$$

Observations and experiences from real power systems show that during disturbances, the angular velocity of the rotor will not deviate significantly from the nominal values, i.e. from ω_{mo} and ω_{eo} , respectively.

$$H = \frac{\frac{1}{2} J \omega_{mo}^2}{S}$$

$$\frac{2H d^2\theta_e}{\omega_{eo} dt^2} = P_m \text{ (p.u.)} - P_e \text{ (p.u.)} \quad (6)$$

The index (e) and superscript (p.u) can be omitted in eq. (6), then the form of the swing equation:

$$\frac{2H d^2\theta}{\omega_o dt^2} = P_m - P_e \quad (7)$$

Appendix C

The load & Generation of the Iraqi National Super Grid System (400 kV)

Bus Bar Number	Bus Bar Name	Type	Generation		Load	
			MW	M _{VAR}	MW	M _{VAR}
1	BAJ	Slack	570.592	100.4455	200.00	98.00
2	SDM	P,V	700.00	- 23.2248	5.00	2.00
3	HAD	P,V	500.00	- 0.8474	100.00	60.00
4	QAM	P,Q	.00	.00	60.00	40.00
5	MOS	P,Q	.00	.00	300.00	180.00
6	KRK	P,Q	.00	.00	70.00	40.00
7	BQB	P,Q	.00	.00	150.00	80.00
8	BGW	P,Q	.00	.00	500.00	360.00
9	BGE	P,Q	.00	.00	500.00	360.00
10	BGS	P,Q	.00	.00	100.00	50.00
11	BGN	P,Q	.00	.00	300.00	200.00
12	MSB	P,V	600.00	420.6564	120.00	70.00
13	BAB	P,Q	.00	.00	100.00	50.00
14	KUT	P,Q	.00	.00	100.00	60.00
15	KDS	P,Q	.00	.00	200.00	100.00
16	NAS	P,V	650.00	- 69.1434	100.00	54.00
17	KAZ	P,Q	.00	.00	350.00	200.00
18	HRT	P,V	380.00	35.9855	38.00	22.00
19	QRN	P,Q	.00	.00	70.00	30.00
Total			3400.592	463.8716	3363	2056

Appendix D

INSG System Line Data

From	To	R (P.U)	X (P.U)	B (P.U)
BAJ4	SDM4	0.00542	0.0487	1.4384
MOS4	SDM4	0.00143	0.0124	0.36439
MOS4	BAJ4	0.00399	0.03624	1.074
BAJ4	HAD4	0.00364	0.03024	0.8676
QAM4	HAD4	0.0035	0.03	0.7413
BGE4	BQB4	0.00076	0.00689	0.2043
BAJ4	KRK4	0.00182	0.01654	0.49031
BAJ4	BGW4-2	0.0055	0.05004	1.4826
BAJ4	BGW4-1	0.00483	0.04393	1.3017
HAD4	BGW4	0.00483	0.04393	1.3017
BGW4	BGN4	0.00093	0.00847	0.25099
BGN4	BGE4	0.00029	0.00265	0.0788
KRK4	BGE4	0.00481	0.04373	1.29581
BGE4	BGS4	0.00105	0.00955	0.28309
BGW4	BGS4	0.00144	0.0131	0.38816
BGS4	MSB4-1	0.00121	0.0102	0.30944
BGS4	MSB4-2	0.00121	0.0102	0.30944
BAB4	MSB4-1	0.00077	0.00648	0.19666
BAB4	MSB4-2	0.00077	0.00648	0.19666
BGS4	KUT4	0.00245	0.02236	0.6625
BGS4	KDS4	0.00292	0.02659	0.788
KDS4	NSR4	0.00383	0.03486	1.03314
KAZ4	NSR4	0.00439	0.03999	1.1849
KUT4	NSR4	0.00433	0.0394	1.1674
KAZ4	HRT4	0.00119	0.01083	0.32104
QRN4	HRT4	0.0013	0.01182	0.35022
QRN4	KUT4	0.00628	0.05713	1.6927

Appendix E

Machine's Parameters

Node Name	Armature ARG (Per Unit)	Transient XD (Per Unit)	Inertia Constant H (SECS)
BAJ4	0.0	0.0122242	132
SDM4	0.0	0.037	91.008
HAD4	0.0	0.04948	36.096
MSB4	0.0	0.017225	104
NSR4	0.0	0.0285	99.94
HRT4	0.0	0.0508	47.5

Appendix F

Limits of Generation and Load Buses

Bus Bar	$Q_{\text{generation}} [M_{\text{var}}]$		Voltage [P.V]	
	Q_{min}	Q_{max}	V_{min}	V_{max}
1	- 200	200	0.95	1.05
2	- 257.15	433.82	0.95	1.05
3	- 183.68	309.87	0.95	1.05
4	0	0	0.95	1.05
5	0	0	0.95	1.05
6	0	0	0.95	1.05
7	0	0	0.95	1.05
8	0	0	0.95	1.05
9	0	0	0.95	1.05
10	0	0	0.95	1.05
11	0	0	0.95	1.05
12	- 220.42	371.85	0.95	1.05
13	0	0	0.95	1.05
14	0	0	0.95	1.05
15	0	0	0.95	1.05
16	- 238.77	402.83	0.95	1.05
17	0	0	0.95	1.05
18	- 139.6	235.5	0.95	1.05
19	0	0	0.95	1.05
20	- 200	200	0.95	1.05
21	- 257.15	433.82	0.95	1.05
22	- 183.68	309.87	0.95	1.05
23	- 220.42	371.85	0.95	1.05
24	- 238.77	402.83	0.95	1.05
25	- 139.6	235.5	0.95	1.05

Table (5.8): Sensitivity and Losses when Injecting the Same Value of Active Power

P_i	Losses [Mw]	Bus 7 $\partial P_{\text{loss}}/\partial P_i$	Bus 9 $\partial P_{\text{loss}}/\partial P_i$	Bus 11 $\partial P_{\text{loss}}/\partial P_i$	Bus 8 $\partial P_{\text{loss}}/\partial P_i$	Bus 10 $\partial P_{\text{loss}}/\partial P_i$	Bus 15 $\partial P_{\text{loss}}/\partial P_i$
0	37.592	- 0.0392	- 0.0361	- 0.0359	- 0.0279	- 0.0258	- 0.0230
10	35.7077	- 0.0365	- 0.0337	- 0.0335	- 0.0259	- 0.0233	- 0.0186
20	33.982	- 0.0339	- 0.0312	- 0.0311	- 0.024	- 0.0209	- 0.0172
40	31.000	- 0.0286	- 0.0264	- 0.0263	- 0.0201	- 0.0161	- 0.0115
60	28.631	- 0.0234	- 0.0216	- 0.0216	- 0.0163	- 0.0113	- 0.0058
80	26.864	- 0.0182	- 0.0168	- 0.0170	- 0.0125	- 0.0066	- 0.0001
100	25.687	- 0.0131	- 0.0121	- 0.0127	- 0.0087	- 0.0019	0.0054
120	25.091	- 0.0080	- 0.0074	- 0.0078	- 0.0050	0.0028	0.0110
140	25.069	- 0.0030	- 0.0028	- 0.0033	- 0.0013	0.0074	0.0165
150	25.255	- 0.0005	- 0.0005	- 0.0010	- 0.0006	0.0097	0.0186
160	25.614	0.0020	0.0018	0.0012	0.0024	0.0120	0.0220
180	26.685	0.0070	0.0064	0.0057	0.0061	0.0166	0.0268

Table (5.10): Sensitivity and Losses when Injecting Same Reactive Power

Q_{inj}	Losses [Mw]	Bus 5 Sensitivity	Bus 6 Sensitivity	Bus 7 Sensitivity	Bus 8 Sensitivity	Bus 9 Sensitivity	Bus 10 Sensitivity	Bus 11 Sensitivity	Bus 15 Sensitivity
10	36.903	- 0.0033	- 0.0017	- 0.0095	- 0.0062	- 0.0088	- 0.0027	- 0.0091	- 0.0016
20	36.279	- 0.0031	- 0.0012	- 0.0084	- 0.0055	- 0.0079	- 0.0022	- 0.0082	- 0.0010
30	35.717	- 0.0028	- 0.0007	- 0.0073	- 0.0049	- 0.0070	- 0.0018	- 0.0073	- 0.0004
40	35.217	- 0.0026	- 0.0002	- 0.0063	- 0.0043	- 0.0061	- 0.0014	- 0.0064	0.0002
50	34.77	- 0.0024	0.0003	- 0.0052	- 0.0036	- 0.0053	- 0.0009	- 0.0056	0.0008
60	34.397	- 0.0022	0.0008	- 0.0042	- 0.0031	- 0.0044	- 0.0005	- 0.0047	0.0014
70	34.073	- 0.0019	0.0013	- 0.0032	- 0.0024	- 0.0035	- 0.0001	- 0.0039	0.0019
80	33.807	- 0.0017	0.0018	- 0.0022	- 0.0018	- 0.0027	0.0003	- 0.0030	0.0025
90	33.595	- 0.0015	0.0023	- 0.0012	- 0.0012	- 0.0019	0.0007	- 0.0022	0.0031
100	33.438	- 0.0013	0.0028	- 0.0002	- 0.0007	- 0.0011	0.0011	0.0014	0.0036
110	33.335	- 0.0011	0.0032	0.0007	- 0.0001	- 0.0003	0.0015	- 0.0006	0.0042
115	33.309	- 0.0010	0.0035	0.0012	0.0002	0.0001	0.0017	- 0.002	0.0044
120	33.283	- 0.0008	0.0037	0.0017	0.0005	0.0005	0.0019	0.0002	0.0047
130	33.2827	- 0.0006	0.0042	0.0026	0.0010	0.0013	0.0023	0.0016	0.0053
140	33.3324	- 0.0004	0.0044	0.0034	0.0016	0.0020	0.0027	0.0017	0.0057
150	33.431	- 0.0002	0.0051	0.0044	0.0022	0.0028	0.0031	0.0025	0.0063

Table (5.18): System Losses in Mw for Different Operation Cases

Contingency	Ordinary LF	Optimal $P_{\text{injection}}$ at load buses	Optimal Generation	Optimal $(P_{\text{injection}} + Q_{\text{injection}})$	Optimal $(P_{\text{generation}} + P_{\text{injection}})$ at load buses	Optimal $Q_{\text{injection}}$ at load buses
Removing line (1-6)	48.315	22.59	32.96	18.96	17.808	41.29
Removing line (3-4)	36.439	25.57	28.18	20.98	29.01	31.3
Removing lines (1-6), (3-4)	47.28	24.252	35.1	20.93	29.45	39.54
Removing lines (1-6), (3-4) and (18-19)	49.894	26.64	37.26	23.56	31.44	42.34
Removing line (1-6) and generator (HAD)	56.08	22.03	37.86	18.56	17.11	48.39
Removing line (1-6) and generator (HRT)	74.04	28.29	55.75	24.10	20.71	64.13

الخلاصة

في هذه الأطروحة تمت دراسة مسألة الانسياب الأمثل للقدرة في شبكة الضغط الفائق (400kV) في العراق المتكونة من ١٩ عمومي حمل و ٦ عموميات توليد عند اقل خسائر في الشبكة مقارنة مع الخسائر في حالة الانسياب الاعتيادي والبالغة ٣٧٥٩٢ ميكاواط بموجب بيانات الحمل والتوليد ليوم ٢٠٠٣/١/٢ وذلك باستخدام نموذج رياضي بطريقة لاكرانج تمت برمجته بلغة Matlab5.3 لتقليل الخسائر الفعالة في الشبكة عن طريق حقن قدرة فعالة أو غير فعالة في عموميات الشبكة اعتمادا على حساسية كل عمومي لتقليل الخسائر نسبة إلى القدرة المحقونة. وقد وجد أن اقل خسائر في الشبكة تساوي ٢١,٨٢٤ ميكاواط وذلك عند حقن ١٨٠، ٢٠٠، ٢١٠ و ٣٠٠ ميكاواط في عموميات الحمل ٧، ٨، ٩ و ١١ على التوالي. كما أن اقل خسائر في الشبكة تساوي ٣٢,٦٤ ميكاواط وذلك عند حقن ١٥٠، ١٢٠، ١٢٠، ١٢٠، ١٠٠، ٣١٠ ميكاوار في عموميات الحمل ٥، ٧، ٨، ٩، ١٠ و ١١ على التوالي.

كما تم حساب القدرة التوليدية المثلى لمحطات التوليد الستة الحالية والتي تعطي اقل خسائر في الشبكة. كذلك تمت دراسة تأثير رفع خطوط نقل أو محطات توليد على الانسياب الأمثل و مقارنة النتائج عند ست حالات تشغيل مختلفة.

وأخيرا دراسة تأثير حدوث أعطال ثلاثية الأطوار مع الأرضي عند منتصف خطوط النقل على الانسياب الأمثل وتأثير ذلك على الاستقرار العابرة للمنظومة ، حيث وجد أن أسوأ حالة هي خروج المنظومة من حالة الاستقرار عند حدوث عطل ثلاثي الأطوار في منتصف خط النقل (٣-٤) حديثة-قائم.

Republic of Iraq
Ministry of Higher Education and
Scientific Research
University of Technology



Minimum Power Losses Based Optimal Power Flow for Iraqi National Super Grid (INSG) and its Effect on Transient Stability

A thesis

Submitted to the Department of Technical Education of
University of Technology in a partial fulfillment of the requirements
for the Degree of Doctor of Philosophy in
Educational Technology/Electrical Engineering

by

Samir Sadon Mustafa Al-Jubory

supervised by

Dr. Nihad M. Al-Rawi

Dr. Samira A. Al-Mosawi

2007



الانسياب الأمثل عند اقل خسائر في القدرة لشبكة الضغط الفائق في العراق وتأثيره على الاستقرارية العابرة

أطروحة
مقدمة إلى قسم التعليم التكنولوجي في الجامعة التكنولوجية
و هي جزء من متطلبات نيل شهادة الدكتوراه
في تكنولوجيا التعليم الهندسي / الهندسة الكهربائية

من قبل
سمير سعدون مصطفى الجبوري

بإشراف

د. نهاد محمد الراوي

د. سميرة عبد الله الموسوي

بسم الله الرحمن الرحيم

وقل رب زدني علما

صدق الله العظيم

Chapter Two

Power Flow and Transient Stability Problem

2.1 Introduction:

All analyses in the engineering sciences start with the formulation of appropriate models. A mathematical model is a set of equations or relations, which appropriately describe the interactions between different quantities in the time frame studies and with the desired accuracy of a physical or engineering component or system. Hence, depending on the purpose of the analysis different models might be valid. In many engineering studies the selection of correct model is often the most difficult part of the study.

2.2 Simulation:

Simulation is an educational tool that is commonly used to teach processes that are infeasible to practice in the real world. Software process education is a domain that has not yet taken full advantage of benefits of simulation.

Simulation is a powerful tool for the analysis of new system designs, retrofits to existing systems and proposed changes to operating rules. Conducting a valid simulation is both an art and a science.

A simulation model is a descriptive model of a process or system, and usually includes parameters that allow the model to be configurable, that is, to represent a number of somewhat different systems or process configurations.

As a descriptive model, we can use a simulation model to experiment with, evaluate and compare any number of system alternatives. Evaluation,

comparison and analysis are the key reasons for doing simulation. Prediction of system performance and identification of system problems and their causes are the key results [13-16]. Simulation is most useful in the following situations:

- 1- There is no simple analytic model.
- 2- The real system has some level of complexity, interaction or interdependence between various components, which makes it difficult to grasp in its entirety. In particular, it is difficult or impossible to predict the effect of proposed changes.
- 3- Designing a new system, and facing a new different demand.
- 4- System modification of a type that we have little or no experience and hence face considerable risk.
- 5- Simulation with animation is an excellent training and educational device, for managers, supervisors, and engineers. In systems of large physical scale, the simulation animation may be the only way in which most participants can visualize how their work contributes to overall system success or problems [17, 18].

2.2.1 Simulation Techniques:

Simulation techniques are fundamental to aid the process of large-scale design and network operation.

Simulation models provide relatively fast and inexpensive estimates of the performance of alternative system configuration and / or alternative operating procedures. The value and usage of simulation have increased due to improvement in both computing power and simulation software.

In order for the simulation to be a successful educational tool, it must be based on an appropriate economic model with correct “fundamental laws” of software engineering and must encode them quantitatively into accurate mathematical relationship [19-23].

2.2.2 Simulation Model Used in this Work:

The simulation model used in this work is (**Law and McComas Approach**)[24] which is called Seven Steps Approach for conducting a successful simulation study as shown in Figure (2.1), which presents techniques for building valid and credible simulation models, and determines whether a simulation model is an accurate representation of the system for the particular objectives of the study. In this approach, a simulation model should always be developed for a particular set of objectives, where a model that is valid for one objective may not be for another. The important activities that take place in the seven steps model are used in this work:

Step 1. Formulation the Problem

The following things are studied in this step:

- 1- The overall objectives of the study.
- 2- The scope of the model.
- 3- The system configuration to be modeled.
- 4- The time frame for the study and the required resources.

Step 2. Collection of information/Data and Construction a Conceptual Model

- 1- Collecting information on the system layout and operating procedures.
- 2- Collecting data to specify model parameters.
- 3- Documentation of the model assumptions, algorithms and data summaries.

Step 3. Validation of Conceptual Model

If errors or omissions are discovered in the conceptual model, it must be updated before proceeding to programming in step 4.

Step 4. Programming the Model

- 1- Programming the conceptual model in a programming language.
- 2- Verification (debugging) of the computer program.

Step 5. The Programmed Model Validity

- 1- If there is an existing system (as in this work), then compare model performance measures with the comparable performance measures collected from the system.
- 2- Sensitivity analyses should be performed on the programmed model to see which model factors have the greatest effect on the performance measured and, thus, have to be modeled carefully.

Step 6. Designing and Analyzing Simulation Experiments

Analyzing the results and deciding if additional experiments are required.

Step 7. Documenting and Presenting the Simulation Results

The documentation for the model should include a detailed description of the computer program, and the results of the study [24].

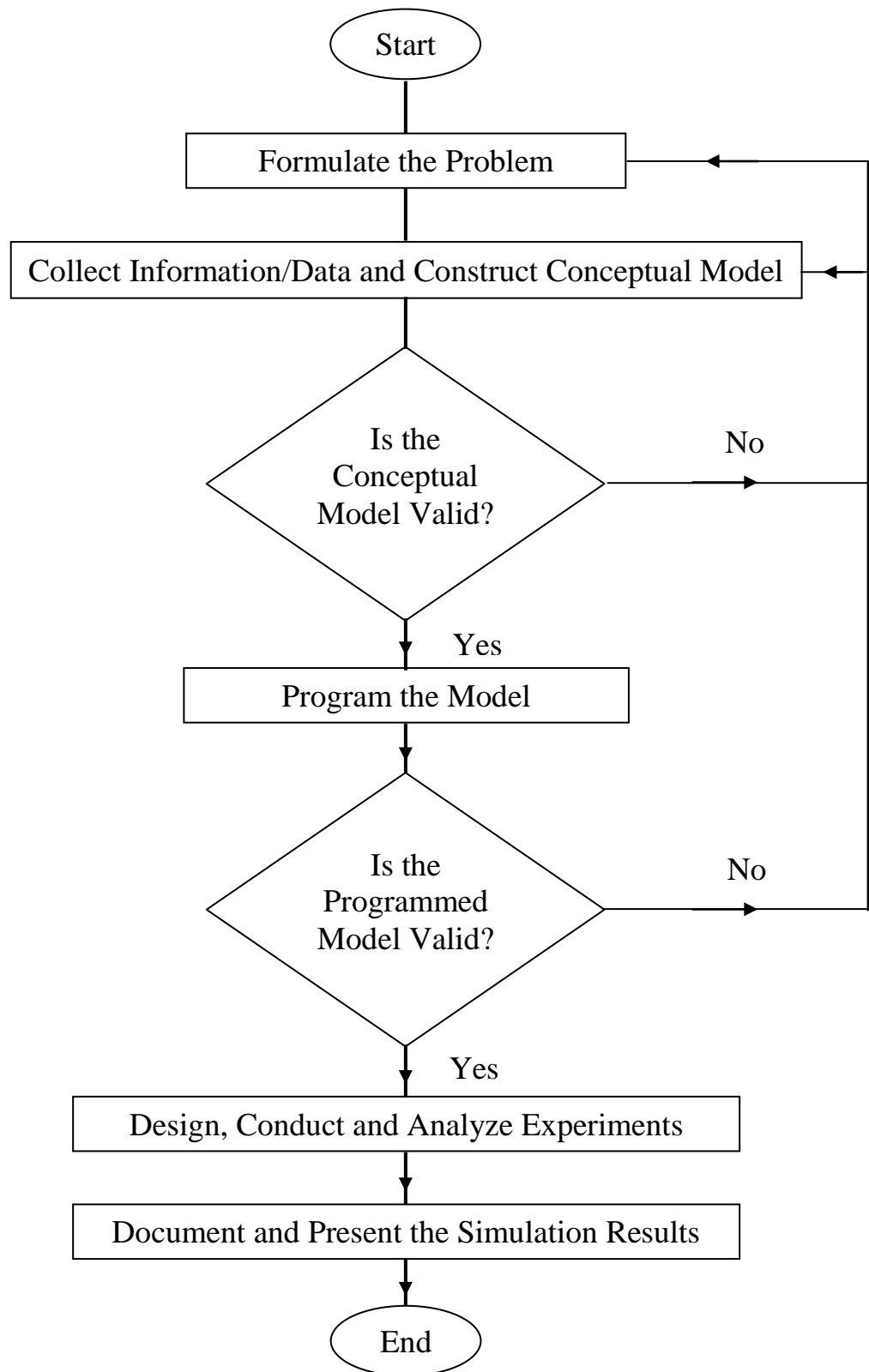


Figure (2.1): Law and McComas Simulation Model [24]

2.3 Network Modeling:

Transmission plant components are modeled by their equivalent circuits in terms of inductance, capacitance and resistance. Among many methods of describing transmission systems to comply with Kirchhoff's laws, two methods, mesh and nodal analysis are normally used. Nodal analysis has been found to be particularly suitable for digital computer work, and almost exclusively used for routine network calculations.

2.3.1 Line Modeling:

The equivalent π -model of a transmission line section is shown in Figure (2.2) and it is characterized by parameters:

$$Z_{km} = R_{km} + jX_{km} = \text{series impedance } (\Omega)$$

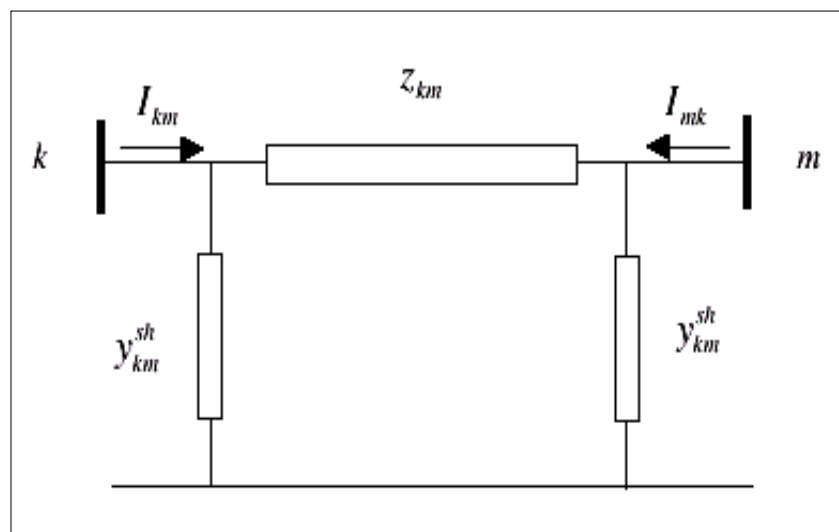


Figure (2.2): Equivalent (π - Model) of a Transmission Line [25]

$$Y_{km} = Z_{km}^{-1} = G_{km} + jB_{km} = \text{series admittance (siemens).}$$

$$Y_{km}^{sh} = G_{km}^{sh} + jB_{km}^{sh} = \text{shunt admittance (siemens).}$$

where:

G_{km} and G_{km}^{sh} are series and shunt conductance respectively.

B_{km} and B_{km}^{sh} are series and shunt Susceptance respectively.

The value of G_{km}^{sh} is so small that it could be neglected [25, 26].

2.3.2 Generator Modeling:

In load flow analysis, generators are modeled as current injections as shown in Figure (2.3).

In steady state a generator is commonly controlled so that the active power injected into the bus and the voltage at the generator terminal are kept constant. Active power from the generator is determined by the turbine control and must of course be within the capability of the turbine generator system. Voltage is primarily determined by reactive power injection into the node, and since the generator must operate within its reactive capability curve, it is not possible to control the voltage outside certain limits [25].

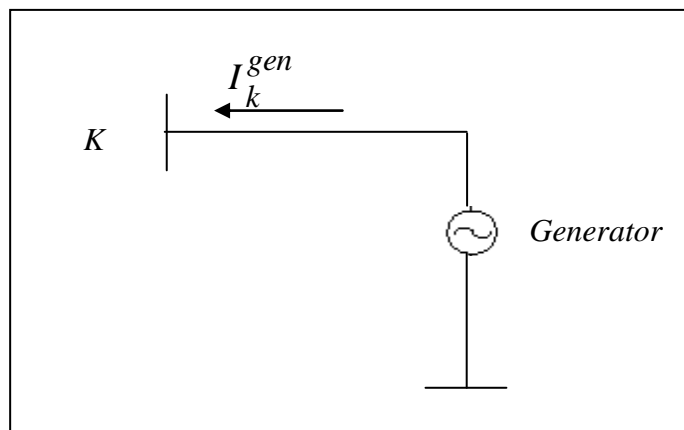


Figure (2.3): Generator Modeling [25]

2.3.3 Load Modeling:

Accurate representation of electric loads in power system is very important in stability calculations. Electric loads can be treated in many ways during the transient period. The common representation of loads are static impedance or admittance to ground, constant current at fixed power factor, constant real and reactive power, or a combination of these representations [27]. For a constant current and a static admittance representation of a load, the following equations are used respectively:

$$I_{Lo} = \frac{P_L - jQ_L}{V_L^*} \quad (2.1)$$

$$Y_{Lo} = \frac{P_L - jQ_L}{V_L^* V_L} \quad (2.2)$$

where:

P_L and Q_L are the scheduled bus loads.

V_L is calculated bus voltage.

I_{Lo} current flows from bus L to ground.

2.4 Power Flow Problem:

The power flow problem can be formulated as a set of non-linear algebraic equality/inequality constraints. These constraints represent both Kirchhoff's laws and network operation limits. In the basic formulation of the power flow problem, four variables are associated with each bus (network node) k:

- V_k – voltage magnitude.
- δ_k – voltage angle.
- P_k – net active power (algebraic sum of generation and load).
- Q_k – net reactive power (algebraic sum of generation and load) [25, 28].

2.5 Bus Types:

Depending on which of the above four variables are known (scheduled) and which ones are unknown (to be calculated), the basic types of buses can be defined as in Table (2-1).

Table (2.1): Power Flow Bus Specification [29]

Bus Type	Active Power, P	Reactive Power, Q	Voltage Magn., E 	Voltage Angle, θ
Constant Power Load, Constant Power Bus	Scheduled	Scheduled	Calculated	Calculated
Generator/Synchronous Condenser, Voltage Controlled Bus	Scheduled	Calculated	Scheduled	Calculated
Reference / Swing Generator, Slack Bus	Calculated	Calculated	Scheduled	Scheduled

2.6 Solution to the PF Problem:

In all realistic cases the power flow problem cannot be solved analytically and hence iterative solutions implemented in computers must be used. Gauss iteration with a variant called Gauss-Seidel iterative method and Newton Raphson method are some of the solutions methods of PF problem. A problem with the Gauss and Gauss-Seidel iteration schemes is that convergence can be very slow and sometimes even the iteration does not converge although a solution exists. Therefore more efficient solution methods are needed, Newton-Raphson method is one such method that is widely used in power flow computations [25, 30].

2.6.1 Newton-Raphson Method [25]:

A system of nonlinear algebraic equations can be written as:

$$f(x) = 0 \quad (2.3)$$

where x is an (n) vector of unknowns and (f) is an (n) vector function of (x). Given an appropriate starting value x^0 , the Newton-

Raphson method solves this vector equation by generating the following sequence:

$$\left. \begin{aligned} J(x^v) \Delta x^v &= -f(x^v) \\ x^{v+1} &= x^v + \Delta x^v \end{aligned} \right\} \quad (2.4)$$

where $J(x^v) = \frac{\partial f(x)}{\partial x}$ is the Jacobian matrix.

The Newton-Raphson algorithm for the n-dimensional case is thus as follows:

1. Set $v=0$ and choose an appropriate starting value x^0 .
2. Compute $f(x^v)$.
3. Test convergence:
If $|f_i(x^v)| \leq \epsilon$ for $i=1, 2, \dots, n$, then x^v is the solution otherwise go to 4.

4. Compute the Jacobian matrix $J(x^v)$.

5. Update the solution

$$\left. \begin{aligned} \Delta x^v &= -J^{-1}(x^v) f(x^v) \\ x^{v+1} &= x^v + \Delta x^v \end{aligned} \right\} \quad (2.5)$$

6. Update iteration counter $v+1 \rightarrow v$ and go to step 2. Note that the linearization of $f(x)$ at x^v is given by the Taylor expansion.

$$f(x^v + \Delta x^v) \approx f(x^v) + J(x^v) \Delta x^v \quad (2.6)$$

where the Jacobian matrix has the general form:

$$J = \frac{\partial f}{\partial x} = \begin{bmatrix} \frac{\partial f_1}{\partial x_1} & \frac{\partial f_1}{\partial x_2} & \dots & \frac{\partial f_1}{\partial x_n} \\ \frac{\partial f_2}{\partial x_1} & \frac{\partial f_2}{\partial x_2} & \dots & \frac{\partial f_2}{\partial x_n} \\ \vdots & \vdots & \ddots & \vdots \\ \frac{\partial f_n}{\partial x_1} & \frac{\partial f_n}{\partial x_2} & \dots & \frac{\partial f_n}{\partial x_n} \end{bmatrix} \quad (2.7)$$

To formulate the Newton-Raphson iteration of the power flow equation, firstly, the state vector of unknown voltage angles and magnitudes is ordered such that:

$$x = \begin{bmatrix} \delta \\ V \end{bmatrix} \quad (2.8)$$

And the nonlinear function f is ordered so that the first component corresponds to active power and the last ones to reactive power:

$$f(x) = \begin{bmatrix} P(x) \\ Q(x) \end{bmatrix} \quad (2.9)$$

$$f(x) = \begin{bmatrix} P_2(x) - P_2 \\ \vdots \\ P_m(x) - P_m \\ \hline Q_2(x) - Q_2 \\ Q_n(x) - Q_n \end{bmatrix} \quad (2.10)$$

In eq. (2.10) the function $P_m(x)$ are the active power which flows out from bus k and the P_m are the injections into bus k from generators and loads, and the functions $Q_n(x)$ are the reactive power which flows out from bus k and Q_n are the injections into bus k from generators and loads. The first $m-1$ equations are formulated for PV and PQ buses, and the last $n-1$ equations can only be formulated for PQ buses. If there are N_{PV} PV buses and N_{PQ} PQ buses, $m-1 = N_{PV} + N_{PQ}$ and $n-1 = N_{PQ}$.

The load flow equations can be written as:

$$f(x) = \begin{bmatrix} P(x) \\ Q(x) \end{bmatrix} = 0 \quad (2.11)$$

And the functions $P(x)$ and $Q(x)$ are called active and reactive power mismatches. The updates to the solutions are determined from the equation:

$$J(x^v) \begin{bmatrix} \Delta\delta^v \\ \Delta V^v \end{bmatrix} + \begin{bmatrix} P(x^v) \\ Q(x^v) \end{bmatrix} = 0 \quad (2.12)$$

The Jacobian matrix J can be written as:

$$J = \begin{bmatrix} \frac{\partial P}{\partial \delta} & \frac{\partial P}{\partial V} \\ \frac{\partial Q}{\partial \delta} & \frac{\partial Q}{\partial V} \end{bmatrix} \quad (2.13)$$

2.6.2 Equality and Inequality Constraints [25]:

The complex power injection at bus k is:

$$S_k = P_k + jQ_k = E_k I_k^* = V_k e^{j\delta_k} I_k^* \quad (2.14)$$

$$\text{where } I_k = \sum Y_{km} E_m \quad (2.15)$$

E_m : complex voltage at bus $m = V_m e^{j\delta}$

$$\text{So } I_k = \sum_{m=1}^N (G_{km} + jB_{km}) V_m e^{j\delta_m} \quad (2.16)$$

$$\text{And } I_k^* = \sum_{m=1}^N (G_{km} - jB_{km}) V_m e^{-j\delta_m} \quad (2.17)$$

$$S_k = V_k e^{j\delta_k} \sum_{m=1}^N (G_{km} - jB_{km}) (V_m e^{-j\delta_m}) \quad (2.18)$$

Where N is the number of buses

The expression for active and reactive power injections is obtained by identifying the real and imaginary parts of eq. (2.18), yielding:

$$P_k = V_k \sum V_m (G_{km} \cos \delta_{km} + B_{km} \sin \delta_{km}) \quad (2.19)$$

$$Q_k = V_k \sum V_m (G_{km} \sin \delta_{km} - B_{km} \cos \delta_{km}) \quad (2.20)$$

Complex power S_{km} flows from bus k to bus m is given by:

$$P_{km} = V_k^2 G_{km} - V_k V_m G_{km} \cos \delta_{km} - V_k V_m B_{km} \sin \delta_{km} \quad (2.21)$$

$$Q_{km} = -V_k^2 (B_{km} + B_{km}^{sh}) + V_k V_m B_{km} \cos \delta_{km} - V_k V_m G_{km} \sin \delta_{km} \quad (2.22)$$

The active and reactive power flows in opposite directions, P_{mk} and Q_{mk} can be obtained in the same way:

$$P_{mk} = V_m^2 G_{km} - V_k V_m G_{km} \cos \delta_{km} + V_k V_m B_{km} \sin \delta_{km} \quad (2.23)$$

$$Q_{mk} = -V_m^2 (B_{km} + B_{km}^{sh}) + V_k V_m B_{km} \cos \delta_{km} + V_k V_m G_{km} \sin \delta_{km} \quad (2.24)$$

The active and reactive power losses of the lines are easily obtained as:

$$P_{km} + P_{mk} = \text{active power losses.}$$

$$Q_{km} + Q_{mk} = \text{reactive power losses.}$$

where:

$k = 1, \dots, n$ (n is the number of buses in the network).

Or: active power loss is calculated using the following equation:

$$P_{loss} = \sum_{i=1}^N \sum_{\substack{j=1 \\ j \neq i}}^N \frac{r_{ij}}{|V_i||V_j|} [(P_i P_j + Q_i Q_j) \cos(\delta_i - \delta_j) + (Q_i P_j - Q_j P_i) \sin(\delta_i - \delta_j)] \quad (2.25)$$

also

$$P_{loss} = \sum_{i=1}^N \sum_{\substack{j=1 \\ j \neq i}}^N G_{ij} [|V_i|^2 + |V_j|^2 - 2|V_i||V_j| \cos(\delta_i - \delta_j)] \quad (2.26)$$

V_k, V_m : voltage magnitudes at the terminal buses of branch k-m.

δ_k, δ_m : voltage angles at the terminal buses of branch k-m.

P_{km} : active power flow from bus k to bus m.

Q_{km} : reactive power flow from bus k to bus m.

Q_k^{sh} = component of reactive power injection due to the shunt element (capacitor or reactor) at bus k ($Q_k^{sh} = b_k^{sh} V_m^2$)

A set of inequality constraints imposes operating limits on variables such as the reactive power injections at PV buses (generator buses) and voltage magnitudes at PQ buses (load buses):

$$V_k^{\min} \leq V_k \leq V_k^{\max}$$

$$Q_k^{\min} \leq Q_k \leq Q_k^{\max}$$

When no inequality constraints are violated, nothing is affected in the power flow equations, but if the limit is violated, the bus status is changed and it is enforced as an equality constraint at the limiting value [25].

2.7 Optimal Power Flow:

2.7.1 Introduction:

The OPF problem has been discussed since 1962 by Carpentier [31]. Because the OPF is a very large, non-linear mathematical programming problem, it has taken decades to develop efficient algorithms for its solution.

Many different mathematical techniques have been employed for its solution. The majority of the techniques in the references [32-37] use one of the following methods:

- 1- Lambda iteration method.
- 2- Gradient method.
- 3- Newton's method.
- 4- Linear programming method.
- 5- Interior point method.

The first generation of computer programs that aimed at a practical solution of the OPF problem did appear until the end of the sixties. Most of these used a gradient method i.e. calculation of the first total derivatives of the objective function related to the independent variables of the problem. These derivatives are known as the gradient vector [38].

2.7.2 Goals of the OPF:

Optimal power flow (OPF) has been widely used in planning and real-time operation of power systems for active and reactive power dispatch to minimize generation costs and system losses and improve voltage profiles.

The primary goal of OPF is to minimize the costs of meeting the load demand for a power system while maintaining the security of the system [39]. The cost associated with the power system can be attributed to the cost of generating power (megawatts) at each generator, keeping each device in the power system within its desired operation range. This will

include maximum and minimum outputs for generators, maximum MVA flows on transmission lines and transformers, as well as keeping system bus voltages within specified ranges.

OPF program is to determine the optimal Operation State of a power system by optimizing a particular objective while satisfying certain specified physical and operating constraints.

Because of its capability of integrating the economic and secure aspects of the concerned system into one mathematical formulation, OPF has been attracting many researchers. Nowadays, power system planners and operators often use OPF as a powerful assistant tool both in planning and operating stage [2]. To achieve these goals, OPF will perform all the steady-state control functions of power system.

These functions may include generator control and transmission system control. For generators, the OPF will control generator MW outputs as well as generator voltage. For the transmission system, the OPF may control the tap ratio or phase shift angle for variable transformers, switched shunt control, and all other flexible ac transmission system (FACTS) devices [31,40].

2.7.3 Nonlinear Programming Methods Applied to OPF Problems:

In a linear program, the constraints are linear in the decision variables, and so is the objective function. In a nonlinear program, the constraints and/or the objective function can also be nonlinear function of the decision variables [41].

In the last three decades, many nonlinear programming methods have been used in the solution of OPF problems, resulting in three classes of approaches:

- a) Extensions of conventional power flow method. In this type of approach, a sequence of optimization problem is alternated with solutions of conventional power flow.
- b) Direct solution of the optimality conditions for Newton's method. In this type of methodology, the approximation of the Lagrangian function by a quadratic form is used, the inequality constraints being handled through penalty functions.
- c) Interior point algorithm, has been extensively used in both linear and nonlinear programming. With respect to optimization algorithm, some alternative versions of the primal-dual interior point algorithm have been developed. One of the versions more frequently used in the OPF is the Predictor-corrector interior point method, proposed for linear programming. This algorithm aims at reducing the number of iterations to the convergence [42-49].

2.7.4 Analysis of System Optimization and Security Formulation of the Optimization Problems:

Optimization and security are often conflicting requirements and should be considered together. The optimization problem consists of minimizing a scalar objective function (normally a cost criterion) through the optimal control of vector [u] of control parameters, i.e.

$$\text{Min } f ([x], [u]) \quad (2.27)$$

subject to:

- ◆ equality constraints of the power flow equations:

$$[g ([x], [u])] = 0 \quad (2.28)$$

- ◆ inequality constraints on the control parameters (parameter constraints):

$$V_{i, \min} \leq V_i \leq V_{i, \max}$$

- ◆ dependent variables and dependent functions (functional constraints):

$$X_{i, \min} \leq X_i \leq X_{i, \max}$$

$$h_i ([x], [u]) \leq 0 \quad (2.29)$$

Examples of functional constraints are the limits on voltage magnitudes at PQ nodes and the limits on reactive power at PV nodes.

The optimal dispatch of real and reactive powers can be assessed simultaneously using the following control parameters:

- ◆ Voltage magnitude at slack node.
- ◆ Voltage magnitude at controllable PV nodes.
- ◆ Taps at controllable transformers.
- ◆ Controllable power P_{Gi} .
- ◆ Phase shift at controllable phase-shifting transformers.
- ◆ Other control parameters.

We assume that only part (P_{Gi}) of the total net power (P_{Ni}) is controllable for the purpose of optimization.

The objective function can then be defined as the sum of instantaneous operating costs over all controllable power generation:

$$f ([x], [u]) = \sum_i c_i (P_{Gi}) \quad (2.30)$$

where c_i is the cost of producing P_{Gi} .

The minimization of system losses is achieved by minimizing the power injected at the slack node.

The minimization of the objective function $f ([x], [u])$ can be achieved with reference to the Lagrange function (L).

$$L = f ([x], [u]) - [\lambda]^T \cdot [g] \quad (2.31)$$

For minimization, the partial derivatives of L with respect to all the variables must be equal to zero, i.e. setting them equal to zero will then give the necessary conditions for a minimum:

$$\left[\frac{\partial L}{\partial \lambda} \right] \equiv [g] = 0 \quad (2.32)$$

$$\left[\frac{\partial L}{\partial x} \right] \equiv \left[\frac{\partial f}{\partial x} \right] - \left[\frac{\partial g}{\partial x} \right]^T \cdot [\lambda] = 0 \quad (2.33)$$

$$\left[\frac{\partial L}{\partial u} \right] \equiv \left[\frac{\partial f}{\partial u} \right] - \left[\frac{\partial g}{\partial u} \right]^T \cdot [\lambda] = 0 \quad (2.34)$$

When we have found $[\lambda]$ from equation (2.33), $[\nabla f]$ the gradient of the objective function (f) with respect to $[u]$ can now be calculated when the minimum has been found, the gradient components will be:

$$\frac{\partial f}{\partial u_i} \begin{cases} = 0 & \text{if } V_{\min} \leq V_i \leq V_{\max} \\ > 0 & \text{if } V_i = V_{\max} \\ < 0 & \text{if } V_i = V_{\min} \end{cases} \quad (2.35)$$

A simplified flow diagram of an optimal power flow program is shown in Figure (2.4) [49].

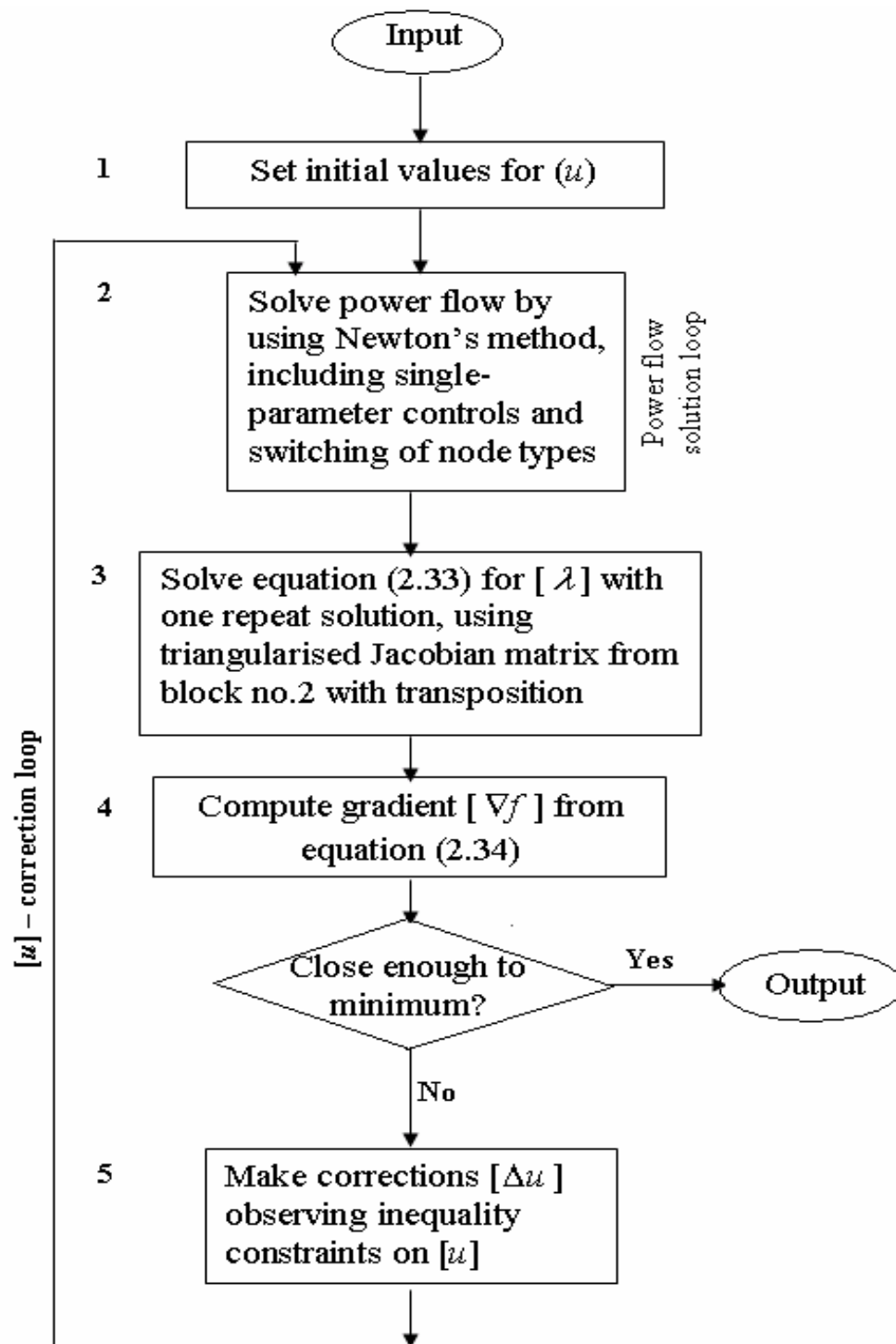


Figure (2.4): Flow Chart of the Optimal Power Flow [49]

2.7.5 Linear Programming Technique (LP):

The nonlinear power loss equation is:

$$P_{\text{loss}} = \sum_{i=1}^N \sum_{j=1}^N G_{ij} [|V_i|^2 + |V_j|^2 - 2|V_i||V_j|\cos(\delta_i - \delta_j)] \quad (2.36)$$

The linearized sensitivity model relating the dependent and control variables can be obtained by linearizing the power equations around the operating state. Despite the fact that any load flow techniques can be used, N-R load flow is most convenient to use to find the incremental losses as shown in Appendix (A). The change in power system losses, ΔP_L , is related to the control variables by the following equation [32]:

$$\Delta P_L = \begin{bmatrix} \frac{\partial P_L}{\partial V_1} & \dots & \frac{\partial P_L}{\partial V_m} & \dots & \frac{\partial P_L}{\partial Q_{m+1}} & \dots & \frac{\partial P_L}{\partial Q_{m+w}} \end{bmatrix} \begin{bmatrix} \Delta V_1 \\ \vdots \\ \Delta V_m \\ \Delta Q_{m+1} \\ \Delta Q_{m+w} \end{bmatrix} \quad (2.37)$$

2.8 Transient Stability:

2.8.1 Introduction:

Power system stability may be defined as the property of the system, which enables the synchronous machines of the system to respond to a disturbance from a normal operating condition so as to return to a condition where their operation is again normal.

Stability studies are usually classified into three types depending upon the nature and order of disturbance magnitude. These are:

- 1- Steady-state stability.
- 2- Transient stability.
- 3- Dynamic stability.

Our major concern here is transient stability (TS) study. TS studies aim at determining if the system will remain in synchronism following major disturbances such as:

- 1- Transmission system faults.
- 2- Sudden or sustained load changes.
- 3- Loss of generating units.
- 4- Line switching.

Transient stability problems can be subdivided into first swing and multi-swing stability problems. In first swing stability, usually the time period under study is the first second following a system fault.

If the machines of the system are found to remain in synchronism within the first second, the system is said to be stable. Multi-swing stability problems extend over a longer study period.

In all stability studies, the objective is to determine whether or not the rotors of the machines being perturbed return to constant speed operation. We can find transient stability definitions in many references such as [50-57].

A transient stability analysis is performed by combining a solution of the algebraic equations describing the network with a numerical solution of the differential equations describing the operation of synchronous machines. The solution of the network equations retains the identity of the system and thereby provides access to system voltages and currents during the transient period. The modified Euler and Runge-Kutta methods have been applied to the solution of the differential equations in transient stability studies [37, 58].

2.8.2 Power Transfer between Two Equivalent Sources:

For a simple lossless transmission line connecting two equivalent generators as shown in Figure (2.5), it is well known that the active power, P , transferred between two generators can be expressed as:

$$p = \frac{E_s * E_R}{X} * \sin \delta \quad (2.38)$$

where E_s is the sending-end source voltage magnitude, E_R is the receiving-end source voltage magnitude, δ is the angle difference between two sources and X is the total reactance of the transmission line and the two sources (X_s, X_R) [50, 59].

$$X = X_s + X_L + X_R \quad (2.39)$$

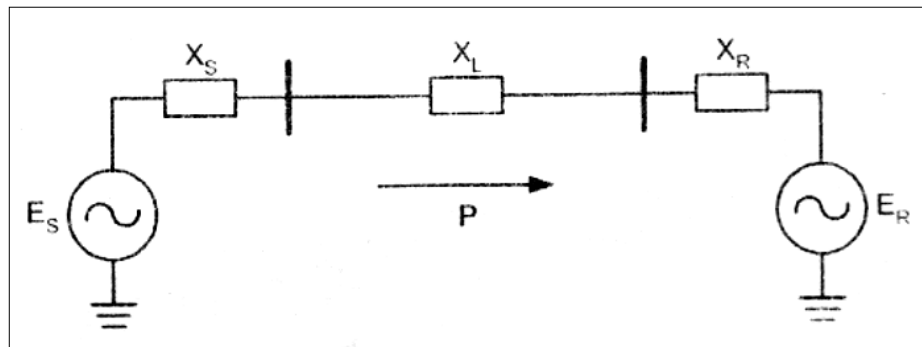


Figure (2.5): A Two-Source System [50]

2.8.3 The Power Angle Curve:

With fixed E_s , E_R and X values, the relationship between P and δ can be described in a power angle curve as shown in Figure (2.6). Starting from $\delta = 0$, the power transferred increases as δ increases. The power transferred between two sources reaches the maximum value P_{MAX} when δ is 90 degrees. After that point, further increase in δ will result in a decrease of power transfer. During normal operations of a generation system without losses, the mechanical power P_0 from a prime mover is converted into the same amount of electrical power and transferred over the transmission line. The angle difference under this balanced normal operation is δ_0 [50, 58].

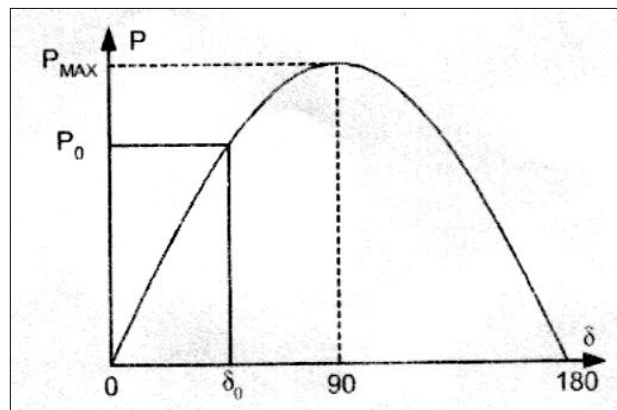


Figure (2.6): The Power Angle Curve [50]

2.8.4 Transiently Stable and Unstable Systems:

During normal operations of a generator, the output of electric power from the generator produces an electric torque that balances the mechanical torque applied to the generator rotor shaft. The generator rotor therefore runs at a constant speed with this balance of electric and mechanical torques. When a fault reduces the amount of power transmission, the electric torque that counters the mechanical torque is also decreased. If the mechanical power is not reduced during the period of the fault, the generator rotor will accelerate with a net surplus of torque input.

Assume that the two-source power system in Figure (2.5) initially operates at a balance point of δ_0 , transferring electric power P_0 . After a fault, the power output is reduced to P_F , the generator rotor therefore starts to accelerate, and δ starts to increase. At the time that the fault is cleared when the angle difference reaches δ_C , there is decelerating torque acting on the rotor because the electric power output P_C at the angle δ_C is larger than the mechanical power input P_0 . However, because of the inertia of the rotor system, the angle does not start to go back to δ_0 immediately. Rather, the angle continues to increase to δ_F when the energy lost during

deceleration in area 2 is equal to the energy gained during acceleration in area 1. This is the so-called equal-area criterion [50, 60].

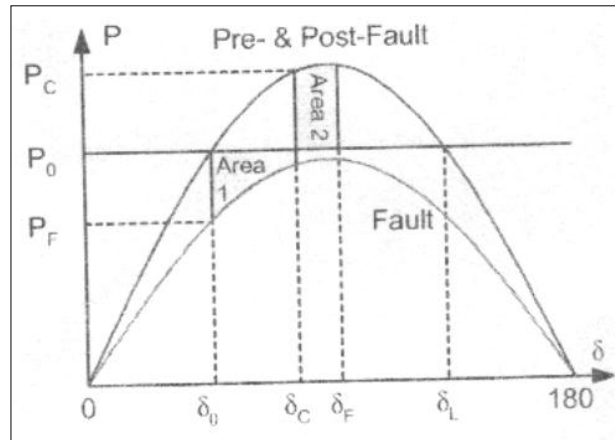


Figure (2.7): A Transiently Stable System [50]

If δ_F is smaller than δ_L , then the system is transiently stable as shown in Figure (2.7). With sufficient damping, the angle difference of the two sources eventually goes back to the original balance point δ_0 . However, if area 2 is smaller than area 1 at the time the angle reaches δ_L , then further increase in angle δ will result in an electric power output that is smaller than the mechanical power input. Therefore, the rotor will accelerate again and δ will increase beyond recovery. This is a transiently unstable scenario, as shown in Figure (2.8). When an unstable condition exists in the power system, one equivalent generator rotates at a speed that is different from the other equivalent generator of the system. We refer to such an event as a loss of synchronism or an out-of-step condition of the power system.

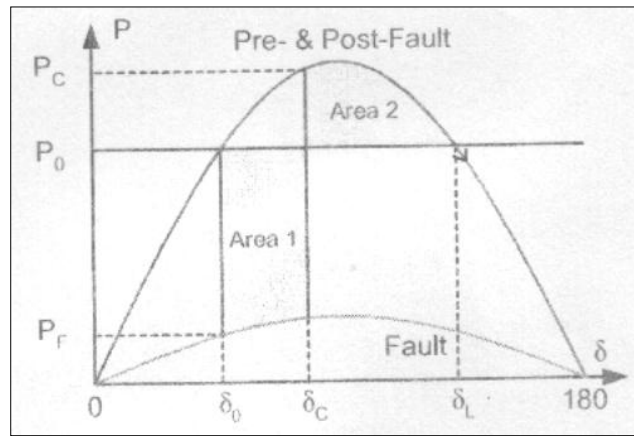


Figure (2.8): A Transiently Unstable System [50]

2.8.5 The Swing Equation:

Electromechanical oscillations are an important phenomenon that must be considered in the analysis of most power systems, particularly those containing long transmission lines. In normal steady state operation all synchronous machines in the system rotate with the same electrical angular velocity, but as a consequence of disturbances one or more generators could be accelerated or decelerated and there is risk that they can fall out of step i.e. lose synchronism. This could have a large impact on system stability and generators losing synchronism must be disconnected otherwise they could be severely damaged. The differential equation describing the rotor dynamics is[25]:

$$J \frac{d^2 \theta_m}{dt^2} = T_m - T_e \quad (2.40)$$

where:

J = the total moment of inertia of the synchronous machine (kg m^2).

θ_m = the mechanical angle of the rotor (rad.).

T_m = mechanical torque from turbine or load (N.m). Positive T_m corresponds to mechanical power fed into the machine, i.e. normal generator operating in steady state.

T_e = electrical torque on the rotor (N.m). Positive T_e is the normal generator operation. Sometimes equation (2.40) is expressed in terms of frequency (f) and inertia constant (H) then the swing equation becomes:

$$\frac{H}{180f} \frac{d^2\theta}{dt^2} = P_m - P_e \quad (2.41)$$

The swing equation is of fundamental importance in the study of power oscillations in power systems. The derivation of this equation is given in Appendix (B) [25].

2.8.6 Step-by-Step Solution of the Swing Curve:

For large systems we depend on the digital computer which determines δ versus t for all the machines in the system. The angle δ is calculated as a function of time over a period long enough to determine whether δ will increase without limit or reach a maximum and start to decrease although the latter result usually indicates stability. On an actual system where a number of variables are taken into account it may be necessary to plot δ versus t over a long enough interval to be sure that δ will not increase again without returning in a low value.

By determining swing curves for various clearing times the length of time permitted before clearing a fault can be determined. Standard interrupting times for circuit breakers and their associated relays are commonly (8, 5, 3 or 2) cycles after a fault occurs, and thus breaker speeds may be specified. Calculations should be made for a fault in the position, which will allow the least transfer of power from the machine, and for the most severe type of fault for which protection against loss of stability is justified.

A number of different methods are available for the numerical evaluation of second-order differential equations in step-by-step computations for small increments of the independent variable. The more

elaborate methods are practical only when the computations are performed on a digital computer by making the following assumptions:

- 1- The accelerating power P_a computed at the beginning of an interval is constant from the middle of the preceding interval considered.
- 2- The angular velocity is constant throughout any interval at the value computed for the middle of the interval. Of course, neither of the assumptions is true, since δ is changing continuously and both P_a and ω are functions of δ . As the time interval is decreased, the computed swing curve approaches the true curve. Figure (2.9) will help in visualizing the assumptions. The accelerating power is computed for the points enclosed in circles at the ends of the $n-2$, $n-1$, and n intervals, which are the beginning of the $n-1$, n and $n+1$ interval. The step curve of P_a in Figure (2.9) results from the assumption that P_a is constant between mid points of the intervals.

Similarly, ω_r , the excess of angular velocity ω over the synchronous angular velocity ω_s , is shown as a step curve that is constant throughout the interval at the value computed for the midpoint. Between the ordinates $n-\frac{3}{2}$ and $n-\frac{1}{2}$ there is a change of speed caused by the constant accelerating power. The change in speed is the product of the acceleration and the time interval, and so

$$\omega_{r,n-1/2} - \omega_{r,n-3/2} = \frac{d^2\delta}{dt^2} \Delta t = \frac{180f}{H} P_{a,n-1} \Delta t \quad (2.42)$$

The change in δ over any interval is the product of ω_r for the interval and the time of the interval. Thus, the change in δ during the $n-1$ interval is:

$$\Delta \delta_{n-1} = \delta_{n-1} - \delta_{n-2} = \Delta t \omega_{r,n-3/2} \quad (2.43)$$

and during the n^{th} interval.

$$\Delta \delta_n = \delta_n - \delta_{n-1} = \Delta t \omega_{r,n-1/2} \quad (2.44)$$

Subtracting Eq. (2.43) from Eq. (2.44) and substituting Eq. (2.42) in the resulting equation to eliminate all values of ω , yields:

$$\Delta \delta_n = \Delta \delta_{n-1} + k P_{a,n-1} \quad (2.45)$$

$$\text{where } k = \frac{180f}{H} (\Delta t)^2 \quad (2.46)$$

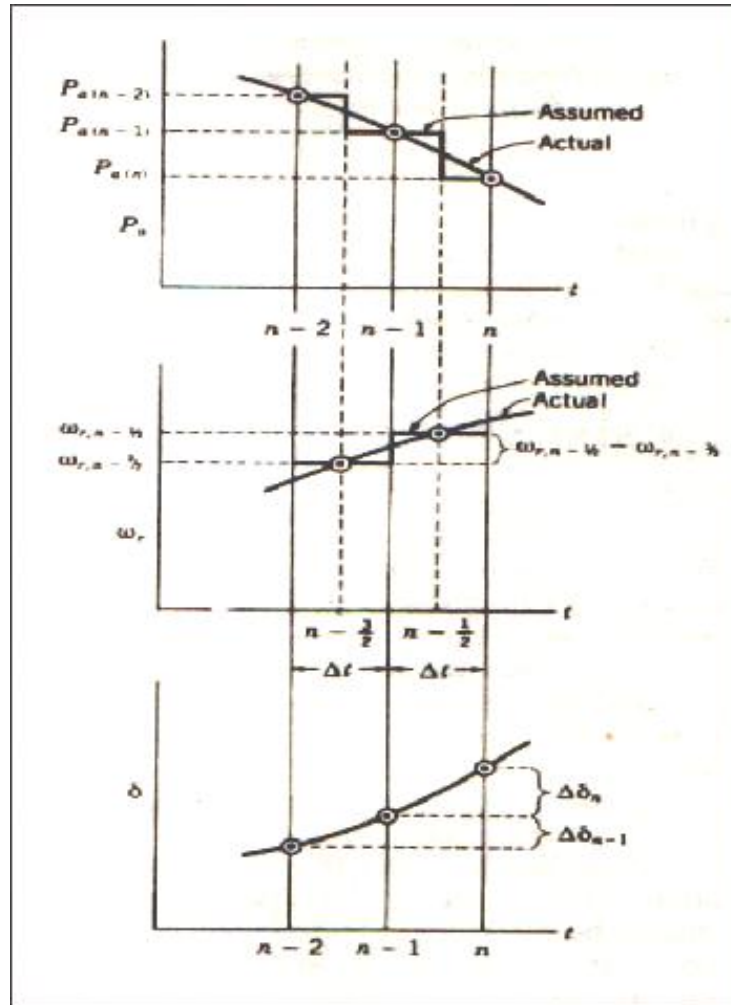


Figure (2.9): Actual and Assumed Values of P_e , ω_r and δ as a Function of Time [37]

Equation (2.45) is the important one for the step-by-step solution of the swing equation with the necessary assumptions enumerated, for it shows how to calculate the change in δ during an interval if the change in δ for the previous interval and the accelerating power for interval are known.

Equation (2.45) shows that, subject to stated assumptions, the change in torque angle during a given interval is equal to change in torque angle during the preceding interval plus the accelerating power at the beginning of the interval times k .

The accelerating power is calculated at the beginning of each new interval. The solution progresses through enough intervals to obtain points for plotting the swing curve. Greater accuracy is obtained when the duration of the intervals is small. An interval of 0.05s is usually satisfactory.

The occurrence of a fault causes a discontinuity in the accelerating power P_a which is zero before the fault and a definite amount immediately following the fault. The discontinuity occurs at the beginning of the interval, when $t=0$. Reference to Figure (2.9) shows that our method of calculation assumes that the accelerating power computed at the beginning of an interval is constant from the middle of the preceding interval to the middle of the interval considered. When the fault occurs, we have two values of P_a at the beginning of an interval, and we must take the average of these two values at our constant accelerating power [37].

Chapter Two

Power Flow and Transient Stability Problem

2.1 Introduction:

All analyses in the engineering sciences start with the formulation of appropriate models. A mathematical model is a set of equations or relations, which appropriately describe the interactions between different quantities in the time frame studies and with the desired accuracy of a physical or engineering component or system. Hence, depending on the purpose of the analysis different models might be valid. In many engineering studies the selection of correct model is often the most difficult part of the study.

2.2 Simulation:

Simulation is an educational tool that is commonly used to teach processes that are infeasible to practice in the real world. Software process education is a domain that has not yet taken full advantage of benefits of simulation.

Simulation is a powerful tool for the analysis of new system designs, retrofits to existing systems and proposed changes to operating rules. Conducting a valid simulation is both an art and a science.

A simulation model is a descriptive model of a process or system, and usually includes parameters that allow the model to be configurable, that is, to represent a number of somewhat different systems or process configurations.

As a descriptive model, we can use a simulation model to experiment with, evaluate and compare any number of system alternatives. Evaluation,

comparison and analysis are the key reasons for doing simulation. Prediction of system performance and identification of system problems and their causes are the key results [13-16]. Simulation is most useful in the following situations:

- 1- There is no simple analytic model.
- 2- The real system has some level of complexity, interaction or interdependence between various components, which makes it difficult to grasp in its entirety. In particular, it is difficult or impossible to predict the effect of proposed changes.
- 3- Designing a new system, and facing a new different demand.
- 4- System modification of a type that we have little or no experience and hence face considerable risk.
- 5- Simulation with animation is an excellent training and educational device, for managers, supervisors, and engineers. In systems of large physical scale, the simulation animation may be the only way in which most participants can visualize how their work contributes to overall system success or problems [17, 18].

2.2.1 Simulation Techniques:

Simulation techniques are fundamental to aid the process of large-scale design and network operation.

Simulation models provide relatively fast and inexpensive estimates of the performance of alternative system configuration and / or alternative operating procedures. The value and usage of simulation have increased due to improvement in both computing power and simulation software.

In order for the simulation to be a successful educational tool, it must be based on an appropriate economic model with correct “fundamental laws” of software engineering and must encode them quantitatively into accurate mathematical relationship [19-23].

2.2.2 Simulation Model Used in this Work:

The simulation model used in this work is (**Law and McComas Approach**)[24] which is called Seven Steps Approach for conducting a successful simulation study as shown in Figure (2.1), which presents techniques for building valid and credible simulation models, and determines whether a simulation model is an accurate representation of the system for the particular objectives of the study. In this approach, a simulation model should always be developed for a particular set of objectives, where a model that is valid for one objective may not be for another. The important activities that take place in the seven steps model are used in this work:

Step 1. Formulation the Problem

The following things are studied in this step:

- 1- The overall objectives of the study.
- 2- The scope of the model.
- 3- The system configuration to be modeled.
- 4- The time frame for the study and the required resources.

Step 2. Collection of information/Data and Construction a Conceptual Model

- 1- Collecting information on the system layout and operating procedures.
- 2- Collecting data to specify model parameters.
- 3- Documentation of the model assumptions, algorithms and data summaries.

Step 3. Validation of Conceptual Model

If errors or omissions are discovered in the conceptual model, it must be updated before proceeding to programming in step 4.

Step 4. Programming the Model

- 1- Programming the conceptual model in a programming language.
- 2- Verification (debugging) of the computer program.

Step 5. The Programmed Model Validity

- 1- If there is an existing system (as in this work), then compare model performance measures with the comparable performance measures collected from the system.
- 2- Sensitivity analyses should be performed on the programmed model to see which model factors have the greatest effect on the performance measured and, thus, have to be modeled carefully.

Step 6. Designing and Analyzing Simulation Experiments

Analyzing the results and deciding if additional experiments are required.

Step 7. Documenting and Presenting the Simulation Results

The documentation for the model should include a detailed description of the computer program, and the results of the study [24].

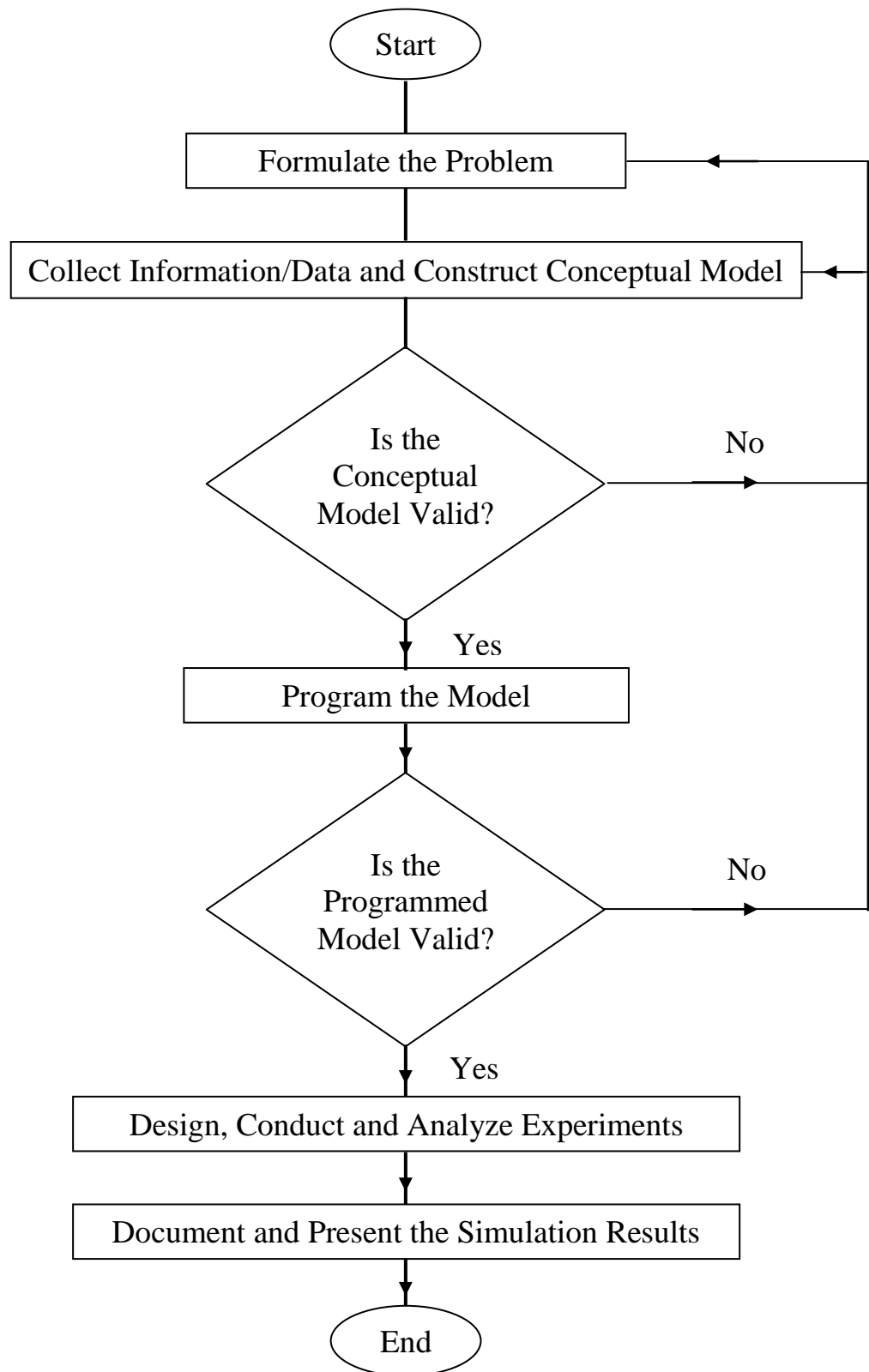


Figure (2.1): Law and McComas Simulation Model [24]

2.3 Network Modeling:

Transmission plant components are modeled by their equivalent circuits in terms of inductance, capacitance and resistance. Among many methods of describing transmission systems to comply with Kirchhoff's laws, two methods, mesh and nodal analysis are normally used. Nodal analysis has been found to be particularly suitable for digital computer work, and almost exclusively used for routine network calculations.

2.3.1 Line Modeling:

The equivalent π -model of a transmission line section is shown in Figure (2.2) and it is characterized by parameters:

$$Z_{km} = R_{km} + jX_{km} = \text{series impedance } (\Omega)$$

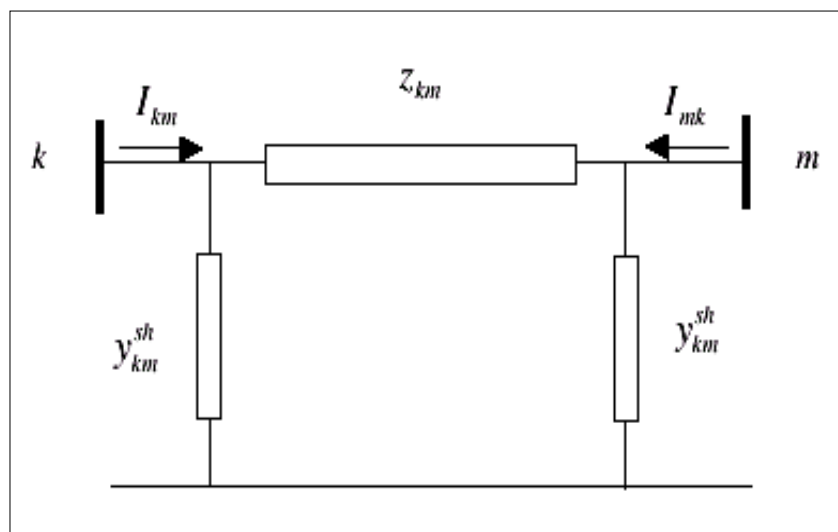


Figure (2.2): Equivalent (π - Model) of a Transmission Line [25]

$$Y_{km} = Z_{km}^{-1} = G_{km} + jB_{km} = \text{series admittance (siemens).}$$

$$Y_{km}^{sh} = G_{km}^{sh} + jB_{km}^{sh} = \text{shunt admittance (siemens).}$$

where:

G_{km} and G_{km}^{sh} are series and shunt conductance respectively.

B_{km} and B_{km}^{sh} are series and shunt Susceptance respectively.

The value of G_{km}^{sh} is so small that it could be neglected [25, 26].

2.3.2 Generator Modeling:

In load flow analysis, generators are modeled as current injections as shown in Figure (2.3).

In steady state a generator is commonly controlled so that the active power injected into the bus and the voltage at the generator terminal are kept constant. Active power from the generator is determined by the turbine control and must of course be within the capability of the turbine generator system. Voltage is primarily determined by reactive power injection into the node, and since the generator must operate within its reactive capability curve, it is not possible to control the voltage outside certain limits [25].

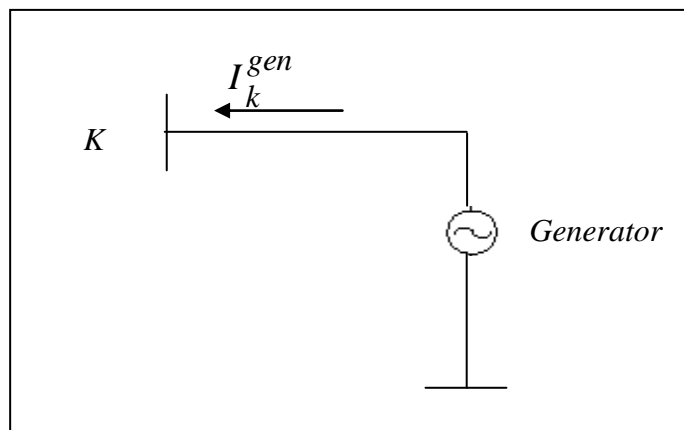


Figure (2.3): Generator Modeling [25]

2.3.3 Load Modeling:

Accurate representation of electric loads in power system is very important in stability calculations. Electric loads can be treated in many ways during the transient period. The common representation of loads are static impedance or admittance to ground, constant current at fixed power factor, constant real and reactive power, or a combination of these representations [27]. For a constant current and a static admittance representation of a load, the following equations are used respectively:

$$I_{Lo} = \frac{P_L - jQ_L}{V_L^*} \quad (2.1)$$

$$Y_{Lo} = \frac{P_L - jQ_L}{V_L^* V_L} \quad (2.2)$$

where:

P_L and Q_L are the scheduled bus loads.

V_L is calculated bus voltage.

I_{Lo} current flows from bus L to ground.

2.4 Power Flow Problem:

The power flow problem can be formulated as a set of non-linear algebraic equality/inequality constraints. These constraints represent both Kirchhoff's laws and network operation limits. In the basic formulation of the power flow problem, four variables are associated with each bus (network node) k:

- V_k – voltage magnitude.
- δ_k – voltage angle.
- P_k – net active power (algebraic sum of generation and load).
- Q_k – net reactive power (algebraic sum of generation and load) [25, 28].

2.5 Bus Types:

Depending on which of the above four variables are known (scheduled) and which ones are unknown (to be calculated), the basic types of buses can be defined as in Table (2-1).

Table (2.1): Power Flow Bus Specification [29]

Bus Type	Active Power, P	Reactive Power, Q	Voltage Magn., E 	Voltage Angle, θ
Constant Power Load, Constant Power Bus	Scheduled	Scheduled	Calculated	Calculated
Generator/Synchronous Condenser, Voltage Controlled Bus	Scheduled	Calculated	Scheduled	Calculated
Reference / Swing Generator, Slack Bus	Calculated	Calculated	Scheduled	Scheduled

2.6 Solution to the PF Problem:

In all realistic cases the power flow problem cannot be solved analytically and hence iterative solutions implemented in computers must be used. Gauss iteration with a variant called Gauss-Seidel iterative method and Newton Raphson method are some of the solutions methods of PF problem. A problem with the Gauss and Gauss-Seidel iteration schemes is that convergence can be very slow and sometimes even the iteration does not converge although a solution exists. Therefore more efficient solution methods are needed, Newton-Raphson method is one such method that is widely used in power flow computations [25, 30].

2.6.1 Newton-Raphson Method [25]:

A system of nonlinear algebraic equations can be written as:

$$f(x) = 0 \quad (2.3)$$

where x is an (n) vector of unknowns and (f) is an (n) vector function of (x). Given an appropriate starting value x^0 , the Newton-

Raphson method solves this vector equation by generating the following sequence:

$$\left. \begin{aligned} J(x^v) \Delta x^v &= -f(x^v) \\ x^{v+1} &= x^v + \Delta x^v \end{aligned} \right\} \quad (2.4)$$

where $J(x^v) = \frac{\partial f(x)}{\partial x}$ is the Jacobian matrix.

The Newton-Raphson algorithm for the n-dimensional case is thus as follows:

1. Set $v=0$ and choose an appropriate starting value x^0 .
2. Compute $f(x^v)$.
3. Test convergence:
If $|f_i(x^v)| \leq \epsilon$ for $i=1, 2, \dots, n$, then x^v is the solution otherwise go to 4.

4. Compute the Jacobian matrix $J(x^v)$.

5. Update the solution

$$\left. \begin{aligned} \Delta x^v &= -J^{-1}(x^v) f(x^v) \\ x^{v+1} &= x^v + \Delta x^v \end{aligned} \right\} \quad (2.5)$$

6. Update iteration counter $v+1 \rightarrow v$ and go to step 2. Note that the linearization of $f(x)$ at x^v is given by the Taylor expansion.

$$f(x^v + \Delta x^v) \approx f(x^v) + J(x^v) \Delta x^v \quad (2.6)$$

where the Jacobian matrix has the general form:

$$J = \frac{\partial f}{\partial x} = \begin{bmatrix} \frac{\partial f_1}{\partial x_1} & \frac{\partial f_1}{\partial x_2} & \dots & \frac{\partial f_1}{\partial x_n} \\ \frac{\partial f_2}{\partial x_1} & \frac{\partial f_2}{\partial x_2} & \dots & \frac{\partial f_2}{\partial x_n} \\ \vdots & \vdots & \ddots & \vdots \\ \frac{\partial f_n}{\partial x_1} & \frac{\partial f_n}{\partial x_2} & \dots & \frac{\partial f_n}{\partial x_n} \end{bmatrix} \quad (2.7)$$

To formulate the Newton-Raphson iteration of the power flow equation, firstly, the state vector of unknown voltage angles and magnitudes is ordered such that:

$$x = \begin{bmatrix} \delta \\ V \end{bmatrix} \quad (2.8)$$

And the nonlinear function f is ordered so that the first component corresponds to active power and the last ones to reactive power:

$$f(x) = \begin{bmatrix} P(x) \\ Q(x) \end{bmatrix} \quad (2.9)$$

$$f(x) = \begin{bmatrix} P_2(x) - P_2 \\ \vdots \\ P_m(x) - P_m \\ \hline Q_2(x) - Q_2 \\ Q_n(x) - Q_n \end{bmatrix} \quad (2.10)$$

In eq. (2.10) the function $P_m(x)$ are the active power which flows out from bus k and the P_m are the injections into bus k from generators and loads, and the functions $Q_n(x)$ are the reactive power which flows out from bus k and Q_n are the injections into bus k from generators and loads. The first $m-1$ equations are formulated for PV and PQ buses, and the last $n-1$ equations can only be formulated for PQ buses. If there are N_{PV} PV buses and N_{PQ} PQ buses, $m-1 = N_{PV} + N_{PQ}$ and $n-1 = N_{PQ}$.

The load flow equations can be written as:

$$f(x) = \begin{bmatrix} P(x) \\ Q(x) \end{bmatrix} = 0 \quad (2.11)$$

And the functions $P(x)$ and $Q(x)$ are called active and reactive power mismatches. The updates to the solutions are determined from the equation:

$$J(x^v) \begin{bmatrix} \Delta \delta^v \\ \Delta V^v \end{bmatrix} + \begin{bmatrix} P(x^v) \\ Q(x^v) \end{bmatrix} = 0 \quad (2.12)$$

The Jacobian matrix J can be written as:

$$J = \begin{bmatrix} \frac{\partial P}{\partial \delta} & \frac{\partial P}{\partial V} \\ \frac{\partial Q}{\partial \delta} & \frac{\partial Q}{\partial V} \end{bmatrix} \quad (2.13)$$

2.6.2 Equality and Inequality Constraints [25]:

The complex power injection at bus k is:

$$S_k = P_k + jQ_k = E_k I_k^* = V_k e^{j\delta_k} I_k^* \quad (2.14)$$

$$\text{where } I_k = \sum Y_{km} E_m \quad (2.15)$$

E_m : complex voltage at bus $m = V_m e^{j\delta}$

$$\text{So } I_k = \sum_{m=1}^N (G_{km} + jB_{km}) V_m e^{j\delta_m} \quad (2.16)$$

$$\text{And } I_k^* = \sum_{m=1}^N (G_{km} - jB_{km}) V_m e^{-j\delta_m} \quad (2.17)$$

$$S_k = V_k e^{j\delta_k} \sum_{m=1}^N (G_{km} - jB_{km}) (V_m e^{-j\delta_m}) \quad (2.18)$$

Where N is the number of buses

The expression for active and reactive power injections is obtained by identifying the real and imaginary parts of eq. (2.18), yielding:

$$P_k = V_k \sum V_m (G_{km} \cos \delta_{km} + B_{km} \sin \delta_{km}) \quad (2.19)$$

$$Q_k = V_k \sum V_m (G_{km} \sin \delta_{km} - B_{km} \cos \delta_{km}) \quad (2.20)$$

Complex power S_{km} flows from bus k to bus m is given by:

$$P_{km} = V_k^2 G_{km} - V_k V_m G_{km} \cos \delta_{km} - V_k V_m B_{km} \sin \delta_{km} \quad (2.21)$$

$$Q_{km} = -V_k^2 (B_{km} + B_{km}^{sh}) + V_k V_m B_{km} \cos \delta_{km} - V_k V_m G_{km} \sin \delta_{km} \quad (2.22)$$

The active and reactive power flows in opposite directions, P_{mk} and Q_{mk} can be obtained in the same way:

$$P_{mk} = V_m^2 G_{km} - V_k V_m G_{km} \cos \delta_{km} + V_k V_m B_{km} \sin \delta_{km} \quad (2.23)$$

$$Q_{mk} = -V_m^2 (B_{km} + B_{km}^{sh}) + V_k V_m B_{km} \cos \delta_{km} + V_k V_m G_{km} \sin \delta_{km} \quad (2.24)$$

The active and reactive power losses of the lines are easily obtained as:

$$P_{km} + P_{mk} = \text{active power losses.}$$

$$Q_{km} + Q_{mk} = \text{reactive power losses.}$$

where:

$k = 1, \dots, n$ (n is the number of buses in the network).

Or: active power loss is calculated using the following equation:

$$P_{loss} = \sum_{i=1}^N \sum_{\substack{j=1 \\ j \neq i}}^N \frac{r_{ij}}{|V_i||V_j|} [(P_i P_j + Q_i Q_j) \cos(\delta_i - \delta_j) + (Q_i P_j - Q_j P_i) \sin(\delta_i - \delta_j)] \quad (2.25)$$

also

$$P_{loss} = \sum_{i=1}^N \sum_{\substack{j=1 \\ j \neq i}}^N G_{ij} [|V_i|^2 + |V_j|^2 - 2|V_i||V_j| \cos(\delta_i - \delta_j)] \quad (2.26)$$

V_k, V_m : voltage magnitudes at the terminal buses of branch k-m.

δ_k, δ_m : voltage angles at the terminal buses of branch k-m.

P_{km} : active power flow from bus k to bus m.

Q_{km} : reactive power flow from bus k to bus m.

Q_k^{sh} = component of reactive power injection due to the shunt element
(capacitor or reactor) at bus k ($Q_k^{sh} = b_k^{sh} V_m^2$)

A set of inequality constraints imposes operating limits on variables such as the reactive power injections at PV buses (generator buses) and voltage magnitudes at PQ buses (load buses):

$$V_k^{\min} \leq V_k \leq V_k^{\max}$$

$$Q_k^{\min} \leq Q_k \leq Q_k^{\max}$$

When no inequality constraints are violated, nothing is affected in the power flow equations, but if the limit is violated, the bus status is changed and it is enforced as an equality constraint at the limiting value [25].

2.7 Optimal Power Flow:

2.7.1 Introduction:

The OPF problem has been discussed since 1962 by Carpentier [31]. Because the OPF is a very large, non-linear mathematical programming problem, it has taken decades to develop efficient algorithms for its solution.

Many different mathematical techniques have been employed for its solution. The majority of the techniques in the references [32-37] use one of the following methods:

- 1- Lambda iteration method.
- 2- Gradient method.
- 3- Newton's method.
- 4- Linear programming method.
- 5- Interior point method.

The first generation of computer programs that aimed at a practical solution of the OPF problem did appear until the end of the sixties. Most of these used a gradient method i.e. calculation of the first total derivatives of the objective function related to the independent variables of the problem. These derivatives are known as the gradient vector [38].

2.7.2 Goals of the OPF:

Optimal power flow (OPF) has been widely used in planning and real-time operation of power systems for active and reactive power dispatch to minimize generation costs and system losses and improve voltage profiles.

The primary goal of OPF is to minimize the costs of meeting the load demand for a power system while maintaining the security of the system [39]. The cost associated with the power system can be attributed to the cost of generating power (megawatts) at each generator, keeping each device in the power system within its desired operation range. This will

include maximum and minimum outputs for generators, maximum MVA flows on transmission lines and transformers, as well as keeping system bus voltages within specified ranges.

OPF program is to determine the optimal Operation State of a power system by optimizing a particular objective while satisfying certain specified physical and operating constraints.

Because of its capability of integrating the economic and secure aspects of the concerned system into one mathematical formulation, OPF has been attracting many researchers. Nowadays, power system planners and operators often use OPF as a powerful assistant tool both in planning and operating stage [2]. To achieve these goals, OPF will perform all the steady-state control functions of power system.

These functions may include generator control and transmission system control. For generators, the OPF will control generator MW outputs as well as generator voltage. For the transmission system, the OPF may control the tap ratio or phase shift angle for variable transformers, switched shunt control, and all other flexible ac transmission system (FACTS) devices [31,40].

2.7.3 Nonlinear Programming Methods Applied to OPF Problems:

In a linear program, the constraints are linear in the decision variables, and so is the objective function. In a nonlinear program, the constraints and/or the objective function can also be nonlinear function of the decision variables [41].

In the last three decades, many nonlinear programming methods have been used in the solution of OPF problems, resulting in three classes of approaches:

- a) Extensions of conventional power flow method. In this type of approach, a sequence of optimization problem is alternated with solutions of conventional power flow.
- b) Direct solution of the optimality conditions for Newton's method. In this type of methodology, the approximation of the Lagrangian function by a quadratic form is used, the inequality constraints being handled through penalty functions.
- c) Interior point algorithm, has been extensively used in both linear and nonlinear programming. With respect to optimization algorithm, some alternative versions of the primal-dual interior point algorithm have been developed. One of the versions more frequently used in the OPF is the Predictor-corrector interior point method, proposed for linear programming. This algorithm aims at reducing the number of iterations to the convergence [42-49].

2.7.4 Analysis of System Optimization and Security Formulation of the Optimization Problems:

Optimization and security are often conflicting requirements and should be considered together. The optimization problem consists of minimizing a scalar objective function (normally a cost criterion) through the optimal control of vector [u] of control parameters, i.e.

$$\text{Min } f ([x], [u]) \quad (2.27)$$

subject to:

- ◆ equality constraints of the power flow equations:

$$[g ([x], [u])] = 0 \quad (2.28)$$

- ◆ inequality constraints on the control parameters (parameter constraints):

$$V_{i, \min} \leq V_i \leq V_{i, \max}$$

- ◆ dependent variables and dependent functions (functional constraints):

$$X_{i, \min} \leq X_i \leq X_{i, \max}$$

$$h_i ([x], [u]) \leq 0 \quad (2.29)$$

Examples of functional constraints are the limits on voltage magnitudes at PQ nodes and the limits on reactive power at PV nodes.

The optimal dispatch of real and reactive powers can be assessed simultaneously using the following control parameters:

- ◆ Voltage magnitude at slack node.
- ◆ Voltage magnitude at controllable PV nodes.
- ◆ Taps at controllable transformers.
- ◆ Controllable power P_{Gi} .
- ◆ Phase shift at controllable phase-shifting transformers.
- ◆ Other control parameters.

We assume that only part (P_{Gi}) of the total net power (P_{Ni}) is controllable for the purpose of optimization.

The objective function can then be defined as the sum of instantaneous operating costs over all controllable power generation:

$$f ([x], [u]) = \sum_i c_i (P_{Gi}) \quad (2.30)$$

where c_i is the cost of producing P_{Gi} .

The minimization of system losses is achieved by minimizing the power injected at the slack node.

The minimization of the objective function $f ([x], [u])$ can be achieved with reference to the Lagrange function (L).

$$L = f ([x], [u]) - [\lambda]^T \cdot [g] \quad (2.31)$$

For minimization, the partial derivatives of L with respect to all the variables must be equal to zero, i.e. setting them equal to zero will then give the necessary conditions for a minimum:

$$\left[\frac{\partial L}{\partial \lambda} \right] \equiv [g] = 0 \quad (2.32)$$

$$\left[\frac{\partial L}{\partial x} \right] \equiv \left[\frac{\partial f}{\partial x} \right] - \left[\frac{\partial g}{\partial x} \right]^T \cdot [\lambda] = 0 \quad (2.33)$$

$$\left[\frac{\partial L}{\partial u} \right] \equiv \left[\frac{\partial f}{\partial u} \right] - \left[\frac{\partial g}{\partial u} \right]^T \cdot [\lambda] = 0 \quad (2.34)$$

When we have found $[\lambda]$ from equation (2.33), $[\nabla f]$ the gradient of the objective function (f) with respect to [u] can now be calculated when the minimum has been found, the gradient components will be:

$$\frac{\partial f}{\partial u_i} \begin{cases} = 0 & \text{if } V_{\min} \leq V_i \leq V_{\max} \\ > 0 & \text{if } V_i = V_{\max} \\ < 0 & \text{if } V_i = V_{\min} \end{cases} \quad (2.35)$$

A simplified flow diagram of an optimal power flow program is shown in Figure (2.4) [49].

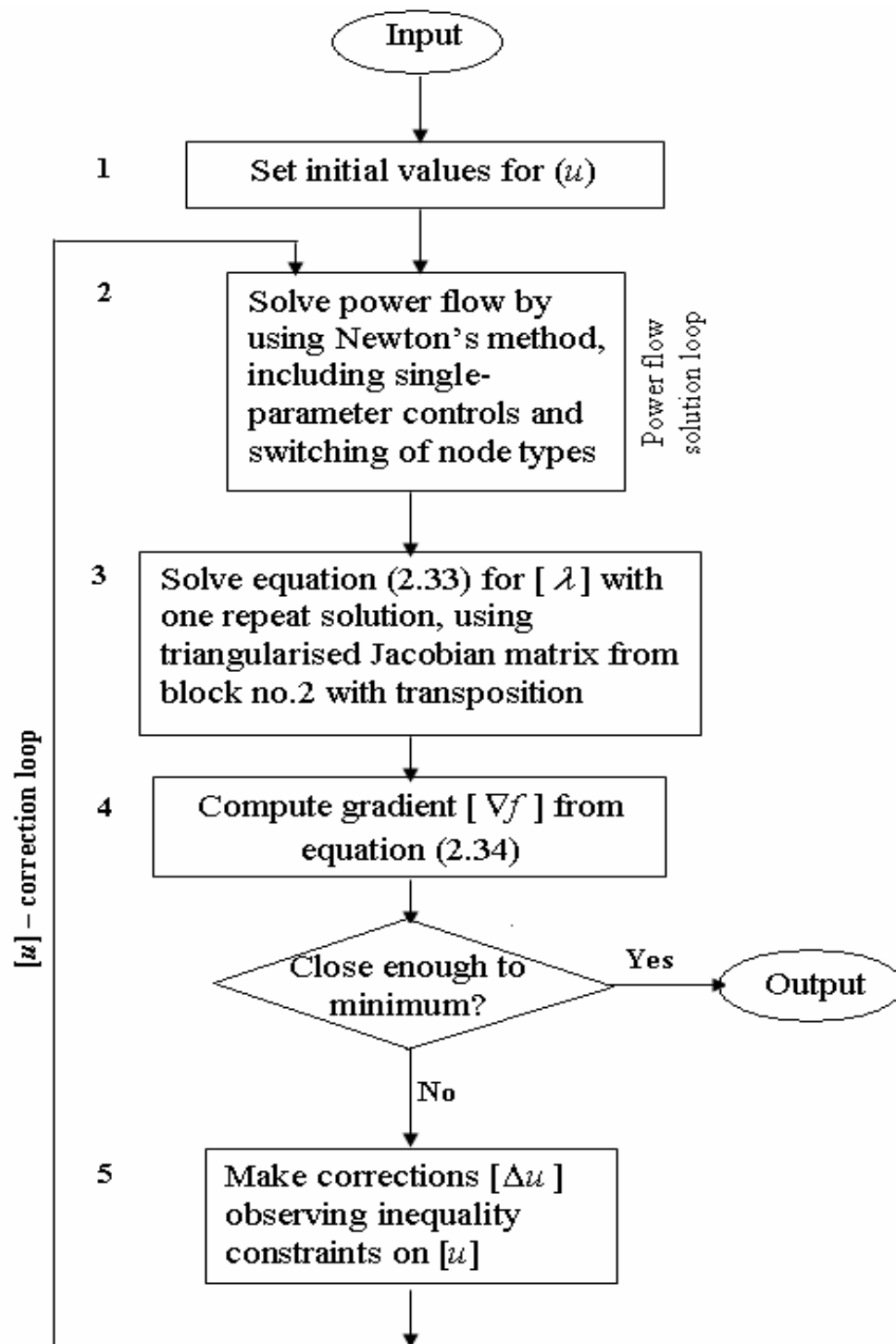


Figure (2.4): Flow Chart of the Optimal Power Flow [49]

2.7.5 Linear Programming Technique (LP):

The nonlinear power loss equation is:

$$P_{\text{loss}} = \sum_{i=1}^N \sum_{j=1}^N G_{ij} [|V_i|^2 + |V_j|^2 - 2|V_i||V_j|\cos(\delta_i - \delta_j)] \quad (2.36)$$

The linearized sensitivity model relating the dependent and control variables can be obtained by linearizing the power equations around the operating state. Despite the fact that any load flow techniques can be used, N-R load flow is most convenient to use to find the incremental losses as shown in Appendix (A). The change in power system losses, ΔP_L , is related to the control variables by the following equation [32]:

$$\Delta P_L = \begin{bmatrix} \frac{\partial P_L}{\partial V_1} & \dots & \frac{\partial P_L}{\partial V_m} & \dots & \frac{\partial P_L}{\partial Q_{m+1}} & \dots & \frac{\partial P_L}{\partial Q_{m+w}} \end{bmatrix} \begin{bmatrix} \Delta V_1 \\ \vdots \\ \Delta V_m \\ \Delta Q_{m+1} \\ \Delta Q_{m+w} \end{bmatrix} \quad (2.37)$$

2.8 Transient Stability:

2.8.1 Introduction:

Power system stability may be defined as the property of the system, which enables the synchronous machines of the system to respond to a disturbance from a normal operating condition so as to return to a condition where their operation is again normal.

Stability studies are usually classified into three types depending upon the nature and order of disturbance magnitude. These are:

- 1- Steady-state stability.
- 2- Transient stability.
- 3- Dynamic stability.

Our major concern here is transient stability (TS) study. TS studies aim at determining if the system will remain in synchronism following major disturbances such as:

- 1- Transmission system faults.
- 2- Sudden or sustained load changes.
- 3- Loss of generating units.
- 4- Line switching.

Transient stability problems can be subdivided into first swing and multi-swing stability problems. In first swing stability, usually the time period under study is the first second following a system fault.

If the machines of the system are found to remain in synchronism within the first second, the system is said to be stable. Multi-swing stability problems extend over a longer study period.

In all stability studies, the objective is to determine whether or not the rotors of the machines being perturbed return to constant speed operation. We can find transient stability definitions in many references such as [50-57].

A transient stability analysis is performed by combining a solution of the algebraic equations describing the network with a numerical solution of the differential equations describing the operation of synchronous machines. The solution of the network equations retains the identity of the system and thereby provides access to system voltages and currents during the transient period. The modified Euler and Runge-Kutta methods have been applied to the solution of the differential equations in transient stability studies [37, 58].

2.8.2 Power Transfer between Two Equivalent Sources:

For a simple lossless transmission line connecting two equivalent generators as shown in Figure (2.5), it is well known that the active power, P , transferred between two generators can be expressed as:

$$p = \frac{E_s * E_R}{X} * \sin \delta \quad (2.38)$$

where E_s is the sending-end source voltage magnitude, E_R is the receiving-end source voltage magnitude, δ is the angle difference between two sources and X is the total reactance of the transmission line and the two sources (X_s, X_R) [50, 59].

$$X = X_s + X_L + X_R \quad (2.39)$$

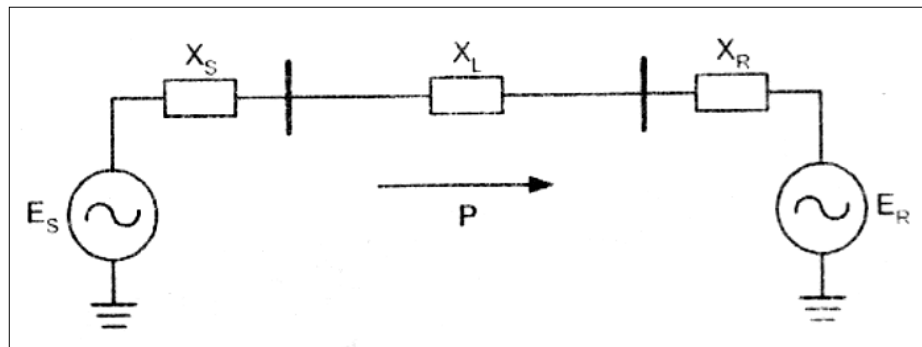


Figure (2.5): A Two-Source System [50]

2.8.3 The Power Angle Curve:

With fixed E_s , E_R and X values, the relationship between P and δ can be described in a power angle curve as shown in Figure (2.6). Starting from $\delta = 0$, the power transferred increases as δ increases. The power transferred between two sources reaches the maximum value P_{MAX} when δ is 90 degrees. After that point, further increase in δ will result in a decrease of power transfer. During normal operations of a generation system without losses, the mechanical power P_0 from a prime mover is converted into the same amount of electrical power and transferred over the transmission line. The angle difference under this balanced normal operation is δ_0 [50, 58].

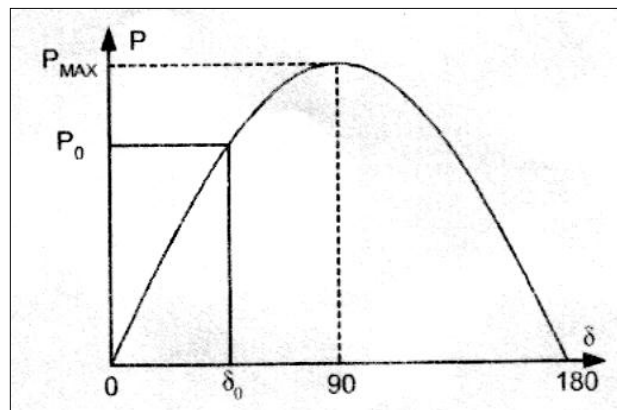


Figure (2.6): The Power Angle Curve [50]

2.8.4 Transiently Stable and Unstable Systems:

During normal operations of a generator, the output of electric power from the generator produces an electric torque that balances the mechanical torque applied to the generator rotor shaft. The generator rotor therefore runs at a constant speed with this balance of electric and mechanical torques. When a fault reduces the amount of power transmission, the electric torque that counters the mechanical torque is also decreased. If the mechanical power is not reduced during the period of the fault, the generator rotor will accelerate with a net surplus of torque input.

Assume that the two-source power system in Figure (2.5) initially operates at a balance point of δ_0 , transferring electric power P_0 . After a fault, the power output is reduced to P_F , the generator rotor therefore starts to accelerate, and δ starts to increase. At the time that the fault is cleared when the angle difference reaches δ_C , there is decelerating torque acting on the rotor because the electric power output P_C at the angle δ_C is larger than the mechanical power input P_0 . However, because of the inertia of the rotor system, the angle does not start to go back to δ_0 immediately. Rather, the angle continues to increase to δ_F when the energy lost during

deceleration in area 2 is equal to the energy gained during acceleration in area 1. This is the so-called equal-area criterion [50, 60].

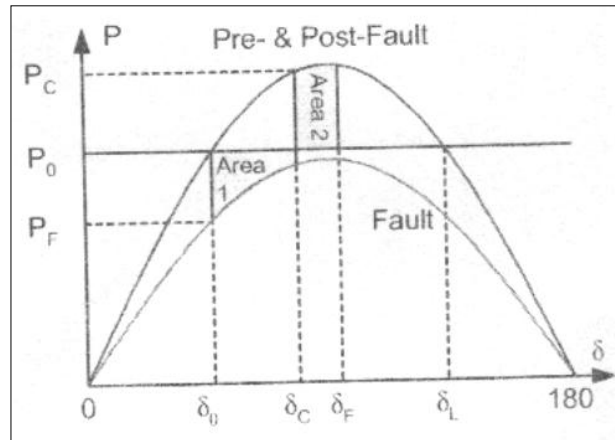


Figure (2.7): A Transiently Stable System [50]

If δ_F is smaller than δ_L , then the system is transiently stable as shown in Figure (2.7). With sufficient damping, the angle difference of the two sources eventually goes back to the original balance point δ_0 . However, if area 2 is smaller than area 1 at the time the angle reaches δ_L , then further increase in angle δ will result in an electric power output that is smaller than the mechanical power input. Therefore, the rotor will accelerate again and δ will increase beyond recovery. This is a transiently unstable scenario, as shown in Figure (2.8). When an unstable condition exists in the power system, one equivalent generator rotates at a speed that is different from the other equivalent generator of the system. We refer to such an event as a loss of synchronism or an out-of-step condition of the power system.

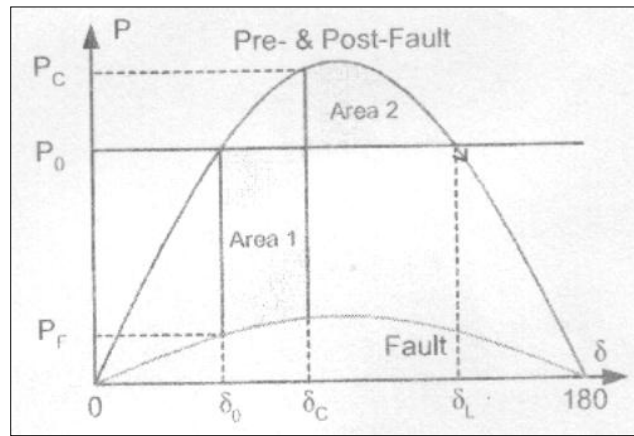


Figure (2.8): A Transiently Unstable System [50]

2.8.5 The Swing Equation:

Electromechanical oscillations are an important phenomenon that must be considered in the analysis of most power systems, particularly those containing long transmission lines. In normal steady state operation all synchronous machines in the system rotate with the same electrical angular velocity, but as a consequence of disturbances one or more generators could be accelerated or decelerated and there is risk that they can fall out of step i.e. lose synchronism. This could have a large impact on system stability and generators losing synchronism must be disconnected otherwise they could be severely damaged. The differential equation describing the rotor dynamics is[25]:

$$J \frac{d^2 \theta_m}{dt^2} = T_m - T_e \quad (2.40)$$

where:

J = the total moment of inertia of the synchronous machine (kg m^2).

θ_m = the mechanical angle of the rotor (rad.).

T_m = mechanical torque from turbine or load (N.m). Positive T_m corresponds to mechanical power fed into the machine, i.e. normal generator operating in steady state.

T_e = electrical torque on the rotor (N.m). Positive T_e is the normal generator operation. Sometimes equation (2.40) is expressed in terms of frequency (f) and inertia constant (H) then the swing equation becomes:

$$\frac{H}{180f} \frac{d^2\theta}{dt^2} = P_m - P_e \quad (2.41)$$

The swing equation is of fundamental importance in the study of power oscillations in power systems. The derivation of this equation is given in Appendix (B) [25].

2.8.6 Step-by-Step Solution of the Swing Curve:

For large systems we depend on the digital computer which determines δ versus t for all the machines in the system. The angle δ is calculated as a function of time over a period long enough to determine whether δ will increase without limit or reach a maximum and start to decrease although the latter result usually indicates stability. On an actual system where a number of variables are taken into account it may be necessary to plot δ versus t over a long enough interval to be sure that δ will not increase again without returning in a low value.

By determining swing curves for various clearing times the length of time permitted before clearing a fault can be determined. Standard interrupting times for circuit breakers and their associated relays are commonly (8, 5, 3 or 2) cycles after a fault occurs, and thus breaker speeds may be specified. Calculations should be made for a fault in the position, which will allow the least transfer of power from the machine, and for the most severe type of fault for which protection against loss of stability is justified.

A number of different methods are available for the numerical evaluation of second-order differential equations in step-by-step computations for small increments of the independent variable. The more

elaborate methods are practical only when the computations are performed on a digital computer by making the following assumptions:

- 1- The accelerating power P_a computed at the beginning of an interval is constant from the middle of the preceding interval considered.
- 2- The angular velocity is constant throughout any interval at the value computed for the middle of the interval. Of course, neither of the assumptions is true, since δ is changing continuously and both P_a and ω are functions of δ . As the time interval is decreased, the computed swing curve approaches the true curve. Figure (2.9) will help in visualizing the assumptions. The accelerating power is computed for the points enclosed in circles at the ends of the $n-2$, $n-1$, and n intervals, which are the beginning of the $n-1$, n and $n+1$ interval. The step curve of P_a in Figure (2.9) results from the assumption that P_a is constant between mid points of the intervals.

Similarly, ω_r , the excess of angular velocity ω over the synchronous angular velocity ω_s , is shown as a step curve that is constant throughout the interval at the value computed for the midpoint. Between the ordinates $n-\frac{3}{2}$ and $n-\frac{1}{2}$ there is a change of speed caused by the constant accelerating power. The change in speed is the product of the acceleration and the time interval, and so

$$\omega_{r,n-1/2} - \omega_{r,n-3/2} = \frac{d^2\delta}{dt^2} \Delta t = \frac{180f}{H} P_{a,n-1} \Delta t \quad (2.42)$$

The change in δ over any interval is the product of ω_r for the interval and the time of the interval. Thus, the change in δ during the $n-1$ interval is:

$$\Delta \delta_{n-1} = \delta_{n-1} - \delta_{n-2} = \Delta t \omega_{r,n-3/2} \quad (2.43)$$

and during the n^{th} interval.

$$\Delta \delta_n = \delta_n - \delta_{n-1} = \Delta t \omega_{r,n-1/2} \quad (2.44)$$

Subtracting Eq. (2.43) from Eq. (2.44) and substituting Eq. (2.42) in the resulting equation to eliminate all values of ω , yields:

$$\Delta \delta_n = \Delta \delta_{n-1} + k P_{a,n-1} \quad (2.45)$$

$$\text{where } k = \frac{180f}{H} (\Delta t)^2 \quad (2.46)$$

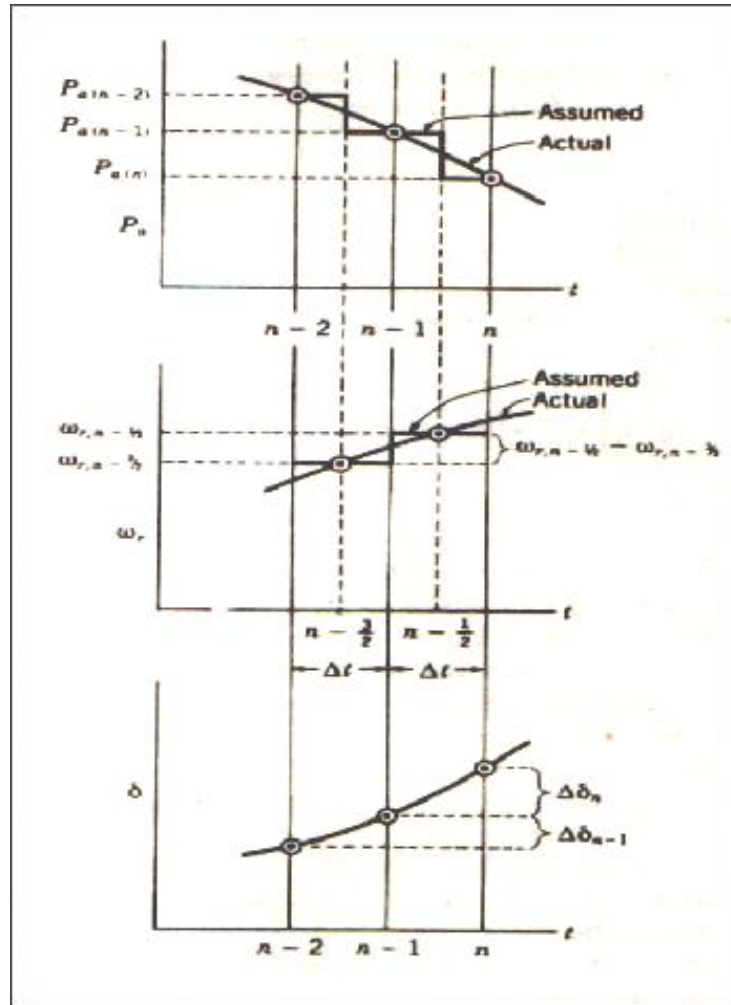


Figure (2.9): Actual and Assumed Values of P_e , ω_r and δ as a Function of Time [37]

Equation (2.45) is the important one for the step-by-step solution of the swing equation with the necessary assumptions enumerated, for it shows how to calculate the change in δ during an interval if the change in δ for the previous interval and the accelerating power for interval are known.

Equation (2.45) shows that, subject to stated assumptions, the change in torque angle during a given interval is equal to change in torque angle during the preceding interval plus the accelerating power at the beginning of the interval times k .

The accelerating power is calculated at the beginning of each new interval. The solution progresses through enough intervals to obtain points for plotting the swing curve. Greater accuracy is obtained when the duration of the intervals is small. An interval of 0.05s is usually satisfactory.

The occurrence of a fault causes a discontinuity in the accelerating power P_a which is zero before the fault and a definite amount immediately following the fault. The discontinuity occurs at the beginning of the interval, when $t=0$. Reference to Figure (2.9) shows that our method of calculation assumes that the accelerating power computed at the beginning of an interval is constant from the middle of the preceding interval to the middle of the interval considered. When the fault occurs, we have two values of P_a at the beginning of an interval, and we must take the average of these two values at our constant accelerating power [37].

Chapter Four

The Application of the Developed Program to the INSG

4.1 Introduction:

The Electrical Energy Generation companies try always to improve the system performance through reducing the active power losses. This problem is investigated by using a mathematical model to find the best location to inject active and reactive power at selected local buses.

In this work the INSG 400 kV has been taken as an example and interesting results have been found.

The objective function of the study is to minimize the system total power loss. The control variables include generator voltage, active power generation, the reactive power generation of VAR sources (capacitive or inductive). The constraints of the load flow are voltage limits at load buses, VAR voltage limits of the generators, and VAR source limits.

OPF and swing equations were solved sequentially. Integration format is used in step-by-step integration (SBSI) and that in the algebraic nonlinear problem should be consistent.

Lagrangian method was applied to find the best solution to optimal load flow. The process was repeated according to control variables. Also different constraints were used according to objective function.

4.2 General Description of the Iraqi National Super Grid (INSG) System:

INSG network consists of 19 busbars and 27 transmission lines; the total length of the lines is 3711 km., six generating stations are connected to the grid. They are of various types of generating units, thermal and hydro

turbine kinds, with different capabilities of MW and MVAR generation and absorption.

Figure (4.1) shows the single line diagram of the INSG (400) kV system [69]. The diagram shows all the busbars, the transmission lines connecting the busbars with their lengths in km marked on each one of them. The per unit data of the system is with the following base values:

Base voltage is 400 kV, base MVA is 100 MVA, and base impedance is 1600Ω . In the single-line diagram the given loads represent the actual values of the busbar's loads. The busbars are numbered and named in order to simplify the input data to the computer programs (the load flow and transient stability programs), which are employed in this thesis. The load and generation of INSG system on the 2nd of January 2003 are tabulated in Appendix (C). Lines and machines parameters are tabulated in Appendixes D, and E and used for a program formulated in MATLAB version (5.3).

The transmission system parameters for both types of conductors (TAA and ACSR) are given in p.u /km in Table (4.1) at the base of 100 MVA [7, 69].

Table (4.1): Transmission Lines Parameters

Conductor Type	R (p.u/km)	X (p.u/km)	B (p.u/km)
TAA *	0.2167×10^{-4}	0.1970×10^{-4}	0.5837×10^{-2}
ACSR **	0.2280×10^{-4}	0.1908×10^{-4}	0.5784×10^{-2}

*TAA is Twin Aluminum Alloy.

** ACSR is Aluminum Conductor Steel-Reinforced.

The cross-section area of the conductors in Table (4.1) is $551 \times 2 \text{ mm}^2$ bundle. These overhead lines can be over loaded 25% more than thermal

limits with these types of conductors. Each 1 mm² can handle 1.25 ampere [7].

The INSG system configuration has been taken as given in Figure (4.1) without any rearrangement and reduction of system buses.

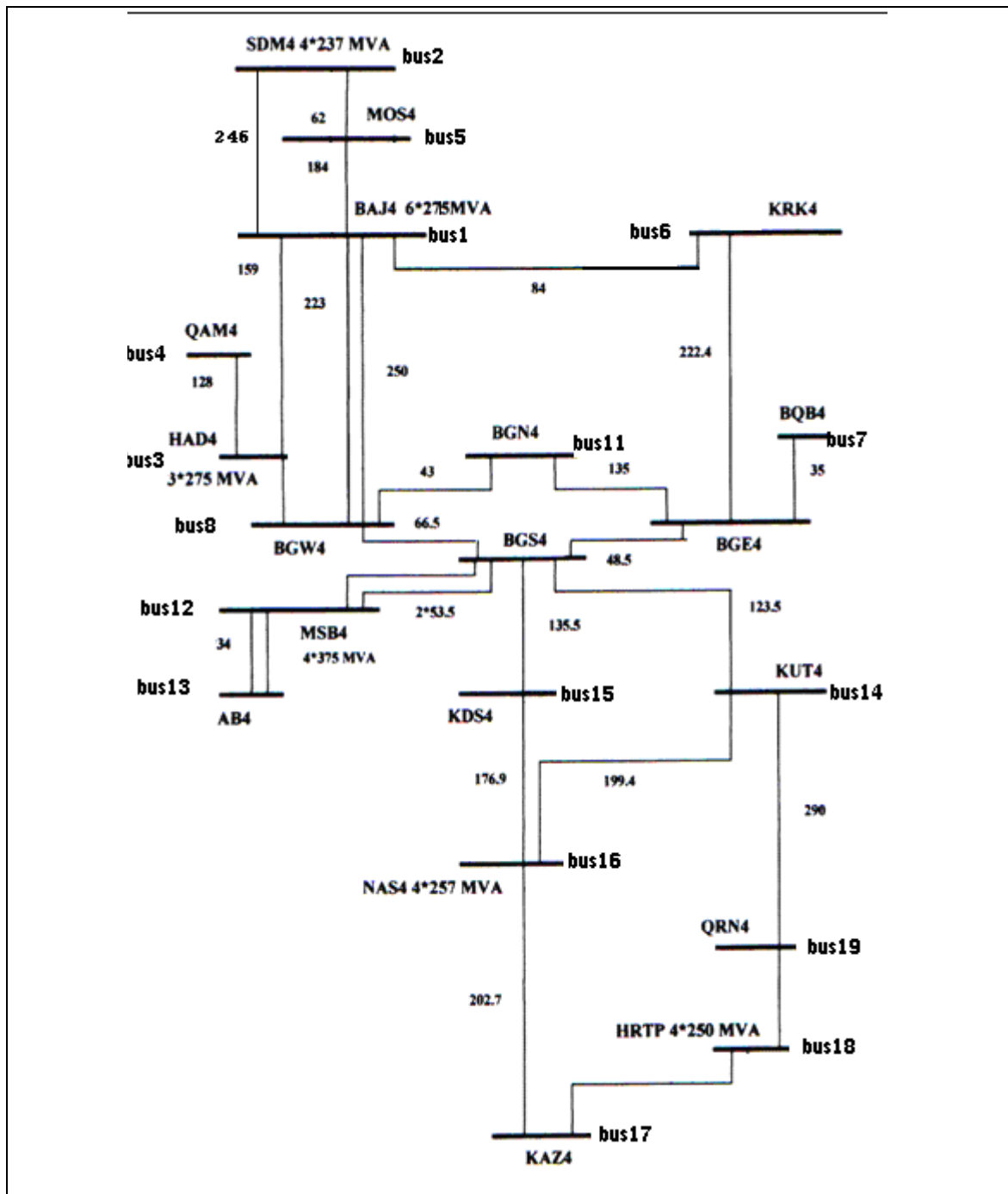


Figure (4.1): Configuration of the 400 kV Network [69]

4.3 The Program Used:

A problem for electric power system students is the solution to problems in text books. In the case of load flow problem, most of the efforts is focused on iterative calculations, not on how the problem is solved. The same is true for stability studies.

A software package [58] is developed to perform electrical power system analysis on a personal computer. The software is capable of performing admittance calculations, load flow studies, optimal load flow studies and transient stability analysis of electric power systems.

It is intended for electric power system students, and is realized in such a manner that a problem can be solved using alternative methods.

Each step during calculations can be visualized. The program has been developed under MATLAB 5.3 for Microsoft Windows. The students are also able to see the inner structure of the program. Load flow analysis is performed by means of Newton-Raphson or Fast-Decoupled methods. Gradient method is used for optimal power flow analysis. This feature enables the power system students to examine differences in the performance of alternative algorithms. A simplified model is used for transient stability, which takes the data from the load flow module. After defining the fault duration, fault clearance time and total analysis time, modified-Euler method is used. The results are displayed and written to corresponding output files. The graphs for angle vs. time for each generator in the system are plotted.

4.4 The Instructional Program:

Power Analysis User Manual

In MATLAB command window, the program is called by typing:

```
>> Main_program
```

which results in the main program menu as shown in Figure (4.2).

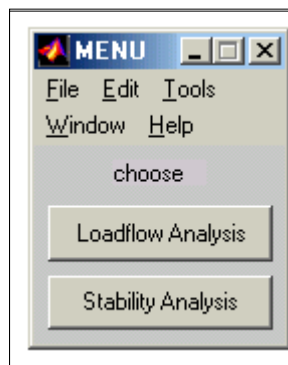


Figure (4.2): Main Program Menu

Load Flow Analysis:

1. Choosing the load flow option, a sub menu is displayed. This menu provides the choice of power flow with and without contingency as shown in Figure (4.3).

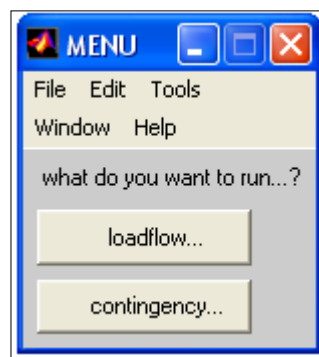


Figure (4.3): Sub Menu of Load Flow Analysis

2. Choosing the Load Flow without contingency, the program will ask the user to enter the data file name. The results consist of two text files (bus result.txt and flow result.txt). The bus result contains: bus number, name, voltage magnitude and phase in degrees, generated and demand power, total series and shunt losses as shown in Figure (4.4). Flow result.txt contains the over loaded lines, the power flow through the lines from send to receive and vice verse as shown in Figure (4.5).

```

LOAD FLOW BUS RESULTS
Name |v| angle(deg) PG(MW) QG(MVAR)
BAJG 399.9996 -0.00032593 0 0
SDMG 400.0001 6.3145 0 0
HADG 400 0.73618 0 0
QAM4 398.9524 -0.082643 0 0
MOS4 394.1607 3.2424 0 0
KRK4 394.4911 -2.7952 0 0
BQB4 373.5296 -9.2764 0 0
BGW4 382.455 -6.8138 0 0
BGE4 376.1397 -8.6367 0 0
BGS4 391.5996 -6.5426 0 0
BGN4 375.7272 -8.5621 0 0
MSBG 399.9983 -5.5487 0 0
BAB4 398.0503 -5.6635 0 0
KUT4 400.656 -5.0389 0 0
KDS4 392.4906 -5.8886 0 0
NSRG 400.0003 -1.0043 0 0
KAZ4 394.1097 -3.9273 0 0
HRTG 399.9999 -2.6124 0 0
QRN4 402.6102 -3.4641 0 0
BAJ4 400 0 570.5925 100.4455
SDM4 400 6.3149 700 -23.22485
HAD4 400 0.73647 500 -0.8474983
MSB4 400 -5.5484 600 420.6564
NSR4 400 -1.004 650 -69.14344
HRT4 400 -2.6121 380 35.9855
TOTAL 3400.5925 463.8716
THE TOTAL AMOUNT OF SERIES LOSSES ARE 37.59249-330.18861
THE TOTAL AMOUNT OF SHUNT LOSSES ARE 0+1922.31691

```

Figure (4.4): Load Flow Bus Results

NS	Name	NR	Name	P(Mw)
2	SDMG	21	SDM4	-700
5	MOS4	2	SDMG	-455.4206
5	MOS4	1	BAJG	155.4206
1	BAJG	2	SDMG	-233.3049
1	BAJG	20	BAJ4	-570.5925
4	QAM4	3	HADG	-60
3	HADG	22	HAD4	-500
1	BAJG	3	HADG	-45.1666
3	HADG	8	BGW4	294.6566
1	BAJG	8	BGW4	238.7362
1	BAJG	8	BGW4	267.6415
1	BAJG	6	KRK4	296.9418
9	BGE4	7	BQB4	150.2395
8	BGW4	11	BGN4	340.7821
11	BGN4	9	BGE4	39.3459
8	BGW4	10	BGS4	-51.5339
9	BGE4	10	BGS4	-388.5388
13	BAB4	12	MSBG	-50
13	BAB4	12	MSBG	-50
12	MSBG	23	MSB4	-600
10	BGS4	12	MSBG	-188.9261
10	BGS4	12	MSBG	-188.9261
10	BGS4	15	KDS4	-41.4485
10	BGS4	14	KUT4	-124.3212

Figure (4.5): Line Flow Results

3. Choosing the Load Flow with contingency, a sub menu is displayed; this menu provides the choice of different contingencies as shown in Figure (4.6).

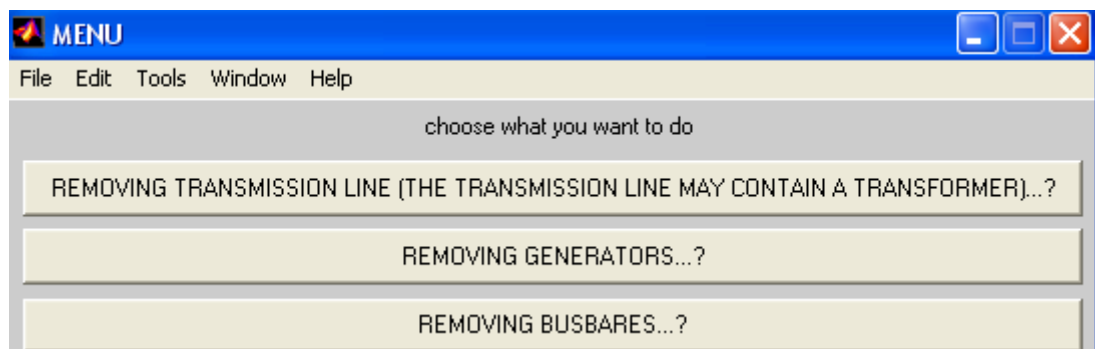


Figure (4.6): Sub Menu of Load Flow with Contingency

4. Choosing one or many of these options gives a system with new configuration. The result consists of two text files similar to that without contingency, but according to the new configuration. The

user has a lot of alternatives to study the system with many contingencies.

Transient Stability Analysis:

1. Choosing the T.S option in the main program, the program will ask for the data file name. The results are displayed at each time step and graphs for angle vs. time for each generator in the system are plotted as shown in Figure (4.7) for one of the generators.

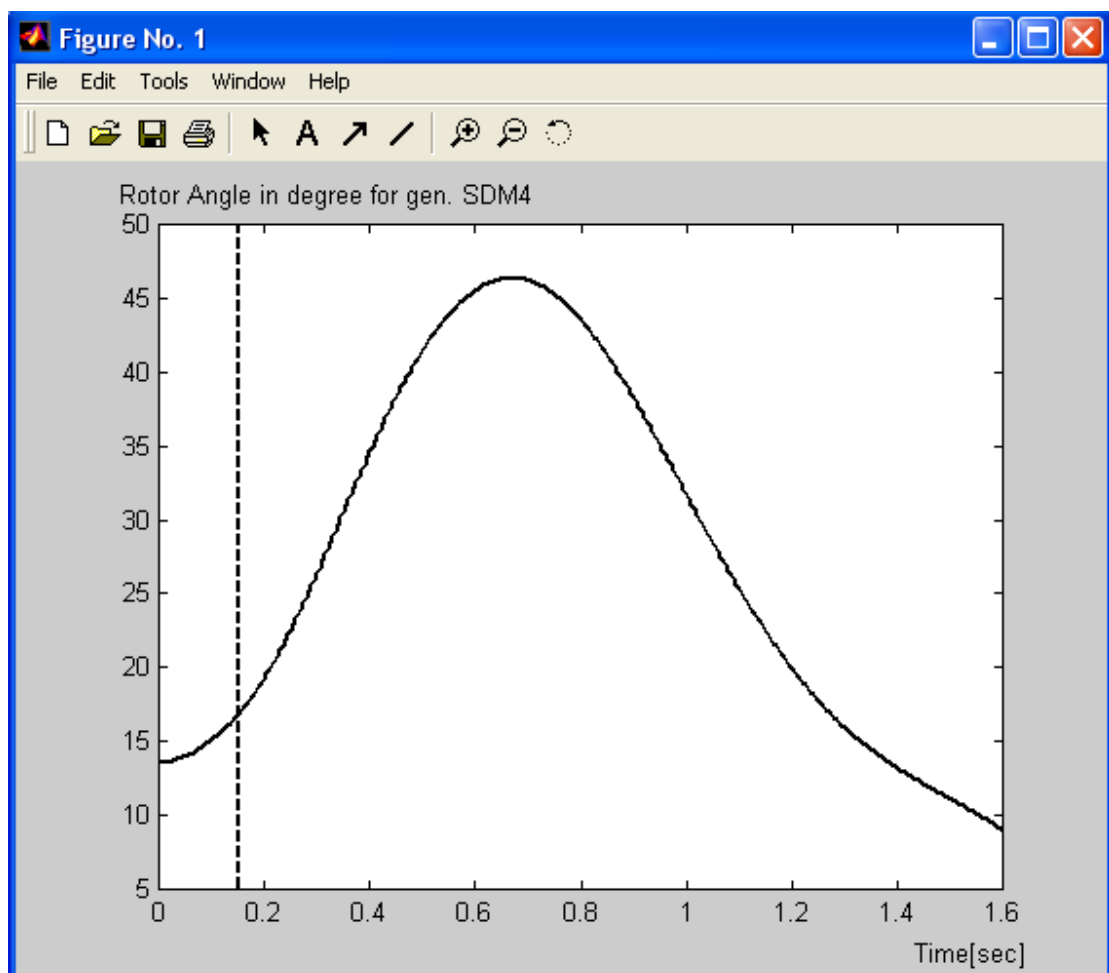


Figure (4.7): Swing Curve for SDM Generation Bus

2. Choosing any type of three phase fault (Line fault, generator fault and load fault) will give a new situation of system stability and a new plot for swing curve is plotted.

Optimal Load Flow:

1. Choosing the OPF option, a sub menu is displayed. This menu provides a choice of minimum losses calculation, bus sensitivity to decrease losses w.r.t real power injecting and bus sensitivity to decrease losses w.r.t reactive power injection as shown in Figure (4.8).

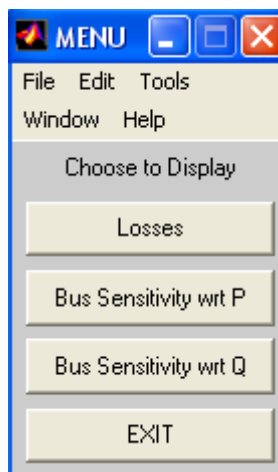
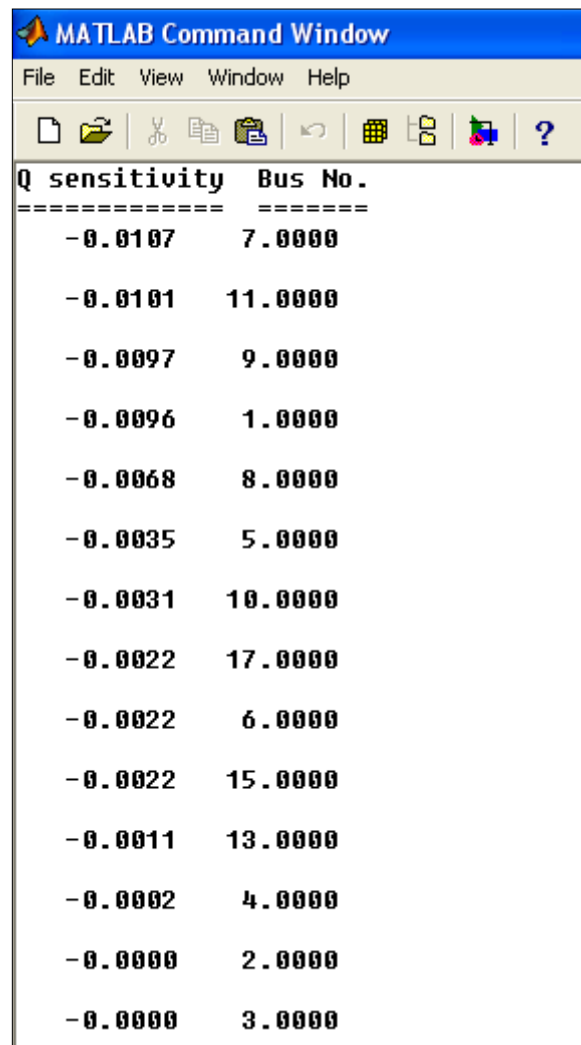


Figure (4.8): Optimal Load Flow

2. Choosing (losses) option will give the magnitude of total system losses.
3. Choosing (P sensitivity) or (Q sensitivity) will give the sequence of the buses according to these sensitivities to reduce system losses with respect to real or reactive power injection in load buses or power generated in generation buses, this will give the best allocation for generator or shunt capacitor in the system which gives minimum losses as shown in Figure (4.9).



The image shows a screenshot of the MATLAB Command Window. The window title is "MATLAB Command Window" and it has a menu bar with "File", "Edit", "View", "Window", and "Help". Below the menu bar is a toolbar with various icons. The main area of the window displays a table with two columns: "Q sensitivity" and "Bus No.". The table is separated from the rest of the window by a dashed line. The data in the table is as follows:

Q sensitivity	Bus No.
-0.0107	7.0000
-0.0101	11.0000
-0.0097	9.0000
-0.0096	1.0000
-0.0068	8.0000
-0.0035	5.0000
-0.0031	10.0000
-0.0022	17.0000
-0.0022	6.0000
-0.0022	15.0000
-0.0011	13.0000
-0.0002	4.0000
-0.0000	2.0000
-0.0000	3.0000

Figure (4.9): Sequence of Bus Sensitivities w.r.t Reactive Power Injection

Chapter Four

The Application of the Developed Program to the INSG

4.1 Introduction:

The Electrical Energy Generation companies try always to improve the system performance through reducing the active power losses. This problem is investigated by using a mathematical model to find the best location to inject active and reactive power at selected local buses.

In this work the INSG 400 kV has been taken as an example and interesting results have been found.

The objective function of the study is to minimize the system total power loss. The control variables include generator voltage, active power generation, the reactive power generation of VAR sources (capacitive or inductive). The constraints of the load flow are voltage limits at load buses, VAR voltage limits of the generators, and VAR source limits.

OPF and swing equations were solved sequentially. Integration format is used in step-by-step integration (SBSI) and that in the algebraic nonlinear problem should be consistent.

Lagrangian method was applied to find the best solution to optimal load flow. The process was repeated according to control variables. Also different constraints were used according to objective function.

4.2 General Description of the Iraqi National Super Grid (INSG) System:

INSG network consists of 19 busbars and 27 transmission lines; the total length of the lines is 3711 km., six generating stations are connected to the grid. They are of various types of generating units, thermal and hydro

turbine kinds, with different capabilities of MW and MVAR generation and absorption.

Figure (4.1) shows the single line diagram of the INSG (400) kV system [69]. The diagram shows all the busbars, the transmission lines connecting the busbars with their lengths in km marked on each one of them. The per unit data of the system is with the following base values:

Base voltage is 400 kV, base MVA is 100 MVA, and base impedance is 1600Ω . In the single-line diagram the given loads represent the actual values of the busbar's loads. The busbars are numbered and named in order to simplify the input data to the computer programs (the load flow and transient stability programs), which are employed in this thesis. The load and generation of INSG system on the 2nd of January 2003 are tabulated in Appendix (C). Lines and machines parameters are tabulated in Appendixes D, and E and used for a program formulated in MATLAB version (5.3).

The transmission system parameters for both types of conductors (TAA and ACSR) are given in p.u /km in Table (4.1) at the base of 100 MVA [7, 69].

Table (4.1): Transmission Lines Parameters

Conductor Type	R (p.u/km)	X (p.u/km)	B (p.u/km)
TAA *	0.2167×10^{-4}	0.1970×10^{-4}	0.5837×10^{-2}
ACSR **	0.2280×10^{-4}	0.1908×10^{-4}	0.5784×10^{-2}

*TAA is Twin Aluminum Alloy.

** ACSR is Aluminum Conductor Steel-Reinforced.

The cross-section area of the conductors in Table (4.1) is $551 \times 2 \text{ mm}^2$ bundle. These overhead lines can be over loaded 25% more than thermal

limits with these types of conductors. Each 1 mm^2 can handle 1.25 ampere [7].

The INSG system configuration has been taken as given in Figure (4.1) without any rearrangement and reduction of system buses.

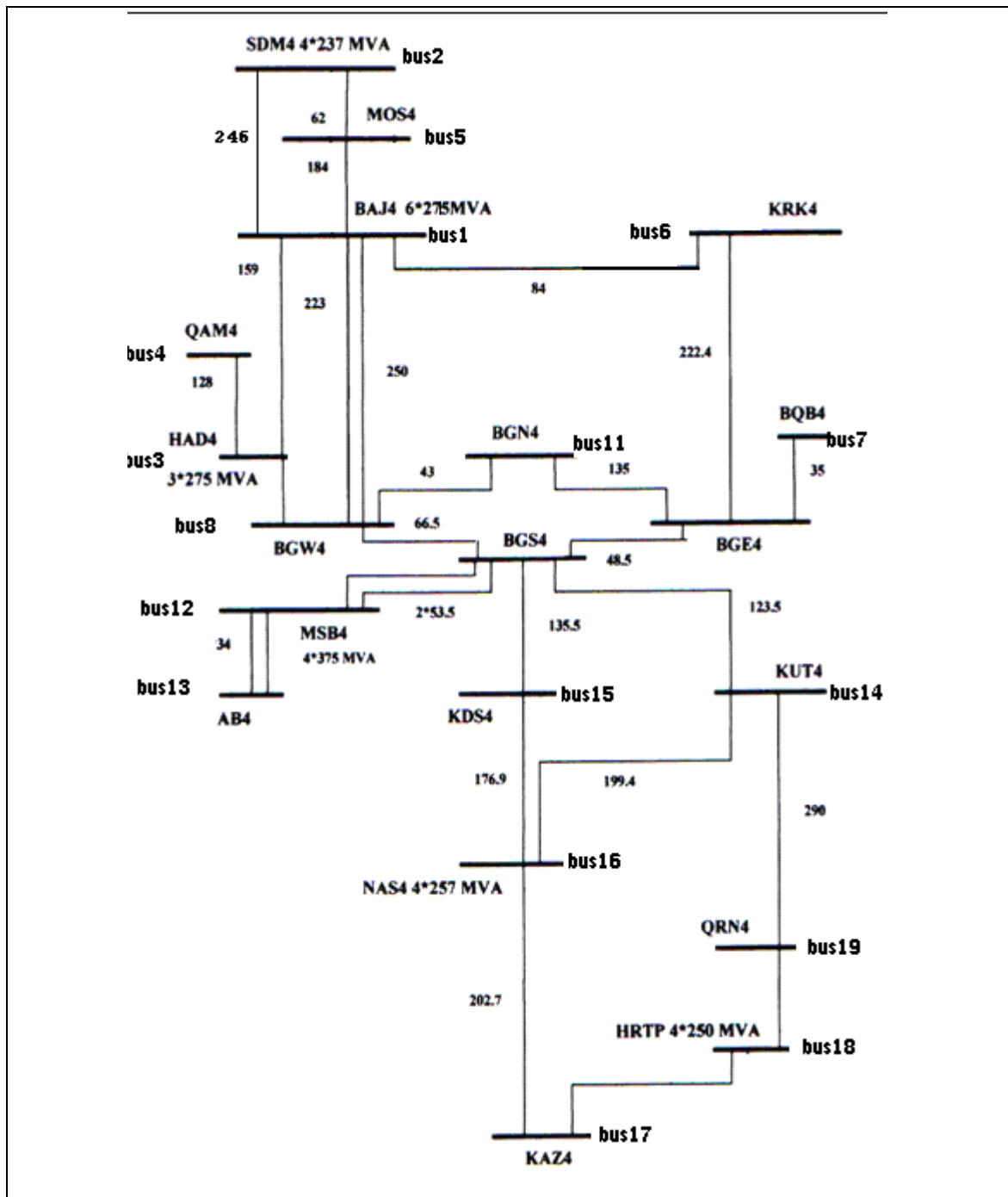


Figure (4.1): Configuration of the 400 kV Network [69]

4.3 The Program Used:

A problem for electric power system students is the solution to problems in text books. In the case of load flow problem, most of the efforts is focused on iterative calculations, not on how the problem is solved. The same is true for stability studies.

A software package [58] is developed to perform electrical power system analysis on a personal computer. The software is capable of performing admittance calculations, load flow studies, optimal load flow studies and transient stability analysis of electric power systems.

It is intended for electric power system students, and is realized in such a manner that a problem can be solved using alternative methods.

Each step during calculations can be visualized. The program has been developed under MATLAB 5.3 for Microsoft Windows. The students are also able to see the inner structure of the program. Load flow analysis is performed by means of Newton-Raphson or Fast-Decoupled methods. Gradient method is used for optimal power flow analysis. This feature enables the power system students to examine differences in the performance of alternative algorithms. A simplified model is used for transient stability, which takes the data from the load flow module. After defining the fault duration, fault clearance time and total analysis time, modified-Euler method is used. The results are displayed and written to corresponding output files. The graphs for angle vs. time for each generator in the system are plotted.

4.4 The Instructional Program:

Power Analysis User Manual

In MATLAB command window, the program is called by typing:

```
>> Main_program
```

which results in the main program menu as shown in Figure (4.2).

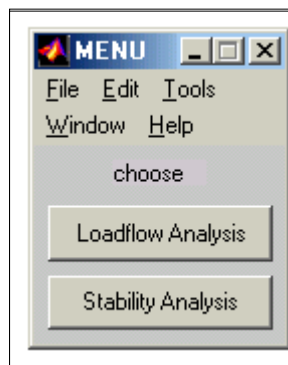


Figure (4.2): Main Program Menu

Load Flow Analysis:

1. Choosing the load flow option, a sub menu is displayed. This menu provides the choice of power flow with and without contingency as shown in Figure (4.3).

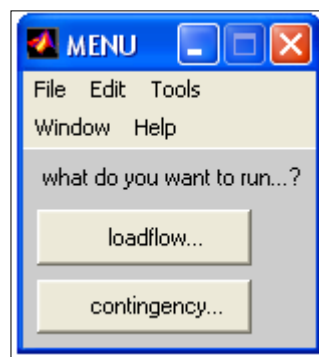


Figure (4.3): Sub Menu of Load Flow Analysis

2. Choosing the Load Flow without contingency, the program will ask the user to enter the data file name. The results consist of two text files (bus result.txt and flow result.txt). The bus result contains: bus number, name, voltage magnitude and phase in degrees, generated and demand power, total series and shunt losses as shown in Figure (4.4). Flow result.txt contains the over loaded lines, the power flow through the lines from send to receive and vice verse as shown in Figure (4.5).

```

LOAD FLOW BUS RESULTS
Name |V| angle(deg) PG(MW) QG(MVAR)
BAJG 399.9996 -0.00032593 0 0
SDMG 400.0001 6.3145 0 0
HADG 400 0.73618 0 0
QAM4 398.9524 -0.082643 0 0
MOS4 394.1607 3.2424 0 0
KRK4 394.4911 -2.7952 0 0
BQB4 373.5296 -9.2764 0 0
BGW4 382.455 -6.8138 0 0
BGE4 376.1397 -8.6367 0 0
BGS4 391.5996 -6.5426 0 0
BGN4 375.7272 -8.5621 0 0
MSBG 399.9983 -5.5487 0 0
BAB4 398.0503 -5.6635 0 0
KUT4 400.656 -5.0389 0 0
KDS4 392.4906 -5.8886 0 0
NSRG 400.0003 -1.0043 0 0
KAZ4 394.1097 -3.9273 0 0
HRTG 399.9999 -2.6124 0 0
QRN4 402.6102 -3.4641 0 0
BAJ4 400 0 570.5925 100.4455
SDM4 400 6.3149 700 -23.22485
HAD4 400 0.73647 500 -0.8474983
MSB4 400 -5.5484 600 420.6564
NSR4 400 -1.004 650 -69.14344
HRT4 400 -2.6121 380 35.9855
TOTAL 3400.5925 463.8716
THE TOTAL AMOUNT OF SERIES LOSSES ARE 37.59249-330.18861
THE TOTAL AMOUNT OF SHUNT LOSSES ARE 0+1922.31691

```

Figure (4.4): Load Flow Bus Results

NS	Name	NR	Name	P(Mw)
2	SDMG	21	SDM4	-700
5	MOS4	2	SDMG	-455.4206
5	MOS4	1	BAJG	155.4206
1	BAJG	2	SDMG	-233.3049
1	BAJG	20	BAJ4	-570.5925
4	QAM4	3	HADG	-60
3	HADG	22	HAD4	-500
1	BAJG	3	HADG	-45.1666
3	HADG	8	BGW4	294.6566
1	BAJG	8	BGW4	238.7362
1	BAJG	8	BGW4	267.6415
1	BAJG	6	KRK4	296.9418
9	BGE4	7	BQB4	150.2395
8	BGW4	11	BGN4	340.7821
11	BGN4	9	BGE4	39.3459
8	BGW4	10	BGS4	-51.5339
9	BGE4	10	BGS4	-388.5388
13	BAB4	12	MSBG	-50
13	BAB4	12	MSBG	-50
12	MSBG	23	MSB4	-600
10	BGS4	12	MSBG	-188.9261
10	BGS4	12	MSBG	-188.9261
10	BGS4	15	KDS4	-41.4485
10	BGS4	14	KUT4	-124.3212

Figure (4.5): Line Flow Results

3. Choosing the Load Flow with contingency, a sub menu is displayed; this menu provides the choice of different contingencies as shown in Figure (4.6).

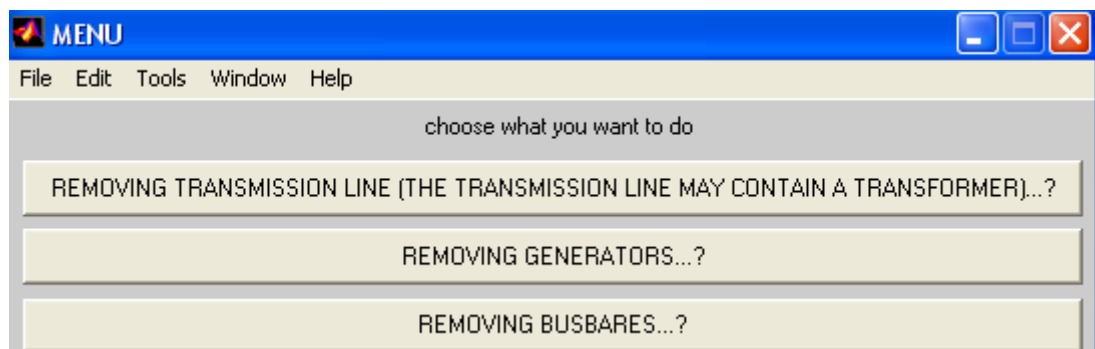


Figure (4.6): Sub Menu of Load Flow with Contingency

4. Choosing one or many of these options gives a system with new configuration. The result consists of two text files similar to that without contingency, but according to the new configuration. The

user has a lot of alternatives to study the system with many contingencies.

Transient Stability Analysis:

1. Choosing the T.S option in the main program, the program will ask for the data file name. The results are displayed at each time step and graphs for angle vs. time for each generator in the system are plotted as shown in Figure (4.7) for one of the generators.

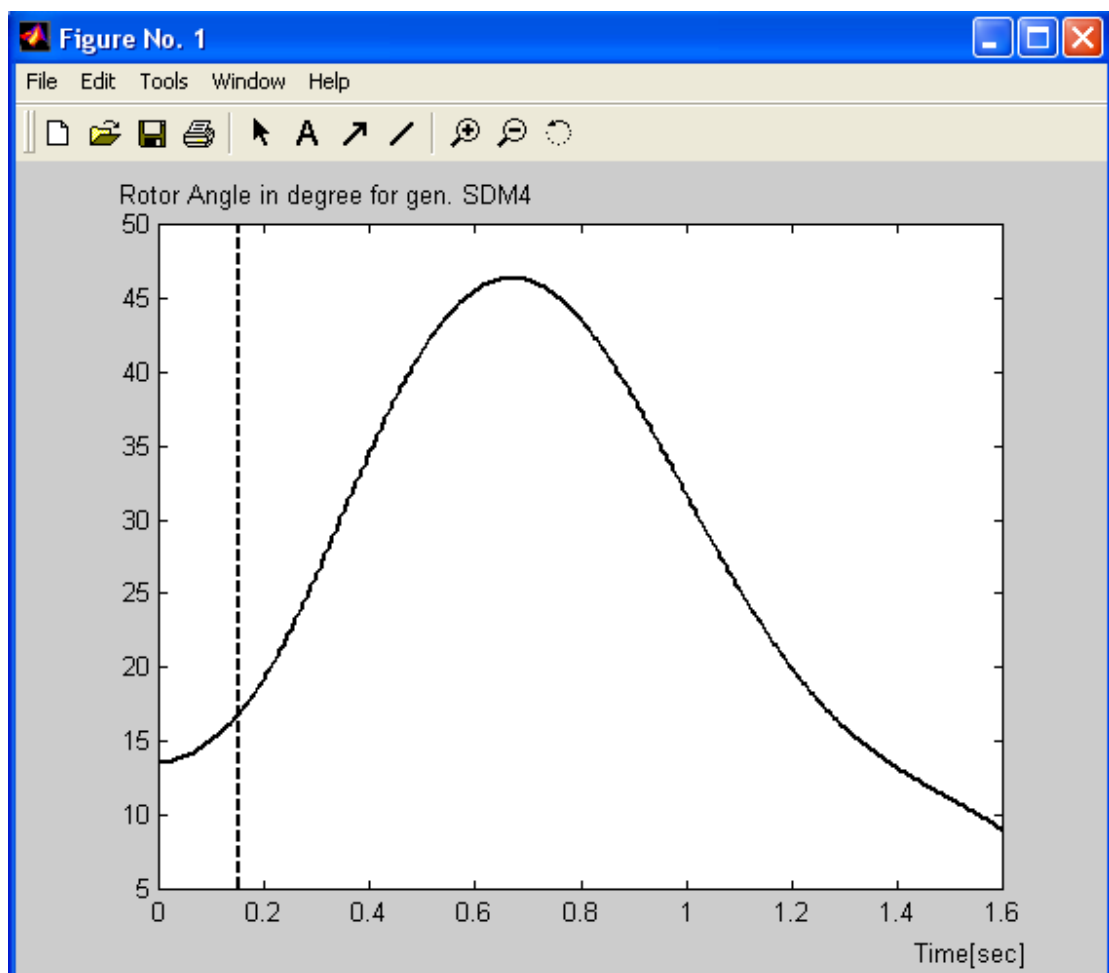


Figure (4.7): Swing Curve for SDM Generation Bus

2. Choosing any type of three phase fault (Line fault, generator fault and load fault) will give a new situation of system stability and a new plot for swing curve is plotted.

Optimal Load Flow:

1. Choosing the OPF option, a sub menu is displayed. This menu provides a choice of minimum losses calculation, bus sensitivity to decrease losses w.r.t real power injecting and bus sensitivity to decrease losses w.r.t reactive power injection as shown in Figure (4.8).

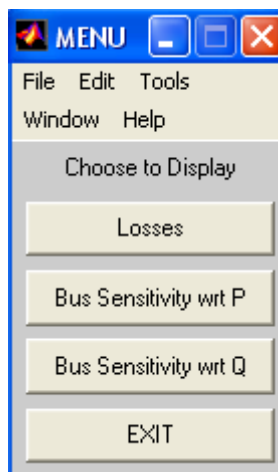
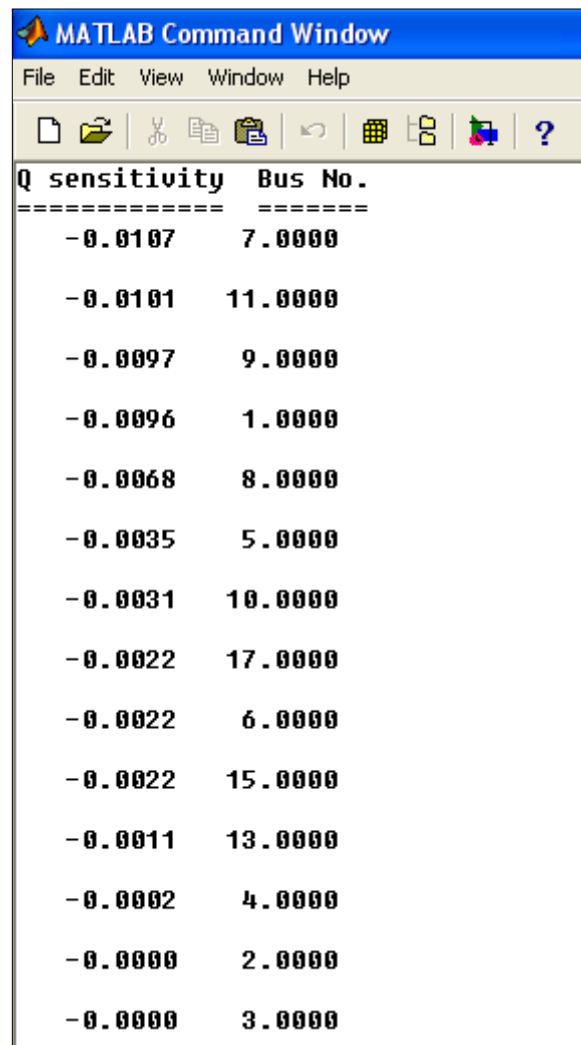


Figure (4.8): Optimal Load Flow

2. Choosing (losses) option will give the magnitude of total system losses.
3. Choosing (P sensitivity) or (Q sensitivity) will give the sequence of the buses according to these sensitivities to reduce system losses with respect to real or reactive power injection in load buses or power generated in generation buses, this will give the best allocation for generator or shunt capacitor in the system which gives minimum losses as shown in Figure (4.9).



The image shows a screenshot of the MATLAB Command Window. The window title is "MATLAB Command Window" and it has a menu bar with "File", "Edit", "View", "Window", and "Help". Below the menu bar is a toolbar with various icons. The main area of the window displays a table with two columns: "Q sensitivity" and "Bus No.". The table is separated from the rest of the window by a dashed line. The data in the table is as follows:

Q sensitivity	Bus No.
-0.0107	7.0000
-0.0101	11.0000
-0.0097	9.0000
-0.0096	1.0000
-0.0068	8.0000
-0.0035	5.0000
-0.0031	10.0000
-0.0022	17.0000
-0.0022	6.0000
-0.0022	15.0000
-0.0011	13.0000
-0.0002	4.0000
-0.0000	2.0000
-0.0000	3.0000

Figure (4.9): Sequence of Bus Sensitivities w.r.t Reactive Power Injection